Western Graduate&PostdoctoralStudies

Western University

Scholarship@Western

Electronic Thesis and Dissertation Repository

2-27-2019 10:00 AM

The Purification of Human Adult Progenitor Cell Types to Promote Angiogenesis

Stephen E. Sherman, *The University of Western Ontario*

Supervisor: Hess, David A., *The University of Western Ontario*

A thesis submitted in partial fulfillment of the requirements for the Doctor of Philosophy degree in Physiology and Pharmacology

© Stephen E. Sherman 2019

Follow this and additional works at: https://ir.lib.uwo.ca/etd

Part of the Cardiovascular Diseases Commons, Circulatory and Respiratory Physiology Commons, Medical Cell Biology Commons, and the Medical Physiology Commons

Recommended Citation

Sherman, Stephen E., "The Purification of Human Adult Progenitor Cell Types to Promote Angiogenesis" (2019). *Electronic Thesis and Dissertation Repository*. 6026.
https://ir.lib.uwo.ca/etd/6026

This Dissertation/Thesis is brought to you for free and open access by Scholarship@Western. It has been accepted for inclusion in Electronic Thesis and Dissertation Repository by an authorized administrator of Scholarship@Western. For more information, please contact wlswadmin@uwo.ca.

Abstract

Cellular transplantation strategies have aimed to combat critical limb ischemia (CLI) by inducing endogenous blood vessel regeneration. Transplantation of mesenchymal stromal cells (MSC) for CLI has proven safe and well-tolerated but demonstrated only modestly improved clinical outcomes explained in part by a lack of MSC survival and/or potency in ischemic tissues. This thesis focuses on the development of improved transplantation strategies for patients with CLI utilizing purified pro-angiogenic subsets of MSC and endothelial colony forming cells (ECFC) seeded within decellularized adipose tissue (DAT) bioscaffolds. First, I investigated whether purification of bone marrow-derived MSC based on a conserved stem cell function, high ALDH-activity, could isolate a pro-vascular MSC subset after culture. Conditioned media generated by ALDH^{hi} MSC promoted endothelial cell proliferation, survival, and tube forming functions under serum-free conditions, and a robust recruitment of mouse derived endothelial cells was observed after subcutaneous implantation of ALDH^{hi} MSC within immunodeficient mice. Interestingly, isolating ECFC based on high ALDH-activity did not improve endothelial cell functions. Instead, isolation of ECFC expressing the progenitor cell surface marker, CD34 purified for ECFC with a mature endothelial cell surface phenotype and diminished colony- and tubule-forming functions *in vitro*. Before transplanting ECFC and MSC within human DAT scaffolds, I sought to develop robust methodologies to extract cells from DAT scaffolds, without generation of autofluorescent debris that impaired flow cytometric cellular evaluations. After protease dissociation, DAT scaffolds were centrifuged using a density gradient to produce samples with >99% purity. This method enabled accurate quantification of changes in ECFC surface marker expression alongside a decline in ECFC proliferation when co-cultured with MSC on DAT scaffolds *in vitro*. After intramuscular injection, or DAT scaffold implantation of ECFC and/or MSC into NOD.SCID mice with acute unilateral hindlimb ischemia, the level of blood perfusion in the ischemic limb was unaffected compared to saline injection. Importantly, implanted DAT scaffolds became vascularized and enhanced survival of ECFC or MSC. Taken together, this body of work indicates the importance of purifying pro-regenerative subsets to maximize cellular potency for clinical benefit.

Keywords

Cardiovascular disease, Peripheral artery disease, Critical limb ischemia, Ischemia, Angiogenesis, Cell therapy, Stem cell, Progenitor cell, Mesenchymal stromal cell, Endothelial progenitor cell, Aldehyde dehydrogenase, Fluorescence activated cell sorting, Flow cytometry, Biomaterials, Decellularized scaffolds, Cell transplantation, Regenerative medicine.

Co-Authorship Statement

All studies presented in this thesis were completed by Stephen Sherman in the laboratory of Dr. David Hess with experimental contributions from the co-authors listed below. Dr. David Hess contributed to design, analysis, interpretation, and manuscript preparation for all experiments.

Chapter 1:

The section on Mesenchymal stromal cells was previously published in a book chapter co-authored with Dr. David Hess.

Sherman SE, Hess DA. Immunogenicity and Immunomodulation of Fetal Stem Cells. In Fetal Stem Cells in Regenerative Medicine 2016 (pp. 57-79). Springer, New York, NY.

Chapter 2:

Dr. Miljan Kuljanin helped with the cell lysate preparation and analysis by mass spectrometry. Tyler Cooper provided support with processing the directed in vivo angiogenesis assay. Dr. David Putman provided training and support for the MSC differentiation assays *in vitro*. Dr. Gilles Lajoie provided mass spectrometry expertise to perform the proteomic analysis.

Sherman SE, Kuljanin M, Cooper TT, Putman DM, Lajoie GA, Hess DA. High aldehyde dehydrogenase activity identifies a subset of human mesenchymal stromal cells with vascular regenerative potential. Stem Cells. 2017 Jun;35(6):1542-53.

Chapter 3:

Dr. Miljan Kuljanin assisted in the isolation of the cell surface proteins from ECFC after FACS purification. He also aided with the protein preparation and analysis by mass spectrometry. Dr. Gilles Lajoie provided mass spectrometry expertise to perform the proteomic analysis. Manuscript for submission:

Sherman SE, Kuljanin M, Lajoie GA, and Hess DA. Characterization of CD34-expressing endothelial colony forming cell subsets during *ex vivo* expansion

Chapter 4:

Anna Kornmuller provided decellularized cartilage foam scaffolds and prepared the collagen-based scaffolds. Dr. Lauren Flynn provided biomaterials expertise and aided in the presentation of some figures for this chapter.

Chapter 5:

Tyler Cooper helped with the staining and quantification of blood vessel density within the ischemic and non-ischemic thigh muscle. Gillian Bell provided assistance with the optimization of the vector blue staining alongside staining for blood vessel density within the ischemic and non-ischemic hind limbs. Manuscript for submission:

Sherman SE, Cooper TT, Bell GI, and Hess DA. Transplantation of endothelial and mesenchymal progenitor cells in decellularized adipose tissue scaffolds for the recovery of acute ischemic injury.

Acknowledgments

I would like to begin with thanking my supervisor Dr. David Hess for giving me the opportunity to work in the lab and for providing continuous support throughout my time in the lab. Dr. Hess’ patience and understanding was instrumental to nurturing my development as a scientist. Allowing me the opportunity to have my own autonomy during experimental design and execution kindled my passion for science and fostered my scientific mindset. Thank you, I would not be able to pursue this dream without you.

I would like to thank Ayesh Seneviratne for training me in the lab and providing me with the initial molecular techniques to begin my career in research. I would also like to thank Tyler Cooper for being the best colleague I could ask for. Our common understanding that science is a lifestyle has enabled many discussions which have changed my perspective in life and in the laboratory. Although working on different projects, we were able to challenge each other which not only accelerated our growth as individuals, but also as scientists. From learning to handle disagreement to identifying bias in one’s approach to science, there have been many invaluable outcomes from our interaction. Although I was surprised to accrue a life-long collaborator early in my scientific career, accruing a good friendship in my graduate career was truly unexpected. To many more years!

I would like to thank the members of my advisory committee: Dr. Zia Khan, Dr. Robert Gros, Dr. Dean Betts, and Dr. Lauren Flynn. The collective insight of my committee pointed out my weaknesses and challenged me to fix my flaws (which I still have many!). Furthermore, our interactions got me back on track when I would get caught up in my projects which I’ve since been able to begin identifying on my own. This skill is something that I feel is invaluable to be an efficient scientist.

I would like to thank the Children’s hospital foundation and OGS for providing funding to subsidize my studies and ultimately allow me to make the next steps in my career.

I would like to thank a good friend of mine, Austin Montgomery for lending me enough money so I could pay tuition through rough times and carry on with my studies without the worry of financial burden holding me back from completing this journey.

Lastly, I would like to thank my partner in crime Dr. Sydney Todorovich and her family for being my support structure when no one else was. Your unwavering support and understanding of my science-related stresses has allowed me to be as efficient as I can be and to push my comfort levels to maximize my growth as a person and as a scientist.

Table of Contents

Abstract i

Co-Authorship Statement iii

Acknowledgments v

Table of Contents vii

List of Tables xiv

List of Figures xv

List of Appendices xix

List of Abbreviations xx

Chapter 1 1

1 Introduction[i] 1

1.1 Vascular disease 1

1.1.1 Atherosclerosis 1

1.1.2 Coronary Artery disease 2

1.1.3 Peripheral artery disease 3

1.2 Vascular biology 4

1.2.1 Blood Vessel anatomy 4

1.2.2 Endothelial cells 5

1.2.3 Pericytes 6

1.2.4 Vascular smooth muscle cells 7

1.2.5 Development of the vascular system 7

1.2.6 Hemangioblasts 8

1.3 Neovascular formation 8

1.3.1 Hypoxic responses 9

1.3.2 Angiogenesis 9

1.3.3 Vasculogenesis 10
1.3.4 Arteriogenesis 11
1.3.5 Pro-angiogenic Cytokines and endothelial cell activation 12
1.3.6 Vessel patterning and Guidance cues. 13
1.3.7 Extracellular matrix remodeling during neovessel formation. 14
1.3.8 Vessel remodeling. 14
1.4 Cell therapy for vascular diseases 17
1.4.1 Stem/progenitor cells 17
1.4.2 Adult endothelial progenitor cells 18
1.4.3 Mesenchymal stromal cells 21
1.4.4 Selecting for cells with high aldehyde dehydrogenase activity 23
1.4.5 Cell free therapies using extracellular vesicles 24
1.5 Decellularized scaffolds 25
1.6 Thesis overview and hypotheses 26
1.6.1 Chapter 2: Objective/Hypothesis 33
1.6.2 Chapter 3: Objectives 33
1.6.3 Chapter 4: Objectives/Hypothesis 34
1.6.4 Chapter 5: Objectives/Hypothesis 34
1.7 References 35
Chapter 2 55
2 High aldehyde dehydrogenase activity identifies a subset of human mesenchymal stromal cells with vascular regenerative potential. 55
2.1 Introduction 56
2.2 Methods 58
2.2.1 Selection of ALDH^{lo} versus ALDH^{hi} MSC subsets 58
2.2.2 Cell surface phenotype analysis 58

2.2.3 *In vitro* differentiation assays 59

2.2.4 Generation of conditioned media (CDM) 59

2.2.5 HMVEC expansion assays 59

2.2.6 HMVEC tubule forming assays 60

2.2.7 Directed *in vivo* angiogenesis assay (DIVAA) 60

2.2.8 Microarray analysis 60

2.2.9 Proteomic analysis of CDM 61

2.2.10 Cytokine arrays 63

2.2.11 Statistical analyses 63

2.3 Results 63

2.3.1 ALDH^{lo} and ALDH^{hi} MSC demonstrated multipotent differentiation potential *in vitro*. 63

2.3.2 CDM generated by ALDH^{lo} or ALDH^{hi} MSC augmented HMVEC expansion *in vitro*. 67

2.3.3 Contact co-culture with ALDH^{lo} or ALDH^{hi} MSC did not promote HMVEC expansion. 70

2.3.4 ALDH^{hi} MSC CDM augmented HMVEC tube formation. 73

2.3.5 ALDH^{hi} MSC augmented EC recruitment into DIVAA inserts. 76

2.3.6 ALDH^{lo} and ALDH^{hi} MSC demonstrated similar mRNA expression. 78

2.3.7 ALDH^{hi} MSC demonstrated a pro-angiogenic secretome. 81

2.4 Discussion 87

2.5 References 89

Chapter 3 93

3 Characterization of CD34-expressing endothelial colony forming cell subsets during ex vivo expansion. 93

3.1 Introduction 94

3.2 Methods 96

3.2.1 Collection and isolation of ECFC. 96

3.2.2 Flow cytometric characterization of ECFC. 97

3.2.3 Cell sorting and colony forming assays. 97

3.2.4 Tube forming assay. 97

3.2.5 Growth kinetics and surface marker kinetics. 97

3.2.6 Preparation of cells for cell surface proteome analysis. 98

3.2.7 Mass spectrometry analysis of cell surface protein expression. 98

3.2.8 Surface marker identification. 99

3.2.9 *In vivo* implantation of purified ECFC in Matrigel. 99

3.3 Results 99

3.3.1 ECFC express hematopoietic progenitor cell markers CD34 and ALDH. 99

3.3.2 Colony forming capacity was increased in CD34$^-$/CXCR4$^-$ ECFC. 104

3.3.3 Tube forming capacity was increased by CD34$^-$ ECFC. 106

3.3.4 CD34-expression on ECFC was increased in confluent culture conditions. 108

3.3.5 CD34-expression was reversible and CD34$^-$ ECFC showed increased growth kinetics. 110

3.3.6 The frequency of CD34$^+$ ECFC remained stable over several passages. 112

3.3.7 ECFC surface proteomics revealed enrichment of known endothelial cell pathways on CD34$^+$ ECFC. 114

3.3.8 Angiotensin converting enzyme expression was enriched on CD34$^+$ ECFC but did not impact colony forming capacity. 117

3.3.9 In vivo transplantation of CD34$^{+/-}$ ECFC subsets in Matrigel enabled the formation of vessel-like structures. 121

3.4 Discussion 125

3.5 References 128

Chapter 4 133

4 Methods for the analysis of cells seeded in matrix-derived bioscaffolds using flow cytometry 133

4.1 Introduction 134

4.2 Methods 136

4.2.1 Human adipose tissue decellularization. 136

4.2.2 Porcine cartilage decellularization. 136

4.2.3 Bovine collagen scaffolds. 137

4.2.4 ECM-derived foam fabrication. 137

4.2.5 Human progenitor cell isolation and culture. 137

4.2.6 Scaffold Seeding. 138

4.2.7 Protease preparation. 138

4.2.8 Determining scaffold autofluorescence. 138

4.2.9 Cell extraction methodologies for flow cytometry. 139

4.2.10 Determining cell viability. 139

4.2.11 Antibody staining. 140

4.2.12 MSC and ECFC co-culture on scaffolds. 140

4.2.13 Statistics. 140

4.3 Results 141

4.3.1 Digested bioscaffolds produce autofluorescent debris that complicate flow cytometric analyses. 141

4.3.2 Scaffold debris obscures cell populations visualized by flow cytometry. 149

4.3.3 TrypLE express^{TM} digestion enabled cell preparation suitable for flow cytometry 152

4.3.4 Cell extraction efficiency was proportional to the length of enzymatic treatment. 155

4.3.5 Cell extraction using a density gradient improved cell purity, yield, and viability. 157

4.3.6 Cell extraction did not impair detection of cell viability or cell surface phenotype. 159

4.4 Discussion 164

4.5 References 166

Chapter 5 169

5 Transplantation of endothelial and mesenchymal progenitor cells in decellularized adipose tissue scaffolds for the recovery of acute ischemic injury. 169

5.1 Introduction 170

5.2 Methods 173

5.2.1 MSC and ECFC isolation and culture. 173

5.2.2 DAT preparation and seeding. 173

5.2.3 Determining cell proliferation and cell surface phenotype via flow cytometry. 174

5.2.4 Femoral artery ligation and transplantation. 175

5.2.5 Measurement of perfusion by laser doppler perfusion imaging. 175

5.2.6 Analysis of hind limb and scaffold tissue by immunofluorescence. 175

5.2.7 Immunohistochemical analysis of human cell engraftment and blood vessel recruitment within DAT foam scaffolds. 176

5.2.8 Statistical analyses. 176

5.3 Results 177

5.3.1 Seeding and culture in DAT scaffolds altered the surface marker expression of ECFC and MSC. 177

5.3.2 ECFC proliferation was diminished during culture with MSC or on DAT scaffolds. 179

5.3.3 Intramuscular injection of ECFC and/or MSC did not improve perfusion in NOD.SCID mice with FAL. 181

5.3.4 ECFC and/or MSC seeded DAT foam scaffolds did not improve perfusion in NOD.SCID mice with FAL. 183

5.3.5 Transplantation of ECFC and/or MSC increase blood vessel density within the ischemic thigh muscle. 185

5.3.6 Human ECFC or MSC engraftment was improved within the DAT scaffolds. 189

5.3.7 The murine cells recruited to the DAT scaffolds were primarily MAC-1+ and took up HLA from the DAT scaffolds. 194

5.3.8 DAT scaffolds contained CD31+ vessel-like structures. 199

5.4 Discussion 201

5.5 References 204

Chapter 6 209

6 Summary and Discussion 209

6.1 Summary of findings 209

6.1.1 Chapter 2 – ALDH^{hi} MSC demonstrate enhanced vascular regenerative potential 210

6.1.2 Chapter 3 – CD34^{+} ECFC have attenuated vascular functions *in vitro*. 212

6.1.3 Chapter 4 – Purification of human cells seeded within decellularized bioscaffolds for analysis by multiparametric flow cytometry. 213

6.1.4 Chapter 5 – ECFC and MSC demonstrate pro-vascular properties *in vivo*. 214

6.2 Clinical significance 218

6.3 Limitations of *in vitro* culture. 220

6.4 Future directions 221

6.5 References 223

Appendices 228

Curriculum Vitae 237

List of Tables

Table 2.1 Parameters for mass spectrometry proteomic analyses. 62

Table 2.2 Differentially expressed mRNAs comparing ALDH^{lo} versus ALDH^{hi} MSC subsets. 80

Table 2.3 Secreted proteins unique to CDM generated by ALDH^{hi} MSC or ALDH^{lo} MSC. 83

Table 2.4 Proteins differentially secreted from ALDH^{hi} versus ALDH^{lo} MSC. 85

Table 3.1 List of gene ontology (GO) terms by DAVID gene enrichment analysis for the CD34^{-} versus CD34^{+} ECFC surface proteomics. 115

Table 3.2 Comparison of the surface proteomics of CD34^{-} versus CD34^{+} ECFC by DAVID gene enrichment analysis. 116

Table 5.1 T-test comparison of CD31^{+} vessel density between the ischemic and normal thigh within treatment groups 35 days post FAL surgery. 188

List of Figures

Figure 1.1 A schematic overview of sprouting angiogenesis. 16

Figure 1.2 Proposed *in vivo* model of revascularization through ECFC and MSC transplantation. 28

Figure 1.3 Schematic of Aldefluor^{TM} staining and subsequent FACS purification of ALDH^{hi} cells. 30

Figure 1.4 Schematic of the *in vivo* transplantation strategies for ECFC and MSC to determine pro-vascular potential 32

Figure 2.1 ALDH^{lo} and ALDH^{hi} MSC subsets expressed stromal and pericyte markers and demonstrated multipotent differentiation *in vitro*. 65

Figure 2.2 Flow cytometric analyses of HMVEC proliferation and survival *in vitro*. 68

Figure 2.3 Conditioned media generated by ALDH^{lo} or ALDH^{hi} MSC stimulated HMVEC expansion *in vitro* 69

Figure 2.4 Contact co-culture with ALDH^{lo} or ALDH^{hi} MSC did not augment HMVEC expansion *in vitro* 71

Figure 2.5 Contact co-culture with HMVEC augmented ALDH^{lo} and ALDH^{hi} MSC expansion *in vitro* 72

Figure 2.6 Conditioned media generated by ALDH^{hi} MSC augmented HMVEC tube formation *in vitro*. 74

Figure 2.7 Implantation of ALDH^{hi} MSC increased endothelial cell invasion into Directed *In Vivo* Angiogenesis Assay (DIVAA) Inserts. 77

Figure 2.8 Global mRNA expression was similar comparing ALDH^{lo} versus ALDH^{hi} MSC subsets. 79

Figure 2.9 Comparison of protein content in conditioned media generated from ALDH^{lo} versus ALDH^{hi} MSC. 84

Figure 2.10 Multiplex-ELISA of conditioned media from ALDH^{lo} versus ALDH^{hi} MSC. 86

Figure 3.1 Cultured UCB ECFC expressed endothelial cell surface antigens and lack the hematopoietic cell surface marker CD45. 101

Figure 3.2 Identification of progenitor cell surface marker expression by flow cytometry. 102

Figure 3.3 ECFC contained intracellular stores of CXCR4. 103

Figure 3.4 ECFC expressing CD34 and CXCR4 exhibit deceased colony formation *in vitro*. 105

Figure 3.5 ECFC expressing CD34 exhibit decreased tube forming capacity *in vitro*. 107

Figure 3.6 ECFC cultured at high density increased CD34 expression and altered ECFC colony and tubule formation *in vitro*. 109

Figure 3.7 CD34-expression increased with endothelial cell density. 111

Figure 3.8 CD34-expression reached a steady state for each cell line. 113

Figure 3.9 Angiotensin converting enzyme co-localized with CD34 expression on ECFC and did not affect the colony forming capacity of ECFC. 118

Figure 3.10 ECFC contain intracellular stores of collagen 13A1 (Col13A1) and tyrosine-protein kinase receptor UFO (AXL). 120

Figure 3.11 ECFC had the capacity to vascularize Matrigel plugs *in vivo*. 122

Figure 3.12 Purified CD34$^{+/-}$ ECFC did not improve vascularization of Matrigel plugs after subcutaneous injection into immunodeficient mice. 123

Figure 4.1 Enzyme digested DAT particles were autofluorescent across the visible spectrum. 143

Figure 4.2 Enzyme digested DCT was autofluorescent across the visible spectrum........... 145

Figure 4.3 Enzyme digested pure bovine collagen was autofluorescent across the visible spectrum. 147

Figure 4.4 Debris particles from digested ECM obscured ECFC detected by flow cytometry. 150

Figure 4.5 Debris particles from digested ECM obscured MSC detected by flow cytometry. 151

Figure 4.6 TrypLE Express^{TM}-treated bioscaffolds produced cell preparations suitable for flow cytometry. 153

Figure 4.7 Cell extraction efficiency is proportional to protease treatment time. 156

Figure 4.8 Cell extraction using Hypaque-Ficoll improved cell purity, yield, and viability. 158

Figure 4.9 Prolonged enzymatic extraction reduced ECFC survival in collagenase-treated bovine collagen bioscaffolds... 160

Figure 4.10 MSC viability was reduced in collagenase-treated bovine collagen bioscaffolds. 162

Figure 4.11 Prolonged enzymatic treatment did alter predicted cell surface antigen detection. 163

Figure 5.1 ECFC and MSC expression of TIE2 and CD105 was altered by culture in DAT foam scaffolds. 178

Figure 5.2 ECFC proliferation was decreased by culture on DAT scaffolds and by co-culture with MSC. 180

Figure 5.3 Intramuscular injection of ECFC and/or MSC did not improve limb perfusion in NOD.SCID mice after FAL. 182

Figure 5.4 Implantation of ECFC and/or MSC seeded into DAT scaffolds did not improve limb perfusion in NOD.SCID mice with FAL. 184

Figure 5.5 Intramuscular injection of ECFC with MSC increased blood vessel density in the ischemic limb of NOD.SCID mice after FAL. 186

Figure 5.6 DAT scaffolds seeded with ECFC and/or MSC improved blood vessel density in the ischemic limb of NOD.SCID mice with FAL. 187

Figure 5.7 Human cell engraftment was rare in the ischemic thigh after scaffold implantation or I.M injection. 190

Figure 5.8 Human cell engraftment was increased in DAT scaffolds at 14 days post-transplantation. 191

Figure 5.9 Human cell detection in the DAT scaffolds at 35 days post-transplantation in MPS type VII NOD.SCID mice. 193

Figure 5.10 Human leukocyte antigen was detected in DAT scaffolds and invading murine cells 14 days post-transplantation. 195

Figure 5.11 Murine cells recruited to DAT scaffolds were primarily MAC-1+ and presented the human-specific marker, HLA. 197

Figure 5.12 DAT scaffolds transplanted at the site of FAL surgery contained CD31+ 200

Figure 6.1 A working model of DAT-seeded ECFC and MSC contribution to revascularization after transplantation in an ischemic hindlimb. 217

List of Appendices

Appendix 1 Permission to reproduce Sherman et al. in Springer eBook............................. 228

Appendix 2 Permission to reproduce Sherman et al. in Stem cells. 230

Appendix 3 Animal use protocol ethics approval... 234

Appendix 4 Human research ethics approval 236

List of Abbreviations

ABC	ATP-binding cassette
ABI	Ankle-brachial index
ACDU	Automated cell deposition unit
ACE	Angiotensin converting enzyme (or CD143)
ADAMTS12	A disintegrin and metalloproteinase with thrombospondin motifs 12
ALDH	Aldehyde dehydrogenase
$ALDH^{hi}$	High aldehyde dehydrogenase activity
$ALDH^{lo}$	Low aldehyde dehydrogenase activity
ALDH1A3	Aldehyde dehydrogenase 1 family member A3
ANGPT 1-4	Angiopoietin (isoforms 1, 2, 3, 4)
ANGPTL3	Angiopoietin-like 3 protein
ARNT	Aryl hydrocarbon nuclear transporter
AXL	AXL receptor tyrosine kinase
BCA	Bicinchoninic acid
bFGF	Basic fibroblast growth factor
BM	Bone marrow
BM-MNC	Bone marrow derived mononuclear cells
BSA	Bovine serum albumin
CAC	Circulating angiogenic cells
CAD	Coronary artery disease
CD	Cluster of differentiation
CDM	Conditioned media
CFU-EC	Colony forming unit endothelial cells
CFU-F	Colony forming units of fibroblasts

CLI	Critical limb ischemia
COL13A1	Collagen 13A1
CVD	Cardiovascular disease
CXCL4	Chemokine (C-X-C motif) ligand 4 (platelet factor-4)
CXCR4	Chemokine (C-X-C motif) receptor 4
DAT	Decellularized adipose tissue
DAPI	4’,6-diamidino-2-phenylindole
DCT	Decellularized cartilage tissue
DDH_2O	Double distilled water
DEAB	Diethylaminobenzaldehyde
DIVAA^{TM}	Directed In Vivo Angiogenesis Assay^{TM}
DLL4	Delta-like ligand 4
DRAQ5	Deep Red Anthraquinone 5
EBM	Endothelial basal media
EC	Endothelial cell
ECFC	Endothelial colony forming ells
ECM	Extracellular matrix
EdU	5-ethynyl-2-deoxyuridine
EGM	Endothelial growth media
ELISA	Enzyme-linked immunosorbent assay
EPC	Endothelial progenitor cells
Eph	Ephrin receptor
Ephrin	Ephrin ligand
FACS	Fluorescence activated cell sorting
FAL	Femoral artery ligation
GRO	Growth related alpha protein (CXCL1)

GVHD	Graft-versus-host disease
HEPES	4-(2-hydroxyethyl)-1-piperazineethanesulfonic acid
HIF	Hypoxia inducible factor
HIFα	Hypoxia inducible factor alpha subunit
HIFβ	Hypoxia inducible factor beta subunit, also known as ARNT
HLA	Human leukocyte antigen
HMVEC	Human microvascular endothelial cells
HPC	Hematopoietic progenitor cell
HPH	HIF-prolyl hydroxylase
ICAM-1	Intracellular adhesion molecule-1
IL	Interleukin
IPSC	Induced pluripotent stem cells
LDPI	Laser Doppler perfusion imaging
MCP-1	Monocyte chemoattractant protein-1
MMP	Matrix metalloproteinases
MNC	Mononuclear cells
MS	Mass spectrometry
MSC	Mesenchymal stromal cells
N-CAD	N-cadherin
NO	Nitric oxide
NOD.SCID	Immunodeficient non-obese, severe-combined immunodeficient
NPN	Neuropilins
PAD	Peripheral artery disease
PBS	Phosphate buffered saline
PDGF	Platelet-derived growth factor
PLAUR	Plasminogen activator, urokinase receptor

RANTES	Regulated upon activation, normal T-cell expressed and secreted
SCL	T cell acute lymphocytic leukemia protein
SDS	Sodium dodecyl sulfate
SDS-PAGE	Sodium dodecyl sulfate polyacrylamide gel electrophoresis
SPB	Sorensen’s phosphate buffer
STZ	Streptozotocin
TACT	Therapeutic angiogenesis by cell transplantation
TBP	Tributyl phosphate
TCP	Tissue culture plastic
TGF-β	Transforming growth factor-β
TIE	Tyrosine kinase with immunoglobulin-like and EGF-like domains
TIMPs	Tissue inhibitors of matrix metalloproteinases
UCB	Umbilical cord blood
VEGF	Vascular endothelial growth factor
VEGF-A-E	Vascular endothelial growth factor (A, B, C, D, E)
VEGFR1-3	Vascular endothelial growth factor receptor (1, 2, 3)
VE-CAD	Vascular endothelial cadherin
vWF	Von Willebrand factor
Wnt5A	Wingless-type MMTV integration site family, member 5A

Chapter 1

1 Introduction[i]

1.1 Vascular disease

According to the American Heart Association, cardiovascular disease (CVD) is broadly defined as a class of diseases which affect the heart or blood vessels. Specifically, CVD includes life-threatening ailments including: heart disease, heart attack, stroke, peripheral artery disease, heart failure, arrhythmia, or heart valve problems. CVD is the leading cause of death worldwide[1] accounting for one in three deaths in North America[2, 3]. In Canada, the cost of CVD to the health care system alone totals more than $22 billion per year[4]. Unfortunately, the etiology of CVD is multi-factorial, influenced by genetic and non-genetic factors and often presenting with comorbidities (i.e. diabetes, obesity, etc.). Regardless, the pathogenesis of CVD is often accelerated by life style choices including: diet, smoking, physical activity, and uncontrolled blood pressure and cholesterol[2, 3]. In regard to hypertension, approximately 23% of the adult population in Canada are hypertensive[5]. As the prevalence of CVD increases, projections estimate that 45.1% of Americans will have some form of CVD by 2035[2], in return increasing health care costs >2-fold[6]. Thus, current research aims on developing effective and novel therapeutic strategies to prevent or to reverse the morbidities of CVD.

1.1.1 Atherosclerosis

Atherosclerosis is a chronic blood vessel disorder characterized by the progressive narrowing of blood vessels through a complex inflammatory process. Chronic inflammation in the vascular endothelium will lead to the formation of fibrous tissues that contain a dense core of lipid and cellular material known as plaques[7, 8].

---

[i] Parts of this chapter have been previously published: **Sherman SE**, Hess DA. Immunogenicity and Immunomodulation of Fetal Stem Cells. In Fetal Stem Cells in Regenerative Medicine 2016 (pp. 57-79). Springer, New York, NY.

The early stages of atherosclerosis begins with the deposition of lipid droplets within the intimal layers of the vasculature in response to a fat-laden environment[9, 10]. Dyslipidemia will promote a pro-inflammatory environment that will alter endothelial cell expression of chemoattractant and adhesion molecules to permit circulating monocytes to invade into the vessel intima[11]. Infiltrating monocytes will rapidly differentiate into macrophages that scavenge extracellular lipids from the interstitium. The accumulation of cytosolic lipids in macrophages will convert these macrophages into foam cells, explained in great detail by Moore *et al.*[12]. As the number of foam cells accumulate in the developing intimal lesion, the plaques present with the earliest visible feature called the ‘fatty streak’[13]. At this stage, the inflammatory signals released by foam cells induce proliferation of smooth muscle cells, thickening the intimal layer and forming a fibrous cap around the foam cells[14, 15]. Foam cells and smooth muscle cells within the lipid core become apoptotic, releasing accumulated cholesterols and lipoproteins, intensifying the pro-inflammatory environment[16]. If efferocytosis is impaired, the inflammatory process is unable to resolve in these early lesions. The accumulation of dead cell bi-products develops into a ‘vulnerable plaque’ whereby invading leukocytes can disrupt the structure of the atherosclerotic plaque[17]. The rupturing of the plaque exposes the thrombotic core to the circulating blood, in return leading to thrombosis formation and vessel occlusion[18]. Thrombotic events have been implicated in >75% of fatal heart attacks in addition to other acute ischemic pathologies such as stroke[19, 20]. The risk factors for developing atherosclerosis include: diabetes, hypertension, smoking, lack of physical activity and dyslipidemia[2, 21].

1.1.2 Coronary Artery disease

Of the atherosclerotic-related diseases, coronary artery disease (CAD) remains one of the most deadly forms of heart disease accounting for 1 in 6 deaths in the United States[22]. CAD is characterized by the blockage of the major vessels surrounding the heart due to atherosclerotic plaque buildup. Typically, CAD progression will lead to myocardial infarction and eventual heart failure where the mortality rate is approximately 60% within 5 years of diagnosis[23]. Treatment options for CAD have been progressively improving since the use of coronary artery bypass surgery[24] including the use of anti-platelet therapies[25] and exercise[26]. Unfortunately, for patients with late stage progressive heart failure, treatment options are limited to highly invasive procedures such as heart transplantation or ventricular assist devices[27]. Although the rates of diagnosis have been steadily increasing, mortality rates have been decreasing for several decades [28, 29]. The development of cell-based therapies for CAD is still in its infancy but holds promise for the CVD field[30].

1.1.3 Peripheral artery disease

Peripheral artery disease (PAD) is a disease of the circulatory system characterized by ischemia in the lower extremities due to a partial or complete occlusion of blood vessels with chronic atherosclerotic plaque accumulation. Clinically, PAD is defined as an ankle-brachial index (ABI) ≤ 0.9, with or without pain during moderate exercise. In Canada, approximately 800,000 individuals are affected by PAD with more than 8.5 million Americans suffering from PAD[2, 31, 32]. With a lack of public awareness of PAD[33] and as many as 40% of PAD patients being symptom free, many cases go undiagnosed[32, 34-36]. Unfortunately, as the severity of atherosclerosis increases, an individual's risk for life-threatening cardiovascular complications will increase 6-fold[31]. The current treatment for PAD include pharmacological therapies to minimize clotting, smoking cessation, surgical intervention, and/or exercise programs[37, 38]. When left untreated, ischemia in the lower extremity will become so severe that the patients will experience severe resting pain, non-healing ulcers, and increased risk of infection in the ischemic limb. This is known as critical limb ischemia (CLI), the most severe form of PAD[39]. Current statistics indicate that 30% of patients within one year of diagnosis will require limb amputation and greater than 60% of patients will have died from cardiovascular complications within 5 years of diagnosis[40]. Unfortunately, patients with CLI often exhibit co-morbidities such as diabetes which impairs endothelial cell functions, accelerating disease progression and symptomatology[41]. Stimulation of angiogenesis through pharmacological targets, gene therapy, or cellular therapy are under investigation to prevent amputations and prolong patient lifespan[38]. The development of cellular therapies for CLI is a central theme within this thesis.

1.2 Vascular biology

Blood vessels are dynamic structures whose primary function is to direct blood flow throughout the body and mediate the exchange of gases, nutrients and waste to maintain homeostasis. Blood vessels are organized in a hierarchical structure with few blood vessels of larger diameter and many small, microscopic vessels[42]. The vascular plexus begins with the arteries that mediate the transport of oxygenated blood which will branch into smaller vessels known as arterioles. Upon further branching, the arterioles will become capillaries which are the smallest functional unit of the vascular system where the erythrocytes release oxygen and gain carbon dioxide. The capillary system will anastomose to form venules which carry deoxygenated blood. Venules will continue to anastomose into larger veins which deliver the deoxygenated blood back to the heart[43]. Systemically, the larger vessels support the movement of large volumes of blood and deal with higher blood pressures required to deliver blood to the tissues and return to the heart[44]. In contrast, the primary function of the smaller blood vessels is to mediate the exchange of nutrients and wastes at the cellular level to maintain organ homeostasis[45].

Lastly, the final component to the vascular system is the lymphatic vessels. Like the vascular plexus, the lymphatic system is organized in a hierarchical structure of few large ducts with many capillaries. Contrary to the vascular system, the lymphatic system promotes a one-way flow of lymphatic fluid (interstitial fluid) towards the heart. Lymph is exchanged from the blood capillaries to the lymphatic capillaries. Like blood capillaries, the capillaries of the lymphatic system anastomose into larger collecting vessels. Collecting vessels then pass through lymph nodes and drain into larger trunks which ultimately drain into ducts which returns the lymph to the blood stream[46].

1.2.1 Blood Vessel anatomy

Arteries (0.1-10mm diameter) are composed of three layers which enable these vessels to withstand the high blood pressures from the heart. The outermost layer is called the Tunica externa and is primarily comprised of elastic fibers which provide elasticity and support to the vessel. The Tunica media is a layer of smooth muscle cells which lies adjacent to the Tunica externa and is separated from the Tunica intima by a basement membrane. The Tunica intima is the innermost layer of the artery which is comprised of a layer of continuous endothelial cells which interface with the blood[47].

Like arteries, arterioles (100-300 µm diameter) can also be divided into the three segments: Tunica externa, media, and intima. Arterioles differ from arteries in their tunica externa and media thicknesses which give arterioles a smaller diameter than arteries. Like arteries, arterioles are lined with a continuous endothelial layer[48, 49].

Capillaries are the smallest units of the vasculature system and are comprised of only a single layer of endothelial cells which interact with pericytes. The architecture of the endothelial cells in capillaries is usually continuous but can be fenestrated to mediate specific functions within different organs[50-52].

Venules interface with the capillaries to bring deoxygenated blood back to the heart. These vessels are similar to arterioles except these vessels contain microscopic valves to prevent the backflow of blood due to the low blood pressures after travel through the capillaries[53].

Veins are large blood vessels which bring blood back to the heart. Like arteries, arterioles, and venules, veins contain three vessel layers: Tunica externa, media, and intima. Veins differ from arteries in their relatively thin structures and large diameter lumens. Veins also contain valves to prevent the backflow of blood as it travels to the heart[47].

1.2.2 Endothelial cells

Endothelial cells are the functional units of blood vessels and are the cells that are responsible for lining blood vessels and directly interacting with the blood. Endothelial cells are highly specialized and must function in a tissue-specific manner to ensure optimal performance of each organ system. The tissue-specific phenotype of endothelial cells is determined by tissue interactions via cell-contact mechanisms as well as paracrine signaling[54, 55]. For example, the phenotypic differences observed between the blood brain barrier endothelium and the endothelium within somatic tissue is due to tissue signaling of the local microenvironment[56]. Furthermore, the permeability and dilation of vessels is a complex, multifactorial process which is tightly controlled by endothelial cells exposed to specific physical and chemical cues[57]. For example, endothelial cells exposed to shear stress will produce nitric oxide synthase[58] which has vasodilatory effects as well as cardio-protective effects and down-stream chemotactic properties for mesenchymal stromal cells[59].

In healthy tissues, endothelial cells in blood vessels are typically quiescent and have slow cell turnover rates. Cellular quiescence and survival is primarily mediated by the delicate balance of maintenance and survival cues such as vascular endothelial growth factor (VEGF), basic fibroblast growth factor (bFGF), angiopoietin (ANGPT), and NOTCH signaling[60, 61]. When endothelial cells are exposed to higher levels of these signals, this will initiate endothelial cell migration and proliferation to form new vasculature in a process called angiogenesis[62]. Importantly, endothelial cells are also crucial in mediating inflammatory responses by up-regulating cell surface proteins to promote thrombosis and to promote extravasation of immune cells into damaged tissues[63, 64].

1.2.3 Pericytes

The vascular structure depends on two main cell types: endothelial cells, and perivascular cells. In the vasculature, these cell types interact with one another in a complex and delicate balance between growth, survival, regression and death [65]. Perivascular cells, or pericytes, wrap around the endothelial cells that make up blood vessels and provide structural support as well as cellular communication through direct contact and perivascular mechanisms. More importantly, pericytes also play a key role in the regulation of vessel formation during angiogenesis[66]. In mature vessels, pericytes interact with endothelial cells through platelet-derived growth factor (PDGF) to promote vessel stability and quiescence[67]. Although closely associated with endothelial cells, pericytes do not express common endothelial markers such as CD31, CD44, or von Willebrand factor (vWF). These $CD146^+$ $CD31^-$ cells can be isolated from almost every human adult and fetal tissue including the umbilical cord and placenta[68]. Pericytes have also been thought to reside on a phenotype continuum which includes vascular smooth muscle cells and mesenchymal stromal cells (MSC)[67, 68].

1.2.4 Vascular smooth muscle cells

Vascular smooth muscle cells (vSMC) are specialized cells which reside within the Tunica media of larger blood vessels and help to regulate vessel integrity and tone. A primary role for vSMC is to regulate conductance of blood flow through vasomotor responses. Specifically, the vasomotor responses within vasculature involves contraction or relaxation of vSMC to control blood conductance by constricting or dilating blood vessels, respectively[69]. The ability for vSMC to contract or relax is tightly controlled by the balance of depolarizing and hyperpolarizing currents generated by ion channels on the plasma membrane[70, 71]. These electrical responses within arterial structures are capable of propagating across the length of vessels through gap junctional connections of coupled vSMC. The conduction of vasomotor responses is not observed in the venous circulation[72]. The initiation of the vasomotor response is driven by endothelial cells responding to physical and chemical signals in the blood. In response to these circulating stimuli, endothelial cells release factors such as nitric oxide and endothelin-1 directly on vSMC to modulate vessel tone[73, 74]. In healthy tissues, vascular smooth muscle cells proliferate at extremely low rates and express contractile proteins to control blood flow distribution[14]. The differentiation and regulation of cell function and phenotype is tightly controlled by the microenvironment and is dependent on the interactions with endothelial cells[75]. In disease conditions such as atherosclerosis, vascular smooth muscle cells exhibit a phenotype switch which causes the cells to become proliferative and may promote the formation of the fibrotic cap[14].

1.2.5 Development of the vascular system

The cardiovascular system is the first organ system to begin its function during embryogenesis. The development of circulation is required to develop and maturate all the other organ systems during development[76]. Development of the vasculature begins by the formation of blood islands within the mesodermal layer of the developing yolk sac[77]. The outer cells of the blood island then give rise to Angioblasts through a common hematopoietic/endothelial cell precursor known as the hemangioblast[78, 79]. Angioblasts then begin to migrate outward and assemble into vascular structures through a process known as vasculogenesis. The proliferation and migration of angioblasts inevitably give rise to a labyrinth of small capillaries known as the primary vascular plexus through VEGF signaling mechanisms[76, 80]. Once the primary vascular plexus is formed from angioblast proliferation and migration, endothelial cells begin to sprout from preexisting capillaries in response to VEGF released from developing organs[81]. During these processes, the primitive heart pushes blood through these early vascular networks which begin to specialize endothelial cells to adopting an arterial or venous identity[82]. The development of arterial and venous identities are tightly controlled by multiple signaling mechanisms crucial to establish and mantain functional vascular system[83]. Through angiogenesis, endothelial cells continue to populate developing organs and subsequently maturate[80].

1.2.6 Hemangioblasts

The concept of a common ancestor between hematopoietic and endothelial cell lineages began with the observations of the close developmental proximity of hematopoietic and endothelial cell development alongside several shared features such as surface phenotype and transcriptional programs[84]. Subsequent studies indicated that there in fact was a common cell type that gave rise to both hematopoietic and endothelial cells which was termed the hemangioblast[85]. During development, the earliest distinguishing phenotype of the hemangioblast is vascular endothelial growth factor receptor 2 (VEGFR2), the primary receptor for VEGF-A[80]. Hemangioblasts have also been demonstrated to require T cell acute lymphocytic leukemia protein (SCL) for development[86]. Hemangioblasts have been demonstrated to populate both the blood islands and the aortic floor during cardiac development[79, 85]. Although controversial, accumulating evidence suggests the existence of the hemangioblast persisting into adulthood[87].

1.3 Neovascular formation

Neovessel formation in adult organisms can occur in two possible ways: angiogenesis or vasculogenesis. Angiogenesis is thought to occur by activation of vessel-resident endothelial cells that become primed to respond to regions of hypoxia through local secretion of pro-angiogenic factors. After activation, the endothelial cells begin proliferating to direct the formation of the new vessel towards the site of ischemia[88]. If stable perfusion is established in the neovessels, perivascular cells will stabilize this new blood vessel network and the endothelial cells will become quiescent [65, 89]. Vasculogenesis, on the other hand, is the formation of new blood vessels by means of circulating endothelial progenitor cells (EPC). Circulating EPC are capable of spontaneously forming tubules *in vitro* and have been shown to directly incorporate into newly forming blood vessels *in vivo* [90, 91].

1.3.1 Hypoxic responses

Cellular responses to a lack of oxygen are crucial to promoting neovessel formation in the embryo and in the adult. The primary signaling pathway that mediates these responses is the hypoxia inducible factor (HIF) pathway. HIF-1 is a basic helix-loop-helix transcription factor which is the primary mediator for transcription of VEGF and other hypoxia-inducible genes[92, 93]. HIF-1 can only bind to DNA and promote transcription as a heterodimer containing an alpha subunit (HIFα) and a beta subunit (HIFβ or aryl hydrocarbon nuclear transporter; ARNT)[94]. Under normal oxygen conditions, HIF-prolyl hydroxylase (HPH) uses oxygen as a co-substrate to ubiquitinate HIF-1α and target it for degradation in the proteasome[95]. During hypoxia, HIF-1α is stabilized by the lack of ubiquitination by HPH which enables dimerization with HIFβ and subsequent localization to the nucleus. Once activated, the HIF pathway targets many genes that control angiogenesis, cell metabolism, vascular tone, and even erythropoiesis[96]. Lastly, the hypoxic response is heavily involved in many pathologic manifestations such as: cancer, wound healing, PAD, sleep apnea, and pulmonary arterial hypertension, making it an attractive target for many therapies[97].

1.3.2 Angiogenesis

The formation of new blood vessels form pre-existing vasculature is termed angiogenesis. Angiogenesis is a complex, multi-step process which is mediated through the delicate balance of signaling proteins to maintain endothelial cell quiescence or proliferation and migration[62]. Angiogenesis can be divided into two main groups: intussusceptive or sprouting angiogenesis[98, 99].

Intussusceptive angiogenesis is characterized by the splitting of pre-existing vessels to form daughter vessels, a phenomena first observed in the rat lung during a developmental process called microvascular maturation[100]. The act of vessel intussusception requires the formation of an intraluminal pillar within the blood vessel to induce splitting. The formation of pillars is thought to occur rapidly without requiring endothelial cell proliferation, expertly reviewed by Burri *et al*.[101]. Intussusceptive angiogenesis has been found in various organs of the body and is thought to be mediated through ANGPT signaling to increase vessel density in maturing organs[102-104].

Sprouting angiogenesis is a more involved process compared to intussusceptive angiogenesis beginning with the tissue response to hypoxia and subsequent release of angiogenic factors such as bFGF, VEGF, and ANGPT [92]. These factors will activate endothelial cells to remodel the vascular structure and surrounding ECM. Endothelial cell proliferation drives the migration of the sprouting vessel to revascularize the hypoxic tissues[99]. Although endothelial cells are the primary driver for sprouting angiogenesis, many hematopoietic cell types contribute to facilitate capillary formation and aid in the joining of migrating endothelial tip cells[105-107].

1.3.3 Vasculogenesis

During development, the differentiation of lateral plate mesoderm to form angioblasts marks the beginning of vasculogenesis. Briefly defined, vasculogenesis is the de-novo formation of blood vessels from endothelial precursors or progenitor cells[76, 82]. After the vascular plexus is formed by the VEGFR2$^+$ (hem)angioblasts, vasculogenesis is primarily replaced by angiogenesis to produce the blood vessels of the developing organism[108]. Although a short-lived process, experimental evidence to demonstrate post-natal vasculogenesis is now abundant.

The conceptualization of postnatal vasculogenesis began with pre-clinical studies involving the use of cytokines and growth factors to promote neovascularization in patients with CLI. In these initial studies, VEGF expression declined with age and in disease states which suggested the need for progenitor cell types to replenish these “exhausted” tissues[109]. Because hematopoietic and endothelial precursors share a common progenitor during development, the observations of hematopoietic stem cells persisting in the adult led Asahara to purify putative endothelial progenitor cells (EPC) using the hematopoietic progenitor cell marker, CD34[110]. The resulting putative EPC isolated from human blood demonstrated endothelial-like properties *in vitro*. After transplantation of the CD34+ peripheral blood mononuclear cells (MNC) into mice that underwent femoral artery ligation (FAL) surgery, the human cells engrafting in the mouse vasculature co-expressed CD31. This seminal work established the field of postnatal EPC biology which has been instrumental in understanding endothelial cell biology.

1.3.4 Arteriogenesis

During the development of the vascular system, the formation of high-resistance, low flow vasculature known as “collateral vessels” enables the vascular system to compensate in times of high flow or vessel blockage. The primary utility of collateral vessels is to undergo a morphogenic process into large-conductance arteries in a process known as arteriogenesis[111]. When blood flow is blocked in large vessels, the collateral vasculature morphologically changes to accommodate the high blood flow and act as a bi-pass mechanism, protecting from ischemia[112, 113]. Contrary to neo-vessel formation, the induction of arteriogenesis is not regulated by hypoxia[114]. The initiation of arteriogenesis is caused by an increase in blood volume passing through collateral vessels, thereby increasing the shear stress on these vessels. The increase in shear stress mechanically influences endothelial cell transcription through the opening of chloride channels and phosphorylation of focal adhesions. As a result, endothelial cells within collateral vessels begin to express monocyte chemoattractant protein-1 (MCP-1) and intracellular adhesion molecule-1 (ICAM-1), primarily attracting monocytes from the circulation[115, 116]. Concurrently, shear stress induces nitric oxide (NO) and PDGF release from endothelial cells causing vasodilation to accommodate blood flow and attracting pericytes and vascular smooth muscle cells to stabilize the vessel[117]. Collectively, the recruitment of circulating monocytes, pericytes, and vascular smooth muscle cells facilitates the remodeling of the vessel structure to form a functional, high-conductance artery[115, 117, 118].

1.3.5 Pro-angiogenic Cytokines and endothelial cell activation

1.3.5.1 VEGF and NOTCH

The VEGF and NOTCH signaling pathways are one of the most studied pathways in endothelial cell biology. The VEGF protein family which contains members (VEGF-A through to VEGF-E) that signal through tyrosine receptor kinases: VEGFR1, VEGFR2, and VEGFR3[119]. VEGF exerts pleiotropic effects on endothelial cells where low levels of VEGF signaling promotes cell survival and quiescence. On the other hand, high levels of VEGF signaling activates endothelial cells for angiogenesis[89]. In a normal physiological state, pericytes provide low levels of VEGF to endothelial cells to promote quiescence. However, endothelial cells will activate upon exposure to higher concentrations of VEGF released from hypoxic tissues, marking the beginning of angiogenesis. Activated endothelial cells begin by loosening tight junctions and secreting matrix metalloproteinases (MMP) to break free from the basement membrane shared by pericytes[120]. Subsequently, endothelial cells will migrate towards the VEGF signals. Notably, the endothelial cell with the highest VEGF exposure will become a “tip cell”. Endothelial tip cells guide the growing vessel towards the angiogenic stimuli through many extended filopodia which sense the environment as the vessel grows[121, 122].

During the phenotypic change into a tip cell, the expression of the NOTCH ligand, delta-like 4 (DLL4) is upregulated. NOTCH is a evolutionarily conserved, contact-dependent signaling pathway which is involved in cell fate decisions such as proliferation, apoptosis and differentiation [82, 123]. The primary function of NOTCH/DLL4 signaling during angiogenesis is to regulate endothelial tip cell formation. The NOTCH signaling pathway will prevent tip cell formation through the down-regulation of VEGF receptors on signal receiving cells, acting as a counterbalance to VEGF signaling[124]. Thus, with the heightened expression of DLL4 on tip cells, the adjacent endothelial cells will decrease VEGFR2 and become less likely to become a tip cell in a process called lateral inhibition[120, 125]. The endothelial cells adjacent to the tip cell then become “stalk” cells which drive vessel elongation through proliferation[89, 123, 125, 126]. Once the sprouting vessel invades the hypoxic tissues, macrophages have been demonstrated to facilitate the joining of incoming vessels to complete the circuit before blood flow can be re-established[106, 127].

1.3.5.2 Angiopoietin

The angiopoietins are a well-studied endothelial-specific growth factor family which contain 4 isoforms (ANGPT 1-4) all capable of binding to the receptor tyrosine kinase with immunoglobulin and epidermal growth factor homology domain (TIE-2)[119]. The major isoforms involved in endothelial cell functions is ANGPT1 and ANGPT2. Interestingly, both ANGPT-1&2 can bind to TIE 2 but ANGPT-1 is the only ligand capable of phosphorylating TIE-2. ANGPT-2 has been implicated in providing antagonistic functions to ANGPT-1[128]. ANGPT-1 signaling is also thought to be context dependent and can act to promote vessel growth on mobilized endothelial cells[62]. Largely, ANGPT-1 signaling promotes endothelial cell quiescence, basement membrane deposition, and further stabilizes pericyte interactions[129]. Upon activation, endothelial tip cells will secrete ANGPT-2 to antagonize TIE-2 signaling and promote pericyte detachment, further destabilizing the vessel[130, 131].

1.3.6 Vessel patterning and Guidance cues.

Ephrin signaling plays an important role in several developmental processes and are a major player in the regulation of tissue patterning and axon/blood vessel guidance. Like NOTCH signaling, ephrin receptors (Eph) and ligands (Ephrin) are membrane-bound and require cell-contact to signal[126, 132]. Ephrin signaling is also bi-directional, meaning that ligand-expressing cells can signal through ligand-receptor interactions[133, 134]. Eph4, is found on cells of the venous circulation whereas EphrinB2, the ligand for Eph4, marks cells of the arterial circulation. It is thought that the expression of Eph4 and EphrinB2 are primarily to maintain arterial and venous identity[62, 82, 135]. Ephrin’s bi-directional signaling cascades have been implicated in vessel wall assembly with pericytes and vascular smooth muscle cells expressing EphrinB2[136]. Ephrins have also been implicated in promoting vessel sprouting and migration of activated endothelial cells[137].

Semaphorins are a large family of soluble guidance signals that all share a 500 amino acid sema domain[138]. Semaphorins play a crucial role in the regulation of blood vessel and axon growth in development and in adult tissues. There are 2 main receptor types which bind semaphorins and initiate intracellular signaling: the Plexin family and Neuropilins (NPN). The primary function of semaphorin-signaling through plexin receptors is to reduce cell adhesion through destabilization of the actin cytoskeleton. Neuropilins on the other hand, are thought to modify the growth cone of migrating cells[126, 139]. Collectively, semaphorins are largely implicated with repulsive cues during sprouting angiogenesis. However, semaphorins can elicit a repulsive or attractive signal to cells depending on protein kinase G activity within the cell[140].

1.3.7 Extracellular matrix remodeling during neovessel formation.

Once endothelial cells become activated, the basement membrane common to endothelial cells and pericytes must be degraded to enable vessel sprouting (angiogenesis) or remodeling (arteriogenesis)[141]. To perform this function, endothelial cells secrete matrix metalloproteinases (MMPs), a family of endopeptidases involved in extracellular matrix (ECM) remodeling processes[142]. Endothelial cells secrete various MMPs which may be regulated by the tissue microenvironment[143]. To ensure that matrix remodeling does not occur in excess, tissue inhibitors of matrix metalloproteinases (TIMPs) are secreted to limit ECM degradation by MMPs[144]. Thus, proper angiogenesis depends on a fine balance between MMP and TIMP activities where too little MMP activity will prevent angiogenic sprouting and too much activity will prevent the formation of stable vasculature[145]. Lastly, an important feature of MMP-mediated ECM remodeling is through the release of pro-angiogenic factors sequestered in the ECM to further promote angiogenesis and tip cell migration[146].

1.3.8 Vessel remodeling.

After angiogenic sprouts invade the hypoxic tissues, there are many connections made between different sprouts but also dead ends which failed to form a circuit to the systemic circulation. The resulting microvasculature in these sites of angiogenesis are randomly oriented and chaotic, creating turbid and inefficient blood flow[104, 147]. These new vessels also lack pericyte stabilization and thus, are poorly perfused and leaky[148]. Therefore, vessel maturation and remodeling of the newly developed vascular tree to select for efficient vessels needs to occur.

Vessel maturation is primarily mediated through endothelial cell secretion of PDGF which is responsible for recruiting pericytes to wrap and stabilize vessels [149]. Additionally, ANGPT-1 and transforming growth factor-β (TGF-β) are secreted by endothelial cells to promote pericyte-endothelial cell binding[89, 150]. Finally, the pericyte-endothelial interactions promote matrix deposition to form a common basement membrane at the interface between the two cell populations. Up-regulation of N-cadherin (N-CAD) and vascular endothelial cadherin (VE-CAD) stabilizes cell-cell interactions within the vessel to minimize leakiness[149].

Remodeling of the chaotic vascular network through the pruning of inefficient vascular connections is regulated by multiple mechanisms. First, the secretion of pro-angiogenic factors will decrease as the newly invading vasculature will provide the hypoxic tissues with oxygen. As vascularization of the tissues reaches a maximum, the lack of pro-angiogenic signals will halt further vessel sprouting[151, 152]. Concurrently, the release of anti-angiogenic factors will counteract the survival signals from the pro-angiogenic factors, promoting vessel regression[153]. Next, the vessels that have made efficient connections will experience adequate sheer stress, acting as a pro-survival signal in endothelial cells. The vessels which carry the least blood flow will undergo apoptosis due to a lack of sheer stress and nutrients[154]. After the tissues reach an optimal partial pressure of oxygen, the process of vessel regression and maturation is concluded which marks the end of the angiogenic process (overviewed in Figure 1.1).

Figure 1.1

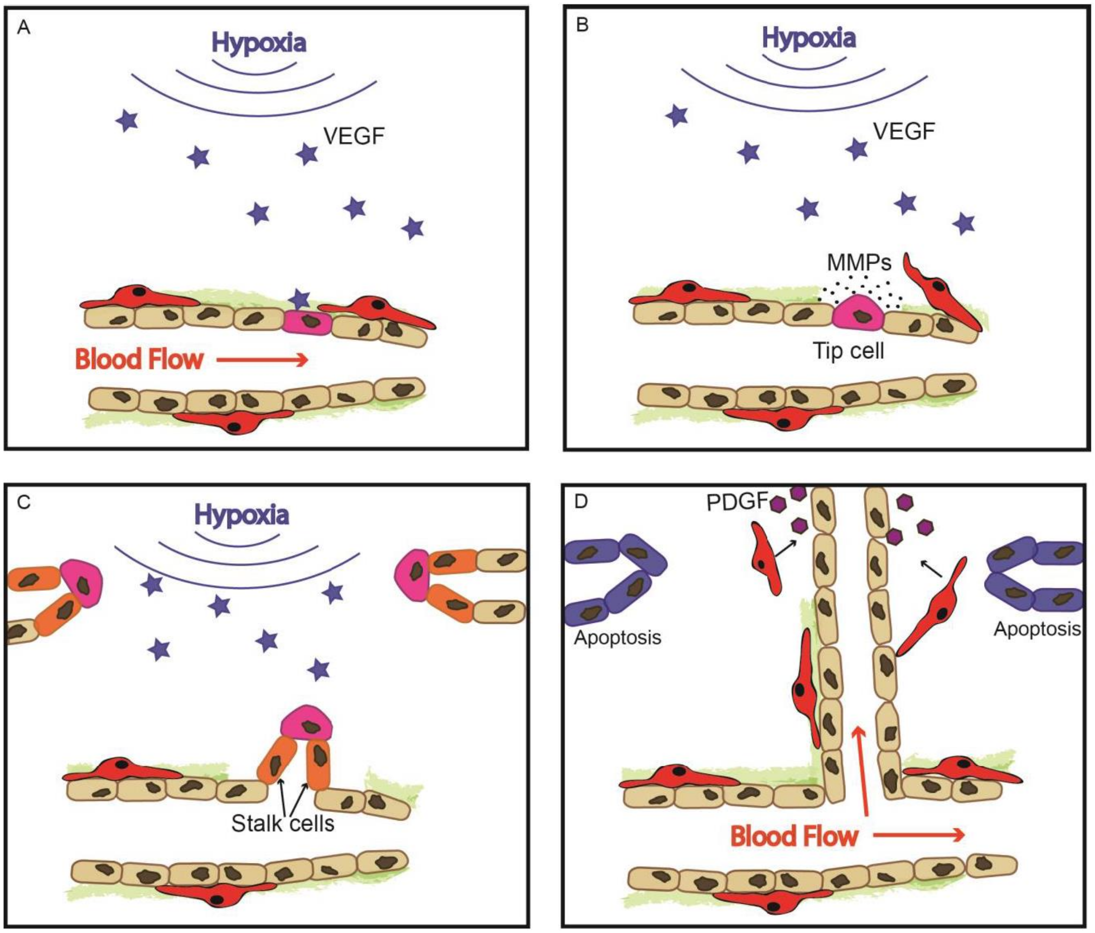

Figure 1.1. A schematic overview of sprouting angiogenesis. (A) Hypoxic tissues up-regulate the secretion of pro-angiogenic factors (i.e. VEGF) through activation of the HIF pathway. The pro-angiogenic factors will diffuse through tissues and activate endothelial cells of surrounding blood vessels. (B) VEGF signaling will activate endothelial cells to secrete ANGPT-2 and MMPs to degrade the basement membrane and detach pericytes that are stabilizing the blood vessel. (C) The endothelial cell experiencing the most VEGF signaling will become the tip cell and begin to migrate towards the source of hypoxia. Tip cells promote the formation of stalk cells by decreasing VEGFR2 expression through lateral inhibition (NOTCH/DLL4 signaling). Proliferation of the stalk cells will drive the migration of the vessel towards hypoxic signals. (D) After forming a blood vessel circuit at the source of hypoxia, endothelial cells will secrete PDGF to recruit pericytes to the newly formed vessels. Blood flow kinetics and vessel stabilization through pericyte interactions will enable vessel maturation and protect against diminished pro-survival signals in the microenvironment. Subsequently, the inefficient vessels are regressed or 'pruned' through apoptotic mechanisms.

1.4 Cell therapy for vascular diseases

The focus of many emerging clinical therapies for patients suffering from CVD is to promote angiogenesis to revascularize damaged or diseased tissues. Many of the clinical trials for cellular therapies have involved direct injection of bone marrow derived mononuclear cells (BM-MNC), a heterogeneous cell population which contains hematopoietic, endothelial, and mesenchymal cell lineages that directly and indirectly aid in neovessel formation. For example, the therapeutic angiogenesis by cell transplantation (TACT) trial was able to demonstrate efficacy in patients with CLI by improving ankle brachial pressure index as well as tissue oxygen saturation through transplantation of BM-MNC[155]. In a follow-up study to the TACT trial, there was significant improvement in pain scale, walking time as well as improvements in ulcer healing after 2 years post-transplantation[156]. The potential for cellular therapeutics is a field of research that is thoroughly being explored for various diseases from cancer to CVD[157, 158].

1.4.1 Stem/progenitor cells

The field of stem cell biology began with seminal experiments by James Till and Ernest McCulloch to identify a cell type in the mouse bone marrow which could engraft and form colonies in the spleen after whole-body irradiation[159]. Subsequently, two crucial observations eventually lead to the widely accepted definition of a stem cell: The ability for a cell to self-renew and the ability to differentiate[160]. Stem cells are also defined by their potency or their ability to give rise to specialized tissue types. Stem cell potency is arranged in a hierarchy beginning with totipotent stem cells: a cell type that can give rise to all the tissues of an organism including the extra-embryonic tissues[161]. Stem cells that are only able to differentiate into the 3 germ layers of the embryo proper are termed pluripotent. Multipotency refers to the ability for a cell to differentiate into multiple different cell types within a given germ layer. For example, Mesenchymal stromal cell (MSC) differentiation into bone, cartilage, and adipose tissues within the mesenchymal germ line. Unipotency refers to the ability for a cell to differentiate into a specific tissue type while the bottom of the hierarchy contains mature cells with minimal proliferative capacity[162].

More recently, the discovery of induced pluripotent stem cells (iPSC) has enabled the production of pluripotent stem cells from mature, somatic cells. The seminal work of Takahashi and Yamanaka led to the discovery of 4 transcription factors capable of converting mouse or human fibroblasts into pluripotent cells[163, 164]. This discovery was instrumental in progressing the stem cell field by providing an alternative method to derive a pluripotent human cell type instead of using human embryonic stem cells (hESC). Likewise, iPSC have provided the capacity to model genetic diseases in a dish which has great potential to develop effective clinical treatments[165].

Importantly, tissue-resident stem/progenitor cells can be found in tissues throughout adult organisms. These cells are responsible for the maintenance of tissues throughout the lifespan of the organism[166]. In many cases of disease, tissue-resident stem/progenitor cells are overwhelmed by the severity of damage or unable to compensate properly for the burden of disease and fail to repair or replace damaged tissues. For example, in patients with CLI, the endothelial progenitor cells do not respond adequately to tissue ischemia[167, 168]. The lack of progenitor cell response is due to a concept referred to as stem cell exhaustion. With increased age or prolonged chronic disease states such as type 2 diabetes, the regenerative function of the tissue-resident stem/progenitor cells can be gradually diminished[169, 170]. Thus, the use of stem cells in clinical therapies to aid in tissue replacement or repair is an attractive option to maximize therapeutic outcomes. Discussed below are two leading progenitor cell types that hold promise for cellular therapies to treat vascular-related diseases through the replacement of vasculature.

1.4.2 Adult endothelial progenitor cells

The field of postnatal vasculogenesis began with the seminal discovery of $CD34^+$ peripheral blood mononuclear cells (MNC) that could incorporate into sites of ischemia and promote vascularization after transplantation[110]. This was the first demonstration of the existence of a circulating EPC population within adult blood. This work lead to the subsequent isolation of “EPC” from human bone marrow blood sources and propagation *ex vivo*. Three distinct culture techniques emerged, producing three different resulting cell populations termed: (1) colony forming unit – endothelial cells (CFU-EC)[110, 171], (2) circulating angiogenic cells (CAC)[167, 172, 173], and (3) endothelial colony forming cells

(ECFC)[174-176]. Two main variables where these isolation techniques diverge is the culture of adherent versus the non-adherent cells of the MNC fraction, and the length of time before colonies emerge. The technique used to isolate CFU-EC involves the depletion of the adherent cells on fibronectin where the non-adherent cells are subsequently collected and cultured. Cell colonies from this technique formed within 4-7 days and are also known as early outgrowth endothelial cells[110, 171, 177]. The isolation of CAC involves the seeding of MNC on fibronectin where the non-adherent cells are removed after 3 days in culture and the adherent, early outgrowth cells are then formed within 10 days after plating[167, 172, 173]. Lastly, the final technique involves the culture of the adherent MNC on collagen until late outgrowth colonies form (approximately 14 days), termed outgrowth endothelial cells or endothelial colony forming cells (ECFC)[174-176, 178].

It has since become established that CFU-EC are comprised mainly of hematopoietic cells[91, 172]. Similarly, CAC are a hematopoietic population composed primarily of monocytes/macrophages which display endothelial-like characteristics, inducible with endothelial growth factors[179-181]. Methodologically, CACs are closest to ECFC. The difference between the CAC and ECFC preparations is that ECFC gets established after 14 days in culture whereas CAC are established and used less than 10 days in culture. Thus, the CAC population most likely contains ECFC, but the culture technique used to isolate CAC does not allow ECFC to establish before the 14-day point. Interestingly, other groups have demonstrated that established monocytes from blood-derived MNC begin to die off in the first 2-3 weeks of culture[174, 177]. Therefore, it appears that monocytes dominate the early CAC culture and the ECFC begin to establish and become selected for as monocytes decline in number. By later passages, expression of hematopoietic cell surface markers is diminished, and the cultures are largely endothelial in nature[177, 182].

In summary, it appears that culture techniques selecting for the non-adherent cell fraction of MNC from blood sources yield pro-angiogenic hematopoietic cells in culture. However, if the adherent cell fraction is used, this population is largely comprised of monocytes/macrophages with a minority population of endothelial cells. At this point, if the cultures are taken out past 14 days in endothelial cell-specific culture media, then

ECFC are selected for. Although there has been controversy surrounding the culture and identification of true EPC; the fact remains that putative endothelial progenitor cell content in peripheral blood MNC is used as clinical diagnostic to indicate cardiovascular disease risk[171] and potential recovery[183] in patients with cardiovascular complications.

Despite being fairly well established that many "EPC" cultures are largely contaminated with hematopoietic cells, there continues to be confusing nomenclature whereby proangiogenic hematopoietic cells are referred to as EPC[184]. For example, the use of the term early EPC – early outgrowth EPC – versus late EPC – ECFC – adds confusion as the early EPC are hematopoietic cells with pro-angiogenic capacity with the capability to become endothelial-like[177, 185]. Another large contributor of the controversies surrounding the defining criteria of EPC is the promiscuity of both hematopoietic and endothelial cell surface markers. For example, the isolation and differentiation of monocytes into endothelial cells[186] is controversial as the CD14 antigen, largely used for purification of monocytes, is expressed on various other cell types, including endothelial cells[187]. Experiments aiming to differentiate MNC into endothelial cells depends on having pure starting cell populations which is confounded by deposition of cell surface markers by platelet microparticles [188].

A trademark indication of endothelial cell function is the ability to incorporate into the vasculature. Thus, heterogeneous cell populations can be deemed endothelial in nature when one of the cell types incorporate into vasculature[181]. The isolation of $CD34^+$ MNC has been demonstrated to produce a heterogeneous population of endothelial and hematopoietic cells depending on the isolation and propagation techniques[110, 189]. Macrophages are also pivotal in the generation of new blood vessels by the recruitment of proangiogenic cell types as well as moderating the physical interaction between endothelial cells during sprouting angiogenesis [106]. Because of the potential interchangeability of cell surface markers and cell-cell interactions between cells of the monocyte lineage and endothelial cells, defining a true EPC population remains a challenge.

1.4.3 Mesenchymal stromal cells

In the 1970s, Alexander Friedenstein and colleagues were the first to identify clonogenic, plastic adherent cells from murine bone marrow termed colony forming units of fibroblasts (CFU-F). These cells differentiated into multiple mesodermal cell types including osteocytes, chondrocytes and adipocytes, but did not contribute to hematopoietic tissue[190, 191]. Soon after, similar cells from adult human bone marrow were characterized (reviewed in[192]) and were shown to engraft multiple human tissues (mesenchymal and non-mesenchymal) after systemic infusion. Multiple tissues within the human body, including both fetal and adult sources, have been shown to contain mesodermal precursors capable of differentiating into cartilage, bone, adipose, and muscle tissue[193-195]. In subsequent studies these cells were given many names including marrow stromal stem cells or more accurately mesenchymal stromal cells (MSC) based on their diverse differentiative potential. In 1991, Arnold Caplan coined the term mesenchymal stem cells to describe these cells, highlighting their developmental origin and considerable therapeutic potential[196]. These different nomenclatures have been highly debated in the field because not all bones are derived from embryonic mesenchymal tissue, and the self-renewal capacity of MSC remains highly disputed[197, 198].

In addition to the supportive role of fibroblasts in human tissues, MSC are thought to play an instructive role in a paracrine fashion to aid in the repair and regeneration of organs, and in the modulation of the immune system at sites of tissue injury[199-202]. MSC have been shown to exert their effects via both soluble factors and direct cell-cell contact, demonstrating their ability to ameliorate autoimmune disease conditions through anti-inflammatory mediators and to support regenerative processes[203-205]. However, MSC from various adult sources, including human bone marrow, have been shown to possess considerable variability in the degree of immunosuppression and in the secretion of regenerative factors depending on the health status of the individual from which the cells are obtained[206]. Because of this tissue-specific heterogeneity, preclinical research has focused on the regenerative prowess and immunomodulatory capacity of MSC isolated from tissues of early ontogeny that are untouched by chronic disease pathologies[207].

Despite establishment of unifying standards[208], MSC-like populations of variable purity demonstrate significant heterogeneity in cell surface marker expression when isolated from different tissue sources. Unfortunately, little progress has been made in identifying uniquely-expressed cell surface markers *in situ* as a way to prospectively purify MSC from human sources. Unlike hematopoietic precursors, the MSC field has yet to develop an accepted means of isolating MSC from tissues using cell-surface markers or enzymatic progenitor functions. Recently, the isolation of a perivascular associated MSC subset (also known as pericytes) has been demonstrated using melanoma cell adhesion molecule or CD146 expressed *in situ* and to varying degrees during *ex vivo* culture[68]. In culture these perivascular MSC, which are depleted of CD34-expressing endothelial cells, meet the minimal criteria to define MSC by cell surface marker expression and trilineage differentiative capacity. Notably, CD146+ MSC can be isolated from both adult and placental tissues at varying frequencies. Likewise, the nerve growth factor receptor (CD271) may represent another cell-surface marker expressed on MSC with active immunomodulatory properties[209]. Whether or not these markers can be used interchangeably to purify MSC from umbilical cord of placental tissues remains a topic of debate. Perhaps the most consistent method to purify both adult and perinatal-derived MSC is through the conservation of known progenitor cell functions. One such function is aldehyde dehydrogenase activity (ALDH), a cytosolic enzyme highly expressed in precursors from multiple lineages that protects essential, or long-lived cells against oxidative environmental insults. High ALDH activity (ALDH^{hi}) has been demonstrated as a conserved function in primitive cells from hematopoietic, mesenchymal, endothelial, and neural progenitor lineages[210]. Indeed, human adult BM ALDH^{hi} cells form CFU-F at a frequency of 1 colony in approximately 1500 cells. By using ALDH function, either before or after MSC expansion, we can prospective enrich for progenitor cells higher in the MSC hierarchy, thereby reducing variability between samples and unwanted heterogeneity as cells are expanded *ex vivo*.

The isolation of MSC from adult, fetal or perinatal sources is accomplished through very similar procedures. To obtain a single cell suspension from fetal tissues such as the fetal liver, the tissues are homogenized and strained through a filter[211]. Umbilical cord blood-derived MSC has been isolated from the umbilical vein using similar protocols as BM

MSC[212] but require the addition of collagenase prior to release adherent cells *in situ*[213]. Once the cells are in single cell suspension, mononuclear cells are separated through density gradient centrifugation and plated for selection via plastic adherence. While fetal tissues contain a higher frequency of MSC relative to adult sources[211], the major disadvantage to fetal stem cells becoming a viable source of MSC is that there remains ethical controversy regarding the accrual of cells from pre-natal sources. These ethical barriers delay the use of fetal stem cells for widespread therapeutic purposes. However, umbilical cord and placental-derived MSC are ethically obtained at birth from normally discarded material and can be propagated efficiently for therapeutic application.

The first clinical trial aimed at supporting hematopoiesis used autologous MSC during myeloablative therapies for breast cancer and demonstrated the ability to safely transplant MSC free from side effects or adverse reactions[214]. As MSC became recognized for their immunomodulatory properties, MSC became ideal candidates for treating the hematopoietic transplantation-induced complication graft-versus-host disease (GVHD). Clinical studies have demonstrated that infusion of allogeneic or autologous MSC increased survival rates in steroid-resistant GVHD patients without MSC-related toxicity or ectopic tissue formation[215-217]. Other trials have also been conducted using MSC to treat Crohn's disease-related fistulas, resulting in improved fistula recovery post-surgery and increased quality of life for the patients[218, 219]. Type I diabetes is another autoimmune disease where MSC therapy currently holds promise. MSC have been shown to increase beta cell mass in the injured pancreas of STZ-treated mice allowing for partial restoration of blood glucose levels[220, 221]. Alongside endogenous regeneration, MSC may help to inhibit the autoimmune response towards beta cells, making it a very attractive option as a cellular therapy for type I diabetes[222]. With a focus on MSC, companies such as Osiris Therapeutics are currently performing larger-scale clinical trials to combat autoimmune and inflammatory diseases including cell-based implants for diabetes.

1.4.4 Selecting for cells with high aldehyde dehydrogenase activity

In search to purify progenitor cell populations from the bone marrow, we have previously used a clinically applicable fluorescent probe (Aldefluor™) to isolate cells based on a conserved, functional enzyme known as ALDH[223]. ALDH is a cytosolic enzyme highly expressed in progenitor cells from multiple lineages that protects essential, or long-lived cells against oxidative environmental insults. In general, as progenitor cell differentiation occurs towards a more restricted and expendable phenotype, ALDH-activity reduces. Our group has previously demonstrated that ALDH^{hi} human hematopoietic cells display enhanced hematopoietic re-constitution when transplanted into irradiated, immunodeficient non-obese, severe-combined immunodeficient (NOD.SCID) mice[224, 225]. There have also been clinical trials to demonstrate the efficacy of transplanting ALDH^{hi} BM-MNC in patients with intermittent claudication[226]. Although the ALDH^{hi} fraction of human BM-MNC represents less than 0.8% of the total cell population, this ALDH^{hi} fraction of BM-MNC is enriched for hematopoietic, endothelial, and mesenchymal progenitors. When isolating BM-derived ALDH^{hi} cells, the MSC population is greatly enriched and form CFU-F at a frequency of 1 colony in 1500 cells relative to 1 in 150,000 cells, the common yield of CFU-F in standard isolation procedures[210].

1.4.5 Cell free therapies using extracellular vesicles

Cellular signaling mechanisms include the secretion of protein signals to elicit a variety of effects from chemotaxis to controlling cellular survival and differentiation. Many of these processes are mediated through the cellular release of various cytokines, chemokines and other effectors. A vital form of cellular communication and a quickly emerging field is the study of extracellular vesicles (EVs). Broadly, extracellular vesicles are defined as membraneous bodies released by cells which enable the exchange and communication of intracellular components[227]. EVs can be further broken down into more defined cellular products: Apoptotic bodies, microparticles and exosomes[228]. These different classes of EVs are largely defined by their size; for example, Apoptotic bodies range from 50-5000 nm, Microparticles range from 100-1000nm, and exosomes range from 30-100 nm[229, 230]. EVs have been observed within many bodily tissues such as saliva, blood, synovial fluid, urine etc. and thus have been an attractive target as biomarkers for diseases ranging from cancer to cardiovascular disease[231, 232]. Studies throughout the literature point to the idea that secreted products from cells may have therapeutic benefit[233]. For example, recent work from the Hess lab has demonstrated that conditioned media generated from MSC rapidly reduced hyperglycemia in diabetic mice induced by streptozotocin[234]. Although many factors have been identified to potentiate these regenerative effects, the localization of these proteins within conditioned media is under intense investigation. Conditioned media generated from endothelial cells has been demonstrated to contain EVs which harbor miRNA which has been demonstrated to modulate immune responses during atherosclerosis[235]. Overall, EVs and other secreted products may prove beneficial as cell-free therapeutic agents and potentially even drug delivery vectors[236].

1.5 Decellularized scaffolds

The application of biomaterials in regenerative medicine is a promising treatment modality in many injury or disease conditions requiring tissue repair and/or replacement. A biomaterial represents a bio-compatible material that can integrate into tissues and may provide biological activity after transplantation[237]. Decellularized scaffolds are a subset of biomaterials which provide a substrate for tissues to grow or can be used as a vector for cell delivery strategies. Decellularized bioscaffolds represent the intact, insoluble ECM components of tissues which are devoid of immunogenic cellular material[238]. The major constituents of ECM include evolutionarily conserved proteins: Collagens, proteoglycans, glycoproteins, and other secreted, matrix-associated proteins[239]. These components of ECM lack immunogenicity and have proven safe after transplantation in clinical trials[240, 241]. Because decellularized bioscaffolds resemble native tissue, the host response is minimized by the mechanical behavior, biochemical composition, and tissue ultrastructure of the bioscaffold[242]. Decellularized bioscaffolds also encourage cell-ECM interactions which mediate intracellular signaling cascades to promote cell implantation and survival[243, 244]. Decellularized scaffolds also contain embedded growth factors to aid in cellular processes during the natural remodeling process[245]. Lastly, decellularized scaffolds have demonstrated the ability to re-model and degrade within tissues after exerting their regenerative effect, removing the concern that foreign scaffold materials will remain within the patient [246]. Collectively, the combination of conserved ECM signals and 3-D architecture of decellularized bioscaffolds provide an attractive means to promote the survival and engraftment of transplanted cells[247].

Decellularized bioscaffolds have been utilized in many pre-clinical trials to aid in revascularization therapies for patients with CVD. Many studies have focused on utilizing various scaffold-based platforms to promote revascularization and repair of cardiac tissue after myocardial infarction [248, 249]. Several scaffold-based transplantation strategies have focused on the use of synthetic bioengineered materials for vascular repair. The use of synthetic materials for vascular-related therapies have been documented to increase vessel calcification, atherosclerosis, or result in the formation of excess scar tissue[250, 251]. Alternatively, the use of naturally-derived scaffold materials have been an attractive modality to encourage soft tissue repair and revascularization of ischemic tissues[252, 253]. In a mouse model of hind limb ischemia, ECM-based matrices were demonstrated to recruit circulating progenitor cells to the ischemic muscle and elicit a pro-angiogenic effect[254]. Similarly, decellularized adipose tissue (DAT) is an abundant ECM source which has been implicated to augment soft tissue reconstruction[255]. Without modifying the chemical structure of the ECM, additional processing steps have been developed to generate alternative DAT scaffold formats tailored for specific applications[256]. Lastly, DAT scaffolds have been demonstrated to establish a pro-regenerative and pro-angiogenic microenvironment after transplantation in animal models of adipose tissue regeneration or cutaneous wound repair[257, 258].

1.6 Thesis overview and hypotheses

Patients with atherosclerosis-induced CLI will exhibit decreased pro-vascular cell functions and thus will be less responsive to pro-angiogenic therapies or autologous cell transplantation[168, 169]. ECFC have been demonstrated to be a robust and proliferative endothelial cell type capable of revascularization after transplantation. Similarly, MSC can be readily obtained from allogeneic sources, expanded efficiently in cultures, and are able to support angiogenesis while demonstrating very low immunogenicity[259]. Because of the complementarity between endothelial and mesenchymal cell types, ECFC and

MSC represent an attractive means to promote vascularization in patients with CLI[260, 261]. During the course of my thesis, I focused on the development of a cell-based revascularization therapy using ECFC and MSC in a xenotransplanation model of hind limb ischemia. Furthermore, we also included a decellularized adipose tissue (DAT) scaffold construct to augment cellular engraftment and investigate if the pro-vascular potential of these cells was affected (Figure 1.2).

Figure 1.2

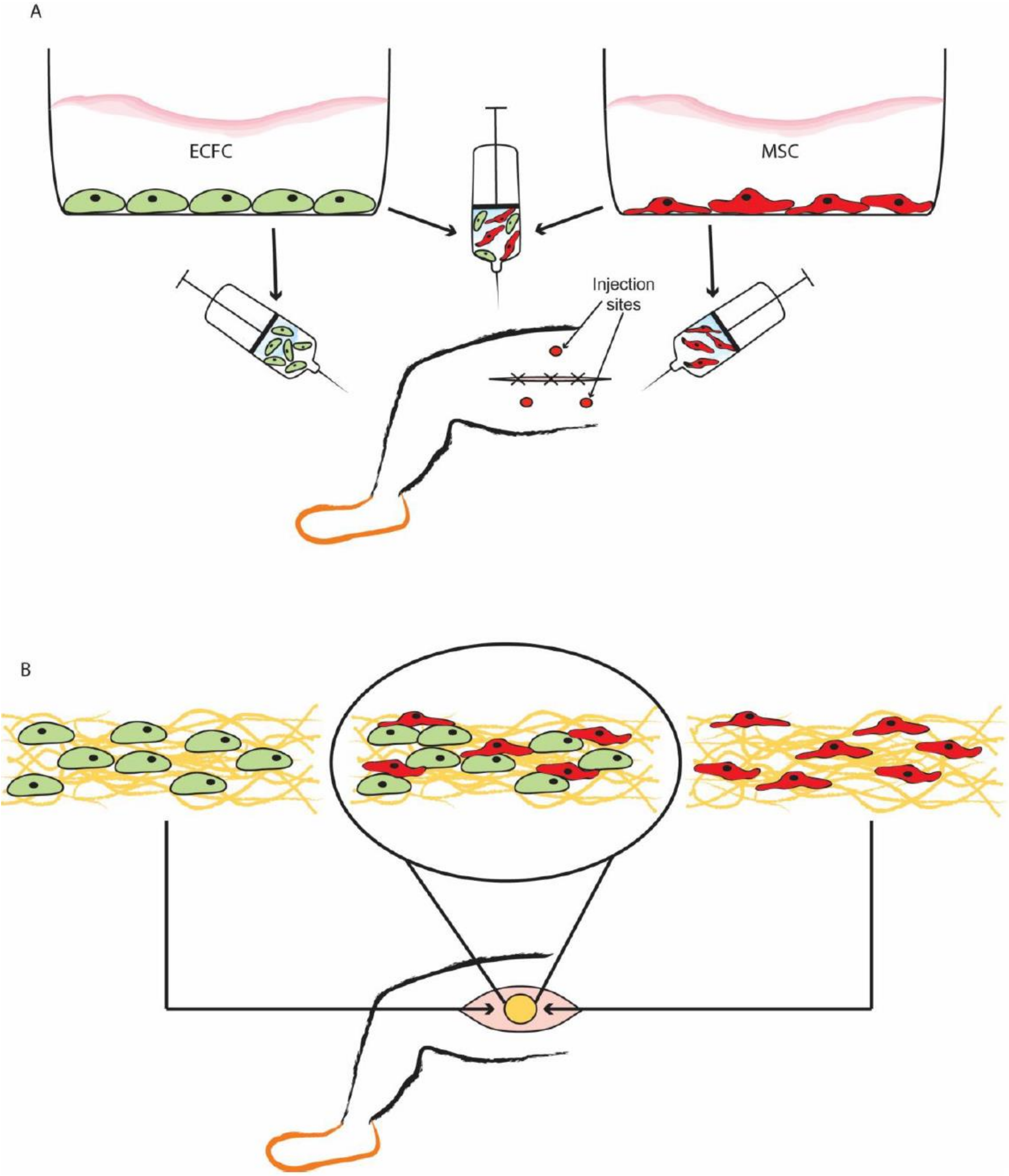

Figure 1.2. Proposed *in vivo* model of revascularization through ECFC and MSC transplantation. After femoral artery ligation surgery on NOD.SCID mice, (A) ECFC and/or MSC were injected into the hindlimb of the mouse at 3 different sites surrounding the surgical incision. Alternatively, (B) ECFC and/or MSC were seeded into decellularized adipose tissue scaffolds prior to transplantation. Scaffolds were directly implanted at the surgical site before the incision was closed.

As MSC exhibit prolonged culture, we have previously demonstrated that MSC can lose their regenerative capacity, suggesting that these cells become more heterogeneous during prolonged culture[221]. We have also previously demonstrated the use of ALDH activity to purify progenitor cells from umbilical cord blood with potent pro-angiogenic activities[262]. Thus, *we hypothesized that using ALDH activity as a selection factor within the ECFC and MSC cell populations would purify a pro-vascular cellular subset.* Herein, I also focused on the purification of progenitor cell types from the ECFC and MSC lineages using Aldefluor^{TM} (Figure 1.3). To validate the improved ability for ECFC to form vasculature and the MSC to recruit vasculature after purification, each cell type was loaded in a basement membrane extract and subcutaneously transplanted in a NOD.SCID mouse (Figure 1.4). *The overarching hypothesis of my thesis is that both ECFC and MSC will contain rare progenitor cell populations identifiable in culture which will exhibit enhanced pro-vascular activities in vivo.* The specific objectives of my studies are described below.

Figure 1.3

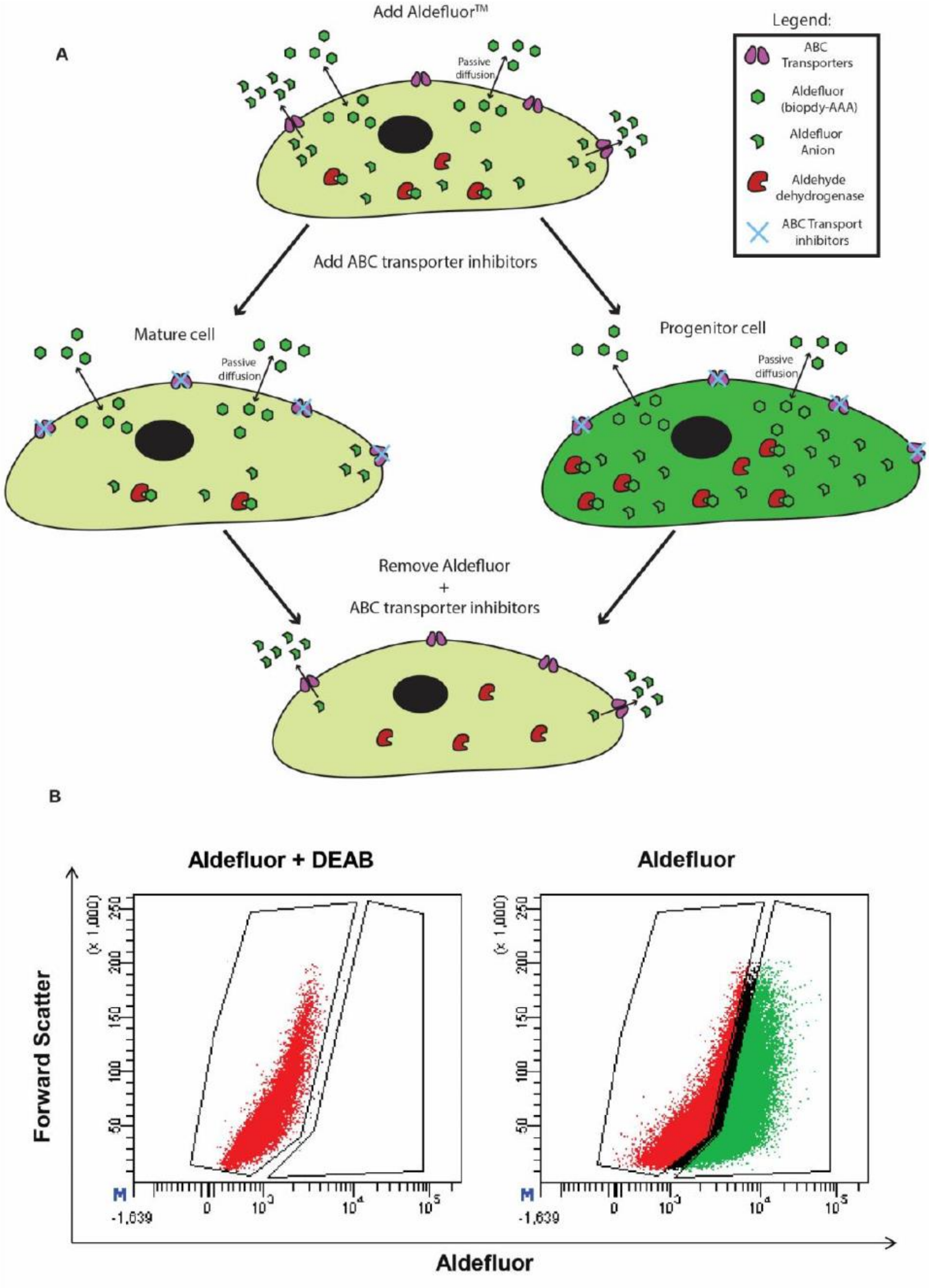
A
Add Aldefluor™
Legend:
ABC Transporters
Aldefluor (biopdy-AAA)
Aldefluor Anion
Aldehyde dehydrogenase
ABC Transport inhibitors
Passive diffusion
Add ABC transporter inhibitors
Mature cell
Progenitor cell
Passive diffusion
Passive diffusion
Remove Aldefluor
+
ABC transporter inhibitors
B
Aldefluor + DEAB
Aldefluor
Forward Scatter
(x 1,000)
250
200
150
100
50
M
-1,639
0
10³
10⁴
10⁵
Aldefluor

Figure 1.3. Schematic of Aldefluor^{TM} staining and subsequent FACS purification of ALDH^{hi} cells.

(A) Aldefluor^{TM} passively diffuses into the cell where it is converted to a fluorescent anion through the enzymatic activity of ALDH. In this state, the anion can only leave the cell through active transport of ABC transporters on the plasma membrane. Adding ABC transport inhibitors will allow the accumulation of fluorescent signal in progenitor cells with high ALDH activity (ALDH^{hi}). Removal of the ABC transporter inhibitors allows complete efflux of the ALDH dye, underscoring the clinical applicability of the Aldefluor^{TM} dye. (B) ALDH activity is subsequently measured via flow cytometry, an ALDH inhibitor, DEAB, is added to establish an ALDH^{lo} threshold. By utilizing the Aldefluor^{TM} stain, cells can be efficiently sorted by fluorescence activated cell sorting and the dye can be effluxed thereafter making this methodology clinically applicable. Because ALDH is an intracellular enzyme, no other staining methodologies exist that maintain cell viability.

Figure 1.4

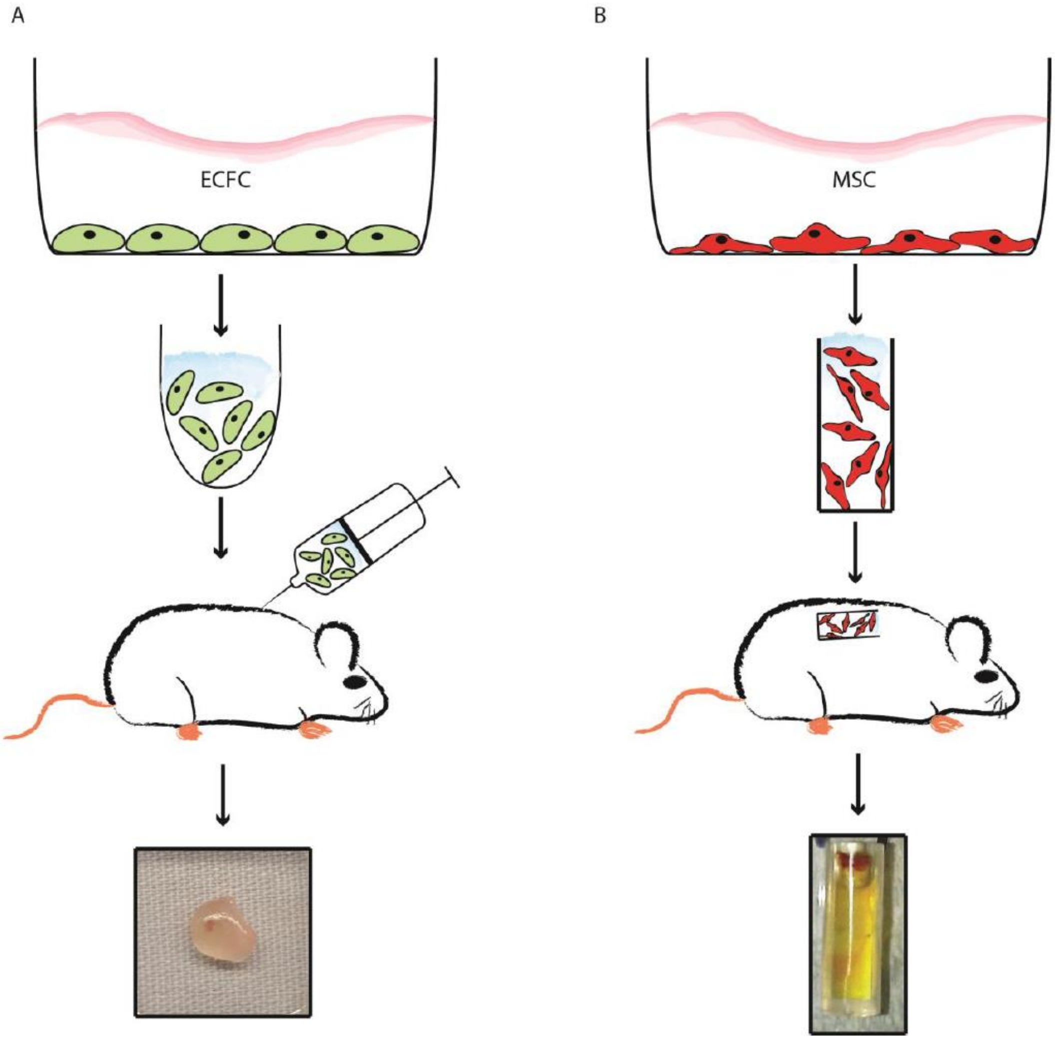

Figure 1.4. Schematic of the *in vivo* transplantation strategies for ECFC and MSC to determine pro-vascular potential. (A) ECFC and (B) MSC were established and cultured on tissue culture plastic before purification using fluorescence activated cell sorting (FACS). ECFC were subsequently suspended in a Matrigel (a basement membrane extract; composed of basement membrane and ECM proteins) and injected into the flank of NOD.SCID mice. MSC were suspended in a basement membrane extract (proprietary) and loaded into 'angioreactors' before subcutaneous implantation. ECFC and MSC were incubated <10 days when the Matrigel plugs and angioreactors were removed from the mice for subsequent analysis.

1.6.1 Chapter 2: Objective/Hypothesis

1. To compare ALDH^{lo} versus ALDH^{hi} MSC subsets for cell surface marker expression, differentiative capacity, mRNA expression profiles, and cytokine secretion.
2. To assess whether endothelial cell growth and tubule formation is augmented by conditioned media or direct co-culture with ALDH^{lo} versus ALDH^{hi} MSC subsets.
3. To determine the vasculogenic capacity of ALDH^{lo} versus ALDH^{hi} MSC subsets after subcutaneous implantation of DIVAA implants into immunodeficient mice.

In chapter 2, *I hypothesized that BM-derived MSC that retained high ALDH activity during ex vivo expansion will demonstrate enhanced pro-angiogenic factor secretion, will promote endothelial cell proliferation and tube forming function in vitro, and will promote vascularization of subcutaneously transplanted membrane extracts in immunodeficient mice*.

1.6.2 Chapter 3: Objectives

1. Ascertain the frequency of common progenitor cell markers on ECFC using flow cytometry and identify other potential surface markers to identify endothelial progenitor cells.
2. Assess colony forming capacity, tube formation, and growth kinetics of progenitor marker-positive ECFC.
3. Determine the capacity for progenitor marker-positive ECFC to incorporate into form blood vessel networks in Matrigel after subcutaneous transplantation into NOD.SCID mice.

In chapter 3, *I hypothesized that umbilical cord blood-derived ECFC will contain a primitive cell subset with enhanced progenitor cell functions in vitro and enhanced vessel forming function in vivo.*

1.6.3 Chapter 4: Objectives/Hypothesis

1. Determine the autofluorescent properties of decellularized adipose and cartilage scaffold materials.
2. Determine the enzymatic digestion methodology to maximize cell yield and cell viability of ECFC and MSC seeded in decellularized adipose and cartilage scaffolds.

** This chapter is focused around the development of a methodology to enable the flow cytometric analysis of cell populations that have been seeded on decellularized scaffold materials in the following chapter.

In chapter 4, *I hypothesized that treatment of decellularized scaffolds with collagenase-containing proteases would effectively digest the scaffold materials leaving both the ECFC or MSC in suspension suitable for flow cytometry*.

1.6.4 Chapter 5: Objectives/Hypothesis

1. Determine phenotypic or functional changes in the ECFC and MSC when cultured in the DAT foam scaffolds.
2. Assess the pro-angiogenic properties of the DAT foam scaffold, the human MSC, and ECFC after transplantation into femoral artery ligated NOD/SCID mice.
3. Determine if the DAT scaffold augments human cell engraftment and overall vascularization of the scaffold 35 days post transplantation.

In chapter 5, *I hypothesized that human ECFC and MSC will create functional vasculature, increase limb perfusion, and have enhanced engraftment capacity when transplanted in decellularized adipose tissue scaffolds in immunodeficient mice with femoral artery ligation.*

1.7 References

1. Mendis, S., P. Puska, and B. Norrving, *Global atlas on cardiovascular disease prevention and control*. 2011: World Health Organization.
2. Benjamin, E.J., et al., *Heart Disease and Stroke Statistics&#x2014;2018 Update: A Report From the American Heart Association.* Circulation, 2018. **137**(12): p. e67-e492.
3. Wilkins, E., et al., *European cardiovascular disease statistics 2017.* 2017.
4. Smolderen, K.G., et al., *One-year costs associated with cardiovascular disease in Canada: insights from the REduction of Atherothrombosis for Continued Health (REACH) registry.* 2010. **26**(8): p. e297-e305.
5. Padwal, R.S., et al., *Epidemiology of hypertension in Canada: an update.* 2016. **32**(5): p. 687-694.
6. Khavjou, O., D. Phelps, and A. Leib, *Projections of cardiovascular disease prevalence and costs: 2015–2035.* Dallas: American Heart Association, 2016.
7. Ross, R., *Atherosclerosis—an inflammatory disease.* New England journal of medicine, 1999. **340**(2): p. 115-126.
8. Stoll, G. and M. Bendszus, *Inflammation and atherosclerosis: novel insights into plaque formation and destabilization.* Stroke, 2006. **37**(7): p. 1923-1932.
9. Smith, E.B., *The relationship between plasma and tissue lipids in human atherosclerosis*, in *Advances in lipid research*. 1974, Elsevier. p. 1-49.
10. Guyton, J., et al., *Extracellular lipid deposition in atherosclerosis.* European heart journal, 1990. **11**(suppl_E): p. 20-28.
11. Mestas, J. and K. Ley, *Monocyte-endothelial cell interactions in the development of atherosclerosis.* Trends in cardiovascular medicine, 2008. **18**(6): p. 228-232.
12. Moore, K.J. and I. Tabas, *Macrophages in the pathogenesis of atherosclerosis.* Cell, 2011. **145**(3): p. 341-355.
13. Stary, H.C., et al., *A definition of advanced types of atherosclerotic lesions and a histological classification of atherosclerosis: a report from the Committee on Vascular Lesions of the Council on Arteriosclerosis, American Heart Association.* Circulation, 1995. **92**(5): p. 1355-1374.
14. Gomez, D. and G.K. Owens, *Smooth muscle cell phenotypic switching in atherosclerosis.* Cardiovascular research, 2012. **95**(2): p. 156-164.

15. Schwartz, S.M., R. Virmani, and M.E. Rosenfeld, *The good smooth muscle cells in atherosclerosis.* Current atherosclerosis reports, 2000. **2**(5): p. 422-429.

16. Geng, Y.-J. and P. Libby, *Evidence for apoptosis in advanced human atheroma. Colocalization with interleukin-1 beta-converting enzyme.* The American journal of pathology, 1995. **147**(2): p. 251.

17. Tabas, I., *Macrophage death and defective inflammation resolution in atherosclerosis.* Nature Reviews Immunology, 2010. **10**(1): p. 36.

18. Schaar, J.A., et al., *Terminology for high-risk and vulnerable coronary artery plaques.* European heart journal, 2004. **25**(12): p. 1077-1082.

19. Falk, E., *Pathogenesis of atherosclerosis.* Journal of the American College of Cardiology, 2006. **47**(8 Supplement): p. C7-C12.

20. Bekwelem, W., et al., *Carotid Atherosclerosis and stroke in atrial fibrillation: the Atherosclerosis Risk in Communities study.* Stroke, 2016. **47**(6): p. 1643-1646.

21. Association, A.D., *8. Cardiovascular disease and risk management.* Diabetes care, 2016. **39**(Supplement 1): p. S60-S71.

22. Go, A.S., et al., *Heart disease and stroke statistics—2014 update: a report from the American Heart Association.* Circulation, 2013: p. 01. cir. 0000441139.02102. 80.

23. McMurray, J.J. and S. Stewart, *Epidemiology, aetiology, and prognosis of heart failure.* Heart, 2000. **83**(5): p. 596-602.

24. Killip, T., E. Passamani, and K. Davis, *Coronary artery surgery study (CASS): a randomized trial of coronary bypass surgery. Eight years follow-up and survival in patients with reduced ejection fraction.* Circulation, 1985. **72**(6 Pt 2): p. V102-9.

25. Dans, A.L., et al., *Concomitant use of antiplatelet therapy with dabigatran or warfarin in the Randomized Evaluation of Long-Term Anticoagulation Therapy (RE-LY) trial.* Circulation, 2013. **127**(5): p. 634-640.

26. Hambrecht, R., et al., *Effect of exercise on coronary endothelial function in patients with coronary artery disease.* New England Journal of Medicine, 2000. **342**(7): p. 454-460.

27. Stokes, M., P. Bergin, and D. McGiffin, *Role of long-term mechanical circulatory support in patients with advanced heart failure.* Internal medicine journal, 2016. **46**(5): p. 530-540.

28. Rosamond, W.D., et al., *Trends in the incidence of myocardial infarction and in mortality due to coronary heart disease, 1987 to 1994.* New England Journal of Medicine, 1998. **339**(13): p. 861-867.

29. Sanchis-Gomar, F., et al., *Epidemiology of coronary heart disease and acute coronary syndrome.* Annals of translational medicine, 2016. **4**(13).

30. Braunwald, E., *The war against heart failure: the Lancet lecture.* The Lancet, 2015. **385**(9970): p. 812-824.

31. Makowsky, M., et al., *Prevalence and treatment patterns of lower extremity peripheral arterial disease among patients at risk in ambulatory health settings.* Can J Cardiol, 2011. **27**(3): p. 389 e11-8.

32. Lovell, M., et al., *Peripheral arterial disease: Lack of awareness in Canada.* Canadian Journal of Cardiology, 2009. **25**(1): p. 39-45.

33. Cronin, C., et al., *Peripheral artery disease: a marked lack of awareness in Ireland.* European Journal of Vascular and Endovascular Surgery, 2015. **49**(5): p. 556-562.

34. Hirsch, A.T., et al., <*Peripheral arterial disease detection, awareness and treatment in primary care.pdf*>. JAMA, 2001. **286**(11): p. 8.

35. Alahdab, F., et al., *A systematic review for the screening for peripheral arterial disease in asymptomatic patients.* Journal of vascular surgery, 2015. **61**(3): p. 42S-53S.

36. Papia, G., et al. *Just leg pain? Think again: what health leaders must know about peripheral arterial disease*. in *Healthcare management forum*. 2015. SAGE Publications Sage CA: Los Angeles, CA.

37. Aggarwal, S., et al., *Rehabilitation therapy in peripheral arterial disease.* Canadian Journal of Cardiology, 2016. **32**(10): p. S374-S381.

38. Berger, J.S. and W.R. Hiatt, *Medical therapy in peripheral artery disease.* Circulation, 2012. **126**(4): p. 491-500.

39. Wennberg, P.W., *Approach to the patient with peripheral arterial disease.* Circulation, 2013. **128**(20): p. 2241-2250.

40. Davies, J.E., *Criticial Limb Ischemia: Epidemiology.* MDCVJ, 2012. **3**(4): p. 1.

41. Gupta, N.K., E.J. Armstrong, and S.A. Parikh, *The current state of stem cell therapy for peripheral artery disease.* Current cardiology reports, 2014. **16**(2): p. 447.

42. Adams, R.H., *Molecular control of arterial–venous blood vessel identity.* Journal of anatomy, 2003. **202**(1): p. 105-112.

43. Heinke, J., C. Patterson, and M. Moser, *Life is a pattern: vascular assembly within the embryo.* Frontiers in bioscience (Elite edition), 2012. **4**: p. 2269.

44. Kobari, M., et al., *Blood flow velocity in the pial arteries of cats, with particular reference to the vessel diameter.* Journal of Cerebral Blood Flow & Metabolism, 1984. **4**(1): p. 110-114.

45. Mayrovitz, H.N., R.F. Tuma, and M.P. Wiedeman, *Relationship between microvascular blood velocity and pressure distribution.* American Journal of Physiology-Heart and Circulatory Physiology, 1977. **232**(4): p. H400-H405.

46. Swartz, M.A., *The physiology of the lymphatic system.* Advanced drug delivery reviews, 2001. **50**(1-2): p. 3-20.

47. Rhodin, J.A., *Architecture of the vessel wall.* Handbook of physiology, the cardiovascular system, 1980. **2**: p. 1-31.

48. Mulvany, M. and C. Aalkjær, *Structure and function of small arteries.* Physiological reviews, 1990. **70**(4): p. 921-961.

49. Rhodin, J.A., *The ultrastructure of mammalian arterioles and precapillary sphincters.* Journal of ultrastructure research, 1967. **18**(1-2): p. 181-223.

50. Han, S.S. and J.K. Avery, *The ultrastructure of capillaries and arterioles of the hamster dental pulp.* The Anatomical Record, 1963. **145**(4): p. 549-571.

51. Tilton, R.G., C. Kilo, and J.R. Williamson, *Pericyte-endothelial relationships in cardiac and skeletal muscle capillaries.* Microvascular research, 1979. **18**(3): p. 325-335.

52. Nehls, V., K. Denzer, and D. Drenckhahn, *Pericyte involvement in capillary sprouting during angiogenesis in situ.* Cell and tissue research, 1992. **270**(3): p. 469-474.

53. Caggiati, A., et al., *Valves in small veins and venules.* European Journal of Vascular and Endovascular Surgery, 2006. **32**(4): p. 447-452.

54. Cleaver, O. and D.A. Melton, *Endothelial signaling during development.* Nature medicine, 2003. **9**(6): p. 661.

55. Kumar, S., D.C. West, and A. Ager, *Heterogeneity in endothelial cells from large vessels and microvessels.* Differentiation, 1987. **36**(1): p. 57-70.

56. Stewart, P. and M. Wiley, *Developing nervous tissue induces formation of blood-brain barrier characteristics in invading endothelial cells: a study using quail-chick transplantation chimeras.* Developmental biology, 1981. **84**(1): p. 183-192.

57. Mehta, D. and A.B. Malik, *Signaling mechanisms regulating endothelial permeability.* Physiological reviews, 2006. **86**(1): p. 279-367.

58. Ballermann, B.J., et al., *Shear stress and the endothelium.* Kidney International, 1998. **54**: p. S100-S108.

59. Li, N., et al., *Endothelial Nitric Oxide Synthase Promotes Bone Marrow Stromal Cell Migration to the Ischemic Myocardium via Upregulation of Stromal Cell-Derived Factor-1α.* Stem Cells, 2009. **27**(4): p. 961-970.

60. Noseda, M., et al., *Notch activation induces endothelial cell cycle arrest and participates in contact inhibition: role of p21Cip1 repression.* Molecular and cellular biology, 2004. **24**(20): p. 8813-8822.

61. Cines, D.B., et al., *Endothelial cells in physiology and in the pathophysiology of vascular disorders.* Blood, 1998. **91**(10): p. 3527-3561.

62. Carmeliet, P., *Angiogenesis in health and disease.* Nature medicine, 2003. **9**(6): p. 653.

63. Schiffrin, E.L., *The endothelium and control of blood vessel function in health and disease.* Clinical and investigative medicine, 1994. **17**(6): p. 602.

64. Hansson, G.K. and P. Libby, *The immune response in atherosclerosis: a double-edged sword.* Nature reviews immunology, 2006. **6**(7): p. 508.

65. Carmeliet, P., *Mechanisms of angiogenesis and arteriogenesis.* Nature Medicine, 2000. **6**(3): p. 7.

66. Bergers, G. and S. Song, *The role of pericytes in blood-vessel formation and maintenance.* Neuro Oncol, 2005. **7**(4): p. 452-64.

67. Betsholtz, C., P. Lindblom, and H. Gerhardt, *Role of pericytes in vascular morphogenesis,* in *Mechanisms of Angiogenesis*. 2005, Springer. p. 115-125.

68. Crisan, M., et al., *A perivascular origin for mesenchymal stem cells in multiple human organs.* Cell Stem Cell, 2008. **3**(3): p. 301-13.

69. Segal, S.S., *Cell-to-cell communication coordinates blood flow control.* Hypertension, 1994. **23**(6 Pt 2): p. 1113-1120.

70. Sancho, M., et al., *KIR channels tune electrical communication in cerebral arteries.* Journal of Cerebral Blood Flow & Metabolism, 2017. **37**(6): p. 2171-2184.

71. Harraz, O.F., et al., *CaV1. 2/CaV3. x channels mediate divergent vasomotor responses in human cerebral arteries.* The Journal of general physiology, 2015. **145**(5): p. 405-418.

72. Welsh, D.G., et al., *The conducted vasomotor response: function, biophysical basis, and pharmacological control.* Annual review of pharmacology and toxicology, 2018. **58**: p. 391-410.

73. Haynes, W.G. and D.J. Webb, *Contribution of endogenous generation of endothelin-1 to basal vascular tone.* The Lancet, 1994. **344**(8926): p. 852-854.

74. Vanhoutte, P.M., *Endothelial control of vasomotor function.* Circulation journal, 2003. **67**(7): p. 572-575.

75. Owens, G.K., M.S. Kumar, and B.R. Wamhoff, *Molecular regulation of vascular smooth muscle cell differentiation in development and disease.* Physiological reviews, 2004. **84**(3): p. 767-801.

76. Risau, W. and I. Flamme, *Vasculogenesis.* Annual review of cell and developmental biology, 1995. **11**(1): p. 73-91.

77. Gonzalez-Crussi, F., *Vasculogenesis in the chick embryo. An ultrastructural study.* American Journal of Anatomy, 1971. **130**(4): p. 441-459.

78. Choi, K., et al., *A common precursor for hematopoietic and endothelial cells.* Development, 1998. **125**(4): p. 725-732.

79. Jaffredo, T., et al., *Tracing the hemangioblast during embryogenesis: developmental relationships between endothelial and hematopoietic cells.* International Journal of Developmental Biology, 2003. **49**(2-3): p. 269-277.

80. Risau, W., *Development and differentiation of endothelium.* Kidney International, 1998. **54**: p. S3-S6.

81. Fruttiger, M., *Development of the retinal vasculature.* Angiogenesis, 2007. **10**(2): p. 77-88.

82. Swift, M.R. and B.M. Weinstein, *Arterial–venous specification during development.* Circulation research, 2009. **104**(5): p. 576-588.

83. Fish, J.E. and J.D. Wythe, *The molecular regulation of arteriovenous specification and maintenance.* Developmental Dynamics, 2015. **244**(3): p. 391-409.

84. Pardanaud, L., F. Yassine, and F. Dieterlen-Lievre, *Relationship between vasculogenesis, angiogenesis and haemopoiesis during avian ontogeny.* Development, 1989. **105**(3): p. 473-485.

85. Mikkola, H.K. and S.H. Orkin, *The search for the hemangioblast.* Journal of hematotherapy & stem cell research, 2002. **11**(1): p. 9-17.

86. Choi, K., *The hemangioblast: a common progenitor of hematopoietic and endothelial cells.* Journal of hematotherapy & stem cell research, 2002. **11**(1): p. 91-101.

87. Bailey, A.S. and W.H. Fleming, *Converging roads: evidence for an adult hemangioblast.* Experimental hematology, 2003. **31**(11): p. 987-993.

88. Adams, R.H. and K. Alitalo, *Molecular regulation of angiogenesis and lymphangiogenesis.* Nature reviews Molecular cell biology, 2007. **8**(6): p. 464.

89. Carmeliet, P. and R.K. Jain, *Molecular mechanisms and clinical applications of angiogenesis.* Nature, 2011. **473**(7347): p. 298-307.

90. Critser, P.J. and M.C. Yoder, *Endothelial colony-forming cell role in neoangiogenesis and tissue repair.* Curr Opin Organ Transplant, 2010. **15**(1): p. 68-72.

91. Yoder, M.C., et al., *Redefining endothelial progenitor cells via clonal analysis and hematopoietic stem/progenitor cell principals.* Blood, 2007. **109**(5): p. 10.

92. Semenza, G.L., et al., *Transcriptional Responses Mediated by Hypoxia-Inducible Factor 1*, in *Oxygen Homeostasis and Its Dynamics*. 1998, Springer. p. 421-427.

93. Forsythe, J.A., et al., *Activation of vascular endothelial growth factor gene transcription by hypoxia-inducible factor 1.* Molecular and cellular biology, 1996. **16**(9): p. 4604-4613.

94. Semenza, G.L., et al., *Structural and functional analysis of hypoxia-inducible factor 1.* Kidney international, 1997. **51**(2): p. 553-555.

95. Berra, E., et al., *HIF prolyl-hydroxylase 2 is the key oxygen sensor setting low steady-state levels of HIF-1α in normoxia.* The EMBO journal, 2003. **22**(16): p. 4082-4090.

96. Ke, Q. and M. Costa, *Hypoxia-inducible factor-1 (HIF-1).* Molecular pharmacology, 2006. **70**(5): p. 1469-1480.

97. Semenza, G.L., *Hypoxia-inducible factors in physiology and medicine.* Cell, 2012. **148**(3): p. 399-408.

98. Djonov, V., O. Baum, and P.H. Burri, *Vascular remodeling by intussusceptive angiogenesis.* Cell and tissue research, 2003. **314**(1): p. 107-117.

99. Risau, W., *Mechanisms of angiogenesis.* nature, 1997. **386**(6626): p. 671.

100. Caduff, J., *Scanning electron microscopic study of the developing microvasculature in thepostnatal rat lung*. 1986, Caduff, J.

101. Burri, P.H., R. Hlushchuk, and V. Djonov, *Intussusceptive angiogenesis: its emergence, its characteristics, and its significance.* Developmental dynamics: an official publication of the American Association of Anatomists, 2004. **231**(3): p. 474-488.

102. Logothetidou, A., et al., *Intussusceptive angiogenesis and expression of Tie receptors during porcine metanephric kidney development.* Histology and histopathology, 2017. **32**(8): p. 817-824.

103. OHASHI, Y., S. KITA, and T. MURAKAMI, *Microcirculation of the rat small intestine as studied by the injection replica scanning electron microscope method.* Archivum histologicum japonicum, 1976. **39**(4): p. 271-282.

104. Arpino, J.-M., et al., *4D microvascular analysis reveals that regenerative angiogenesis in ischemic muscle produces a flawed microcirculation.* Circulation research, 2017: p. CIRCRESAHA. 116.310535.

105. De Palma, M., D. Biziato, and T.V. Petrova, *Microenvironmental regulation of tumour angiogenesis.* Nature Reviews Cancer, 2017. **17**(8): p. 457.

106. Schmidt, T. and P. Carmeliet, *Blood-vessel formation: Bridges that guide and unite.* Nature, 2010. **465**(7299): p. 697-699.

107. Takakura, N., et al., *A role for hematopoietic stem cells in promoting angiogenesis.* Cell, 2000. **102**(2): p. 199-209.

108. Huber, T.L., et al., *Haemangioblast commitment is initiated in the primitive streak of the mouse embryo.* Nature, 2004. **432**(7017): p. 625.

109. Isner, J.M. and T. Asahara, *Angiogenesis and vasculogenesis as therapeutic strategies for postnatal neovascularization.* The Journal of clinical investigation, 1999. **103**(9): p. 1231-1236.

110. Asahara, T., *Isolation of Putative Progenitor Endothelial Cells for Angiogenesis.* Science, 1997. **275**(5302): p. 964-966.

111. Buschmann, I. and W. Schaper, *The pathophysiology of the collateral circulation (arteriogenesis).* The Journal of pathology, 2000. **190**(3): p. 338-342.

112. Qadura, M., et al., *Concise review: cell therapy for critical limb ischemia: an integrated review of preclinical and clinical studies.* Stem Cells, 2018. **36**(2): p. 161-171.

113. Iwasawa, E., et al., *Acute development of collateral circulation and therapeutic prospects in ischemic stroke.* Neural regeneration research, 2016. **11**(3): p. 368.

114. Heil, M., et al., *Arteriogenesis versus angiogenesis: similarities and differences.* Journal of cellular and molecular medicine, 2006. **10**(1): p. 45-55.

115. Schaper, W. and D. Scholz, *Factors regulating arteriogenesis.* Arteriosclerosis, thrombosis, and vascular biology, 2003. **23**(7): p. 1143-1151.

116. Helisch, A. and W. Schaper, *Arteriogenesis The Development and Growth of Collateral Arteries.* Microcirculation, 2003. **10**(1): p. 83-97.

117. Carmeliet, P., G. Eelen, and J. Kalucka, *Arteriogenesis versus angiogenesis*, in *The ESC Textbook of Vascular Biology*. 2017, Oxford University Press.

118. Bergmann, C.E., et al., *Arteriogenesis depends on circulating monocytes and macrophage accumulation and is severely depressed in op/op mice.* Journal of leukocyte biology, 2006. **80**(1): p. 59-65.

119. Li, J., Y.P. Zhang, and R.S. Kirsner, *Angiogenesis in wound repair: angiogenic growth factors and the extracellular matrix.* Microscopy research and technique, 2003. **60**(1): p. 107-114.

120. Potente, M., H. Gerhardt, and P. Carmeliet, *Basic and therapeutic aspects of angiogenesis.* Cell, 2011. **146**(6): p. 873-887.

121. Carmeliet, P. and M. Tessier-Lavigne, *Common mechanisms of nerve and blood vessel wiring.* Nature, 2005. **436**(7048): p. 193.

122. De Smet, F., et al., *Mechanisms of vessel branching: filopodia on endothelial tip cells lead the way.* Arteriosclerosis, thrombosis, and vascular biology, 2009. **29**(5): p. 639-649.

123. Blanco, R. and H. Gerhardt, *VEGF and Notch in tip and stalk cell selection.* Cold Spring Harbor perspectives in medicine, 2013. **3**(1): p. a006569.

124. Leslie, J.D., et al., *Endothelial signalling by the Notch ligand Delta-like 4 restricts angiogenesis.* Development, 2007. **134**(5): p. 839-844.

125. Hellström, M., L.-K. Phng, and H. Gerhardt, *VEGF and Notch signaling: the yin and yang of angiogenic sprouting.* Cell adhesion & migration, 2007. **1**(3): p. 133-136.

126. Adams, R.H. and A. Eichmann, *Axon guidance molecules in vascular patterning.* Cold Spring Harbor perspectives in biology, 2010: p. a001875.

127. Ribatti, D., *The seminal work of Werner Risau in the study of the development of the vascular system*, in *Protagonists of Medicine*. 2010, Springer. p. 83-91.

128. Procopio, W.N., et al., *Angiopoietin-1 and-2 coiled coil domains mediate distinct homo-oligomerization patterns, but fibrinogen-like domains mediate ligand activity.* Journal of Biological Chemistry, 1999. **274**(42): p. 30196-30201.

129. Eklund, L. and P. Saharinen, *Angiopoietin signaling in the vasculature.* Experimental cell research, 2013. **319**(9): p. 1271-1280.

130. Saharinen, P., et al., *Angiopoietins assemble distinct Tie2 signalling complexes in endothelial cell–cell and cell–matrix contacts.* Nature cell biology, 2008. **10**(5): p. 527.

131. Augustin, H.G., et al., *Control of vascular morphogenesis and homeostasis through the angiopoietin–Tie system.* Nature reviews Molecular cell biology, 2009. **10**(3): p. 165.

132. Adams, R.H., et al., *Roles of ephrinB ligands and EphB receptors in cardiovascular development: demarcation of arterial/venous domains, vascular morphogenesis, and sprouting angiogenesis.* Genes & development, 1999. **13**(3): p. 295-306.

133. Xu, N.-J. and M. Henkemeyer. *Ephrin reverse signaling in axon guidance and synaptogenesis*. in *Seminars in cell & developmental biology*. 2012. Elsevier.

134. Kania, A. and R. Klein, *Mechanisms of ephrin–Eph signalling in development, physiology and disease.* Nature reviews Molecular cell biology, 2016. **17**(4): p. 240.

135. Cheng, N., D.M. Brantley, and J. Chen, *The ephrins and Eph receptors in angiogenesis.* Cytokine & growth factor reviews, 2002. **13**(1): p. 75-85.

136. Salvucci, O., et al., *EphrinB reverse signaling contributes to endothelial and mural cell assembly into vascular structures.* Blood, 2009. **114**(8): p. 1707-1716.

137. Wang, Y., et al., *Ephrin-B2 controls VEGF-induced angiogenesis and lymphangiogenesis.* Nature, 2010. **465**(7297): p. 483.

138. Yazdani, U. and J.R. Terman, *The semaphorins.* Genome biology, 2006. **7**(3): p. 211.

139. Alto, L.T. and J.R. Terman, *Semaphorins and their signaling mechanisms*, in *Semaphorin Signaling*. 2017, Springer. p. 1-25.

140. Song, H.-j. and M.-m. Poo, *The cell biology of neuronal navigation.* Nature cell biology, 2001. **3**(3): p. E81.

141. Deindl, E. and W. Schaper, *The art of arteriogenesis.* Cell biochemistry and biophysics, 2005. **43**(1): p. 1-15.

142. Rohani, M.G. and W.C. Parks, *Matrix remodeling by MMPs during wound repair.* Matrix Biology, 2015. **44**: p. 113-121.

143. Davis, G.E. and D.R. Senger, *Endothelial extracellular matrix: biosynthesis, remodeling, and functions during vascular morphogenesis and neovessel stabilization.* Circulation research, 2005. **97**(11): p. 1093-1107.

144. Arpino, V., M. Brock, and S.E. Gill, *The role of TIMPs in regulation of extracellular matrix proteolysis.* Matrix Biology, 2015. **44**: p. 247-254.

145. Arroyo, A., et al., *Matrix metalloproteinases: new routes to the use of MT1-MMP as a therapeutic target in angiogenesis-related disease.* Current pharmaceutical design, 2007. **13**(17): p. 1787-1802.

146. Deryugina, E.I. and J.P. Quigley, *Pleiotropic roles of matrix metalloproteinases in tumor angiogenesis: contrasting, overlapping and compensatory functions.* Biochimica et Biophysica Acta (BBA)-Molecular Cell Research, 2010. **1803**(1): p. 103-120.

147. Fukumura, D. and R.K. Jain, *Imaging angiogenesis and the microenvironment.* Apmis, 2008. **116**(7-8): p. 695-715.

148. Shaterian, A., et al., *Real-time analysis of the kinetics of angiogenesis and vascular permeability in an animal model of wound healing.* Burns, 2009. **35**(6): p. 811-817.

149. Armulik, A., A. Abramsson, and C. Betsholtz, *Endothelial/pericyte interactions.* Circulation research, 2005. **97**(6): p. 512-523.

150. Hellberg, C., A. Östman, and C.-H. Heldin, *PDGF and vessel maturation*, in *Angiogenesis inhibition*. 2010, Springer. p. 103-114.

151. Baffert, F., et al., *Cellular changes in normal blood capillaries undergoing regression after inhibition of VEGF signaling.* Am J Physiol Heart Circ Physiol, 2006. **290**(2): p. H547-59.

152. Claxton, S. and M. Fruttiger, *Role of arteries in oxygen induced vaso-obliteration.* Experimental eye research, 2003. **77**(3): p. 305-311.

153. Wietecha, M.S., W.L. Cerny, and L.A. DiPietro, *Mechanisms of vessel regression: toward an understanding of the resolution of angiogenesis*, in *New Perspectives in Regeneration*. 2012, Springer. p. 3-32.

154. Korn, C. and H.G. Augustin, *Mechanisms of vessel pruning and regression.* Developmental cell, 2015. **34**(1): p. 5-17.

155. Tateishi-Yuyama, E., et al., *Therapeutic angiogenesis for patients with limb ischaemia by autologous transplantation of bone-marrow cells: a pilot study and a randomised controlled trial.* The Lancet, 2002. **360**(9331): p. 427-435.

156. Matoba, S., et al., *Long-term clinical outcome after intramuscular implantation of bone marrow mononuclear cells (Therapeutic Angiogenesis by Cell Transplantation [TACT] trial) in patients with chronic limb ischemia.* Am Heart J, 2008. **156**(5): p. 1010-8.

157. Trounson, A., et al., *Clinical trials for stem cell therapies.* BMC medicine, 2011. **9**(1): p. 52.

158. Mirzaei, H., et al., *Therapeutic application of multipotent stem cells.* Journal of cellular physiology, 2018. **233**(4): p. 2815-2823.

159. Till, J.E. and E.A. McCulloch, *A direct measurement of the radiation sensitivity of normal mouse bone marrow cells.* Radiation research, 1961. **14**(2): p. 213-222.

160. McCulloch, E.A. and J.E. Till, *Perspectives on the properties of stem cells.* Nature medicine, 2005. **11**(10): p. 1026.

161. Hima Bindu, A. and B. Srilatha, *Potency of various types of stem cells and their transplantation.* J Stem Cell Res Ther, 2011. **1**: p. 115.

162. Singh, V.K., et al., *Describing the stem cell potency: the various methods of functional assessment and in silico diagnostics.* Frontiers in cell and developmental biology, 2016. **4**: p. 134.

163. Takahashi, K. and S. Yamanaka, *Induction of pluripotent stem cells from mouse embryonic and adult fibroblast cultures by defined factors.* cell, 2006. **126**(4): p. 663-676.

164. Takahashi, K., et al., *Induction of pluripotent stem cells from adult human fibroblasts by defined factors.* cell, 2007. **131**(5): p. 861-872.

165. Soldner, F. and R. Jaenisch, *iPSC disease modeling.* Science, 2012. **338**(6111): p. 1155-1156.

166. Barker, N., S. Bartfeld, and H. Clevers, *Tissue-resident adult stem cell populations of rapidly self-renewing organs.* Cell stem cell, 2010. **7**(6): p. 656-670.

167. Kalka, C., et al., *Transplantation of ex vivo expanded endothelial progenitor cells for therapeutic neovascularization.* Proc Natl Acad Sci U S A, 2000. **97**(7): p. 3422-7.

168. Tongers, J.r., J.G. Roncalli, and D.W. Losordo, *Therapeutic angiogenesis for critical limb ischemia: microvascular therapies coming of age*. 2008, Am Heart Assoc.

169. Rauscher, F.M., et al., *Aging, progenitor cell exhaustion, and atherosclerosis.* Circulation, 2003. **108**(4): p. 457-463.

170. Stolzing, A., et al., *Diabetes induced changes in rat mesenchymal stem cells.* Cells Tissues Organs, 2010. **191**(6): p. 453-465.

171. Hill, J.M., et al., *Circulating endothelial progenitor cells, vascular function, and cardiovascular risk.* NEJM, 2003. **348**(7): p. 8.

172. Rehman, J., *Peripheral Blood "Endothelial Progenitor Cells" Are Derived From Monocyte/Macrophages and Secrete Angiogenic Growth Factors.* Circulation, 2003. **107**(8): p. 1164-1169.

173. Dimmeler, S., et al., *HMG-CoA reductase inhibitors (statins) increase endothelial progenitor cells via the PI 3-kinase/Akt pathway.* Journal of Clinical Investigation, 2001. **108**(3): p. 391-397.

174. Lin, Y., et al., *Origins of circulating endothelial cells and endothelial outgrowth from blood.* J Clin Invest, 2000. **105**(1): p. 71-7.

175. Bompais, H., et al., *Human endothelial cells derived from circulating progenitors display specific functional properties compared with mature vessel wall endothelial cells.* Blood, 2004. **103**(7): p. 2577-2584.

176. Ingram, D.A., et al., *Identification of a novel hierarchy of endothelial progenitor cells using human peripheral and umbilical cord blood.* Blood, 2004. **104**(9): p. 2752-60.

177. Hur, J., et al., *Characterization of two types of endothelial progenitor cells and their different contributions to neovasculogenesis.* Arterioscler Thromb Vasc Biol, 2004. **24**(2): p. 288-93.

178. Prater, D.N., et al., *Working hypothesis to redefine endothelial progenitor cells.* Leukemia, 2007. **21**(6): p. 1141-9.

179. Pujol, B.F., et al., *Endothelial-like cells derived from human CD14 positive monocytes.* Differentiation, 2000. **65**(5): p. 287-300.

180. Schmeisser, A., et al., *Monocytes coexpress endothelial and macrophagocytic lineage markers and form cord-like structures in matrigel under angiogenic conditions.* Cardiovascular Research, 2000. **49**: p. 10.

181. Fujiyama, S., et al., *Bone marrow monocyte lineage cells adhere on injured endothelium in a monocyte chemoattractant protein-1-dependent manner and*

accelerate reendothelialization as endothelial progenitor cells. Circ Res, 2003. **93**(10): p. 980-9.

182. Richardson, M.R. and M.C. Yoder, *Endothelial progenitor cells: quo vadis?* J Mol Cell Cardiol, 2011. **50**(2): p. 266-72.

183. Yip, H.K., et al., *Level and value of circulating endothelial progenitor cells in patients after acute ischemic stroke.* Stroke, 2008. **39**(1): p. 69-74.

184. Asahara, T., A. Kawamoto, and H. Masuda, *Concise review: Circulating endothelial progenitor cells for vascular medicine.* Stem Cells, 2011. **29**(11): p. 1650-5.

185. Timmermans, F., et al., *Endothelial outgrowth cells are not derived from CD133+ cells or CD45+ hematopoietic precursors.* Arterioscler Thromb Vasc Biol, 2007. **27**(7): p. 1572-9.

186. Krenning, G., et al., *Efficient differentiation of CD14+ monocytic cells into endothelial cells on degradable biomaterials.* Biomaterials, 2007. **28**(8): p. 1470-9.

187. Jersmann, H.P., *Time to abandon dogma: CD14 is expressed by non-myeloid lineage cells.* Immunol Cell Biol, 2005. **83**(5): p. 462-7.

188. Prokopi, M., et al., *Proteomic analysis reveals presence of platelet microparticles in endothelial progenitor cell cultures.* Blood, 2009. **114**(3): p. 723-32.

189. Delorme, B., et al., *Presence of endothelial progenitor cells, distinct from mature endothelial cells, within human CD146+ blood cells.* Thromb Haemost, 2005. **94**(6): p. 1270-9.

190. Friedenstein, A.J., et al., *Precursors for fibroblasts in different populations of hematopoietic cells as detected by the in vitro colony assay method.* Exp Hematol, 1974. **2**(2): p. 83-92.

191. Friedenstein, A.J., J.F. Gorskaja, and N.N. Kulagina, *Fibroblast precursors in normal and irradiated mouse hematopoietic organs.* Exp Hematol, 1976. **4**(5): p. 267-74.

192. Prockop, D.J., *Marrow stromal cells as steam cells for nonhematopoietic tissues.* Science, 1997. **276**(5309): p. 71-74.

193. Pittenger, M.F., *Multilineage Potential of Adult Human Mesenchymal Stem Cells.* Science, 1999. **284**(5411): p. 143-147.

194. Jiang, Y., et al., *Pluripotency of mesenchymal stem cells derived from adult marrow.* Nature, 2002. **418**(6893): p. 41-49.

195. Phadnis, S.M., et al., *Human bone marrow-derived mesenchymal cells differentiate and mature into endocrine pancreatic lineage in vivo.* Cytotherapy, 2011. **13**(3): p. 279-93.

196. Caplan, A.I., *Mesenchymal stem cells.* Journal of Orthopaedic Research, 1991. **9**(5): p. 641-650.

197. Bianco, P., et al., *"Mesenchymal" stem cells in human bone marrow (skeletal stem cells): a critical discussion of their nature, identity, and significance in incurable skeletal disease.* Human gene therapy, 2010. **21**(9): p. 1057-1066.

198. da Silva Meirelles, L., A.I. Caplan, and N.B. Nardi, *In Search of the In Vivo Identity of Mesenchymal Stem Cells.* STEM CELLS, 2008. **26**(9): p. 2287-2299.

199. Maitra, B., et al., *Human mesenchymal stem cells support unrelated donor hematopoietic stem cells and suppress T-cell activation.* Bone Marrow Transplant, 2004. **33**(6): p. 597-604.

200. Salem, H.K. and C. Thiemermann, *Mesenchymal stromal cells: current understanding and clinical status.* Stem Cells, 2010. **28**(3): p. 585-96.

201. Si, Y., et al., *Infusion of mesenchymal stem cells ameliorates hyperglycemia in type 2 diabetic rats: identification of a novel role in improving insulin sensitivity.* Diabetes, 2012. **61**(6): p. 1616-25.

202. Caplan, A.I. and D. Correa, *The MSC: an injury drugstore.* Cell Stem Cell, 2011. **9**(1): p. 11-5.

203. Nauta, A.J. and W.E. Fibbe, *Immunomodulatory properties of mesenchymal stromal cells.* Blood, 2007. **110**(10): p. 3499-506.

204. Corcione, A., et al., *Human mesenchymal stem cells modulate B-cell functions.* Blood, 2006. **107**(1): p. 367-72.

205. Gopurappilly, R., V. Bhat, and R. Bhonde, *Pancreatic tissue resident mesenchymal stromal cell (MSC)-like cells as a source of in vitro islet neogenesis.* J Cell Biochem, 2013. **114**(10): p. 2240-7.

206. Francois, M., et al., *Human MSC suppression correlates with cytokine induction of indoleamine 2,3-dioxygenase and bystander M2 macrophage differentiation.* Mol Ther, 2012. **20**(1): p. 187-95.

207. Fong, C.Y., et al., *Human Wharton's jelly stem cells have unique transcriptome profiles compared to human embryonic stem cells and other mesenchymal stem cells.* Stem Cell Rev, 2011. **7**(1): p. 1-16.

208. Dominici, M., et al., *Minimal criteria for defining multipotent mesenchymal stromal cells. The International Society for Cellular Therapy position statement.* Cytotherapy, 2006. **8**(4): p. 315-317.

209. Kuci, Z., et al., *Clonal analysis of multipotent stromal cells derived from CD271+ bone marrow mononuclear cells: functional heterogeneity and different mechanisms of allosuppression.* Haematologica, 2013. **98**(10): p. 1609-16.

210. Capoccia, B.J., et al., *Revascularization of ischemic limbs after transplantation of human bone marrow cells with high aldehyde dehydrogenase activity.* Blood, 2009. **113**(21): p. 5340-51.

211. Campagnoli, C., *Identification of mesenchymal stem/progenitor cells in human first-trimester fetal blood, liver, and bone marrow.* Blood, 2001. **98**(8): p. 2396-2402.

212. Lee, O.K., et al., *Isolation of multipotent mesenchymal stem cells from umbilical cord blood.* Blood, 2004. **103**(5): p. 1669-75.

213. Covas, D.T., et al., *Isolation and culture of umbilical vein mesenchymal stem cells.* Brazilian Journal of Medical and Biological Research, 2003. **36**: p. 1179-1183.

214. Koc, O.N., et al., *Rapid hematopoietic recovery after coinfusion of autologous-blood stem cells and culture-expanded marrow mesenchymal stem cells in advanced breast cancer patients receiving high-dose chemotherapy.* J Clin Oncol, 2000. **18**(2): p. 307-16.

215. Lazarus, H.M., et al., *Cotransplantation of HLA-identical sibling culture-expanded mesenchymal stem cells and hematopoietic stem cells in hematologic malignancy patients.* Biol Blood Marrow Transplant, 2005. **11**(5): p. 389-98.

216. Le Blanc, K., et al., *Mesenchymal stem cells for treatment of steroid-resistant, severe, acute graft-versus-host disease: a phase II study.* Lancet, 2008. **371**(9624): p. 1579-86.

217. Ringden, O., et al., *Mesenchymal stem cells for treatment of therapy-resistant graft-versus-host disease.* Transplantation, 2006. **81**(10): p. 1390-7.

218. Duijvestein, M., et al., *Autologous bone marrow-derived mesenchymal stromal cell treatment for refractory luminal Crohn's disease: results of a phase I study.* Gut, 2010. **59**(12): p. 1662-9.

219. Ciccocioppo, R., et al., *Autologous bone marrow-derived mesenchymal stromal cells in the treatment of fistulising Crohn's disease.* Gut, 2011. **60**(6): p. 788-98.

220. Lee, R.H., et al., *Multipotent stromal cells from human marrow home to and promote repair of pancreatic islets and renal glomeruli in diabetic NOD/scid*

mice. Proceedings of the National Academy of Sciences, 2006. **103**(46): p. 17438-17443.

221. Bell, G.I., et al., *Transplanted human bone marrow progenitor subtypes stimulate endogenous islet regeneration and revascularization.* Stem Cells Dev, 2012. **21**(1): p. 97-109.

222. Abdi, R., et al., *Immunomodulation by mesenchymal stem cells: a potential therapeutic strategy for type 1 diabetes.* Diabetes, 2008. **57**(7): p. 1759-67.

223. Storms, R.W., et al., *Isolation of primitive human hematopoietic progenitors on the basis of aldehyde dehydrogenase activity.pdf>.* PNAS, 1999. **96**: p. 6.

224. Hess, D.A., et al., *Functional characterization of highly purified human hematopoietic repopulating cells isolated according to aldehyde dehydrogenase activity.* Blood, 2004. **104**(6): p. 1648-55.

225. Hess, D.A., et al., *Widespread Nonhematopoietic Tissue Distribution by Transplanted Human Progenitor Cells with High Aldehyde Dehydrogenase Activity.* Stem Cells, 2008. **26**(3): p. 611-620.

226. Perin, E.C., et al., *Rationale and design for PACE: patients with intermittent claudication injected with ALDH bright cells.* Am Heart J, 2014. **168**(5): p. 667-73.

227. Simpson, R.J., et al., *Exosomes: proteomic insights and diagnostic potential.* 2009. **6**(3): p. 267-283.

228. Andaloussi, S.E., et al., *Extracellular vesicles: biology and emerging therapeutic opportunities.* 2013. **12**(5): p. 347.

229. Akers, J.C., et al., *Biogenesis of extracellular vesicles (EV): exosomes, microvesicles, retrovirus-like vesicles, and apoptotic bodies.* 2013. **113**(1): p. 1-11.

230. Van Der Pol, E., et al., *Optical and non-optical methods for detection and characterization of microparticles and exosomes.* 2010. **8**(12): p. 2596-2607.

231. Rak, J.J.F.i.p., *Extracellular vesicles–biomarkers and effectors of the cellular interactome in cancer.* 2013. **4**: p. 21.

232. Gaceb, A., et al., *Extracellular vesicles: new players in cardiovascular diseases.* 2014. **50**: p. 24-28.

233. Van der Pol, E., et al., *Classification, functions, and clinical relevance of extracellular vesicles.* 2012. **64**(3): p. 676-705.

234. Kuljanin, M., et al., *Human multipotent stromal cell secreted effectors accelerate islet regeneration.* 2019.

235. Cheng, H.S., et al., *Paradoxical suppression of atherosclerosis in the absence of microRNA-146a.* 2017. **121**(4): p. 354-367.

236. Vader, P., et al., *Extracellular vesicles for drug delivery.* 2016. **106**: p. 148-156.

237. Williams, D.F., *On the mechanisms of biocompatibility.* Biomaterials, 2008. **29**(20): p. 2941-2953.

238. Macchiarini, P., et al., *Clinical transplantation of a tissue-engineered airway.* The Lancet, 2008. **372**(9655): p. 2023-2030.

239. Naba, A., et al., *The extracellular matrix: Tools and insights for the "omics" era.* Matrix Biol, 2016. **49**: p. 10-24.

240. Badylak, S.F., *Xenogeneic extracellular matrix as a scaffold for tissue reconstruction.* Transpl Immunol, 2004. **12**(3-4): p. 367-77.

241. Badylak, S.F., D.O. Freytes, and T.W. Gilbert, *Extracellular matrix as a biological scaffold material: Structure and function.* Acta Biomater, 2009. **5**(1): p. 1-13.

242. Gilbert, T.W., T.L. Sellaro, and S.F. Badylak, *Decellularization of tissues and organs.* Biomaterials, 2006. **27**(19): p. 3675-83.

243. Pawson, T. and J.D. Scott, *Signaling through scaffold, anchoring, and adaptor proteins.* Science, 1997. **278**(5346): p. 2075-2080.

244. Stupack, D.G. and D.A. Cheresh, *Get a ligand, get a life: integrins, signaling and cell survival.* Journal of cell science, 2002. **115**(19): p. 3729-3738.

245. Hoshiba, T., et al., *Decellularized matrices for tissue engineering.* Expert opinion on biological therapy, 2010. **10**(12): p. 1717-1728.

246. Fuchs, J.R., B.A. Nasseri, and J.P. Vacanti, *Tissue engineering: a 21st century solution to surgical reconstruction.* Ann Thorac Surg, 2001. **72**: p. 15.

247. Casadei, A., et al., *Adipose tissue regeneration: a state of the art.* J Biomed Biotechnol, 2012. **2012**: p. 462543.

248. Godier-Furnémont, A.F., et al., *Composite scaffold provides a cell delivery platform for cardiovascular repair.* Proceedings of the National Academy of Sciences, 2011. **108**(19): p. 7974-7979.

249. Wang, B., et al., *Fabrication of cardiac patch with decellularized porcine myocardial scaffold and bone marrow mononuclear cells.* Journal of biomedical materials research Part A, 2010. **94**(4): p. 1100-1110.

250. Vyavahare, N.R., et al., *Prevention of calcification of glutaraldehyde-crosslinked porcine aortic cusps by ethanol preincubation: Mechanistic studies of protein structure and water–biomaterial relationships.* Journal of Biomedical Materials Research: An Official Journal of The Society for Biomaterials, The Japanese Society for Biomaterials, and the Australian Society for Biomaterials, 1998. **40**(4): p. 577-585.

251. Mendelsohn, M. and G. Dunlop, *Gore-tex augmentation grafting in rhinoplasty--is it safe?* Journal of Otolaryngology-Head & Neck Surgery, 1998. **27**(6): p. 337.

252. Hodde, J., *Naturally occurring scaffolds for soft tissue repair and regeneration.* Tissue engineering, 2002. **8**(2): p. 295-308.

253. Singelyn, J.M. and K.L. Christman, *Injectable materials for the treatment of myocardial infarction and heart failure: the promise of decellularized matrices.* Journal of cardiovascular translational research, 2010. **3**(5): p. 478-486.

254. Suuronen, E.J., et al., *An acellular matrix-bound ligand enhances the mobilization, recruitment and therapeutic effects of circulating progenitor cells in a hindlimb ischemia model.* The FASEB Journal, 2009. **23**(5): p. 1447-1458.

255. Wang, L., et al., *Combining decellularized human adipose tissue extracellular matrix and adipose-derived stem cells for adipose tissue engineering.* Acta biomaterialia, 2013. **9**(11): p. 8921-8931.

256. Martin, P.M., et al., *Decellularized Adipose Tissue Scaffolds for Soft Tissue Regeneration and Adipose-Derived Stem/Stromal Cell Delivery.* Adipose-Derived Stem Cells: Methods and Protocols, 2018: p. 53-71.

257. Han, T.T.Y., et al., *Adipose-derived stromal cells mediate in vivo adipogenesis, angiogenesis and inflammation in decellularized adipose tissue bioscaffolds.* Biomaterials, 2015. **72**: p. 125-137.

258. Martin, P.M., et al., *Matrix composition in 3-D collagenous bioscaffolds modulates the survival and angiogenic phenotype of human chronic wound dermal fibroblasts.* Acta biomaterialia, 2018.

259. Caplan, A.I. and D. Correa, *The MSC: an injury drugstore.* Cell stem cell, 2011. **9**(1): p. 11-15.

260. Melero-Martin, J.M., et al., *Engineering robust and functional vascular networks in vivo with human adult and cord blood-derived progenitor cells.* Circ Res, 2008. **103**(2): p. 194-202.

261. Au, P., et al., *Bone marrow derived mesenchymal stem cells facilitate engineering of long lasting functional vasculature*. Blood, 2008. **111**(9): p. 9.

262. Putman, D.M., et al., *Umbilical Cord Blood-Derived Aldehyde Dehydrogenase-Expressing Progenitor Cells Promote Recovery from Acute Ischemic Injury*. Stem Cells, 2012. **30**(10): p. 2248-2260.

Chapter 2

2 High aldehyde dehydrogenase activity identifies a subset of human mesenchymal stromal cells with vascular regenerative potential.

[ii] A version of this chapter has been published: **Sherman SE**, Kuljanin M, Cooper TT, Putman DM, Lajoie GA, Hess DA. High aldehyde dehydrogenase activity identifies a subset of human mesenchymal stromal cells with vascular regenerative potential. Stem Cells. 2017 Jun;35(6):1542-53.

2.1 Introduction

Peripheral artery disease (PAD) is characterized by ischemia in the lower extremities due to narrowing of blood vessels associated with atherosclerotic plaque accumulation. PAD currently affects 8-12 million in North America and >200 million worldwide[1]. The clinical consequences of PAD range from intermittent claudication, to critical limb ischemia (CLI), the most severe form of PAD distinguished by pain at rest with non–healing ulcers in distal extremities. Many patients with CLI are not candidates for vessel bypass or percutaneous interventions[2, 3], and ≈30% will require limb amputation. Those afflicted with CLI have 6-fold increased risk of serious cardiovascular events[4], and >60% of CLI patients will die from complications within 5 years of diagnosis[5]. Thus, there is a compelling need for improved therapies to combat CLI.

Cell transplantation to restore perfusion in ischemic limbs is under intense investigation for the treatment of CLI. In 2002, the therapeutic angiogenesis by cell transplantation (TACT) trial first demonstrated improvements in ankle brachial pressure index and tissue oxygen saturation after transplantation of bone marrow mononuclear cells (BM MNC)[6]. In a follow-up study, there was significant improvement in pain scale and ulcer healing after 2 years post-transplantation[7]. Unfortunately, overall clinical benefit was considered modest and lower limb amputation rates were not improved. However, BM MNC contain cells from multiple (hematopoietic, endothelial, and mesenchymal-stromal) cell lineages that directly or indirectly aid in neovessel formation[8].

In efforts to purify pro-vascular progenitor cell populations from human BM and umbilical cord blood (UCB) with enhanced regenerative functions, we used a clinically-applicable fluorescent substrate (Aldefluor^{TM}) of aldehyde dehydrogenase (ALDH), a conserved detoxification enzyme highly expressed in multiple mesodermal progenitor cell lineages[9]. Essentially, ALDH protects long-lived cells against oxidative environmental insults, and paradoxically represents the rate-limiting enzyme in the intracellular production of the lipid morphogen, retinoic acid. As progenitor cell differentiation occurs towards a more restricted or expendable phenotype, ALDH-activity is generally reduced. Although cells with high aldehyde dehydrogenase activity (ALDH^{hi}) represent a rare fraction of human BM (<0.8% of MNC) or UCB (<0.5% of MNC), ALDH^{hi} cells are highly enriched for expandable progenitor cells with hematopoietic, endothelial, and mesenchymal colony-forming functions[10]. Human cells with high ALDH activity demonstrate a plethora of regenerative functions when transplanted into preclinical immunodeficient mouse models, including strong hematopoietic reconstituting capacity[11, 12], widespread tissue distribution after intravenous delivery [12], elicit islet repair in models of diabetes[13, 14], and demonstrate potent angiogenic stimulatory capacity in ischemic hindlimbs after femoral artery ligation[10, 15]. Recently, a phase I, randomized controlled trial compared unselected autologous BM MNC to purified BM ALDH^{hi} cells in the treatment of CLI[16]. Although significant improvements in ankle-brachial index were observed in both groups, neither ischemic group showed improvement in ischemic ulcer grade or limb salvage[16].

Mesenchymal stromal cells (MSC) are defined as non-hematopoietic, progenitor cells that grow adherent to plastic and differentiate into bone, cartilage and adipose *in vitro*[17]. MSC are also considered potent bio-factories that orchestrate regenerative and immunomodulatory effects in a paracrine fashion at sites of tissue injury[18-21]. BM-derived MSC promote survival and proliferation of endothelial cells (EC) under hypoxic conditions[22]. After transplantation, MSC home to sites of vascular injury, incorporate into vessels as perivascular cells[23, 24], and secrete factors that support angiogenesis such as vascular endothelial growth factor (VEGF) and platelet derived growth factor (PDGF)[25]. Administration of ECs with MSC has been shown to increase vascularization and enhance vessel stability in multiple murine xenograft transplantation models[24, 26]. MSC have been demonstrated to be safe and well tolerated in many clinical studies[27, 28]. Early trials involving intramuscular transplantation into patients with CLI showed increased ankle brachial pressure index, accelerated ulcer healing, and improving overall quality of life and Rutherford scores[29-31]. In a direct comparison of autologous BM MNC to BM MSC administered to patients with CLI, Lu *et al* found that MSC-injected patients showed better perfusion and ulceration recovery scores at 6 months post-transplantation[32]. However, limb salvage compared to MNC administration was not improved by MSC treatment. Overall, MSC represent an attractive cell type to promote vascular regeneration because MSC can be readily obtained from autologous and allogeneic sources, expanded efficiently in culture, and support angiogenesis while demonstrating very low immunogenicity[21]. However, significant challenges remain that prevent the advancement of cellular therapies for CLI, and scientists have been challenged to better understand the functions of active cell subtypes that mediate beneficial effects within heterogenous cell populations. Here we demonstrate that purification using high ALDH-activity (by Aldefluor^{TM} staining) after expansion selects a novel MSC subset with a unique secretory profile that augments EC survival, proliferation, tube formation *in vitro* and promotes the generation of a pro-angiogenic niche *in vivo*.

2.2 Methods

2.2.1 Selection of ALDH^{lo} versus ALDH^{hi} MSC subsets

Human BM aspirates were obtained from healthy allogeneic sibling donors with informed consent from the London Health Sciences Centre (London, ON). MNC were isolated via hypaque-ficoll centrifugation and seeded on tissue culture plastic at 270,000 cells/cm^2. Adherent stromal colonies (CFU-fibroblast) were established within 14 days and expanded in Amniomax media + supplement (Life Technologies, Carlsbad, CA).

At passage 4 (P4), MSC were purified into ALDH^{lo} versus ALDH^{hi} subsets by fluorescence activated cell sorting using the Aldefluor^{TM} assay (StemCell Technologies, Vancouver, BC) as previously described[11, 33]. The ALDH^{hi} subset represented cells with ≈5-fold higher fluorescence intensity compared to ALDH^{lo} gate established using DEAB-inhibition. Purified ALDH^{lo} and ALDH^{hi} MSC subsets also represented no greater than the top or bottom 30% of ALDH fluorescent events, respectively. All BM samples were sorted (FACS Aria III, Beckton Dickenson (BD), Mississauga, ON) in the London Regional Flow Cytometry Facility.

2.2.2 Cell surface phenotype analysis

ALDH^{lo} and ALDH^{hi} MSC were co-stained with antibodies for stromal cell markers: CD73, CD90, and CD105; hematopoietic lineage markers: CD45 and CD14 (monocytes), and the pericellular marker: CD146. Surface marker expression was obtained using an LSR II flow cytometer (Beckton Dickenson), and analysis performed using FloJo software (Treestar, Ashland, OR).

2.2.3 *In vitro* differentiation assays

To assess multipotent differentiation, ALDH^{lo} or ALDH^{hi} MSC (N=3) were grown in adipogenesis or osteogenesis differentiation media (Life Technologies) as per manufacturer's instructions. After 14 or 21 days cells were fixed in formalin and stained for adipocytes or osteocytes using using Oil Red O or Alizarin red respectively. For chondrogenic differentiation, micromasses of purified ALDH^{lo} or ALDH^{hi} MSC (N=3) were cultured for 14 days in chondrogenesis differentiation media (Life Technologies) as previously described[33]. Micromasses were frozen in OCT, sectioned, and stained with Alcian Blue counterstained with Nuclear Fast Red.

2.2.4 Generation of conditioned media (CDM)

FACS-purified ALDH^{lo} and ALDH^{hi} MSC subsets were plated at equal density (13,000 cells/cm^2) and allowed to recover for 8 hours in Amniomax^{TM} media + supplement. After cell adherence, media was replaced with serum and growth-factor deprived endothelial basal media (EBM-2, Lonza, Walkersville, MD) and conditioned for 48 hours before use in subsequent experiments.

2.2.5 HMVEC expansion assays

HMVEC (9,400 cells/cm^2) were cultured in EBM-2, or in CDM generated by purified ALDH^{lo} or ALDH^{hi} MSC subsets generated as described above. As a positive control, HMVEC were also grown in complete Endothelial Growth Medium (EGM-2 = EBM-2 + 5% FBS + IGF, bFGF, EGF, VEGF). Viable HMVEC were enumerated after 72 hours using blinded trypan blue exclusion hemocytometer counts. To assess cell survival and apoptosis kinetics, HMVEC were harvested at 24, 48, and 72 hours analyzed by flow cytometry for Annexin V/7AAD. To quantify cell proliferation, 500 nM EdU was supplemented into HMVEC cultures 24 hours prior to each timepoint. HMVEC were fixed and permeabilized using 10% formalin and 0.1% Triton X and stained for nuclear

EdU-incorporation using the Click-It assay as per manufacturer’s instructions (Life Technologies). Edu-incorporation into proliferating cells was quantified by flow cytometry.

Direct contact co-cultures between HMVEC and MSC subsets were also performed. HMVEC (9,400 cells/mm^2) were seeded at a 1:1 ratio with ALDH^{lo} or ALDH^{hi} MSC and co-cultured in EBM-2 for up to 72 hours. HMVEC alone or ALDH^{lo} or ALDH^{hi} MSC alone were cultured in EBM-2 as controls. Cell survival and proliferation for each cell type was quantified by flow cytometry as described above with addition of CD31 and CD90 antibodies to discern endothelial versus stromal cell types respectively, at each timepoint (24h, 48h, 72h). in mixed cultures.

2.2.6 HMVEC tubule forming assays

To assay for tubule forming function *in vitro*, 120,000 HMVEC were cultured on growth factor-reduced Geltrex^{TM} matrices (Life Technologies) in EBM-2 or in CDM generated from ALDH^{lo} versus ALDH^{hi} MSC subsets. After 24 hours, 4 photomicrographs were taken per well, and tube formation was quantified by manual counting of complete tubes using ImageJ software.

2.2.7 Directed *in vivo* angiogenesis assay (DIVAA)

To compare the pro-angiogenic capacity of ALDH^{lo} versus ALDH^{hi} MSC subsets *in vivo*, the directed *in vivo* angiogenesis assay (DIVAA) was performed as per manufacturer’s instructions. DIVAA inserts with 200,000 ALDH^{lo} and ALDH^{hi} MSC suspended in 20µl basement membrane extract were subcutaneously implanted into the flank of NOD/SCID mice. After 10 days *in vivo*, EC recruitment into each angioreactor was quantified by lectin-uptake, using a SpectraMax plate reader (Molecular Devices, Sunnyvale, CA).

2.2.8 Microarray analysis

mRNA was extracted from 5x10^5 ALDH^{lo} and ALDH^{hi} MSC (N=3) using mRNAeasy mini kits (Qiagen, Dusseldorf, Germany). Sample matched and early-passage (P4) MSC were used to minimize heterogeneity. Nanodrop readings were taken to determine mRNA quality and concentration, and mRNA expression was assessed using Affymetrix 1.0ST human gene array chips (Affymetrix, Santa Clara, CA) at the London Regional Genomics Facility. Data was analyzed using Partek Genomics Suite software (Partek Inc., St. Louis, MO).

2.2.9 Proteomic analysis of CDM

CDM from purified MSC samples (N=3) was generated in biological duplicate and concentrated (≈50-fold) using 3kDa centrifugal filter units (Millipore). Frozen and lyophilized protein extracts were re-suspended in 8M urea, 50mM ammonium bicarbonate, 10mM dithiothreitol and 2% SDS. Protein concentration was measured using the Pierce protein assay (ThermoFisher), and 150 µg total protein was fractionation with SDS-PAGE using 8-20% gels in technical duplicate. Samples were digested using an in-gel protocol with trypsin/LysC (Promega) as previously described[34]. Prepared fractions were injected and separated using a nanoAcuity system (Waters, Milford, MA) on a 25cm long x 75µm inner diameter C18 column maintained at 35°C. All samples were trapped for 5 min at 99% H_2O, 1% acetonitrile, and separated using a 5.0% to 32.5% acetonitrile gradient over 74 min, followed by 60% acetonitrile over 6 min, at a flow rate of 300nL/min. Fractions were quantified using the BCA assay (ThermoFisher Scientific) and 1 µg of material was injected per fraction. Mass spectrometry was performed on an Orbitrap Elite (ThermoFisher Scientific). Full MS parameters are outlined in **Table 2.1**. Data analysis was performed with MaxQuant version 1.5.0.30 using the Andromeda search engine[35]. MS/MS spectra were searched against the Human Uniprot database with trypsin specificity (20264 entries)[36]. Bioinformatic analysis was performed using Perseus version 1.5.0.8. Datasets were filtered for proteins containing a minimum of 1 unique peptide.

Table 2.1 Parameters for mass spectrometry proteomic analyses.

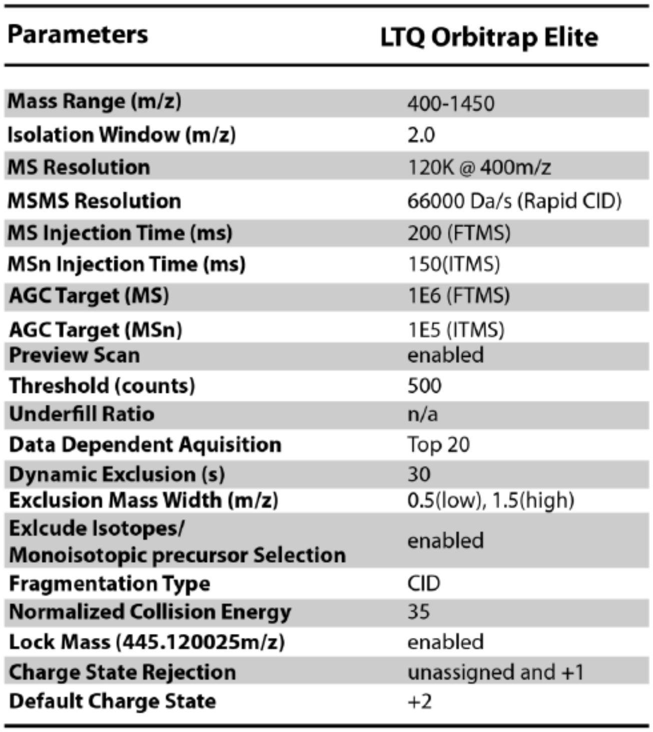

Parameters	LTQ Orbitrap Elite
Mass Range (m/z)	400-1450
Isolation Window (m/z)	2.0
MS Resolution	120K @ 400m/z
MSMS Resolution	66000 Da/s (Rapid CID)
MS Injection Time (ms)	200 (FTMS)
MSn Injection Time (ms)	150(ITMS)
AGC Target (MS)	1E6 (FTMS)
AGC Target (MSn)	1E5 (ITMS)
Preview Scan	enabled
Threshold (counts)	500
Underfill Ratio	n/a
Data Dependent Aquisition	Top 20
Dynamic Exclusion (s)	30
Exclusion Mass Width (m/z)	0.5(low), 1.5(high)
Exlcude Isotopes/ Monoisotopic precursor Selection	enabled
Fragmentation Type	CID
Normalized Collision Energy	35
Lock Mass (445.120025m/z)	enabled
Charge State Rejection	unassigned and +1
Default Charge State	+2

2.2.10 Cytokine arrays

The human angiogenesis array C1 (RayBiotech, Norcross, GA) was used to compare angiogenesis-associated protein composition within CDM from ALDH^{lo} and ALDH^{hi} MSC (N=4). The cytokine arrays were prepared as per manufacturer's instructions and imaged using the Bio-Rad Gel Documentation System (Bio-Rad, Hercules, CA). The relative intensity units for each array feature were quantified by densitometry using the microarray plugin for ImageJ.

2.2.11 Statistical analyses

Analysis of significance for mRNA expression was performed using Partek using algorithms for data normalization, ANOVA, and false discovery rates (FDR<0.05). A multiple sample T-test was performed in Perseus comparing the ALDH^{lo} versus ALDH^{hi} MSC CDM. Analysis of significance was performed by one-way ANOVA with Tukey's multiple comparison tests for the cell survival and proliferation assays, tubule-formation assays, and for the DIVAA experiments.

2.3 Results

2.3.1 ALDH^{lo} and ALDH^{hi} MSC demonstrated multipotent differentiation potential *in vitro*.

At passage 4 (P4), bulk MSC were purified based on ALDH-activity using the Aldefluor^{TM} assay, selecting the top and bottom 30% of fluorescent events while maintaining ≈5-fold difference in fluorescence intensity between ALDH^{lo} and ALDH^{hi} subsets based on DEAB-inhibited controls (**Figure 2.1A**). The ALDH^{lo} and ALDH^{hi} subsets were first assessed for stromal, pericyte, endothelial, and hematopoietic cell surface marker expression. Both subsets showed >95% expression of the stromal markers CD73, CD90, CD105, and the pericyte marker CD146. In contrast, <1% of cells expressed endothelial (CD31) or hematopoietic cell (CD45 and CD14) markers (**Figure 2.1B, C**). Thus, both subsets represented pure stromal cell populations without significant hematopoietic or EC contamination. Next, we performed multipotent differentiation on ALDH^{lo} and ALDH^{hi} subsets. As predicted by cell surface marker expression, both the ALDH^{lo} and ALDH^{hi} subsets equally retained multipotent differentiative capacity into fat, bone, and cartilage lineages *in vitro* (**Figure 2.1D, E**). Collectively, both the ALDH^{lo} and ALDH^{hi} subsets equally fulfill the minimal criteria for MSC established by the International Society of Cellular Therapy[17].

Figure 2.1

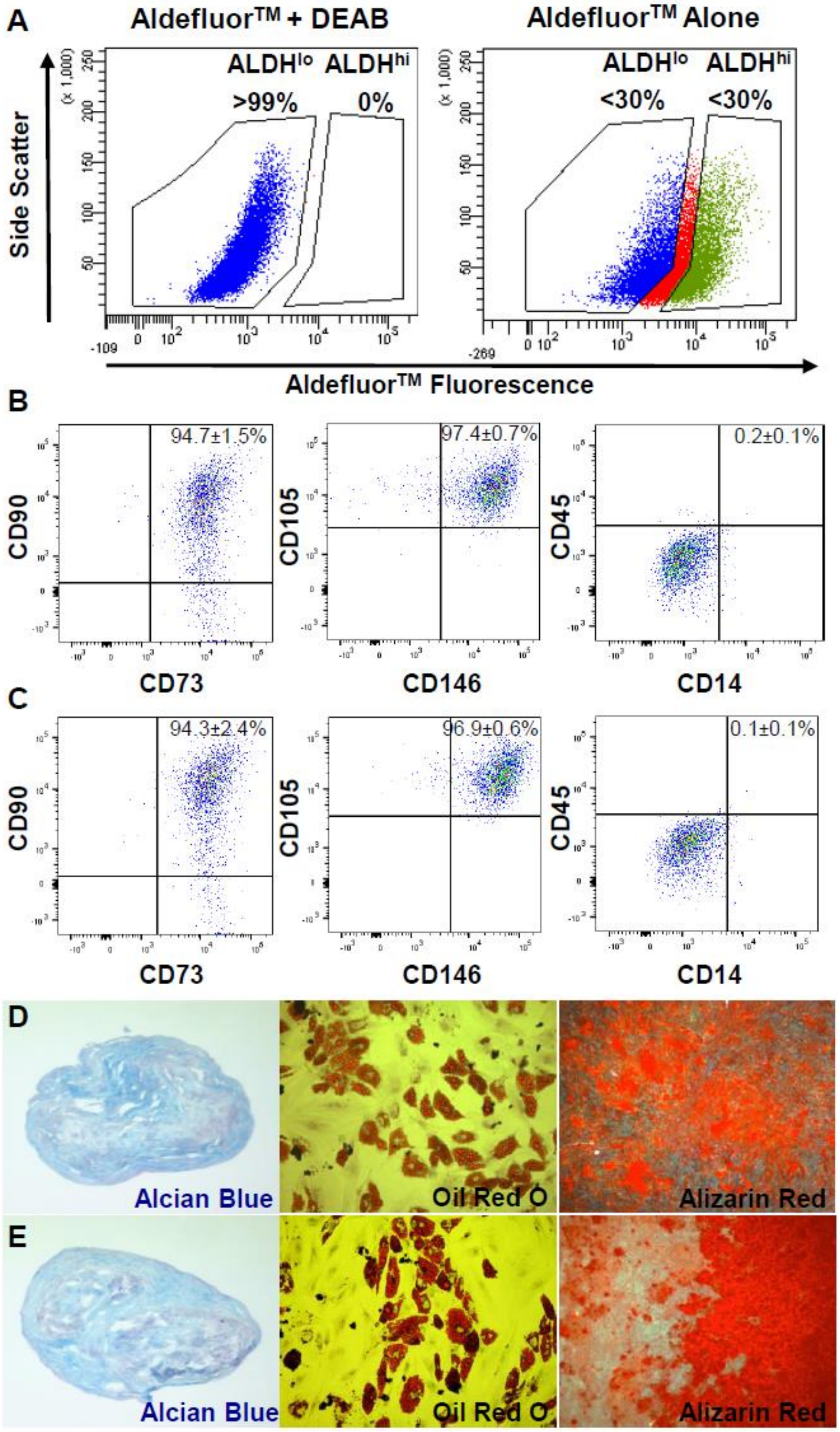
A
Aldefluor™ + DEAB
Aldefluor™ Alone
Side Scatter
(x 1,000)
ALDHlo ALDHhi
>99% 0%
ALDHlo ALDHhi
<30% <30%
Aldefluor™ Fluorescence
-109
-269
B
CD90
CD73
94.7±1.5%
CD105
CD146
97.4±0.7%
CD45
CD14
0.2±0.1%
C
CD90
CD73
94.3±2.4%
CD105
CD146
96.9±0.6%
CD45
CD14
0.1±0.1%
D
Alcian Blue
Oil Red O
Alizarin Red
E
Alcian Blue
Oil Red O
Alizarin Red

Figure 2.1 ALDH^{lo} and ALDH^{hi} MSC subsets expressed stromal and pericyte markers and demonstrated multipotent differentiation *in vitro*. (A) Representative flow cytometry plots showing the selection of human BM-derived MSC with low versus high ALDH activity. ALDH^{hi} MSC were defined as ≈5-fold higher fluorescence than the DEAB control gate, and each subset represented <30% of total events at the bottom and top of fluorescent intensity. (B) ALDH^{lo} and (C) ALDH^{hi} MSC subsets expressed cell surface markers indicating high stromal cell purity (>95% CD73+, CD90+, CD105+, CD45-, CD14-). The perivascular cell marker CD146 was also detected on >95% of ALDH^{lo} and ALDH^{hi} MSC. (D) ALDH^{lo} and (E) ALDH^{hi} MSC demonstrated multipotent differentiation to chondrocytes, adipocytes, and osteocytes. Data is representative of experiments comparing purified MSC from 4-6 human BM samples.

2.3.2 CDM generated by ALDH^{lo} or ALDH^{hi} MSC augmented HMVEC expansion *in vitro*.

To compare the angiogenesis stimulatory potential of the ALDH-purified MSC subsets, HMVEC were grown in CDM generated by ALDH^{lo} versus ALDH^{hi} MSC and cell proliferation and survival were quantified flow cytometric analyses measuring EdU-incorporation and 7AAD / Annexin V detection of apoptotic cells. Representative dot plots for each analysis are shown in **Figure 2.2**. Compared to HMVEC cultured under serum-starved, growth factor-free basal conditions (EBM-2), exposure to ALDH^{lo} or ALDH^{hi} CDM for 72h significantly increased overall HMVEC expansion (**Figure 2.3A**). After 48h exposure to ALDH^{lo} or ALDH^{hi} MSC CDM, HMVEC exhibited increased proliferation (**Figure 2.3B**) and decreased apoptosis (7AAD^{-}/AnnexinV^{+}) (**Figure 2.3C**). The frequency of dead HMVEC (7AAD^{+} / AnnexinV^{+}) was also reduced after 72h exposure to ALDH^{lo} or ALDH^{hi} MSC CDM (**Figure 2.3D**). Thus, CDM from ALDH^{lo} or ALDH^{hi} MSC enhanced HMVEC survival and proliferation under growth-factor depleted conditions *in vitro.*

Figure 2.2

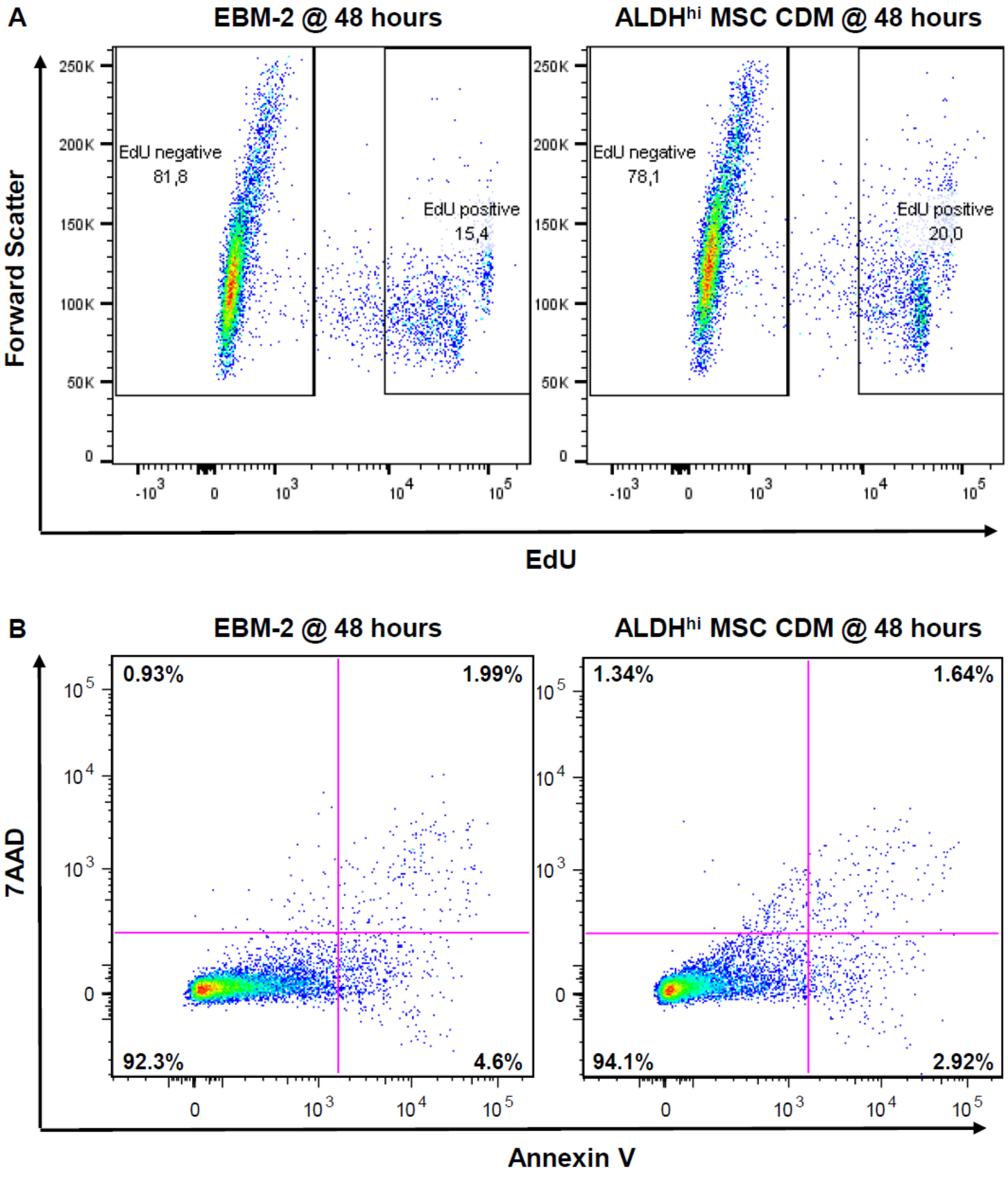

Figure 2.2 Flow cytometric analyses of HMVEC proliferation and survival *in vitro*. Representative flow cytometry plots showing the detection of (A) proliferating (EdU+) cells or (B) viable (7AAD-/Annexin V-), dead (7AAD+/Annexin V+), or apoptotic (7AA-/Annexin V+) cells or under serum-free, growth factor reduced conditions (EBM-2) with or without MSC conditioned media.

Figure 2.3

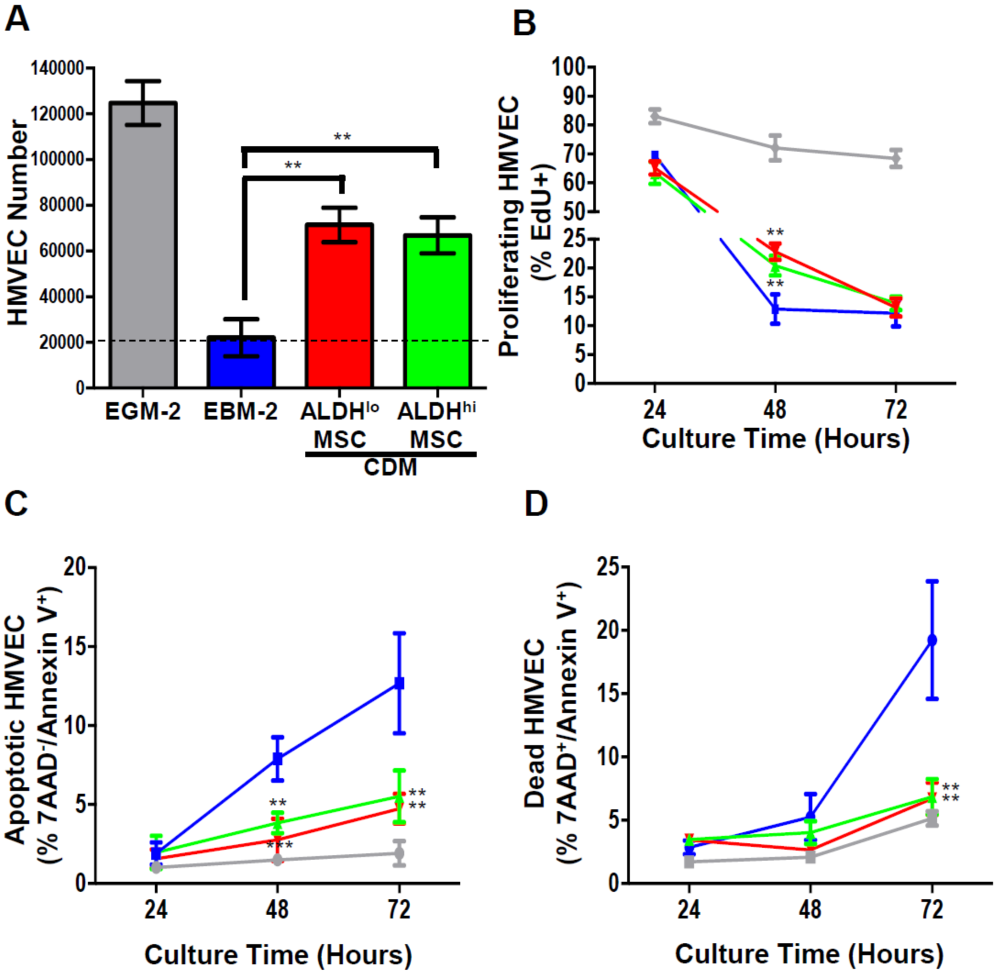

Figure 2.3 Conditioned media generated by ALDH^{lo} or ALDH^{hi} MSC stimulated HMVEC expansion *in vitro*. (A) Exposure to ALDH^{lo} or ALDH^{hi} MSC CDM for 72 hours augmented total HMVEC number compared to serum-free, growth factor-deprived conditions (EBM-2). (B) ALDH^{lo} or ALDH^{hi} MSC CDM increased the frequency of proliferating HMVEC at 48 hours. (C) ALDH^{lo} or ALDH^{hi} MSC CDM decreased the frequency of apoptotic HMVEC (7AAD^{-}/AnnexinV^{+}) at 48 and 72 hours. (D) ALDH^{lo} or ALDH^{hi} MSC CDM reduced the frequency of dead HMVEC (7AAD^{+}/Annexin V^{+}) at 72 hours. Data represents mean ± SEM using purified MSC CDM derived from 3 human BM samples (**p<0.01; ***p<0.001).

2.3.3 Contact co-culture with ALDH^{lo} or ALDH^{hi} MSC did not promote HMVEC expansion.

To assess whether cell contact could further stimulate EC growth, purified MSC subsets were cultured in direct contact with HMVEC under serum-free, growth factor-deprived conditions. Endothelial versus stromal cell phenotype was discerned in mixed cultures using selective CD31 and CD90 expression alongside proliferation and apoptosis assays. Surprisingly, co-culture with ALDH^{lo} or ALDH^{hi} MSC for 72 hours did not augment total HMVEC number compared to uniculture in EBM-2 (**Figure 2.4A**). In fact, contact co-culture with ALDH^{lo} or ALDH^{hi} MSC significantly decreased HMVEC proliferation (**Figure 2.4B**). Although direct co-culture with ALDH^{lo} and ALDH^{hi} MSC significantly decreased the frequency of apoptotic HMVEC at 72 hours (**Figure 2.4C**), there was no difference in the frequency of dead HMVEC over the 72-hour time course (**Figure 2.4D**). Conversely, co-culture with HMVEC significantly increased MSC expansion under serum-free, growth factor-deprived conditions (**Figure 2.5A**). During direct co-culture with HMVEC, the ALDH^{lo} and ALDH^{hi} MSC subsets significantly increased EdU incorporation at 72h compared to the MSC subsets cultured alone (**Figure 2.5B**). Although, no changes were observed in the frequency of apoptotic MSC over 72h (**Figure 2.5C**), the frequency of dead MSC was significantly reduced in ALDH^{lo} and ALDH^{hi} MSC co-cultures at 48 hours compared to the individual MSC controls (**Figure 2.5D**). Contrary to our predicted results, HMVEC presence promoted MSC expansion, whereas MSC presence did not promote HMVEC survival of proliferation under growth factor-restricted conditions.

Figure 2.4

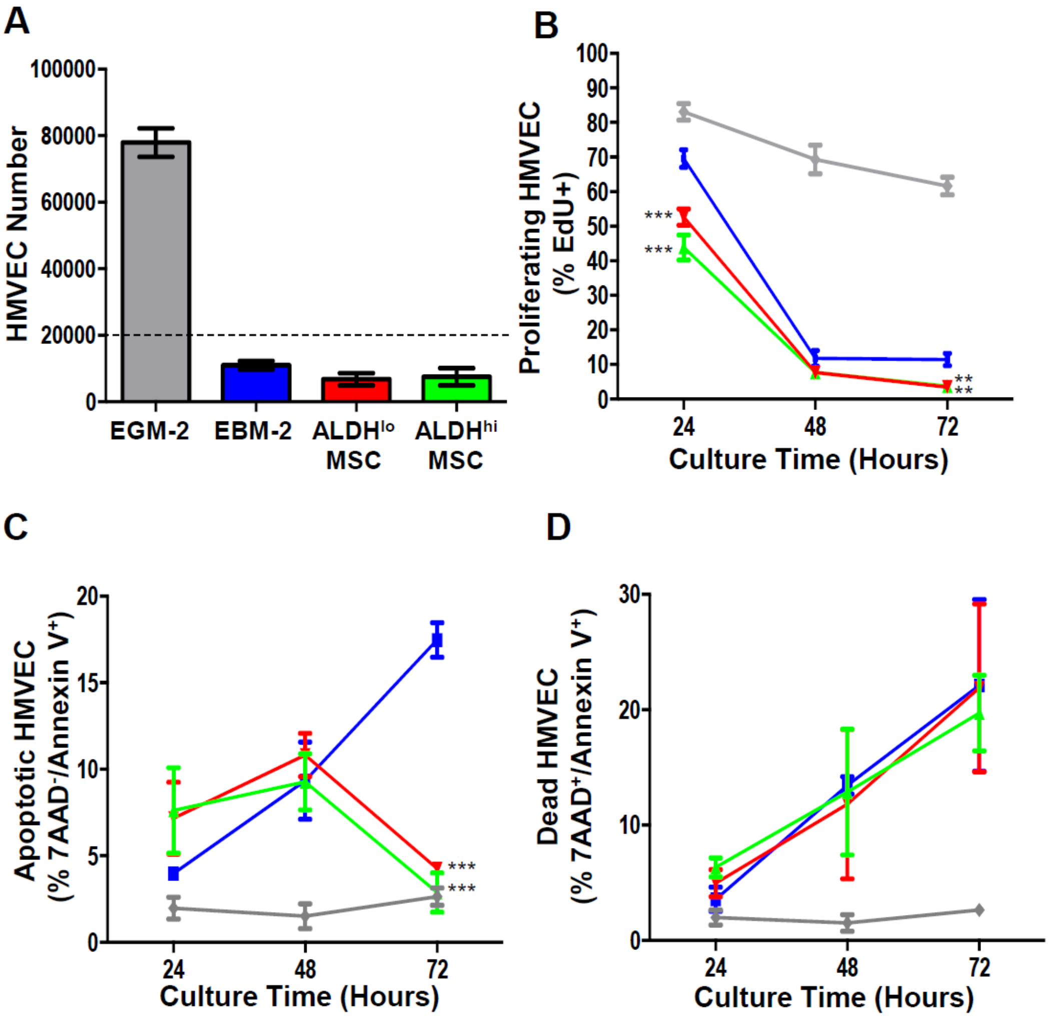

Figure 2.4 Contact co-culture with ALDH^{lo} or ALDH^{hi} MSC did not augment HMVEC expansion *in vitro*. (A) Co-culture with ALDH^{lo} or ALDH^{hi} MSC for 72 hours did not augment total HMVEC number compared to serum-free, growth factor-deprived conditions (EBM-2). (B) Co-culture with ALDH^{lo} and ALDH^{hi} MSC decreased the frequency of proliferating HMVEC at 24 and 72 hours. (C) Co-culture with ALDH^{lo} and ALDH^{hi} MSC decreased the frequency of apoptotic HMVEC (7AAD$^-$/AnnexinV$^+$) at 72 hours only. (D) Co-culture with ALDH^{lo} and ALDH^{hi} MSC did not change the frequency of dead HMVEC (7AAD$^+$/AnnexinV$^+$). Data represents mean ± SEM using purified MSC from 3 human BM samples (**p<0.01; ***p<0.001).

Figure 2.5

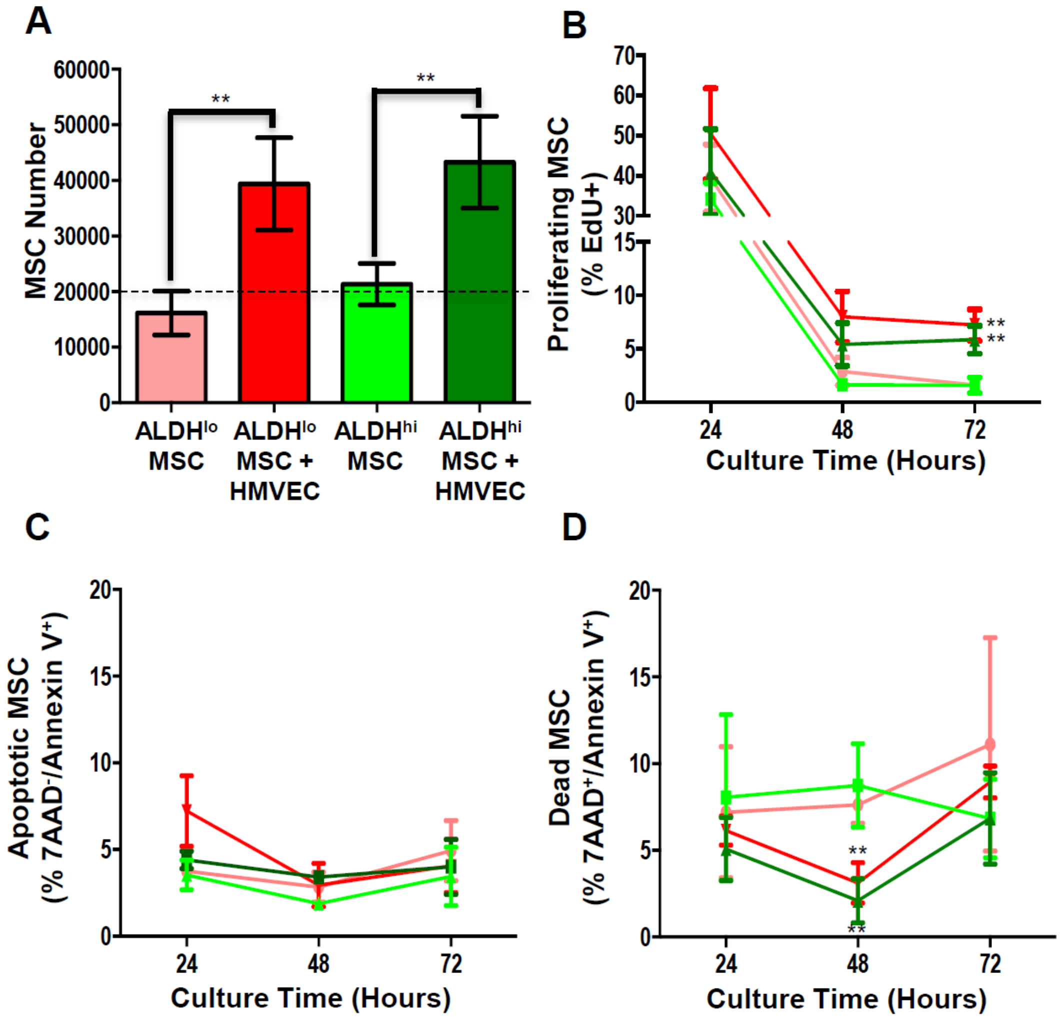

Figure 2.5 Contact co-culture with HMVEC augmented ALDH^{lo} and ALDH^{hi} MSC expansion *in vitro*. (A) Contact co-culture with HMVEC for 72 hours augmented total ALDH^{lo} or ALDH^{hi} MSC number under serum-free, growth factor-deprived conditions. (B) Co-culture with HMVEC increased the frequency of proliferating ALDH^{lo} and ALDH^{hi} MSC at 72 hours. (C) Co-culture with HMVEC did not alter the frequency of apoptotic MSC (7AAD$^-$/AnnexinV$^+$). (D) Co-culture with HMVEC decreased the frequency of dead ALDH^{lo} and ALDH^{hi} MSC (7AAD$^+$/AnnexinV$^+$). Data represents mean ± SEM using purified MSC from 3 human BM samples (**p<0.01).

2.3.4 ALDH^{hi} MSC CDM augmented HMVEC tube formation.

Using a similar strategy to measure HMVEC function, HMVEC were exposed to CDM generated from ALDH^{lo} or ALDH^{hi} MSC subsets and spontaneous tubule formation was quantified in growth factor-reduced Geltrex^{TM} matricies (**Figure 2.6A-D**). Although proliferative and pro-survival effects were demonstrated by CDM from both MSC subsets, only CDM generated by ALDH^{hi} MSC augmented tube forming capacity *in vitro* compared to the EBM-2 condition (**Figure 2.6E**).

Figure 2.6

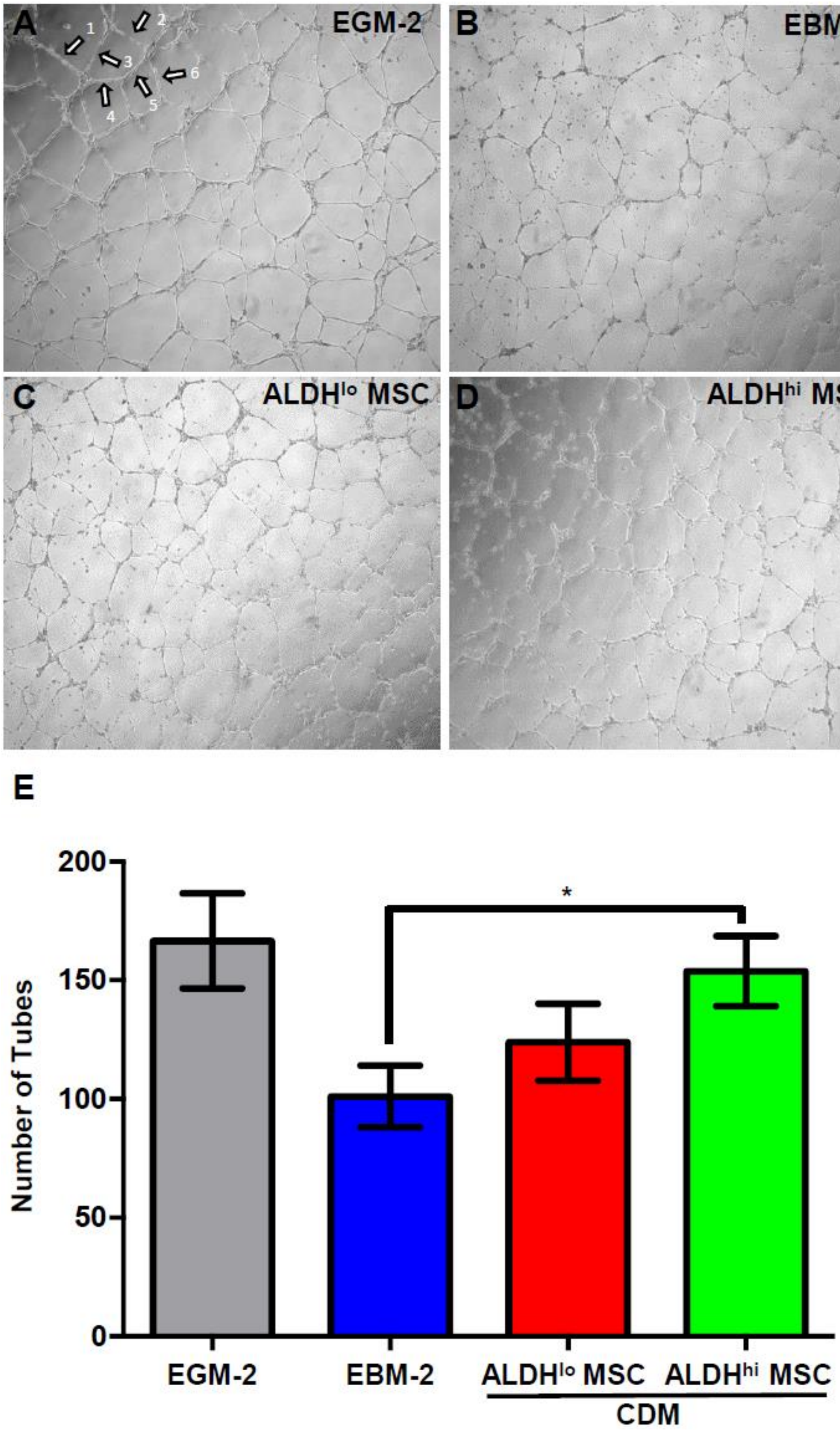
A
EGM-2
1
2
3
4
5
6
B
EBM-2
C
ALDH^{lo} MSC
D
ALDH^{hi} MSC
E
Number of Tubes
200
150
100
50
0
*
EGM-2
EBM-2
ALDH^{lo} MSC
ALDH^{hi} MSC
CDM

Figure 2.6 Conditioned media generated by ALDH^{hi} MSC augmented HMVEC tube formation *in vitro*. (A-D) Representative images of HMVEC tube formation after 24 hours culture in growth factor reduced Geltrex^{TM} matricies supplemented with (A) EGM-2, (B) EBM-2, (C) ALDH^{lo} MSC CDM, or (D) ALDH^{hi} MSC CDM. White arrows indicate examples of enumerated complete tubule branches. (E) Conditioned media derived from the ALDH^{hi} MSC subset augmented tube formation compared to HMVEC grown in EBM-2. Data is represented as mean ± SEM using purified MSC from 4 human BM samples (*$p<0.05$).

2.3.5 ALDH^{hi} MSC augmented EC recruitment into DIVAA inserts.

To assess angiogenesis stimulatory function by human MSC subsets *in vivo*, 2x10^{5} ALDH^{lo} or ALDH^{hi} MSC were loaded into DIVAA inserts and subcutaneously implanted into NOD/SCID mice for 10 days. Representative images of the excised angioreactors shows erythrocyte invasion into the ALDH^{hi} MSC containing angioreactor similar to VEGF/FGF containing controls (**Figure 2.7A**). After measurement of lectin uptake in 6-9 DIVAA inserts per group, the ALDH^{hi} MSC subset significantly increased EC content within the angioreactor compared to the ALDH^{lo} MSC subset (**Figure 2.7B**). Next, concentrated CDM from ALDH^{lo} or ALDH^{hi} MSC subsets was loaded into angioreactors and subcutaneously transplanted into NOD/SCID mice. Lectin uptake was significantly increased in inserts containing ALDH^{hi} MSC CDM compared to ALDH^{lo} MSC CDM or concentrated EBM-2 (**Figure 2.7C)**. Thus, CDM generated specifically by the ALDH^{hi} MSC subset stimulated EC recruitment into angioreactors *in vivo*.

Figure 2.7

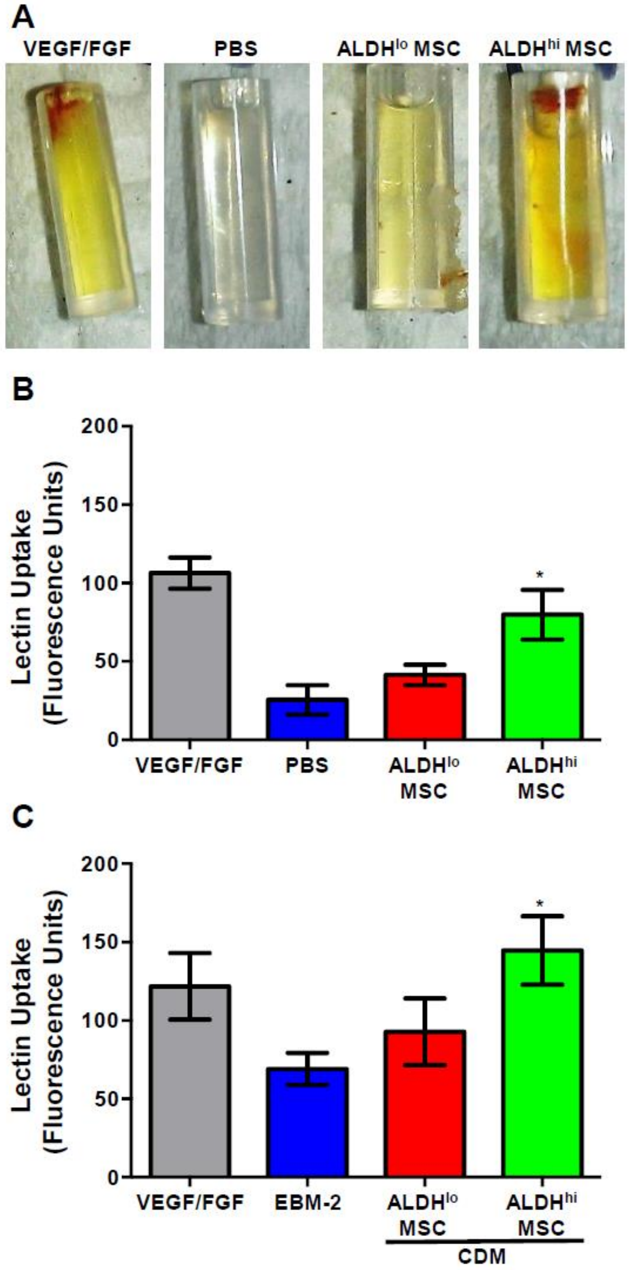

Figure 2.7 Implantation of ALDH^{hi} MSC increased endothelial cell invasion into Directed *In Vivo* Angiogenesis Assay (DIVAA) Inserts. (A) Representative images of DIVAA angioreactors loaded with a BME combined with ALDH$^{hi/lo}$ MSC, EBM, or a VEGF/FGF cocktail retrieved 10 days after subcutaneous implantation. EC invasion was measured using lectin-FITC uptake. (B) Implantation of ALDH^{hi} MSC increased EC invasion into the angioreactor compared to the ALDH^{lo} MSC. (C) Concentrated conditioned media generated from the ALDH^{hi} MSC subset also increased EC invasion into the angioreactor. Data is represented as mean ± SEM for 3 human BM samples performed in triplicate (*p<0.05).

2.3.6 ALDH^{lo} and ALDH^{hi} MSC demonstrated similar mRNA expression.

Affymetrix microarrays were performed to compare global mRNA expression between ALDH^{lo} and ALDH^{hi} MSC subsets. As predicted by functional analyses using HMVEC co-culture *in vitro,* purified ALDH^{lo} and ALDH^{hi} MSC showed remarkably similar mRNA expression patterns. Volcano plot analyses marked only 51 mRNAs with >1.2-fold differential expression ($p<0.05$) (**Figure 2.8A**). Indeed, principal component analyses indicated considerable sample variability between each MSC line with lower variation between sample-matched ALDH^{lo} and ALDH^{hi} MSC subsets (**Figure 2.8B**). Collectively, only 29 mRNAs showed increased expression (>1.2-fold, $p<0.05$) comparing ALDH^{hi} to ALDH^{lo} MSC. Within these mRNAs, 11 had unknown function, 4 were non-coding, and 4 had pseudogene classification. Conversely, only 21 mRNAs showed decreased expression (<-1.2-fold, $p<0.05$) in ALDH^{hi} MSC. Within these mRNAs, 15 had unknown function, were non-coding, or had pseudogene classification. **Table 2.2** annotates the predicted functions of the 15 differentially expressed mRNAs identified. Interestingly, ALDH1A3 mRNA expression was increased 2-fold in the ALDH^{hi} MSC subset. Because ALDH1A3 is a predominant isoform implicated in Aldefluor metabolism, increased ALDH 1A3 expression is expected in MSC selected for high ALDH-activity and validates the accuracy of our sorting and subsequent mRNA expression analyses (**Table 2.2**), Overall, mRNA expression between the ALDH^{lo} and ALDH^{hi} MSC was remarkably similar, and the few differentially expressed mRNAs showed no obvious link to angiogenic secretory functions.

Figure 2.8

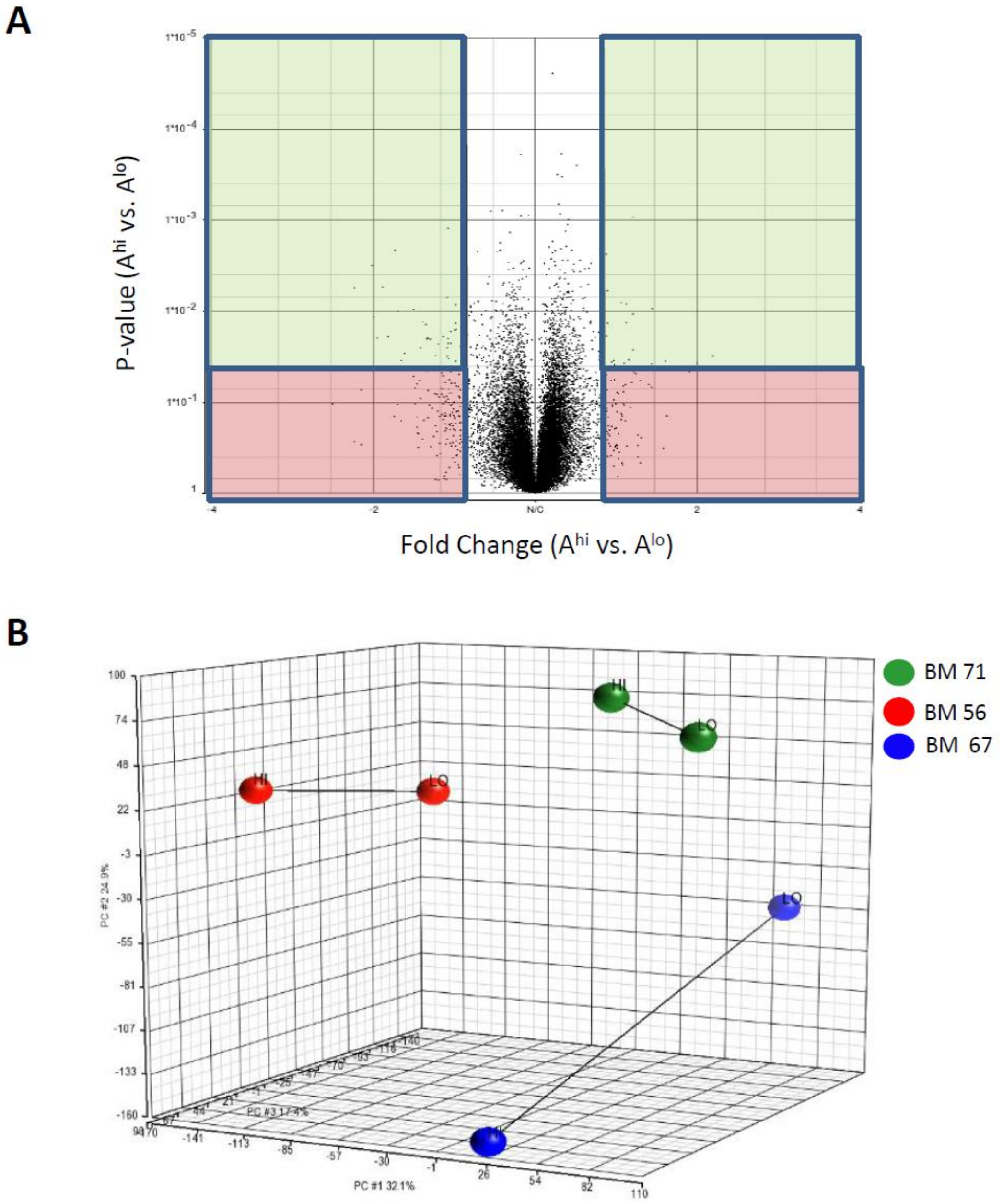

Figure 2.8 Global mRNA expression was similar comparing ALDH^{lo} versus ALDH^{hi} MSC subsets. (A) Volcano plot showing the vast majority of mRNAs had <1.2-fold difference in expression with a P-value >0.05. Only 51 genes met statistical criteria ($p<0.05$) with >1.2-fold expression change between ALDH^{lo} and ALDH^{hi} MSC subsets (see **Table 2.2**). (B) Principal component analysis indicated greater variation existed between individual samples than between sample-matched ALDH^{lo} and ALDH^{hi} MSC subsets.

Table 2.2 Differentially expressed mRNAs comparing ALDH^{lo} versus ALDH^{hi} MSC subsets.

GENE SYMBOL	PROTEIN	FUNCTION	FOLD-CHANGE (HI VS. LO)
ALDH1A3	**Aldehyde Dehydrogenase 1 Family, Member A3**	**Retinal Metabolism**	**2**
ZNF716	Zinc Finger Protein 716	DNA-binding	1.47367
IGSF9B	Immunoglobulin Superfamily, Member 9B	Kinase binding	1.26755
SEC14L4	SEC14-like 4 (S. cerevisiae)	Biogenesis of Golgi-derived vesicles	1.26633
SLC16A12	Solute Carrier Family 16, Member 12	monocarboxylic acid transport	1.25721
KRTAP4-5	Keratin Associated Protein 4-5	Keratin associated proteins - contributes to hair fibre structure	1.21836
DHRS7C	**Dehydrogenase/Reductase SDR Family Member 7C**	**retinol dehydrogenase activity**	**1.21449**
COX7B	Cytochrome C Oxidase Subunit VIIb	Catalyzes electron transfer from cytochrome C to O2 in the ETC	1.2103
MAGEB3	Melanoma Antigen Family B3	Directs expression of tumor antigens	1.20885
AMELX	Amelogenin, X-Linked	Biomineralization during enamel development	1.2029
NGDN	Neuroguidin OR EIF4E Binding Protein	Translational regulatory protein during development of the vertebrate nervous system	-1.20094
ALX1	ARISTALESS-LIKE HOMEOBOX 1 Aristaless-like homeobox 1 (ALX homeobox 1)	(rodents) Survival of the forebrain mesenchyme	-1.20438
TXNIP	Thioredoxin Interacting Protein	Oxidative stress mediator via thioredoxin inhibition	-1.22902
OSGEP	O-Sialoglycoprotein Endopeptidase	Required for the formation of a threonylcarbamoyl group on adenosine	-1.28232
EIF4A2	Eukaryotic Translation Initiation Factor 4A2	ATP-dependent RNA helicase required for mRNA binding to ribosome	-1.30481
AREG	**Amphiregulin**	**Epidermal Growth Factor family**	**-1.31488**

2.3.7 ALDH^{hi} MSC demonstrated a pro-angiogenic secretome.

ALDH^{lo} and ALDH^{hi} MSC subsets (N=3) were incubated in EBM-2 for 48h to generate CDM for global secretome analyses using mass spectrometry. A total of 2482 proteins were detected, 501 proteins were unique to ALDH^{lo} MSC CDM, 264 proteins were unique to ALDH^{hi} MSC CDM, and 1717 proteins were commonly produced by both subsets. These lists were annotated and filtered using GO-cellular component terms associated with the extracellular space or secreted fraction or signal peptide, inclusive of membrane-bound proteins (92 peptides). As an additional criterion, we annotated and filtered based on GO-molecular function terms associated with angiogenesis (tube formation, EC proliferation, migration, matrix modification, etc.). These analyses identified 10 cytokines unique to the ALDH^{hi} CDM (**Table 2.3A**) all associated with the positive regulation of angiogenesis. Several unique factors (VEGFB, PDGFA, Plexin D1, Angiogenin) were directly associated with EC proliferation, differentiation, tubule formation and migration, and several others were important developmental factors (Wnt5A, Spondin1, and activin A receptor) linked angiogenic processes. No proteins unique to the ALDH^{hi} CDM had documented anti-angiogenic effects (**Table 2.3A**). The 501 unique factors in the ALDH^{lo} CDM were analyzed in an identical fashion and revealed 9 secreted proteins (**Table 2.3B**). Only one protein, angiopoietin-like 3 (ANGPTL3), had confirmed pro-angiogenic activity, whereas 3 proteins unique to the ALDH^{lo} MSC CDM (Platelet Factor 4, Tyrosine Kinase 1 (TIE1), and Plasminogen) had documented anti-angiogenic functions (**Table 2.3B**).

A direct comparison of proteins common to the ALDH^{lo} and ALDH^{hi} secretome revealed few differences in the amount of secreted products that were >1.5-fold or <-1.5-fold different in ALDH^{hi} MSC CDM compared to ALDH^{lo} MSC CDM (**Figure 2.9**). Label-free quantitation intensities in >5 of 6 sample replicates (1351 peptides) were again annotated and filtered using GO-cellular component terms associated with the extracellular space or secreted fraction, inclusive of membrane-bound proteins (698 peptides, **Figure 2.9**), and a multiple sample T-test was performed to obtain differentially secreted proteins (**Table 2.4**). Interestingly, there were several factors secreted more highly in the ALDH^{lo} MSC subset with the potential to promote (myeloid derived growth factor and PLAUR) or inhibit angiogenic process such as ADAMTS12 (**Table 2.4**).

To validate the proteomic analyses, ALDH^{lo} and ALDH^{hi} MSC subset CDM (48h in EBM-2) were also assayed for cytokine/chemokine secretion using the Human Angiogenesis array C1 multiplex-ELISA. ALDH^{hi} MSC and ALDH^{lo} MSC showed similar secretory patterns with both MSC subsets secreted similar quantities of angiogenin, GRO, IL-6, IL-8, MCP-1, RANTES, TGF-β, TIMP-1/2 and VEGF (**Figure 2.10**). Overall, these secretome analyses suggested the ALDH^{hi} MSC subset demonstrated a secretory profile consistent with the stimulation of EC proliferation, migration, tube formation and the chemoattraction of pro-angiogenic accessory cells.

Table 2.3 Secreted proteins unique to CDM generated by ALDH^{hi} MSC or ALDH^{lo} MSC.

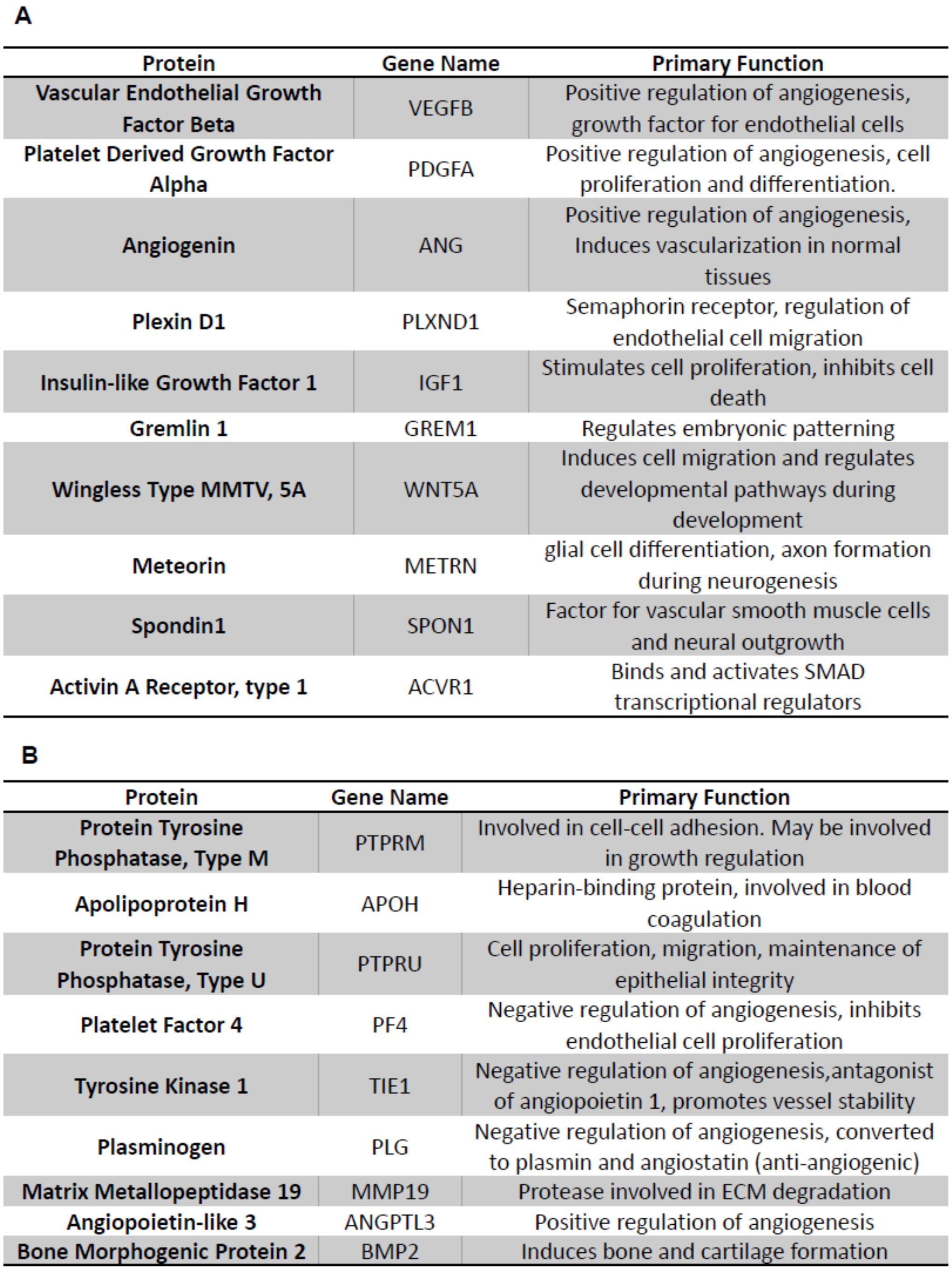

A

Protein	Gene Name	Primary Function
Vascular Endothelial Growth Factor Beta	VEGFB	Positive regulation of angiogenesis, growth factor for endothelial cells
Platelet Derived Growth Factor Alpha	PDGFA	Positive regulation of angiogenesis, cell proliferation and differentiation.
Angiogenin	ANG	Positive regulation of angiogenesis, Induces vascularization in normal tissues
Plexin D1	PLXND1	Semaphorin receptor, regulation of endothelial cell migration
Insulin-like Growth Factor 1	IGF1	Stimulates cell proliferation, inhibits cell death
Gremlin 1	GREM1	Regulates embryonic patterning
Wingless Type MMTV, 5A	WNT5A	Induces cell migration and regulates developmental pathways during development
Meteorin	METRN	glial cell differentiation, axon formation during neurogenesis
Spondin1	SPON1	Factor for vascular smooth muscle cells and neural outgrowth
Activin A Receptor, type 1	ACVR1	Binds and activates SMAD transcriptional regulators

B

Protein	Gene Name	Primary Function
Protein Tyrosine Phosphatase, Type M	PTPRM	Involved in cell-cell adhesion. May be involved in growth regulation
Apolipoprotein H	APOH	Heparin-binding protein, involved in blood coagulation
Protein Tyrosine Phosphatase, Type U	PTPRU	Cell proliferation, migration, maintenance of epithelial integrity
Platelet Factor 4	PF4	Negative regulation of angiogenesis, inhibits endothelial cell proliferation
Tyrosine Kinase 1	TIE1	Negative regulation of angiogenesis,antagonist of angiopoietin 1, promotes vessel stability
Plasminogen	PLG	Negative regulation of angiogenesis, converted to plasmin and angiostatin (anti-angiogenic)
Matrix Metallopeptidase 19	MMP19	Protease involved in ECM degradation
Angiopoietin-like 3	ANGPTL3	Positive regulation of angiogenesis
Bone Morphogenic Protein 2	BMP2	Induces bone and cartilage formation

(A) Within ALDH^{hi} MSC CDM, multiple unique factors were identified that were associated with the positive regulation of angiogenesis (bold). (B) Conversely, multiple proteins unique to the CDM generated by ALDH^{lo} MSC were negative regulators of angiogenesis (*italics*). Unique peptides were identified with a false detection rate (FDR) of 0.01, N=3 MSC samples performed in duplicate. Primary functional annotations were obtained from GeneCards.

Figure 2.9

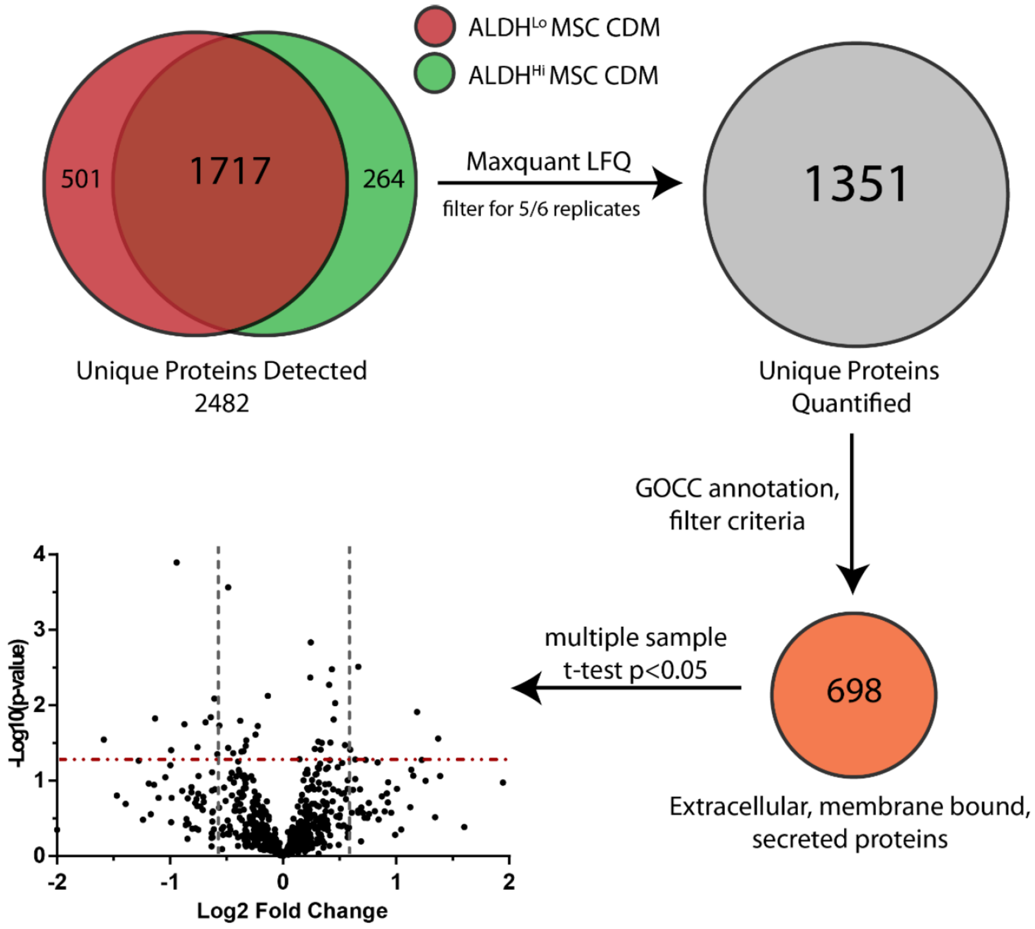
ALDH^{Lo} MSC CDM
ALDH^{Hi} MSC CDM
501
1717
264
Unique Proteins Detected
2482
Maxquant LFQ
filter for 5/6 replicates
1351
Unique Proteins
Quantified
GOCC annotation,
filter criteria
698
Extracellular, membrane bound,
secreted proteins
multiple sample
t-test p<0.05
-Log10(p-value)
4
3
2
1
0
-2
-1
0
1
2
Log2 Fold Change

Figure 2.9 Comparison of protein content in conditioned media generated from ALDH^{lo} versus ALDH^{hi} MSC. Conditioned media generated from 3 bone marrow MSC samples were analyzed in biological duplicate by mass spectrometry. Shared proteins (1717 peptides) were first filtered by label-free quantitation (LFQ) intensities in >5 of 6 sample replicates (1351 peptides). The protein list was annotated and filtered using GO-cellular component terms associated with the extracellular space or secreted fraction, inclusive of membrane-bound proteins (698 peptides). Biological replicates were averaged, and a multiple sample T-test was performed to obtain differentially secreted proteins ($p<0.05$).

Table 2.4 Proteins differentially secreted from ALDH^{hi} versus ALDH^{lo} MSC.

Protein Name	Gene Name	Protein Function	Fold Change (A^{hi} vs. A^{lo})
Prothymosin alpha	PTMA	May be involved in immune resistance	2.967
Thy-1 membrane glycoprotein	THY1	Plays a role in cell-cell/cell-ligand interactions	2.508
Proteoglycan 4	PRG4	Prevents protein deposition onto cartilage in synovial joints	2.420
Cullin-associated NEDD8-dissociated protein 1	CAND1	SCF assembly factor	1.744
Biglycan	BGN	Collagen fibre assembly	-1.509
Neural cell adhesion molecule 1	NCAM1	Cell-cell interaction and cell-matrix interaction	-1.528
Myeloid derived growth factor	C19orf10	Stimulates endothelial cell proliferation and cardiac cell survival	-1.556
Disintegrin and metalloproteinase domain-containing protein 10	ADAM10	Cleaves cell surface proteins including TNF-alpha and E-cadherin	-1.557
Ataxin-10	ATXN10	Neuron survival, differentiation, and neuritogenesis	-1.607
Fibronectin Leucine-rich transmembrane protein	FLRT2	cell adhesion, migration, and axon guidance	-1.808
Urokinase plasminogen activator surface receptor	PLAUR	Promotes plasminogen formation/localization	-1.876
Disintegrin and metalloproteinase with thrombospondin motifs 12	ADAMTS12	Involved in aggrecan cleavage and anti-angiogenic properties	-2.070
Glypican-1	GPC1	Cell division and growth regulation	-2.497
Insulin-like growth factor-binding protein 5	IGFBP5	Prolongs half life of insulin growth factors.	-2.540
Ig gamma-1 chain C region (heavy chain)	IGHG1	heavy chain immunoglobulin	-2.992

* Peptides identified using at least one unique peptide with a false detection rate of 0.01, N=3, performed in duplicate. Functional annotations obtained from GeneCards.org.

Figure 2.10

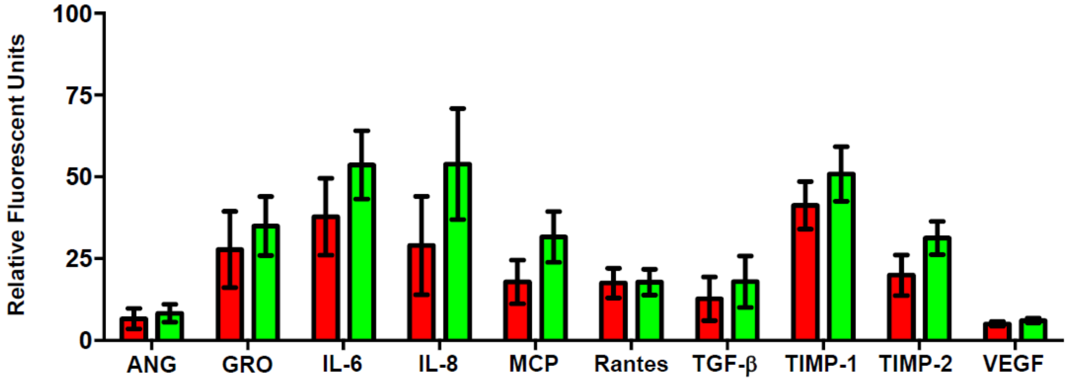

Figure 2.10 Multiplex-ELISA of conditioned media from ALDH^{lo} versus ALDH^{hi} MSC. Conditioned media generated the ALDH^{lo} or ALDH^{hi} MSC subsets was generated for 48 hours in EBM-2 assayed by the human angiogenesis array C1. Both the ALDHl^{o} and ALDH^{hi} MSC subset secreted similar quantities of angiogenin, GRO, IL-6, IL-8, MCP-1, RANTES, TGF-β, TIMP-1/2 and VEGF. All chemo-luminescence values were semi-quantitative. Data is represented as mean ± SEM for 5 human BM samples performed in triplicate.

2.4 Discussion

Cultured MSC represent a heterogeneous mixture of stromal cells amenable to novel cellular therapy applications, due to purported immunomodulatory[37-39] and regenerative paracrine effects[20, 21]. Here we demonstrate expanded MSC purified based on high ALDH-activity selects for an MSC sub-fraction with enhanced pro-angiogenic characteristics. Direct comparison of ALDH^{lo} versus ALDH^{hi} MSC subsets showed identical cell surface marker expression and differentiation into bone, cartilage and adipose tissues *in vitro*. In addition, CDM from both ALDH^{lo} and ALDH^{hi} MSC subsets demonstrated remarkable effects on endothelial cell functions *in vitro*. Detailed comparison of survival / proliferation kinetics every 24 hours revealed MSC CDM increased HMVEC proliferation early in culture (48h), and subsequently reduced apoptosis and cell death later in culture (48-72h). Although CDM from both MSC subtypes augmented HMVEC expansion, only ALDH^{hi} MSC CDM significantly increased HMVEC tubule formation *in vitro*. Thus, only ALDH^{hi} MSC CDM was able to support both endothelial cell expansion and tubule forming functions *in vitro*.

Surprisingly, contact co-culture with ALDH^{lo} or ALDH^{hi} MSC subsets did not augment HMVEC survival or proliferation in serum-free EBM-2 media. In fact, HMVEC proliferation was decreased during co-culture, while MSC subset proliferation and survival was increased. As previously reported by Dhahri et al[40], our co-culture data suggested the presence of HMVEC supported MSC expansion, while the presence of MSC had little effect on HMVEC growth.

After incubation for 10 days in NOD/SCID mice, subcutaneously implanted DIVAA angioreactors containing ALDH^{hi} MSC or ALDH^{hi} MSC CDM increased endogenous vascular cell recruitment measured by lectin uptake. Interestingly, vascularization of angioreactors containing the ALDH^{hi} MSC CDM was equivalent to angioreactors containing a VEGF/FGF cocktail employed as a positive control. Furthermore, ALDH^{lo} MSC or its CDM did not promote endogenous cell recruitment compared to control angioreactors. This data suggests that ALDH^{hi} MSC uniquely support the generation of a pro-angiogenic niche through secretion of chemokines or cytokines that augment recruitment or stimulate the activation of endogenous endothelial cells *in vivo*.

Purified ALDH^{lo} and ALDH^{hi} MSC subsets were also compared for differences in mRNA expression using Affymetrix arrays. The expression patterns of the ALDH^{lo} versus ALDH^{hi} MSC subsets were strikingly similar. Interestingly, PCA analysis of the microarray data indicates that high variability exists between each MSC line and lower variability exists between ALDH^{lo} and ALDH^{hi} MSC within samples. Indeed, the largest mRNA expression difference (2-fold) between purified MSC populations was ALDH1A3, reflecting the enzymatic function used to sort the cells at the onset of experiments. Thus, analyses of transcription profiles using microarray did not account for the enhanced capacity of ALDH^{hi} MSC to induce pro-angiogenic processes.

Next, we carefully analyzed protein secretion into conditioned media generated by ALDH^{lo} and ALDH^{hi} MSC subsets using highly-sensitive proteomic techniques, as post-transcriptional regulation may permit small changes in transcription to give rise to larger changes in protein secretion. Quantitative mass spectrometry analyses revealed that ALDH^{hi} MSC uniquely secreted several well-known pro-angiogenic growth factors (VEGFB, PDGFA, and Angiogenin) not present in the secretome of ALDH^{lo} MSC. Conversely, the ALDH^{lo} MSC CDM contained potent anti-angiogenic factors (platelet factor-4, plasminogen) not present in the ALDH^{hi} MSC CDM. For example, platelet factor 4, or CXCL4, was the first chemokine shown to inhibit endothelial cell proliferation and migration via direct interaction and interference with bFGF, VEGFA and integrin signalling[41]. Plasminogen, through proteolytic conversion to angiostatin enables inhibition of angiogenesis through direct interaction with endothelial cells[42, 43]. Judah Folkman first established the principles of angiogenesis describing that vessel advancement or regression is controlled by a series of on/off switches within the microenvironment[44]. Using this model, the secretome of ALDH^{lo} MSC was consistent with the promotion of anti-angiogenic processes, whereas the ALDH^{hi} MSC secretome was consistent with the promotion of pro-angiogenic processes.

This study outlines several advances relevant to the development of pro-angiogenic therapies. First, ALDH^{hi} MSC can be purified after culture based on a conserved progenitor function where cell surface markers have not been successful identifying MSC with specific regenerative functions. Second, MSC selection can reduces heterogeneity and can purify an “active” MSC subset with enhanced pro-angiogenic secretory functions. Third, the potential use of allogeneic ALDH^{hi} MSC for the treatment of ischemic diseases is an exciting possibility as mounting evidence indicates the potential for cellular dysfunction by autologous MSC in patients with cardiovascular co-morbidities. Finally, only the re-selected MSC progeny with high ALDH-activity retained pro-angiogenic niche forming capacity after implantation *in vivo*. Thus, the delivery of BM ALDH^{hi} MSC into patients with CLI, may be used in future clinical strategies to mediate pro-angiogenic benefit.

2.5 References

1. Fowkes, F.G.R., et al., *Comparison of global estimates of prevalence and risk factors for peripheral artery disease in 2000 and 2010: a systematic review and analysis.* The Lancet, 2013. **382**(9901): p. 1329-1340.

2. Criqui, M.H. and V. Aboyans, *Epidemiology of peripheral artery disease.* Circulation research, 2015. **116**(9): p. 1509-1526.

3. Lawall, H., P. Bramlage, and B. Amann, *Treatment of peripheral arterial disease using stem and progenitor cell therapy.* Journal of vascular surgery, 2011. **53**(2): p. 445-453.

4. Makowsky, M., et al., *Prevalence and treatment patterns of lower extremity peripheral arterial disease among patients at risk in ambulatory health settings.* Can J Cardiol, 2011. **27**(3): p. 389 e11-8.

5. Davies, J.E., *Criticial Limb Ischemia: Epidemiology.* MDCVJ, 2012. **3**(4): p. 1.

6. Tateishi-Yuyama, E., et al., *Therapeutic angiogenesis for patients with limb ischaemia by autologous transplantation of bone-marrow cells: a pilot study and a randomised controlled trial.* The Lancet, 2002. **360**(9331): p. 427-435.

7. Matoba, S., et al., *Long-term clinical outcome after intramuscular implantation of bone marrow mononuclear cells (Therapeutic Angiogenesis by Cell Transplantation [TACT] trial) in patients with chronic limb ischemia.* Am Heart J, 2008. **156**(5): p. 1010-8.

8. Fadini, G.P., D. Losordo, and S. Dimmeler, *Critical reevaluation of endothelial progenitor cell phenotypes for therapeutic and diagnostic use.* Circulation research, 2012. **110**(4): p. 624-637.

9. Storms, R.W., et al., *Isolation of primitive human hematopoietic progenitors on the basis of aldehyde dehydrogenase activity.pdf>.* PNAS, 1999. **96**: p. 6.

10. Capoccia, B.J., et al., *Revascularization of ischemic limbs after transplantation of human bone marrow cells with high aldehyde dehydrogenase activity.* Blood, 2009. **113**(21): p. 5340-51.

11. Hess, D.A., et al., *Functional characterization of highly purified human hematopoietic repopulating cells isolated according to aldehyde dehydrogenase activity.* Blood, 2004. **104**(6): p. 1648-55.

12. Hess, D.A., et al., *Widespread Nonhematopoietic Tissue Distribution by Transplanted Human Progenitor Cells with High Aldehyde Dehydrogenase Activity.* Stem Cells, 2008. **26**(3): p. 611-620.

13. Bell, G.I., et al., *Transplanted human bone marrow progenitor subtypes stimulate endogenous islet regeneration and revascularization.* Stem Cells Dev, 2012. **21**(1): p. 97-109.

14. Bell, G.I., et al., *Intrapancreatic delivery of human umbilical cord blood aldehyde dehydrogenase-producing cells promotes islet regeneration.* Diabetologia, 2012. **55**(6): p. 1755-1760.

15. Putman, D.M., et al., *Umbilical Cord Blood-Derived Aldehyde Dehydrogenase-Expressing Progenitor Cells Promote Recovery from Acute Ischemic Injury.* Stem Cells, 2012. **30**(10): p. 2248-2260.

16. Perin, E.C., et al., *Rationale and design for PACE: patients with intermittent claudication injected with ALDH bright cells.* Am Heart J, 2014. **168**(5): p. 667-73.

17. Dominici, M., et al., *Minimal criteria for defining multipotent mesenchymal stromal cells. The International Society for Cellular Therapy position statement.* Cytotherapy, 2006. **8**(4): p. 315-7.

18. Maitra, B., et al., *Human mesenchymal stem cells support unrelated donor hematopoietic stem cells and suppress T-cell activation.* Bone Marrow Transplant, 2004. **33**(6): p. 597-604.

19. Salem, H.K. and C. Thiemermann, *Mesenchymal stromal cells: current understanding and clinical status.* Stem Cells, 2010. **28**(3): p. 585-96.

20. Si, Y., et al., *Infusion of mesenchymal stem cells ameliorates hyperglycemia in type 2 diabetic rats: identification of a novel role in improving insulin sensitivity.* Diabetes, 2012. **61**(6): p. 1616-25.

21. Caplan, A.I. and D. Correa, *The MSC: an injury drugstore.* Cell Stem Cell, 2011. **9**(1): p. 11-5.

22. Hung, S.C., et al., *Angiogenic effects of human multipotent stromal cell conditioned medium activate the PI3K-Akt pathway in hypoxic endothelial cells to*

inhibit apoptosis, increase survival, and stimulate angiogenesis. Stem Cells, 2007. **25**(9): p. 2363-70.

23. Al-Khaldi, A., et al., *Therapeutic angiogeneis using autologous bone marrow stromal cells: improved blood flow in a Chronic Limb Ischemia model.* Ann Thorac Surg, 2003. **75**: p. 6.

24. Melero-Martin, J.M., et al., *Engineering robust and functional vascular networks in vivo with human adult and cord blood-derived progenitor cells.* Circ Res, 2008. **103**(2): p. 194-202.

25. Ball, S.G., C.A. Shuttleworth, and C.M. Kielty, *Mesenchymal stem cells and neovascularization: role of platelet-derived growth factor receptors.* J Cell Mol Med, 2007. **11**(5): p. 1012-30.

26. Au, P., et al., *Bone marrow derived mesenchymal stem cells facilitate engineering of long lasting functional vasculature.* Blood, 2008. **111**(9): p. 9.

27. Liew, A. and T. O'Brien, *Therapeutic potential for mesenchymal stem cell transplantation in critical limb ischemia.* Stem Cell Research & Therapy, 2012. **3**(4): p. 28.

28. Gupta, P.K., et al., *A double blind randomized placebo controlled phase I/II study assessing the safety and efficacy of allogeneic bone marrow derived mesenchymal stem cell in critical limb ischemia.* J Transl Med, 2013. **11**: p. 143.

29. Dash, N.R., et al., *Targeting nonhealing ulcers of lower extremity in human through autologous bone marrow-derived MSC.* Rejuvenation Research, 2009. **12**(5): p. 8.

30. Lasala, G.P., et al., *Combination stem cell therapy for the treatment of severe limb ischemia: safety and efficacy analysis.* Angiology, 2010. **61**(6): p. 551-6.

31. Lasala, G.P., J.A. Silva, and J.J. Minguell, *Therapeutic angiogenesis in patients with severe limb ischemia by transplantation of a combination stem cell product.* J Thorac Cardiovasc Surg, 2012. **144**(2): p. 377-82.

32. Lu, D., et al., *Comparison of bone marrow mesenchymal stem cells with bone marrow-derived mononuclear cells for treatment of diabetic critical limb ischemia and foot ulcer: a double-blind, randomized, controlled trial.* Diabetes Res Clin Pract, 2011. **92**(1): p. 26-36.

33. Putman, D.M. and D.A. Hess, *Isolation of human umbilical cord blood aldehyde dehydrogenase-expressing progenitor cells that modulate vascular regenerative functions in vitro and in vivo.* Curr Protoc Stem Cell Biol, 2013. **Chapter 2**: p. Unit 2A 10.

34. Bendall, S.C., A.T. Booy, and G. Lajoie, *Proteomic Analysis of Pluripotent Stem Cells*, in *Current Protocols in Stem Cell Biology*. 2007, John Wiley & Sons, Inc.

35. Cox, J. and M. Mann, *MaxQuant enables high peptide identification rates, individualized ppb-range mass accuracies and proteome-wide protein quantification.* Nature biotechnology, 2008. **26**(12): p. 1367-1372.

36. Consortium, U., *UniProt: a hub for protein information.* Nucleic acids research, 2014: p. gku989.

37. Aggarwal, S. and M.F. Pittenger, *Human mesenchymal stem cells modulate allogeneic immune cell responses.* Blood, 2005. **105**(4): p. 1815-1822.

38. Bernardo, M.E. and W.E. Fibbe, *Mesenchymal stromal cells: sensors and switchers of inflammation.* Cell stem cell, 2013. **13**(4): p. 392-402.

39. Melief, S.M., et al., *Multipotent stromal cells induce human regulatory T cells through a novel pathway involving skewing of monocytes toward anti-inflammatory macrophages.* Stem Cells, 2013. **31**(9): p. 1980-1991.

40. Dhahri, D., et al., *Fibrinolytic factor-mediated crosstalk with endothelial cells expands murine bone marrow mesenchymal stromal cells.* Blood, 2016: p. blood-2015-10-673103.

41. Wang, Z. and H. Huang, *Platelet factor-4 (CXCL4/PF-4): an angiostatic chemokine for cancer therapy.* Cancer letters, 2013. **331**(2): p. 147-153.

42. O'Reilly, M.S., et al., *Angiostatin: A novel angiogenesis inhibitor that mediates the suppression of metastases by a lewis lung carcinoma.* Cell, 1994. **79**(2): p. 315-328.

43. Dudani, A.K., et al., *Angiostatin and plasminogen share binding to endothelial cell surface actin.* Biochemistry and Cell Biology, 2005. **83**(1): p. 28-35.

44. Hanahan, D. and J. Folkman, *Patterns and Emerging Mechanisms of the Angiogenic Switch during Tumorigenesis.* Cell, 1996. **86**(3): p. 353-364.

Chapter 3

3 Characterization of CD34-expressing endothelial colony forming cell subsets during ex vivo expansion.

3.1 Introduction

From large caliber vessels to microvascular networks, endothelial cells form the lining of blood vessels and establish a highly regulated interface between circulating blood and systemic tissues. The heterogeneity within vessel derived endothelial cells enables artery, venous and capillary blood vessel networks to serve distinct functions within different organ systems. For example, endothelial cells lining large vessels that are responsible for moving higher volumes of blood interact with smooth muscle cells to tightly control blood pressure and vessel diameter[1]. Alternatively, other endothelial cells can be found with leaky, fenestrated endothelium, as demonstrated in the kidney[2].

Tissue-specific endothelial cell phenotypes are specified by the microenvironment composition and cues that endothelial cells are exposed to during vessel homeostasis[3, 4]. To illustrate this, grafts of non-neural somite tissue transplanted within neural tissues produced fenestrated vasculature with few tight junctions within the grafted tissue. Conversely, when transplanting brain tissue into the coelomic cavity, endothelial cells within the neural graft developed a tight blood brain barrier reflective of neural tissue[5]. Contrary to other mature cell populations, endothelial cells also demonstrate a plastic phenotype *in vitro* despite being “terminally” differentiated. For example, removing endothelial cells from their native environment and sub-cultured *in vitro* can induce a loss of organ-specific phenotype[6, 7]. Endothelial cells will rapidly change their phenotype based on microenvironmental cues or supplemented growth factors encountered during *ex vivo* expansion. Thus, defining a distinct progenitor cell or precursor phenotype for endothelial cells grown in culture has remained a challenge.

The conceptual framework of endothelial precursor cells (EPC) had arisen from seminal experiments by Asahara *et al.* defining the ability of $CD34^+$ peripheral blood mononuclear cells (MNC) to home to sites of ischemia and promote vascularization after transplantation[8]. This work subsequently inspired the isolation and propagation of “EPCs” from blood and/or bone marrow sources. Three distinct culture techniques emerged, producing three different resulting cell populations: colony forming unit – endothelial cells (CFU-EC)[8, 9], circulating angiogenic cells (CAC)[10-12], and endothelial colony forming cells (ECFC)[13-15]. It was later uncovered that the early outgrowth populations from the blood MNC sources (CFU-EC and CAC) were comprised primarily of hematopoietic cells (namely monocytes and macrophages) with a pro-angiogenic secretory phenotype[10, 16-19]. Only the late outgrowth ECFC from the adherent fraction of MNC gave rise to a highly proliferative endothelial cell population able to form vascular networks *in vitro* and *in vivo*[20].

Although consensus has been achieved that only ECFC give rise to endothelial cells *in vitro*, another source of confusion surrounding the term "EPC" lies in the distinction between freshly isolated cells versus cells expanded in culture. For example, freshly isolated $CD34^+/CD45^-$ and/or $CD146^+$ cells can enrich for ECFC in culture[21, 22]; while it has yet to be determined if selection based on CD34 can isolate a comparable EPC subpopulation following expansion *in vitro*. Of note, even within the freshly isolated EPC, there have been many different cell surface markers used to define and purify EPC[23]. Understanding the distinctions between EPC harvested from fresh and/or culture sources is important for accurately comparing results obtained from clinical trials using these cells. Thus far, there are over 350 clinical trials initiated which indicate the use of "Endothelial progenitor cells" (www.clinicaltrials.gov), albeit the minority of trials involve endothelial cell transplantation. Specifically, these trials transplanted "EPC" whose selection parameters ranged from $CD34^+$ and/or $VEGFR2^+$ and $CD133^+$ MNC [24, 25] to MNC cultured similar to CACs on fibronectin-coated plates in endothelial specific media[26, 27]. Regardless, most these early clinical studies demonstrated safety and modest therapeutic benefits, warranting further development of regenerative therapies utilizing EPC or ECFC. Importantly, progenitor cell phenotypes in peripheral blood MNC has been used as clinical diagnostic to non-invasively predict cardiovascular disease risk[9] and recovery rates[28] in patients with cardiovascular complications. Although clinical studies transplanting ECFC are limited, a plethora of pre-clinical studies have elucidated endothelial cell signaling pathways and characterized cellular responses during disease and regeneration, reviewed by Paschalaki *et al.*[29].

To date, ECFC cultures are regarded as the gold standard for the growth of EPC *in vitro* [20]. Although select surface markers may enrich for ECFC from fresh tissue, the initial establishment of ECFC contains a relatively heterogeneous mixture of starting cells, including hematopoietic progeny. However, through adherence and selective culture conditions, highly proliferative ECFC establish a more homogeneous endothelial cell population. Sub-culture and *ex vivo* expansion are necessary steps in order to obtain large numbers of ECFC for cell therapies however, extended culture may stimulate EC maturation as cells differentiate[30, 31]. We hypothesized that ECFC cultures contain a hierarchy of rare, proliferative progenitor cells that drive expansion and subsequently generate more differentiated endothelial cells with lower proliferative rates and conserved endothelial cell functions. Our goal was to accurately define a proliferative endothelial progenitor cell in culture, in order to develop improved strategies to cultivate these cells for therapies, and to delineate a hierarchy marking primitive versus differentiated endothelial cells. Herein, we demonstrate that ECFC expressed CD34 in a density-dependent manner and the expression of CD34 coincided with the increased expression of mature endothelial cell surface antigens, decreased clonogenicity, growth kinetics, and tube-forming capacity compared to the CD34$^-$ ECFC *in vitro*. Nonetheless, the CD34$^{+/-}$ ECFC subsets were equally able to form vessel-like structures within Matrigel plugs after subcutaneous transplantation into the flank of NOD.SCID mice. Collectively, this study describes novel phenotypic and functional characterization of ECFC subsets *in vitro*, although the identity of an endothelial precursor cell *in vitro* remains elusive.

3.2 Methods

3.2.1 Collection and isolation of ECFC.

Human ECFC were established from umbilical cord blood-derived MNC, as previously described[15]. Briefly, MNC were seeded on tissue culture plastic at 70,000 cells/cm^2 in complete endothelial growth media-2 (EGM-2) + 2% FBS + cytokines (Lonza, Basel, Switzerland). Media was replaced every 3 days for up to 14 days when colonies became confluent. Colonies were lifted with TrypLE™ express (ThermoFisher, Waltham, MA) and cells were re-plated at 4000 cells/cm^2. ECFC monolayers were subsequently expanded in EGM-2 and passaged at ≈ 80% confluency. Cells were cryopreserved at passage 3 to be used for subsequent experiments.

3.2.2 Flow cytometric characterization of ECFC.

To prepare ECFC for flow cytometric analyses or fluorescence activated cell sorting (FACS), ECFC were dissociated with trypsin and single cell suspension was treated with Aldefluor^{TM} (StemCell technologies, Vancouver, Canada) to measure ALDH-activity. Surface marker expression was analyzed by co-staining with conjugated anti-human antibodies for CD34, CD31, CD45, VE-Cadherin, CD105, VEGFR2, TIE-2, and CXCR4. Data was acquired using an LSR II flow cytometer (BD biosciences, San Jose, CA) analyzed using FloJo software at the London Regional Flow Cytometry Facility.

3.2.3 Cell sorting and colony forming assays.

An automated cell deposition unit (ACDU) on a FACSAria III cell sorter (BD biosciences), was used to plate single cells into each well of a 96-well plate containing EGM-2. ECFC were initially selected using forward and side scatter profiles to obtain single unpurified cells at random. In subsequent experiments, ECFC subsets were selected based on high versus low ALDH-activity, CXCR4, CD34, or CD143 expression. Single cell deposition was visually checked after plating. Media was replaced after 6 days and colonies were enumerated using an inverted light microscope at day 12 of culture. Enumerated colonies were defined as cell clusters containing >50 cells.

3.2.4 Tube forming assay.

To assess the tubule-forming function of ECFC subsets *in vitro*, 120,000 ALDH$^{hi/lo}$ or CD34$^{+/-}$ FACS purified ECFC were cultured on growth factor-reduced Geltrex matrices (ThermoFisher) in endothelial basal media without serum or cytokines (EBM-2) media or in complete EGM-2. After $\approx$ 20 hours, photomicrographs were taken by light microscopy, and tubule formation was quantified using manual counting of complete tubule number under light microscopy. Tube formation was enumerated using ImageJ software.

3.2.5 Growth kinetics and surface marker kinetics.

FACS-purified CD34$^{+/-}$ ECFC subsets were plated at 4000 cells/cm^2 in 7 different tissue culture flasks. Manual hemocytometer counts and flow cytometry analyses were performed every 24 hours for 7 days to assess ECFC expansion kinetics and CD34 expression patterns. The media was changed on days 3, 5, and 6 as the near confluent monolayer required more frequent media changes to maintain cell growth.

3.2.6 Preparation of cells for cell surface proteome analysis.

Initially, 10^6 FACS-purified CD34$^{+/-}$ ECFC subsets were plated on tissue culture plastic for 8 hours to permit adherence, prior to plasma membrane isolation and analyses of surface proteins by mass spectrometry. For cell surface protein isolation a 10% solution of colloidal silica beads (Sigma Aldrich, St. Louis, MO) was added to ECFC in culture to permit non-specific colloid silica bead/membrane-bound protein interactions, as previously described[32]. A polyacrylamide catalyst (Sigma) was used to stabilize protein/colloidal bead interactions by cross-linking of the silica beads to the cell membrane. Bead-bound ECFC were manually collected using cell scrapers and homogenized via sonication prior to ultra-centrifugation using a HistoDenz gradient (Sigma) to isolate bead/proteins conjugates. The beads, containing membrane bound proteins were resuspended in 8 M urea, 50 mM ammonium bicarbonate, 2% SDS and 5 mM DTT to elute and solubilize proteins off the beads in a sonication bath for 30 min. Protein concentrations were subsequently determined using the Pierce 660 nm protein assay.

3.2.7 Mass spectrometry analysis of cell surface protein expression.

Protein extracts were reduced in 10 mM DTT for 30 min in the dark. Next, samples were alkylated with 100 mM iodoacetamide (IAA) for 45 min at room temperature in the dark. To facilitate the removal of incompatible detergents, reducing and alkylating reagents, proteins were precipitated using chloroform methanol. After protein precipitation, peptides were generated through digestion using trypsin. High pH fractionation was performed using a Waters XBridge BEH130 C18 5µm column. After collection, the protein fractions were vacuum concentrated (SpeedVac^{TM}) and acidified prior to liquid chromatography coupled with tandem mass spectrometry. Data analysis was performed with MaxQuant version 1.5.0.30 using the Andromeda search engine[33]. MS/MS spectra were searched against the Human Uniprot database with trypsin specificity (20264 entries)[34].

3.2.8 Surface marker identification.

Protein expression from the CD34$^+$ ECFC were directly compared with protein expression from the CD34$^-$ ECFC. Bioinformatic analysis was performed using Perseus software version 1.5.0.8. Datasets were filtered for proteins containing a minimum of 1 unique peptide while also meeting the P-value requirement of $P<0.05$. The differentially expressed protein list was exported into DAVID gene ontology (GO) analysis to select for proteins with vascular/endothelial functions.

3.2.9 *In vivo* implantation of purified ECFC in Matrigel.

The ability of CD34-selected ECFC subsets to form functional vasculature *in vivo* was assessed after implantation into immunodeficient NOD/SCID mice. Briefly, 10^6 purified human CD34$^+$ or CD34$^-$ ECFC were mixed with 250,000 mouse aorta smooth muscle cells (4:1 ratio) subcutaneously injected into the flank in 200 µL Matrigel (ThermoFisher) as previously described[35]. After 7 days incubation, the Matrigel plug was removed and mounted in optimal cutting temperature media for subsequent cryosectioning and immunofluorescence. Briefly, 10µM sections were fixed with 10% formalin, permeabilized and stained for CD31 and HLA antibodies to visualize human cell contribution to lumenized vascular structures.

3.3 Results

3.3.1 ECFC express hematopoietic progenitor cell markers CD34 and ALDH.

To validate the purity of ECFC cultures, flow cytometry was used to assess both endothelial and hematopoietic cell surface maker expression. Cultured UCB-derived ECFC highly (>97%) expressed CD31, VEGFR2, VE-Cadherin, CD105, and <5% of ECFC expressed CD45, confirming minimal hematopoietic cell contamination (**Figure 3.1**). Analyses of markers commonly used to assess progenitor cell (ALDH-activity, CD34) or migratory cell (CXCR4) surface phenotype after *ex vivo* expansion is shown in

Figure 3.2. ALDH activity assessed in 4 ECFC samples averaged 64.5 ± 17.9% ALDH^{hi} cells and 28.0 ± 14.7% ALDH^{lo} cells (**Figure 3.2A, D**). Notably, ALDH-activity was highly variable between different UCB samples. In contrast, CD34 (3.3 ± 1.3%) and CXCR4 (1.4 ± 0.6%) expression on cultured ECFC was consistently low (**Figure 3.2B-D**). Because UCB HPC with high-ALDH activity highly co-expressed CD34 (Ref), we used 3-color analyses to assess each parameter simultaneously. Surprisingly, ALDH^{hi} ECFC did not significantly co-express CD34 or CXCR4 (**Figure 3.2E, F**). In contrast, CD34^{+} ECFC co-expressed CXCR4 at 30% (**Figure 3.2G**). Next, we assessed intracellular expression of CD34 or CXCR4. After fixation and permeabilization, ECFC showed considerable stores of CXCR4^{+} whereas CD34 expression was identical on permeabilized or unpermeabilized ECFC (**Figure 3.3**). After culture expansion, ECFC with high ALDH activity did not co-express CD34. Although low expression of CD34 was observed on ECFC, the CD34^{+} ECFC demonstrated increased CXCR4 expression which may represent increased migratory capacity as demonstrated in SCID-repopulating CXCR4^{+}/CD34^{+} hematopoietic progenitor cells[36], and putative circulating endothelial progenitor cells[37].

Figure 3.1

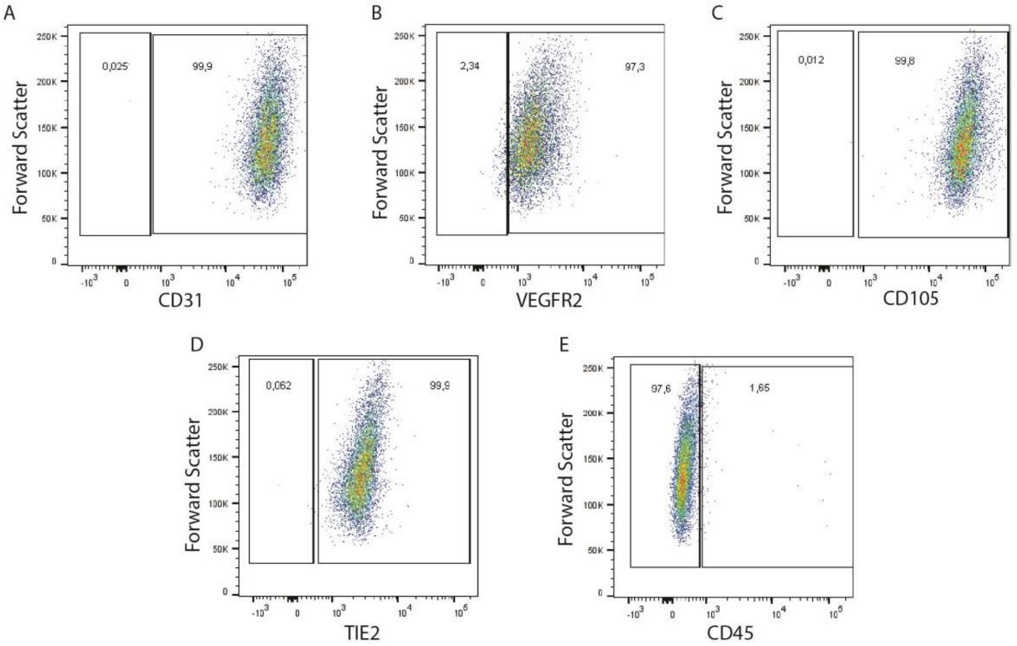

Figure 3.1 Cultured UCB ECFC expressed endothelial cell surface antigens and lack the hematopoietic cell surface marker CD45. Representative flow cytometric analysis of ECFC established from human umbilical cord blood showed >95% expression of the endothelial cell markers: (A) CD31, (B) VEGFR2, (C) CD105, (D) TIE2 and (D) lacking expression of the pan-leukocyte marker, CD45 (N=3).

Figure 3.2

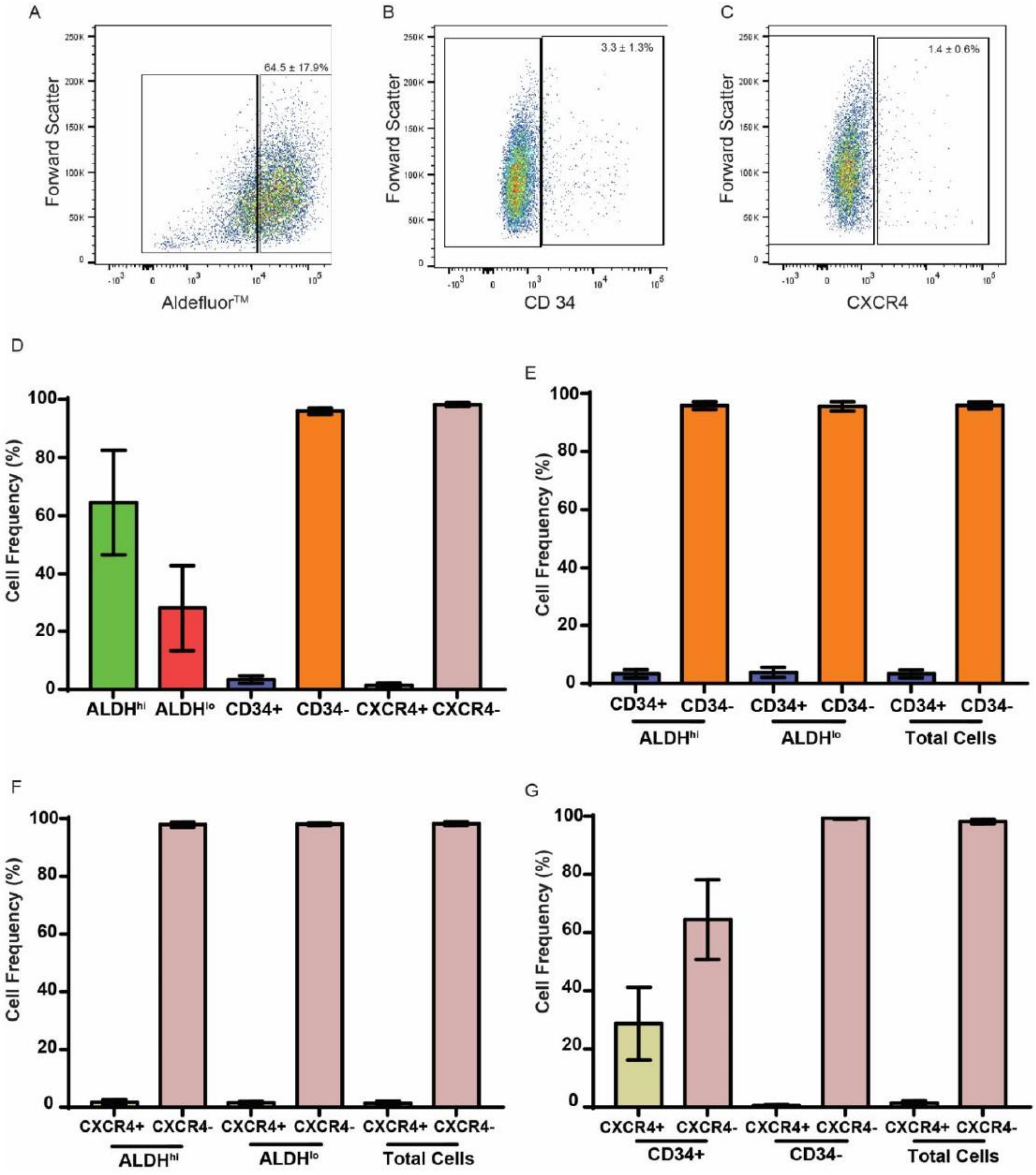

Figure 3.2 Identification of progenitor cell surface marker expression by flow cytometry. After establishment of ECFC in culture, cells were assessed for expression of ALDH, CD34 and CXCR4. Representative flow plots of ECFC for (A) ALDH, (B) CD34, and (C) CXCR4 expression. Aldefluor™ fluorescence was gated using DEAB inhibition of ALDH-activity. Cell surface marker expression was gated based on isotype controls. (D) Approximately 65% of ECFC demonstrated high ALDH-activity but did not co-express (E) CD34 and (F) CXCR4. Conversely, (G) 28% of CD34$^+$ cells also expressed CXCR4, a 19-fold enrichment compared to bulk ECFC. Data represents the mean ± SD using ECFC derived from 4 UCB samples (N=4).

Figure 3.3

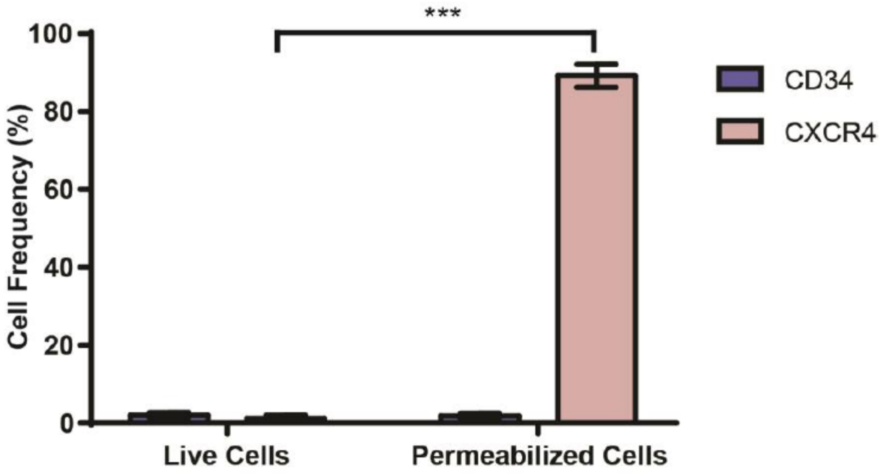

Figure 3.3 ECFC contained intracellular stores of CXCR4. ECFC were fixed and permeabilized before staining with antibodies towards CD34 and CXCR4. The fixed and permeabilized cells were compared to their stained live cell counterparts. Approximately 90% of ECFC contained CXCR4 intracellularly whereas CD34 expression was unchanged after permeabilization of ECFC. Data represents the mean ± SD using ECFC derived from 4 UCB samples (N=4, ***P<0.001).

3.3.2 Colony forming capacity was increased in CD34$^-$/CXCR4$^-$ ECFC.

To assess progenitor-like functions *in vitro*, single ECFC were sorted for ALDH activity, CD34, or CXCR4 expression (**Figure 3.4A-C**) and assessed for their ability to form colonies after 14 days in culture. When acquired without selection using forward and side scatter properties, 34% of total ECFC established colonies (**Figure 3.4D**). After selection of ECFC for ALDH-activity via ACDU, the clonogenic capacity of the ALDH^{hi} ECFC was not significantly different than ALDH^{lo} ECFC (**Figure 3.4D)**. In contrast, CD34$^-$ ECFC efficiently formed colonies (51.3 ± 5.85) compared to CD34$^+$ ECFC (16.3 ± 4.7). Similarly, CXCR4$^-$ ECFC formed significantly more colonies than CXCR4$^+$ ECFC**.** When sorted using both progenitor cell markers, ECFC expressing either CXCR4 and/or CD34 consistently demonstrated reduced colony formation (**Figure 3.4E).** Cells that were CD34$^-$/CXCR4$^-$ or CD34$^-$/ALDH^{hi} formed a significantly higher number of colonies compared to unfractionated ECFC (**Figure 3.4E**). These data suggest that ECFC expressing CD34 or CXCR4 have a reduced ability to establish colonies from single cells *in vitro*.

Figure 3.4

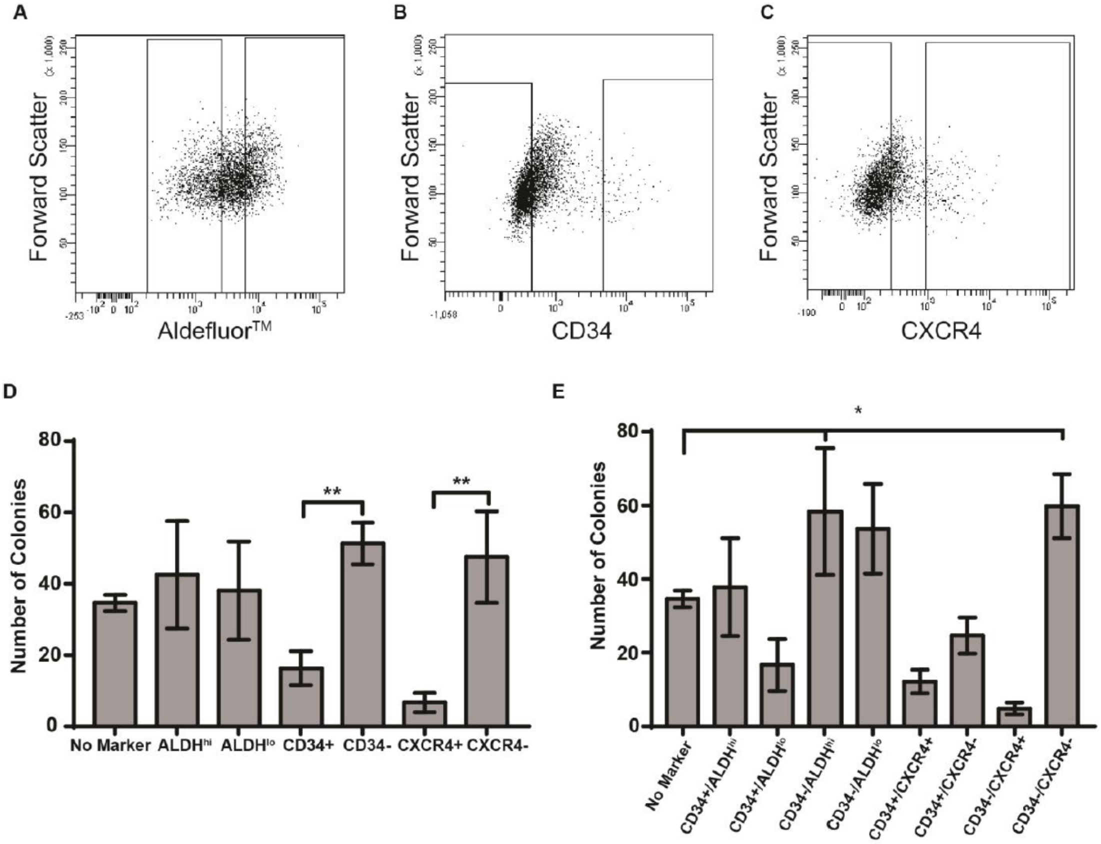

Figure 3.4 ECFC expressing CD34 and CXCR4 exhibit decreased colony formation *in vitro*. Colony forming capacity of single ECFC purified by the expression of (A) ALDH, (B) CD34, or (C) CXCR4, was assessed using (D) single markers or (E) in combination. ECFC expressing CD34 or CXCR4 exhibited a significant decrease in colony forming capacity compared to the CD34 or CXCR4 negative ECFC respectively. $CD34^-/ALDH^{hi}$ ECFC and $CD34^-/CXCR4^-$ ECFC formed significantly more colonies when compared to unselected ECFC. Data represents the mean ± SD using ECFC derived from 3 UCB samples (N=3 **P<0.01; *p<.05).

3.3.3 Tube forming capacity was increased by CD34$^-$ ECFC.

To further assess the relationship between putative progenitor marker expression and a conserved endothelial cell functions *in vitro*, we assessed the tubule-forming capacity of ECFC subsets purified for ALDH-activity or CD34 expression. Briefly, 120,000 purified CD34$^{+/-}$ or ALDH$^{hi/lo}$ ECFC were seeded in growth factor-reduced Geltrex in EBM or fully supplemented EGM-2. Photomicrographs were obtained 20 hours after seeding and total tubule number was enumerated. Regardless of whether ECFC were plated in EGM or EBM, selection for low versus high ALDH-activity did not alter tubule forming capacity of ECFC (**Figure 3.5C**). In contrast, CD34$^-$ ECFC demonstrated increased tubule formation *in vitro*, compared to the CD34$^+$ ECFC (**Figure 3.5D**). Collectively, CD34 expression, and not ALDH-activity, selected ECFC with differential tubule forming capacity *in vitro*.

Figure 3.5

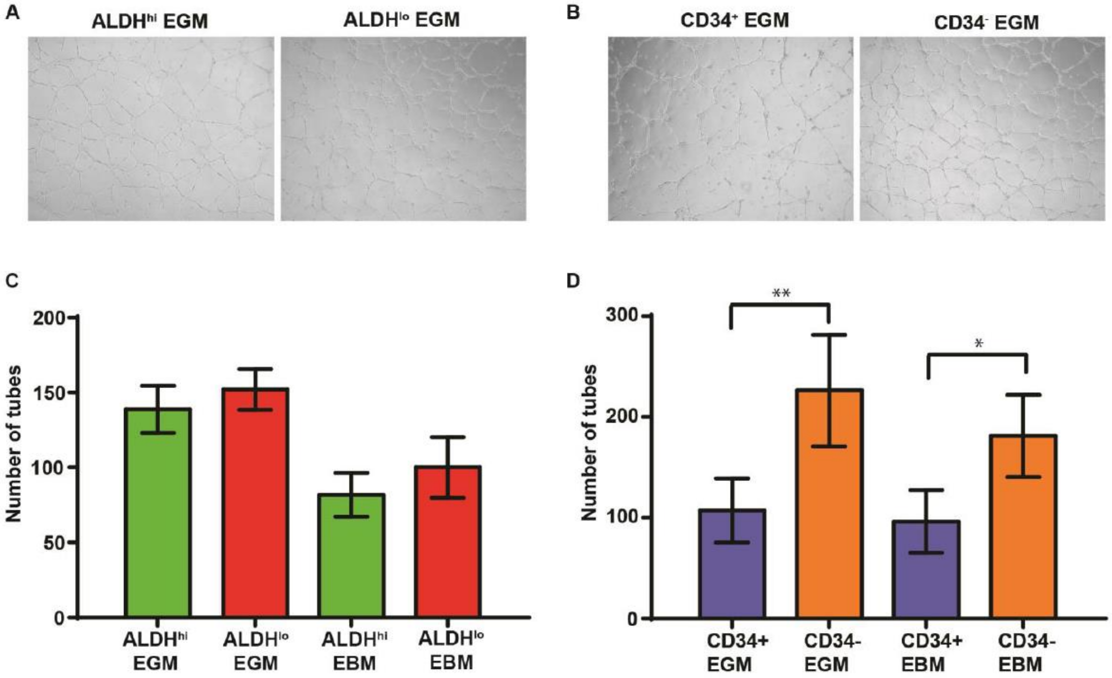

Figure 3.5 ECFC expressing CD34 exhibit decreased tube forming capacity *in vitro*. After *ex vivo* expansion, ECFC were sorted based on ALDH activity or CD34 expression and plated on Geltrex^{TM} for 20 hours. Representative photomicrographs of tube formation for (A) ALDH$^{hi/lo}$ and (B) CD34$^{+/-}$ are presented. Whether using basal media (EBM) or growth media (EGM), the tube forming ability of ECFC with high or low (C) ALDH activity was similar. ECFC expressing (D) CD34 formed significantly less tubules than the CD34^{-} ECFC. Data represents the mean ± SD using ECFC derived from 5 UCB samples, performed in technical duplicate (N = 5; ** $P < 0.01$; * $P < 0.05$).

3.3.4 CD34-expression on ECFC was increased in confluent culture conditions.

We next tested the effects of cultured cell density on ECFC, which has been previously suggested to increase CD34 expression[38]. For ECFC in culture at passage 4, CD34 was expressed on 9% of cells when passaged at <80% confluency (**Figure 3.2**). When ECFC were cultured to >90% confluency, we CD34$^+$ expression was markedly increased. Although the frequency of CD34$^+$ ECFC increased by ~6.5-fold, the other cell markers assessed (ALDH, CXCR4) were not altered at any time point assessed (**Figure 3.6A**). We next sought to assess functional differences between confluent ECFC sorted for CD34 expression compared to ECFC grown under standard culture practices. Of note, no differences in colony formation were observed between CD34$^+$ and CD34$^-$ ECFC after collection at high (>90%) cell density (**Figure 3.6B**). Similarly, the CD34-selected ECFC subsets confluence did not display a significant decrease in the ability to form tubes *in vitro* (**Figure 3.6C**). These findings indicated that culture of ECFC to confluency increases CD34 expression and abrogated functional differences in colony and tubule formation *in vitro.*

Figure 3.6

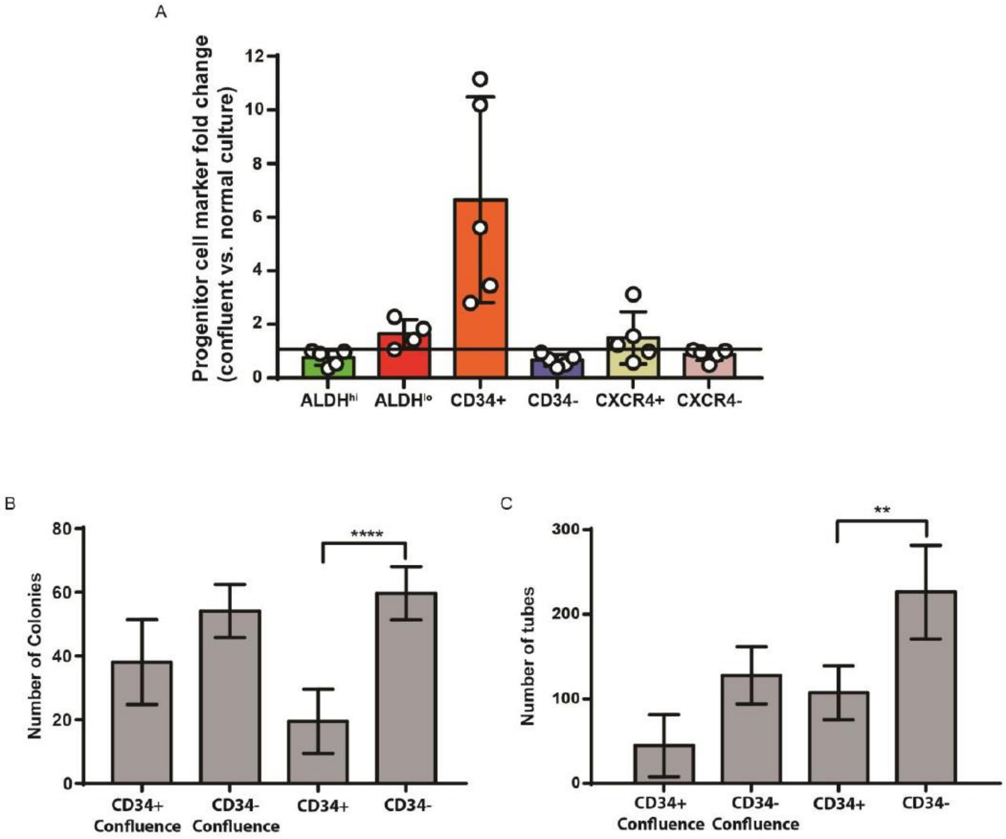

Figure 3.6 ECFC cultured at high density increased CD34 expression and altered ECFC colony and tubule formation *in vitro*. (A) ECFC cultured to >80% confluency for 3 days exhibited ~7-fold increase in the frequency of $CD34^+$ ECFC. (B) Colony and (C) tube forming function were compared to ECFC grown in standard culture conditions. ECFC subsets selected for CD34 = expression at high cell density formed an equal number of colonies or tubules compared to non-confluent counterparts. Data represents the mean ± SD using ECFC derived from 4 UCB samples (N=4; ****p<0.0001; **P<0.01).

3.3.5 CD34-expression was reversible and CD34$^-$ ECFC showed increased growth kinetics.

Based on the previous observation that the CD34 expression was correlated to cell density, we investigated CD34 expression dynamics over 7 days alongside the expansion of CD34$^+$ and CD34$^-$ purified ECFC. Interestingly, the frequency of CD34$^+$ ECFC gradually decreased to <20% over the first 72 hours of culture (**Figure 3.7A**). Notably, the exponential growth phase of the CD34$^-$ ECFC concluded by around day 4.5 whereas exponential growth ended at day 6 for the CD34$^+$ cells. To further illustrate, the number of CD34$^-$ ECFC was significantly greater than the CD34$^+$ ECFC subset at days 2-5 of expansion *in vitro* ($P<0.05$) (**Figure 3.7A, B**). During the expansion of the CD34$^-$ ECFC, the frequency of CD34$^+$ ECFC increased over 7 days (**Figure 3.7B**). In contrast, the CD34$^+$ ECFC population showed a dramatic loss of CD-expression over the first 4 days, followed by increased CD34 expression during the final 3 days as cell density increased (**Figure 3.7B**). These data indicate that CD34 expression on ECFC was reversible and correlated to cell density during expansion. Based on the growth curves, CD34$^+$ ECFC initially expanded at a slower rate but reached a similar cell number after 6 -7 days expansion.

Figure 3.7

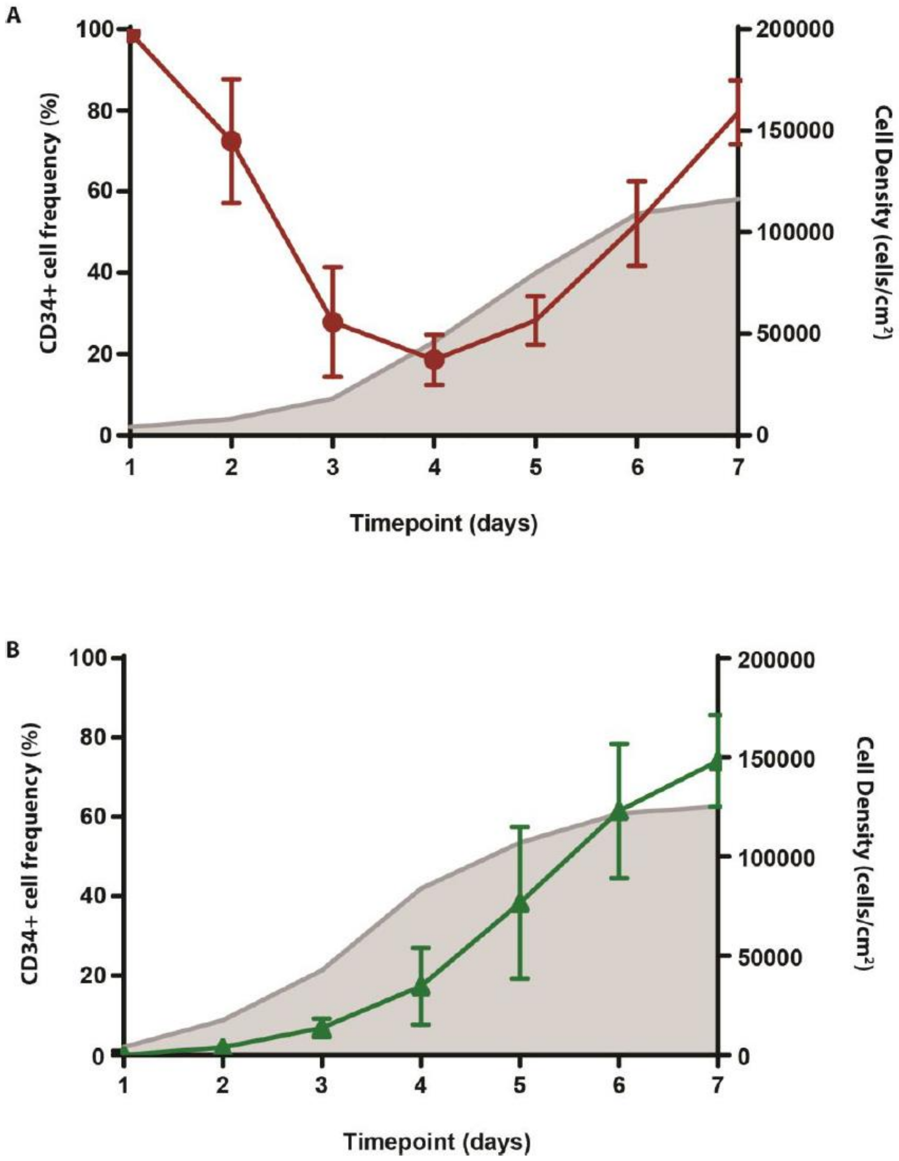

Figure 3.7 CD34-expression increased with endothelial cell density. Cultured ECFC were purified into (A) CD34$^+$ and (B) CD34$^-$ and plated for 7 days to assess CD34 expressional changes and ECFC growth. After being plated at the same density post-sort, the CD34$^+$ ECFC gradually lost the expression of CD34 (red line) which recovered as the cell density (grey shaded area) increased. Similarly, the CD34 expression of the CD34$^-$ ECFC also increased (green line) in response to an increase in cell density (grey shaded area) over 7 days. Notably, the CD34$^-$ ECFC growth curve reached its linear phase by day 4.5 of culture whereas the CD34$^+$ ECFC reached this stage of growth at day 6, indicating a faster growth rate of for the CD34$^-$ ECFC. Data represents the mean ± SD using ECFC derived from 4 UCB samples (N=4).

3.3.6 The frequency of CD34$^+$ ECFC remained stable over several passages.

After observing changes in CD34 expression that occurred as cells were expanded, we also wanted to determine if CD34 frequency was altered over multiple cell passages at <80% confluency. Once the ECFC became established in culture, the first passage of these cells occurred with ≈40% of the ECFC expressing CD34 (**Figure 3.8**). The frequency of CD34$^+$ ECFC decreased below 20% for each cell line by passage 2 but remained at a steady state for the remainder of the experiment. Thus, the CD34$^+$ ECFC frequency remained at a steady state for each cell line after the establishment of a proliferative monolayer in culture.

Figure 3.8

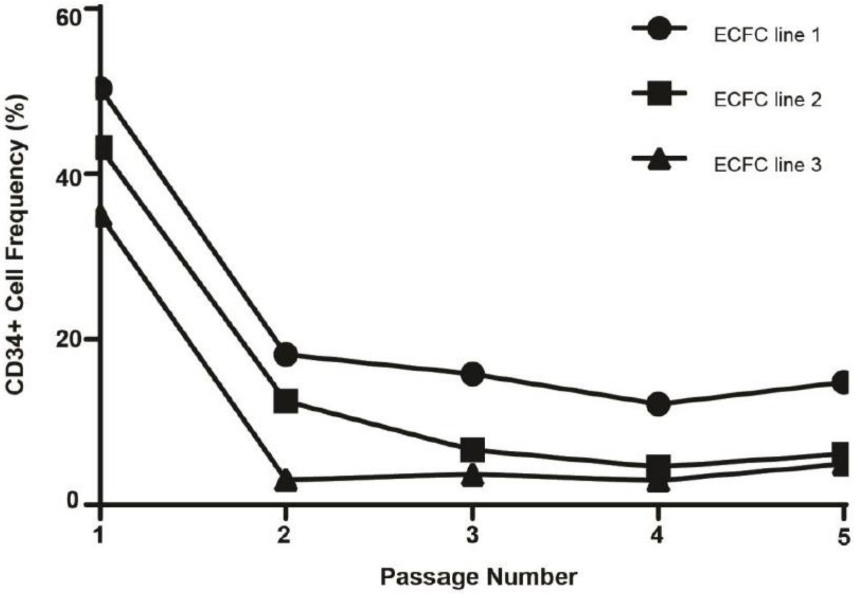

Figure 3.8 CD34-expression reached a steady state for each cell line. During the isolation and establishment of ECFC in culture, the CD34 frequency was determined at the time of passage and was assessed over 5 passages on a per cell line basis. All ECFC lines tested began with higher levels of CD34 expression which rapidly decreased to as low as 3% by passage 1 and remained at a steady state throughout the remaining 4 passages. ECFC were derived from 3 UCB samples (N=3).

3.3.7 ECFC surface proteomics revealed enrichment of known endothelial cell pathways on CD34$^+$ ECFC.

After observing functional differences between the CD34$^+$ and CD34$^-$ ECFC, we sought to identify additional surface markers that may be used to identify ECFC subpopulations with progenitor-like functions. We used mass spectrometry to identify differential cell surface protein expression between CD34$^-$ or CD34$^+$ ECFC. We identified 148 differentially expressed proteins ($P<0.05$), with 67 proteins showed >2-fold increased expression on CD34$^+$ ECFC compared to CD34$^-$ ECFC. Conversely, we identified only 21 proteins >2-fold increased expression on the CD34$^-$ ECFC compared to the CD34$^+$ ECFC. To validate our cell purification procedures, the proteomic comparison between sorted CD34$^-$ and CD34$^+$ ECFC subsets revealed a 36-fold increase in CD34 expression on the CD34$^+$ ECFC. Interestingly, after selecting proteins using GO terms associated with known endothelial cell pathways (**Table 3.1**), the CD34$^+$ ECFC expressed many proteins associated with pro-vascular endothelial cell functions, summarized in **Table 3.2**.

Table 3.1 List of gene ontology (GO) terms by DAVID gene enrichment analysis for the CD34$^-$ versus CD34$^+$ ECFC surface proteomics.

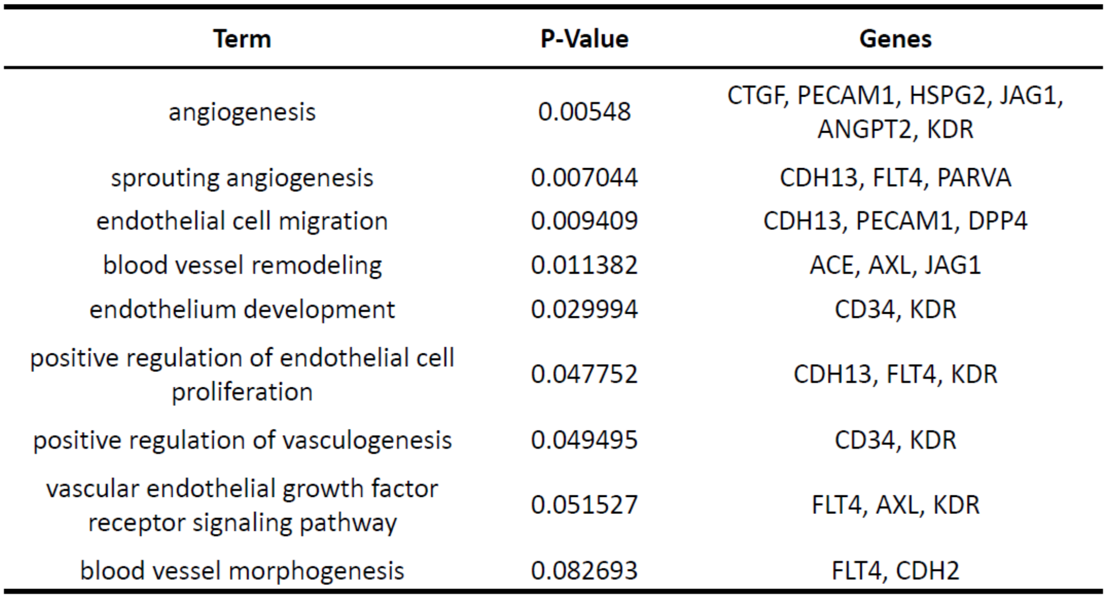

Term	P-Value	Genes
angiogenesis	0.00548	CTGF, PECAM1, HSPG2, JAG1, ANGPT2, KDR
sprouting angiogenesis	0.007044	CDH13, FLT4, PARVA
endothelial cell migration	0.009409	CDH13, PECAM1, DPP4
blood vessel remodeling	0.011382	ACE, AXL, JAG1
endothelium development	0.029994	CD34, KDR
positive regulation of endothelial cell proliferation	0.047752	CDH13, FLT4, KDR
positive regulation of vasculogenesis	0.049495	CD34, KDR
vascular endothelial growth factor receptor signaling pathway	0.051527	FLT4, AXL, KDR
blood vessel morphogenesis	0.082693	FLT4, CDH2

Table 3.2 Comparison of the surface proteomics of CD34$^-$ versus CD34$^+$ ECFC by DAVID gene enrichment analysis.

Fold change	Protein Names	Gene Names
3.690637	Tyrosine-protein kinase receptor UFO	AXL
2.597781	Cadherin-2	CDH2
-2.09914	Alpha-parvin	PARVA
-2.16356	Connective tissue growth factor	CTGF
-2.57701	Protein jagged-1	JAG1
-2.62386	Basement membrane-specific heparan sulfate proteoglycan core protein	HSPG2
-2.76909	Vascular endothelial growth factor receptor 3	FLT4
-3.16141	Platelet endothelial cell adhesion molecule	PECAM1
-4.24958	Vascular endothelial growth factor receptor 2	KDR
-4.90312	Dipeptidyl peptidase 4	DPP4
-6.11232	Cadherin-13	CDH13
-14.3449	Angiopoietin-2	ANGPT2
-27.6667	Angiotensin-converting enzyme	ACE
-36.1126	Hematopoietic progenitor cell antigen CD34	CD34

3.3.8 Angiotensin converting enzyme expression was enriched on CD34$^+$ ECFC but did not impact colony forming capacity.

Angiotensin converting enzyme (ACE or CD143) was shown to have 27-fold greater expression on CD34$^+$ ECFC. Therefore, we sought to determine whether ACE was could be used as a biomarker of mature endothelial cells. When assessing the frequency of ACE expression on ECFC subsets, ≈88% of CD34$^+$ cells expressed ACE while only 12.6% of CD34$^-$ ECFC expressed ACE by flow cytometry (**Figure 3.9A**). Next, we purified ECFC subsets based on CD143 expression, and used single cell deposition to assay for colony formation. Both CD143$^+$ and CD143$^-$ subsets demonstrated equal colony forming capacity (**Figure 3.9B**). Finally, we tried to validate the expression of AXL and Col 13A1 by flow cytometry because both proteins showed increased expression on CD34$^-$ ECFC. Unfortunately, very few unfractionated ECFC demonstrated expression of Col13A1 or AXL on the external cell surface membrane, Cell fixation and permeabilization revealed that >90% of ECFC expressed these proteins on the inside of the cell (**Figure 3.10)**. Of the validated hits from the proteomic screen, the expression of ACE (CD143), Col13A1, and AXL did not provide useable markers for the identification of ECFC after culture with colony forming functions.

Figure 3.9

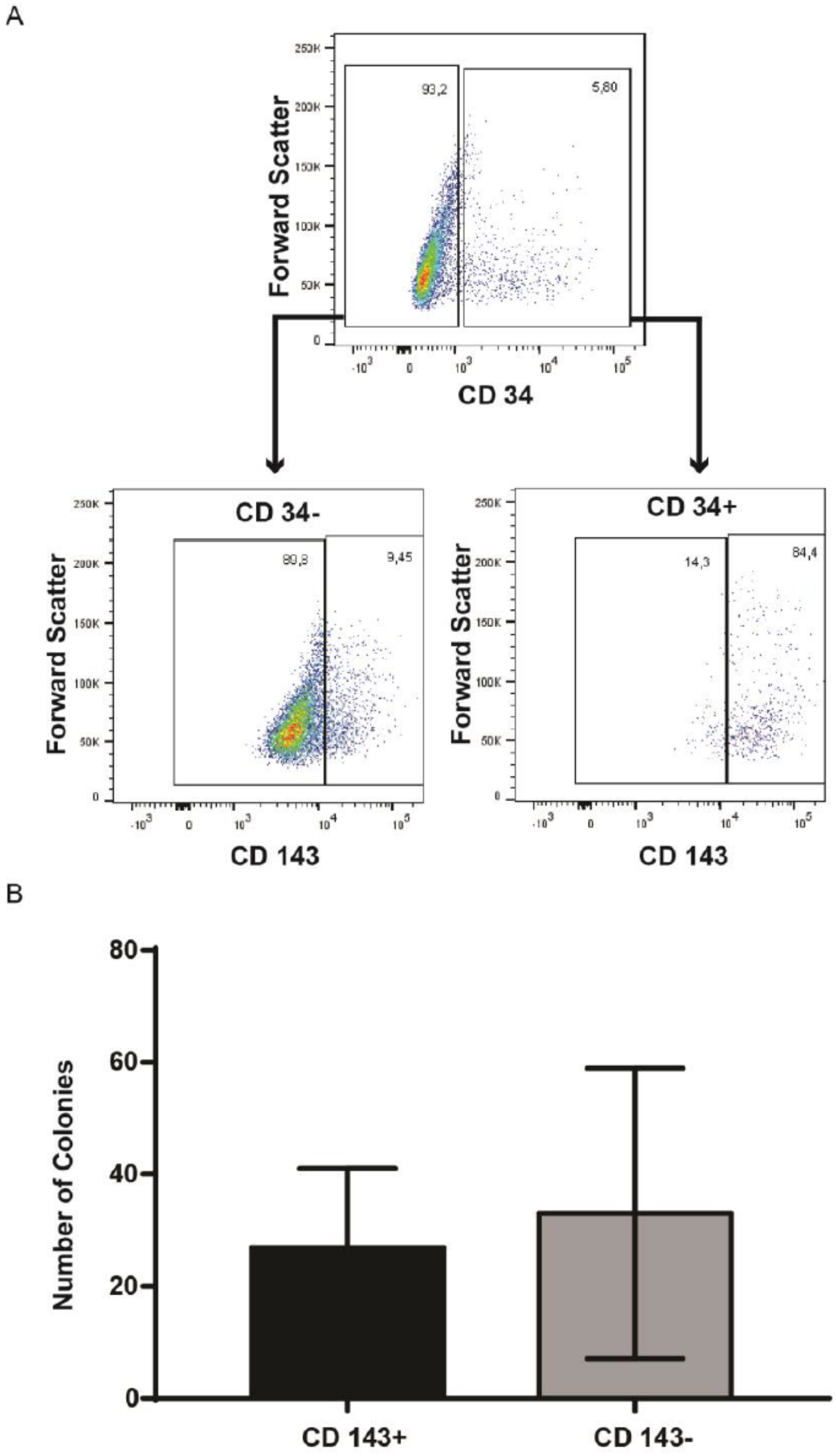
A
250K
200K
150K
100K
50K
0
Forward Scatter
93,2
5,80
-10^3
0
10^3
10^4
10^5
CD 34
CD 34-
80,8
9,45
CD 143
CD 34+
14,3
84,4
CD 143
B
Number of Colonies
80
60
40
20
0
CD 143+
CD 143-

Figure 3.9 Angiotensin converting enzyme co-localized with CD34 expression on ECFC and did not affect the colony forming capacity of ECFC. (A) Cultured ECFC were demonstrated to express angiotensin converting enzyme (ACE) in both the $CD34^+$ and $CD34^-$ subsets. The $CD34^+$ ECFC demonstrated >80% expression of ACE with <10% of $CD34^-$ ECFC expressing ACE. (B) After purification of $ACE^{+/-}$ ECFC, the colony forming capacity for each ECFC subset was equivalent. Data represents the mean ± SD using ECFC derived from 3 UCB samples (N=3).

Figure 3.10

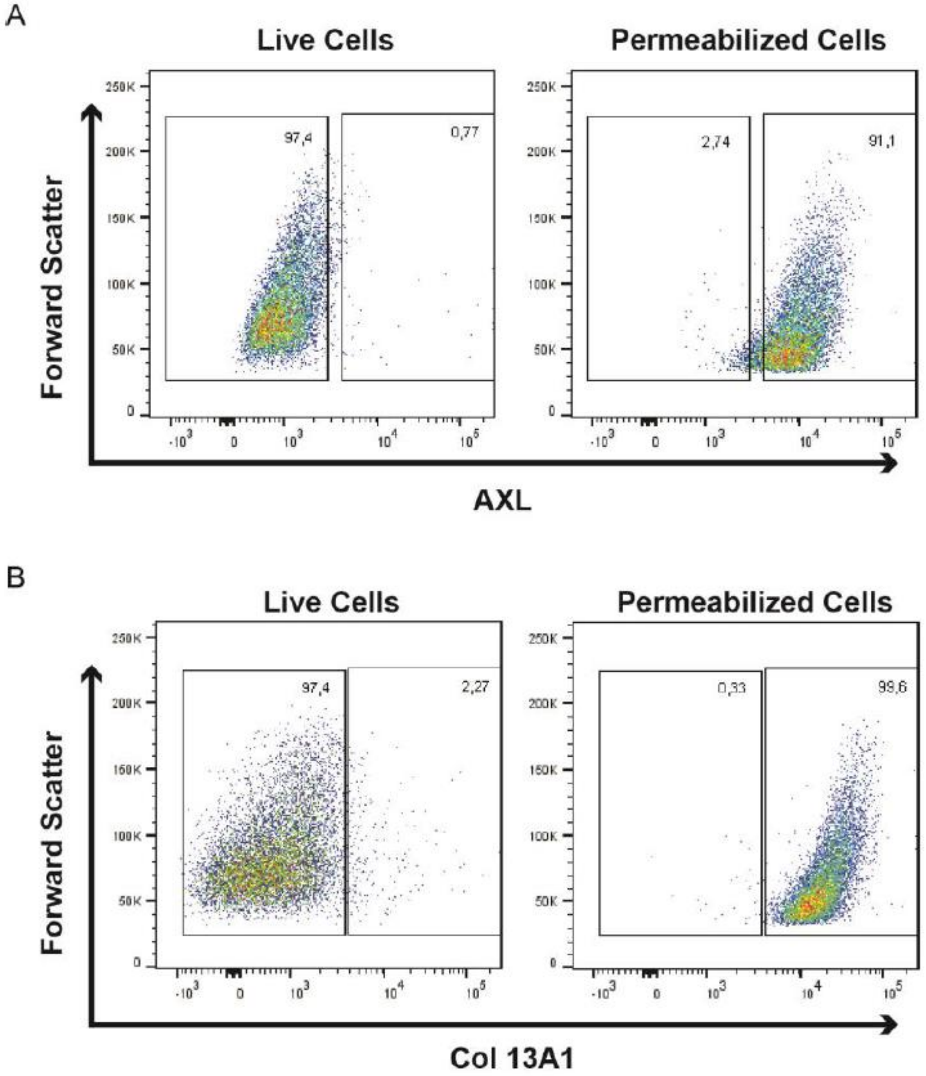

Figure 3.10 ECFC contain intracellular stores of collagen 13A1 (Col13A1) and tyrosine-protein kinase receptor UFO (AXL). After culture, ECFC were stained for the presence of cell-surface and intracellular content of Col13A1 and AXL to validate findings from the ECFC surface proteomics. On the live cells, <2.5% of the cells expressed Col13A1 and <1% of the cells expressed AXL at the cell surface. Once fixed and permeabilized, ECFC demonstrated >90% expression for both markers (N=1).

3.3.9 In vivo transplantation of CD34$^{+/-}$ ECFC subsets in Matrigel enabled the formation of vessel-like structures.

To assess the function of CD34^{+} versus CD34^{-} ECFC subsets to form tubes *in vivo*, CD34^{+} or CD34^{-} ECFC were purified and injected subcutaneously into the flank of immunodeficient NOD/SCID mice within a Matrigel plug. After harvesting the plugs at 7 days, Matrigel plug implanted with both the CD34^{+} and CD34^{-} ECFC showed macroscopic areas of erythrocyte infiltration (**Figure 3.11**). Indeed, Matrigel plugs implanted with CD34^{+} or CD34^{-} ECFC showed vessel-like structures that were HLA positive (**Figure 3.12A**) and infiltration of murine CD31 cells within the Matrigel was rare. The recruitment of murine endothelial cells into the Matrigel plug was equivalent to vehicle control (**Figure 3.12B**). Albeit a rare occurrence, the only interaction between human and mouse endothelial cells was found in the Matrigel plugs containing the CD34^{-} ECFC (**Figure 3.12C**). These data suggested that in an *in vivo* setting, both the CD34^{+} and CD34^{-} ECFC subsets equally generate vasculature at the site of transplantation.

Figure 3.11

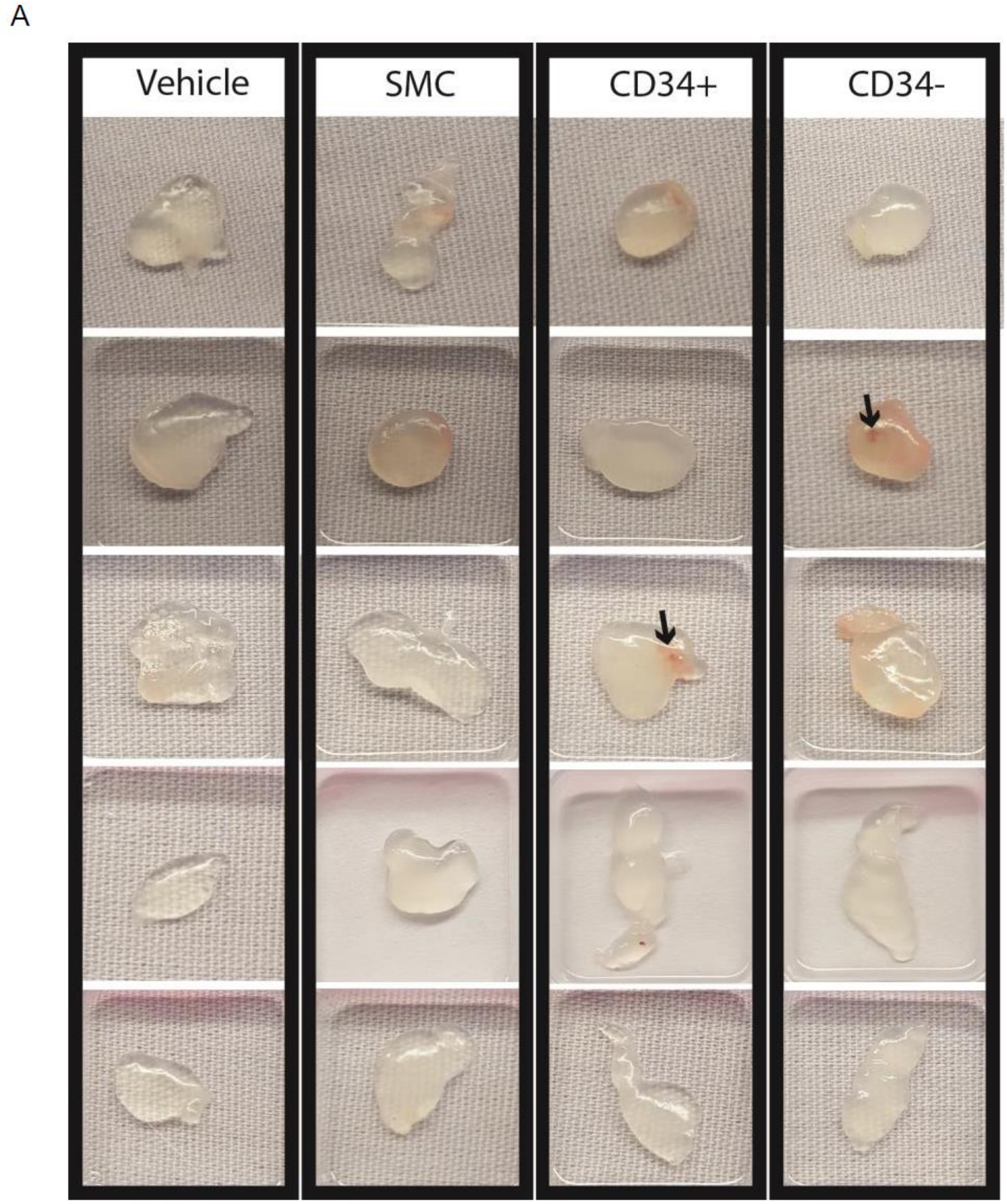

Figure 3.11 ECFC had the capacity to vascularize Matrigel plugs *in vivo*. Removal of 7-day old subcutaneously transplanted Matrigel plugs revealed vascularized sites in 1 out of 5 Matrigel plugs containing CD34$^+$ and CD34$^-$ ECFC (black arrows). (N=5).

Figure 3.12

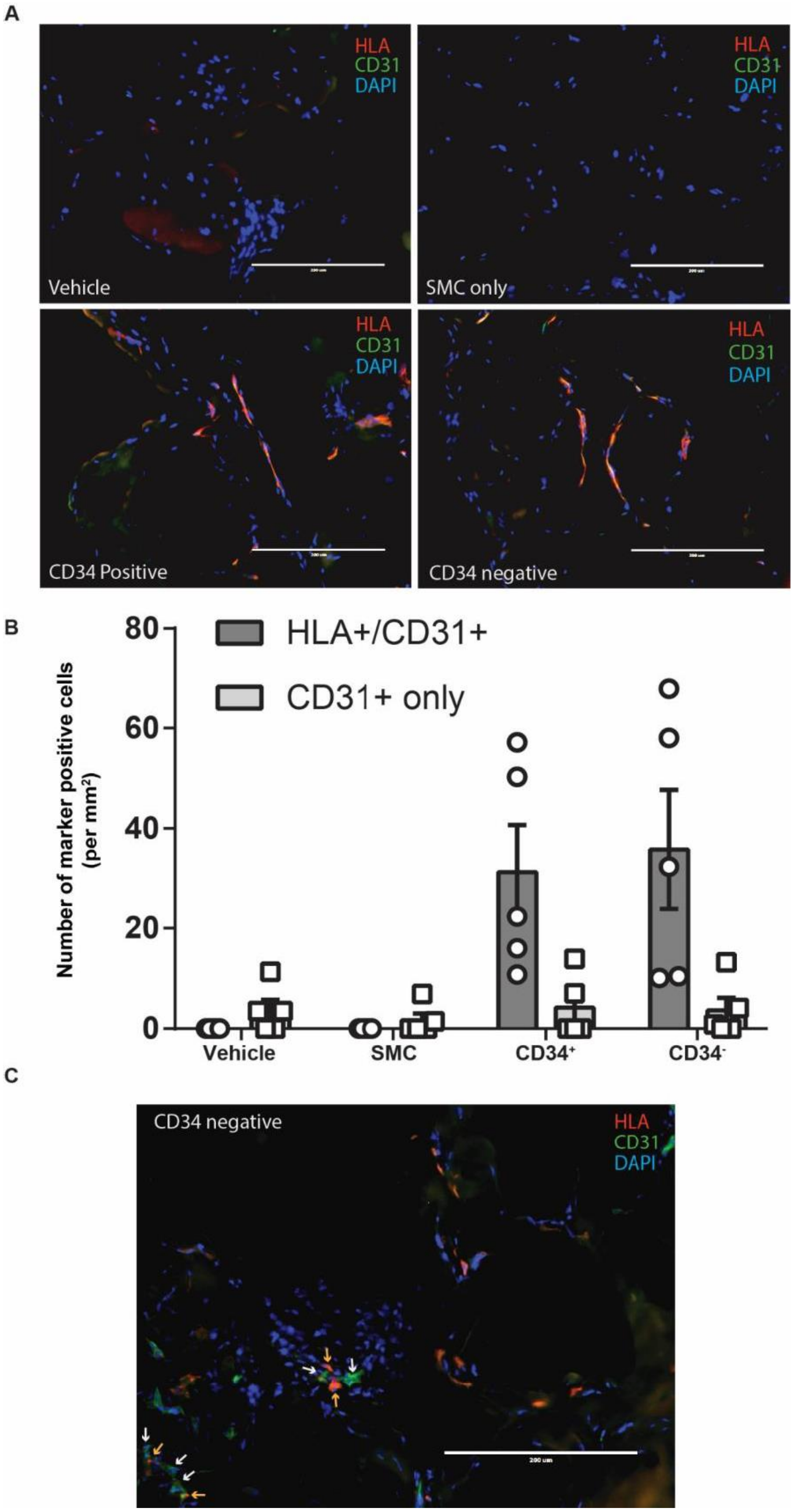
A
HLA
CD31
DAPI
Vehicle
SMC only
CD34 Positive
CD34 negative
B
80
60
40
20
0
Number of marker positive cells (per mm²)
HLA+/CD31+
CD31+ only
Vehicle
SMC
CD34⁺
CD34⁻
C
CD34 negative
200 um

Figure 3.12 Purified CD34$^{+/-}$ ECFC did not improve vascularization of Matrigel plugs after subcutaneous injection into immunodeficient mice. CD34$^{+/-}$ ECFC were purified and combined with mouse smooth muscle cells (SMC) and subcutaneously transplanted into NOD.SCID mice. The Matrigel plugs were extracted after 7 days and assessed for vessel formation within the implants. Vessel structures were visualized by (A) Immunofluorescent staining of human (HLA^{+}) or mouse (HLA^{-}) endothelial (CD31^{+}) cells. Subsequent (B) quantification of human and mouse CD31^{+} cells revealed negligible recruitment of mouse-derived endothelial cells and a similar number of human cells within the scaffolds. Only the CD34^{-} ECFC were observed to co-localize with mouse CD31^{+} cells as seen by (C) Immunofluorescent imaging (human cells – orange arrow; mouse endothelial cells – white arrows) Data represents the mean ± SD using ECFC derived from 5 UCB samples (N=5, P=0.16).

3.4 Discussion

ECFC remain the gold-standard of cultured progenitor-like endothelial cells that harbour potent pro-angiogenic properties *in vitro* and *in vivo*. Even though ECFC can be efficiently expanded in culture, the progeny of these cells lose proliferative capacity as the culture becomes more heterogeneous[20]. Therefore, the ability to define and propagate highly proliferative progenitor cells within heterogeneous ECFC cultures would enable the use of a potent pro-vascular cell population for vascular therapies. In this study we assessed a combination of known progenitor cell functions and cell surface markers[39, 40] to elucidate a distinct progenitor cell subpopulation within ECFC cultures. By using *in vitro* assays to assess putative progenitor cell functions, we observed a reduced cell growth rate, tube-formation, and colony forming ability in the $CD34^+$ ECFC. Next, we used an unbiased proteomic approach to compare membrane proteins between the $CD34^{+/-}$ ECFC subsets by mass spectrometry to identify novel cell surface markers which may enrich for progenitor-like cells in culture. Of the proteins identified, the membrane proteins highly expressed on $CD34^+$ ECFC suggested a mature endothelial cell surface phenotype. However, after sub-cutaneous transplantation into NOD.SCID mice, both the $CD34^{+/-}$ ECFC formed vessel-like structures in the Matrigel plugs.

After assessing the expression of progenitor cell markers: ALDH, CD34, and CXCR4, both $CD34^+$ and $CXCR4^+$ cells were rare while >60% of ECFC demonstrated high ALDH-activity. Interestingly, ALDH-activity did not correlate with the expression of CD34 or CXCR4 as previously suggested by Ferreras *et al.*[41]. We next tested for the presence of intracellular stores of CXCR4 or CD34; a potential for rapid surface localization. Indeed, CXCR4 expression was located within the majority of ECFC which may be likely to localize to the membrane as a rapid response to microenvironmental changes[42]. After confirming the presence of the three prospective progenitor cell markers, we then determined the colony forming capacity of single ECFC purified from using each prospective progenitor marker. Due to the intracellular content of CXCR4, co-localization with CD34, and similar colony forming ability to the CD34-sorted ECFC, we did not pursue other functional assays with the CXCR4-sorted ECFC.

Using our culture conditions, sorting based on ALDH-activity did not significantly change colony forming capacity of the ECFC subsets. We also demonstrated that selection based on ALDH function did not impact the tube forming capacity of the cells. However, purified CD34$^+$ ECFC formed significantly fewer colonies and tubules *in vitro* than the CD34$^-$ ECFC, similar to Ferraras *et al.*[41]. Conversely, other studies have suggested that CD34$^+$ ECFC have an increased capacity to form tube-like structures *in vitro*[38, 43]. The divergence of our results from the other studies may have been due to the differences in ECFC tissue source and/or differences in culture technique. Next we identified a relationship between cell density and CD34 expression as proposed by Tasev *et al.*[38]. However, the expression of other progenitor cell markers was unaffected after growing the ECFC at high density. To further demonstrate the dynamic nature of CD34 expression, we assessed ECFC proliferative capacity alongside the CD34$^+$ cell frequency over the course of a 7-day culture without passaging the cells. This enabled us to identify that ECFC could up- or down-regulate CD34 expression based on the density of the ECFC in culture. Of note, the CD34$^+$ cell frequency began to increase after the exponential phase of the ECFC growth ended, indicating that CD34 expression increases rapidly upon confluence. While monitoring cell expansion, we also noted that the CD34$^-$ ECFC expanded faster than the CD34$^+$ ECFC but the stationary phase of ECFC expansion occurred at approximately the same cell density between the CD34$^+$ and the CD34$^-$ ECFC. These findings suggest that CD34$^-$ ECFC demonstrated higher proliferative potential[41] during the exponential phase of cell expansion but the ECFC growth arrested at a similar density. We also assessed the potential for the CD34$^+$ cell frequency to increase or decrease during culture expansion of ECFC over several passages. Although the CD34 frequency was highest immediately after expansion (40% at passage 1), our previous results suggested that the high density of the established colonies may increase the CD34 cell frequency before re-plating the cells as a monolayer. After this point, the CD34$^+$ cell frequency decreased to a steady state at passage 2 - 5 for each ECFC line tested. Finally, because the CD34 expression on ECFC was dynamic and increased during confluency, we wanted to assess the impact of confluency on endothelial cell function *in vitro*. Although CD34$^+$ cell frequency increased in confluent conditions, the statistical differences in clonogenicity and tubule forming capacity observed between the

$CD34^{+/-}$ ECFC in non-confluent conditions were abrogated when ECFC were cultured in confluent conditions. Thus, this transient state of increasing CD34 expression on ECFC appeared to be in response to the microenvironment while lacking a functional consequence. These findings suggest the need to standardize culture conditions to minimize culture artifacts when comparing studies with ECFC isolated across different tissue types.

Given the functional differences observed between the $CD34^{+}$ and $CD34^{-}$ ECFC subsets *in vitro*, we compared global cell surface protein expression using mass spectrometry identify prospective progenitor cell surface markers. Interestingly, mature endothelial cell surface markers such as CD31, ACE, VEGFR2, and ANGPT2 were expressed at significantly higher levels in $CD34^{+}$ ECFC compared to $CD34^{-}$ ECFC. Alternatively, the proteins more highly expressed on the surface of the $CD34^{-}$ ECFC were not proteins with obvious endothelial cell association. One protein of interest on the $CD34^{-}$ ECFC was AXL; a protein tyrosine kinase which regulates cell proliferation and survival[44]. AXL is also a protein postulated to attenuate immune responses[45], a function of progenitor cell pools in tissues with low turnover rates[46]; a characteristic of endothelial cell populations *in vivo*[47]. Ultimately, a major limitation in this study was the lack of available human-specific antibodies for flow cytometry as a means of prospective cell isolation. For example, the antibodies we tested for COL13A1 and AXL did not detect cell surface expression for these proteins. However, once permeabilized, these antibodies detected the protein expressed in almost 100% of ECFC. This may be due to either the antibody binding to an intracellular epitope or that the protein is anchored on the membrane but is only exposed intracellularly; a limitation of the methodology used for isolating membrane-bound proteins. We also tested an antibody for ACE which we validated to be highly co-expressed with CD34 with reduced expression on the $CD34^{-}$ ECFC. This marker was a promising prospect because the $CD34^{+}$ ECFC which could form colonies and tubules *in vitro* may have been explained by the $ACE^{-}/CD34^{+}$ ECFC. Unfortunately, sorting $ACE^{+/-}$ ECFC, revealed no differences in the generation of colonies after single cell deposition. Similar to CD34 expression on endothelial cells, the expression of ACE has been previously demonstrated to be linked to cell density[48].

Our study suggests that CD34 expressed on endothelial cells after culture *in vitro* does not represent the same populations mentioned in studies where CD34 is used to prospectively isolate endothelial progenitor cells directly from tissue sources. Endothelial cell phenotype plasticity is also described in the literature with changes in endothelial cell phenotype after establishment *in vitro*[49, 50]. The results of the *in vivo* transplantation studies suggest that CD34$^+$ and CD34$^-$ ECFC subsets responded to the *in vivo* environment equally even though obvious functional differences were observed *in vitro*. Thus, this may be suggestive that *in vitro* assays, need to be supported by *in vivo* studies to assess the functions of endothelial progenitor cells relevant to cell therapy applications.

Collectively, our *in vitro* data suggest that CD34$^+$ ECFC represent a more functionally mature endothelial cell population with a diminished ability to form tubes/colonies *in vitro.* In addition, CD34$^+$ ECFC showed increased expression of mature endothelial cell surface markers. However, after transplanting the CD34$^+$ and CD34$^-$ ECFC subsets *in vivo*, functional differences in cell survival, tube formation and murine endothelial cell recruitment were minimal between these populations. Both ECFC subsets formed vessel-like structures in the Matrigel plugs containing a similar number of human cells per mm^2. Although contradictory to similar experiments performed on placental derived ECFC, we observed functional overlap similar to CD34$^+$ peripheral blood-derived ECFC. Thus, differences in cell source, isolation procedure and culture techniques could be responsible for functional differences between these studies. Alternatively, these differences could be due to cultivating different endothelial cell populations that are commonly defined as ECFC by their late outgrowth, expression of endothelial cell markers and high proliferative potential. Nevertheless, standardization for the isolation, culture, and phenotype of ECFC should be addressed for continuity in the potential use of these cells in regenerative therapies.

3.5 References

1. Davies, P.F., *Flow-mediated endothelial mechanotransduction.* Physiological reviews, 1995. **75**(3): p. 519-560.

2. Bennett, H.S., J.H. Luft, and J.C. Hampton, *Morphological classifications of vertebrate blood capillaries.* American Journal of Physiology-Legacy Content, 1959. **196**(2): p. 381-390.

3. Janzer, R.C. and M.C. Raff, *Astrocytes induce blood–brain barrier properties in endothelial cells.* Nature, 1987. **325**(6101): p. 253.

4. Aird, W.C., et al., *Vascular bed–specific expression of an endothelial cell gene is programmed by the tissue microenvironment.* The Journal of cell biology, 1997. **138**(5): p. 1117-1124.

5. Stewart, P. and M. Wiley, *Developing nervous tissue induces formation of blood-brain barrier characteristics in invading endothelial cells: a study using quail-chick transplantation chimeras.* Developmental biology, 1981. **84**(1): p. 183-192.

6. Milici, A., M. Furie, and W. Carley, *The formation of fenestrations and channels by capillary endothelium in vitro.* Proceedings of the National Academy of Sciences, 1985. **82**(18): p. 6181-6185.

7. Rubin, L., et al., *A cell culture model of the blood-brain barrier.* The Journal of cell biology, 1991. **115**(6): p. 1725-1735.

8. Asahara, T., *Isolation of Putative Progenitor Endothelial Cells for Angiogenesis.* Science, 1997. **275**(5302): p. 964-966.

9. Hill, J.M., et al., *Circulating endothelial progenitor cells, vascular function, and cardiovascular risk.* NEJM, 2003. **348**(7): p. 8.

10. Rehman, J., *Peripheral Blood "Endothelial Progenitor Cells" Are Derived From Monocyte/Macrophages and Secrete Angiogenic Growth Factors.* Circulation, 2003. **107**(8): p. 1164-1169.

11. Kalka, C., et al., *Transplantation of ex vivo expanded endothelial progenitor cells for therapeutic neovascularization.* Proc Natl Acad Sci U S A, 2000. **97**(7): p. 3422-7.

12. Dimmeler, S., et al., *HMG-CoA reductase inhibitors (statins) increase endothelial progenitor cells via the PI 3-kinase/Akt pathway.* Journal of Clinical Investigation, 2001. **108**(3): p. 391-397.

13. Lin, Y., et al., *Origins of circulating endothelial cells and endothelial outgrowth from blood.* J Clin Invest, 2000. **105**(1): p. 71-7.

14. Bompais, H., et al., *Human endothelial cells derived from circulating progenitors display specific functional properties compared with mature vessel wall endothelial cells.* Blood, 2004. **103**(7): p. 2577-2584.

15. Ingram, D.A., et al., *Identification of a novel hierarchy of endothelial progenitor cells using human peripheral and umbilical cord blood.* Blood, 2004. **104**(9): p. 2752-60.

16. Yoder, M.C., et al., *Redefining endothelial progenitor cells via clonal analysis and hematopoietic stem/progenitor cell principals.* Blood, 2007. **109**(5): p. 10.

17. Pujol, B.F., et al., *Endothelial-like cells derived from human CD14 positive monocytes.* Differentiation, 2000. **65**(5): p. 287-300.

18. Schmeisser, A., et al., *Monocytes coexpress endothelial and macrophagocytic lineage markers and form cord-like structures in matrigel under angiogenic conditions.* Cardiovascular Research, 2000. **49**: p. 10.

19. Fujiyama, S., et al., *Bone marrow monocyte lineage cells adhere on injured endothelium in a monocyte chemoattractant protein-1-dependent manner and accelerate reendothelialization as endothelial progenitor cells.* Circ Res, 2003. **93**(10): p. 980-9.

20. Medina, R.J., et al., *Endothelial progenitors: a consensus statement on nomenclature.* Stem cells translational medicine, 2017. **6**(5): p. 1316-1320.

21. Case, J., et al., *Human CD34+AC133+VEGFR-2+ cells are not endothelial progenitor cells but distinct, primitive hematopoietic progenitors.* Exp Hematol, 2007. **35**(7): p. 1109-18.

22. Delorme, B., et al., *Presence of endothelial progenitor cells, distinct from mature endothelial cells, within human CD146+ blood cells.* Thromb Haemost, 2005. **94**(6): p. 1270-9.

23. Timmermans, F., et al., *Endothelial progenitor cells: identity defined?* J Cell Mol Med, 2009. **13**(1): p. 87-102.

24. Kinoshita, M., et al., *Long-term clinical outcome after intramuscular transplantation of granulocyte colony stimulating factor-mobilized CD34 positive cells in patients with critical limb ischemia.* Atherosclerosis, 2012. **224**(2): p. 440-445.

25. Baran, Ç., et al., *Effects of preoperative short term use of atorvastatin on endothelial progenitor cells after coronary surgery: a randomized, controlled trial.* Stem Cell Reviews and Reports, 2012. **8**(3): p. 963-971.

26. D'avola, D., et al., *Phase 1–2 pilot clinical trial in patients with decompensated liver cirrhosis treated with bone marrow–derived endothelial progenitor cells.* Translational Research, 2017. **188**: p. 80-91. e2.

27. Wang, X.-X., et al., *Transplantation of autologous endothelial progenitor cells may be beneficial in patients with idiopathic pulmonary arterial hypertension: a*

pilot randomized controlled trial. Journal of the American College of Cardiology, 2007. **49**(14): p. 1566-1571.

28. Yip, H.K., et al., *Level and value of circulating endothelial progenitor cells in patients after acute ischemic stroke.* Stroke, 2008. **39**(1): p. 69-74.

29. Paschalaki, K.E. and A.M. Randi, *Recent advances in Endothelial Colony Forming Cells toward their use in clinical translation.* Frontiers in medicine, 2018. **5**: p. 295.

30. Discher, D.E., D.J. Mooney, and P.W. Zandstra, *Growth factors, matrices, and forces combine and control stem cells.* Science, 2009. **324**(5935): p. 1673-1677.

31. Seneviratne, A.K., et al., *Expanded hematopoietic progenitor cells reselected for high aldehyde dehydrogenase activity demonstrate islet regenerative functions.* Stem Cells, 2016. **34**(4): p. 873-887.

32. Kim, Y., et al., *Use of colloidal silica-beads for the isolation of cell-surface proteins for mass spectrometry-based proteomics.* Immune Receptors: Methods and Protocols, 2011: p. 227-241.

33. Cox, J. and M. Mann, *MaxQuant enables high peptide identification rates, individualized ppb-range mass accuracies and proteome-wide protein quantification.* Nature biotechnology, 2008. **26**(12): p. 1367-1372.

34. Consortium, U., *UniProt: a hub for protein information.* Nucleic acids research, 2014: p. gku989.

35. Melero-Martin, J.M., et al., *In vivo vasculogenic potential of human blood-derived endothelial progenitor cells.* Blood, 2007. **109**(11): p. 4761-4768.

36. Peled, A., et al., *Dependence of human stem cell engraftment and repopulation of NOD/SCID mice on CXCR4.* Science, 1999. **283**(5403): p. 845-848.

37. Egan, C., et al., *Generalised reduction of putative endothelial progenitors and CXCR4-positive peripheral blood cells in type 2 diabetes.* Diabetologia, 2008. **51**(7): p. 1296-1305.

38. Tasev, D., et al., *CD34 expression modulates tube-forming capacity and barrier properties of peripheral blood-derived endothelial colony-forming cells (ECFCs).* Angiogenesis, 2016. **19**(3): p. 325-38.

39. Möhle, R., et al., *The chemokine receptor CXCR-4 is expressed on CD34+ hematopoietic progenitors and leukemic cells and mediates transendothelial migration induced by stromal cell-derived factor-1.* Blood, 1998. **91**(12): p. 4523-4530.

40. Hess, D.A., et al., *Functional characterization of highly purified human hematopoietic repopulating cells isolated according to aldehyde dehydrogenase activity.* Blood, 2004. **104**(6): p. 1648-55.

41. Ferreras, C., et al., *Segregation of late outgrowth endothelial cells into functional endothelial CD34- and progenitor-like CD34+ cell populations.* Angiogenesis, 2015. **18**(1): p. 47-68.

42. Cepeda, E.B., et al., *Mechanisms regulating cell membrane localization of the chemokine receptor CXCR4 in human hepatocarcinoma cells.* Biochimica et Biophysica Acta (BBA)-Molecular Cell Research, 2015. **1853**(5): p. 1205-1218.

43. Patel, J., et al., *Prospective surface marker-based isolation and expansion of fetal endothelial colony-forming cells from human term placenta.* Stem Cells Transl Med, 2013. **2**(11): p. 839-47.

44. Miller, M.A., et al., *Reduced proteolytic shedding of receptor tyrosine kinases is a post-translational mechanism of kinase inhibitor resistance.* Cancer discovery, 2016.

45. Rothlin, C.V., et al., *TAM receptors are pleiotropic inhibitors of the innate immune response.* Cell, 2007. **131**(6): p. 1124-1136.

46. Agudo, J., et al., *Quiescent tissue stem cells evade immune surveillance.* Immunity, 2018. **48**(2): p. 271-285. e5.

47. D'amore, P. and R. Thompson, *Mechanisms of angiogenesis.* Annual review of physiology, 1987. **49**(1): p. 453-464.

48. del Vecchio, P.J. and J.R. Smith, *Expression of angiotensin-converting enzyme activity in cultured pulmonary artery endothelial cells.* Journal of cellular physiology, 1981. **108**(3): p. 337-345.

49. Risau, W., *Differentiation of endothelium.* The FASEB journal, 1995. **9**(10): p. 926-933.

50. Augustin, H.G., D.H. Kozian, and R.C. Johnson, *Differentiation of endothelial cells: analysis of the constitutive and activated endothelial cell phenotypes.* Bioessays, 1994. **16**(12): p. 901-906.

Chapter 4

4 Methods for the analysis of cells seeded in matrix-derived bioscaffolds using flow cytometry.

4.1 Introduction

Decellularized biomaterials have proven useful in a diverse array of cell therapy applications ranging from the development of wound healing matrices to the generation of intact organ scaffolds suitable for tissue engineering[1, 2]. Although diverse sources of biomaterials exist, the use of naturally-derived materials have provided insight into the supportive interactions between the cell and external environment[3-6]. Immunohisochemistry (IHC) has been an extremely useful tool to elucidate cellular distribution and functions within bioscaffolds[7, 8]. However, IHC is laborious and relatively low throughput and does not enable absolute quantification of cell populations/frequencies unless serial sections are analyzed. Thus, novel methodologies are required to enable high throughput analyses of seeded biomatrices. The utility of flow cytometry in a decellularized bioscaffold setting is far reaching as it could enable the investigation of protein and/or gene expression from selected cell types. Furthermore, flow cytometry used in conjunction with IHC analyses of decellularized bioscaffolds can provide insight into cellular distribution as well as quantifying the frequencies of cell phenotypes *in vitro* and *in vivo*.

Flow cytometry is a powerful technique for the multi-parametric analysis of individual cells within heterogeneous cell populations. Furthermore, flow cytometry has proven instrumental in the identification of rare cell types isolated within whole tissues or cultured cells[9]. Although flow cytometry is a very sensitive and high-throughput technique, there are limitations associated with any modality that uses visible light to interrogate cell phenotype. Both autofluorescence and spectral overlap of fluorochromes are important considerations when developing a multichromatic flow cytometric panel[10]. The source for autofluorescence within tissue matrices arises largely from the type and abundance of aromatic amino acids within protein structures[11]. Although many proteins are fluorescent in nature, collagen is a highly abundant ECM protein with strong fluorescent properties that complicates the analyses of cellular components from any solid tissue or ECM-derived scaffold[12]. Moreover, many ECM proteins demonstrate broad emission spectral patterns between 350 and 550 nm, which makes wavelengths closer to the far-red end of the spectrum most practical for imaging purposes[12].

Various techniques have been developed to help minimize autofluorescence, but many of these methods rely on the addition of dyes to quench the autofluorescent signals[13, 14]. The caveat with these methods is that many of the quenching dyes are also fluorescent in the visible light spectra, which make them cumbersome in multichromatic flow cytometric applications. Having to deal with background autofluorescence from the ECM forces the selection of epitopes producing the most intense signal to maximize the resolution between background autofluorescence and true fluorescent signal. Thus, there remains an unmet need to develop protocols whereby ECM contamination is minimized to enable the high-throughput characterization of cells extracted from ECM-derived scaffolds by multichromatic flow cytometry without the use of quenching dyes.

Historically, immunohistochemistry or immunofluorescence microscopy has been typically performed to characterize protein expression by cells seeded within ECM-derived scaffolds[7, 15]. Recognizing the potential utility of flow cytometry as a complementary method for high throughput cell analysis, this study focused on the development of protocols for the efficient extraction and analysis of adherent human cell populations seeded within decellularized scaffolds. The objective was to identify conditions that would enable the isolation of highly purified cell populations with retained cell viability and phenotype. To demonstrate the broad utility of these methods, cell viability and immunophenotype were assessed by flow cytometry using highly adherent human endothelial colony forming cells (ECFC) or mesenchymal stromal cells (MSC) seeded on ECM-derived foams fabricated from human decellularized adipose tissue (DAT), porcine decellularized cartilage tissue (DCT), or commercially-available purified bovine collagen (COL). The selection of the foam format provided a more uniform platform for exploring the effects of the different ECM sources[16]. Enzymatic digestion with TrypLE express^{TM}, Liberase^{TM}, or collagenase were compared to identify the protease formulation that generated the purest cell preparations while minimizing background interference associated with autofluorescent scaffold debris, to enable reliable population analyses throughout the visible spectrum.

4.2 Methods

4.2.1 Human adipose tissue decellularization.

Human adipose tissue was obtained with informed consent from elective lipo-reduction surgeries at the London Health Sciences Centre with Human Research Ethics Board approval from Western University (REB # 105426). Fresh adipose samples were transported on ice in sterile cation-free Dulbecco's phosphate buffered saline (Wisent Inc., Montreal, Quebec) supplemented with 2% bovine serum albumin (BSA). Adipose tissue was prepared by removing cauterized segments and large blood vessels and then processed following an established 5-day detergent-free decellularization protocol that involves mechanical disruption, enzymatic digestion, and polar solvent extraction[17]. All DAT was rinsed with double distilled water (DDH$_2$O) and frozen at -80 ^{o}C before being lyophilized and stored for use.

4.2.2 Porcine cartilage decellularization.

Fresh porcine ears were collected from a local abattoir. The dermis was removed, and the porcine auricular cartilage was surgically extracted and cryomilled to enhance the contact area with the decellularizing agents. The cartilage was decellularized following methods adapted from Xu *et al*[18]. All steps were performed at 37 ^{o}C. In brief, the tissue was subjected to three freeze-thaw cycles in 10 mM Tris buffer (pH 8.0) (Sigma Aldrich, St. Louis, Missouri) before being placed in an extraction solution containing 1.5 M KCl and 2% Triton X-100 (Sigma Aldrich) for 48 h, with solution changes twice per day. Subsequently, the tissue was rinsed 3 times in Sorensen's phosphate buffer (SPB) solution (Sigma Aldrich) for 30 min, followed by digestion in SPB supplemented with 12.5 mg RNase Type III A (from bovine pancreas) and 15,000 U DNase Type II (from bovine pancreas) (Sigma Aldrich) for 5 h. After digestion, the samples were transferred into 50 mM Tris buffer supplemented with 1% tributyl phosphate (TBP) (Sigma Aldrich) for 48 h, replaced twice per day. Subsequently, the samples were rinsed three times in DDH$_2$O for 30 min, and three times in Dulbecco's phosphate buffered saline (D-PBS) for 30 min. Finally, the tissue was incubated for 48 h in 50 mM Tris buffer (pH 9.0), with solution changes 2 times per day. At the end of the process, the DCT was rinsed 3 times in DDH_2O, and frozen at -80 ^oC before being lyophilized.

4.2.3 Bovine collagen scaffolds.

Commercially available, lyophilized bovine tendon collagen type 1 (Advanced Biomatrix, Carlsbad, California) was used as a third extracellular matrix source.

4.2.4 ECM-derived foam fabrication.

DAT, DCT, or commercially-available purified bovine collagen (COL; Tendon source, Advanced Biomatrix, Carlsbad, California) were lyophilized for a minimum of 48 h and minced finely with scissors to 1-2 mm^2 pieces. Following established methods, the ECM samples were cryomilled, digested with 1% (w/w) α-amylase, resuspended in 0.2 M acetic acid (Sigma Aldrich), homogenized and stored at 4 ^oC until use[19, 20]. The ECM suspensions were diluted with 0.2 M acetic acid to a concentration of 25 mg/mL based on the starting mass of ECM. Following previously-established protocols[17], 200 μL of each ECM suspension was transferred into individual wells in 48-well plates and frozen at -80 ^oC before being lyophilized. Prior to cell seeding, the scaffolds were slowly rehydrated through an ethanol series (95, 90, 85, 80, 75, 70, 50, 25, and 0% diluted in sterile D-PBS). Rehydrated foams were incubated in cell-type specific culture media overnight prior to use.

4.2.5 Human progenitor cell isolation and culture.

Mesenchymal stromal cells. Human bone marrow aspirates were obtained from healthy donors with informed consent from the London Health Sciences Centre (London, ON). All studies were approved by the Human Research Ethics Board at Western University (REB # 12934). Mononuclear cells (MNC) were isolated via Hypaque-ficoll centrifugation and seeded on tissue culture polystyrene at 270,000 cells/cm^2. Adherent stromal colonies (CFU-fibroblast) were established within 14 days and expanded in Amniomax media + supplement (Life Technologies, Carlsbad, CA). Established MSCs were cryopreserved at passage 2 used for experiments at passage 4.

Endothelial colony forming cells. Human ECFC were derived from lineage-depleted (Lin-) MNC from umbilical cord blood, as previously described[21]. Briefly, the Lin$^-$ MNC were plated on tissue culture polystyrene at 70,000 cells/cm^2 in endothelial growth media (EGM) (Lonza). Media was changed every 3 days for up to 14 days when colonies became confluent. Cells were lifted with TrypLE^{TM} express and re-plated at 4000 cells/cm^2. ECFC were cryopreserved at passage 2 and used for experiments at passage 4.

4.2.6 Scaffold Seeding.

The day before seeding, the scaffolds were incubated overnight in the cell-type specific media (37 ^{o}C, 5 % CO_2). Each cell type was harvested with TrypLE^{TM} Express enzyme, counted, and 250,000 cells were seeded onto each scaffold in 48-well plates containing 1 mL of growth media for their respective cell types and the plates were incubated at 37 ^{o}C overnight.

4.2.7 Protease preparation.

To extract cells from each scaffold type, 3 different proteolytic enzyme preparations were used: TrypLE express^{TM} (ThermoFisher), Liberase^{TM} TL research grade (Sigma Aldrich), and Worthington's Type I Collagenase (Wisent). The TrypLE express^{TM} was used in stock concentration containing EDTA. Both the Liberase^{TM} TL and Worthington's Type I collagenase were reconstituted within 2 h of use. To reconstitute the Liberase^{TM} TL, 5 mg of Liberase^{TM} TL was dissolved in 25 mL of Dulbecco's PBS (ThermoFisher) to obtain a concentration of 0.5 Collagenase Wünsch units/mL. Briefly, Liberase^{TM} is a proteolytic cocktail containing highly purified collagenase I and II, blended in specific ratios with the neutral protease, Thermolysin. Worthington's type I collagenase was reconstituted at 2 mg/mL (Worthington, Columbus, Ohio) in Krebs Ringer bicarbonate buffer supplemented with 20 mg/mL bovine serum albumin, 3 mM glucose, and 25 mM HEPES, equaling 0.25 Collagenase Wünsch units/mL.

4.2.8 Determining scaffold autofluorescence.

Acellular DAT, DCT or COL scaffolds were incubated at 37 ^{o}C in 1 mL of TrypLE express^{TM}, Liberase^{TM}, or collagenase for 1 hour. Samples were vortexed every 15 minutes and subsequently filtered using a 50 µM cell strainer prior to analysis. For the flow cytometric analyses, an unstained cell suspension collected from tissue culture plastic (TCP) was used to set the fluorescence thresholds prior to measuring fluorescence of the scaffold samples.

4.2.9 Cell extraction methodologies for flow cytometry.

*Cell filtration***.** Seeded DAT, DCT, and COL scaffolds were rinsed once in PBS and transferred to a 5 mL tube containing 1 mL of either Collagenase, Liberase^{TM}, or TrypLE express^{TM}. The samples were incubated in a 37^{o}C water bath and agitated gently every 15 min for 1 h. Samples were incubated for 30 min, 45 min, and 1 h to determine what incubation time maximized cell purity and yield. Subsequently, samples were filtered using 50 µM filters (Sysmex, Kobe, Japan) and centrifuged at 350 x g for 5 min. To determine sample purity, each cell preparation was incubated in Calcein AM (Sigma) stain for 15 min to distinguish cellular content from debris by flow cytometry. All flow cytometric data was obtained using an LSR II flow cytometer (Beckton Dickenson), and analysis was performed using FlowJo software (Treestar, Ashland, OR).

Density gradient. Seeded DAT, DCT, and COL scaffolds were rinsed in PBS and transferred to 5 mL tubes containing 1 mL of Liberase^{TM}. To maximize cell dissociation, Liberase^{TM} was used because it was the strongest protease cocktail containing the most diverse combination of proteases. Samples were incubated in a 37^{o}C water bath and vortexed every 5 min for 15 min until the scaffold structure was evenly homogenized. Sample preparations were layered on 500 µL of Hypaque ficoll density gradient (GE Healthcare, Chicago, IL) and centrifuged at 450 x g for 10 min. Cells were collected at the ficoll-sample interface and filtered using a 50 µM filter. Sample preparations were washed in PBS to dilute residual ficoll and samples were spun at 450 x g for 5 min to pellet the cell sample.

4.2.10 Determining cell viability.

For the cell filtration method, cells were extracted from each of the decellularized scaffold types (DAT and DCT) using TrypLE express^{TM} to minimize the generation of scaffold debris. Cells extracted from the COL scaffolds were incubated in collagenase as it contained the least amount of non-collagenase proteases. For the density gradient method, cells were extracted from each of the decellularized scaffold types (DAT and DCT) using Liberase^{TM} because it contained the highest amount of Wünsch units/mL of the collagenase-containing enzyme cocktails. Cell viability from the scaffolds was determined by staining the extracted cells with Annexin V (Biolegend, San Diego, California), DRAQ5 (ThermoFisher), and Calcein AM. The frequency of apoptotic cells was assessed by enumerating Calcein AM$^+$Annexin V$^+$ cells, while dead cell frequency was determined by quantifying Calcein AM$^-$DRAQ5$^+$ cells. Cell staining was performed according to the manufacturer's instructions.

4.2.11 Antibody staining.

To determine if cell phenotype was affected by the proteolytic enzyme digestion methods, MSC were stained with a multichromatic flow cytometric panel [22] containing conjugated antibodies targeting stromal cell markers: CD73, CD90, and CD105 and the pan leukocyte marker: CD45.

4.2.12 MSC and ECFC co-culture on scaffolds.

To determine if the enzymatic treatment preferentially released MSC or ECFC seeded within scaffolds, the cells were co-cultured at a 1:2, 1:1, and 2:1 ratio. After cell extraction, cells were stained with CD31 and CD90 to discern ECFC and MSC respectively.

4.2.13 Statistics.

Each assay was repeated a total of 3 times. All data is presented as the mean ± standard deviation (SD). For the analysis of significance, a one-way ANOVA with Tukey's multiple comparisons test was performed using Graphpad Prism software.

4.3 Results

4.3.1 Digested bioscaffolds produce autofluorescent debris that complicate flow cytometric analyses.

The characterization of cells extracted from ECM-derived scaffolds with optics-based modalities can be impeded by the autofluorescent properties of the ECM materials. To assess the extent of non-specific event detection associated with debris from scaffolds fabricated with varying ECM sources, the autofluorescent properties of 3 bioscaffolds (human DAT, porcine DCT, and purified bovine COL) digested for 1 hour with the three different enzyme formulations were first assessed in the absence of cells. Due to the heterogeneous makeup of the decellularized ECM, debris particles generated by the TrypLE express^{TM}-digested DAT scaffolds showed significant autofluorescence throughout the visible spectrum (450 nm - 780 nm). Autofluorescence was most pronounced using the violet – blue excitation lasers (>95% of events were autofluorescent at 450 – 610 nm emission) and was reduced when using yellow - green or red excitation lasers (~60% – 70% of events were autofluorescent at 582 – 780 nm emission) (**Figure 4.1A**). In a side-by-side comparison, Liberase^{TM} and collagenase-digested DAT showed considerable autofluorescent events in all emission wavelengths from every excitation laser source (**Figure 4.1B, C**). Similar to the DAT scaffold, the autofluorescent spectra of the DCT digested with TrypLE express^{TM} was most pronounced using the violet – blue excitation lasers (>90% of events at 450 – 610 nm emission) compared to the yellow-green or red excitation lasers (~20% – 50% of events at 582 – 780 nm emission) (**Figure 4.2A**). Similarly, use of Liberase^{TM} or collagenase on the DCT generated more autofluorescent scaffold particles across every channel (**Figure 4.2B, C**). Finally, Liberase^{TM} TL or Worthington’s Type 1 Collagenase treatment resulted in complete digestion of the more homogeneous bovine COL scaffolds (**Figure 4.3B, C**). In contrast to the other ECM sources, TrypLE express^{TM} digestion was the only condition that generated autofluorescent particles for this material. Autofluorescent particles were most pronounced using the violet laser (~75-95% of events at 450 – 610 nm emission), as compared to the blue, yellow – green, or red excitation lasers (~15% – 80% of events at 530 – 780 nm emission) (**Figure 4.3A**). Thus, the presence of autofluorescent scaffold debris within each sample preparations had the potential to complicate flow cytometric analyses of cells enzymatically extracted from the scaffold after seeding.

Figure 4.1

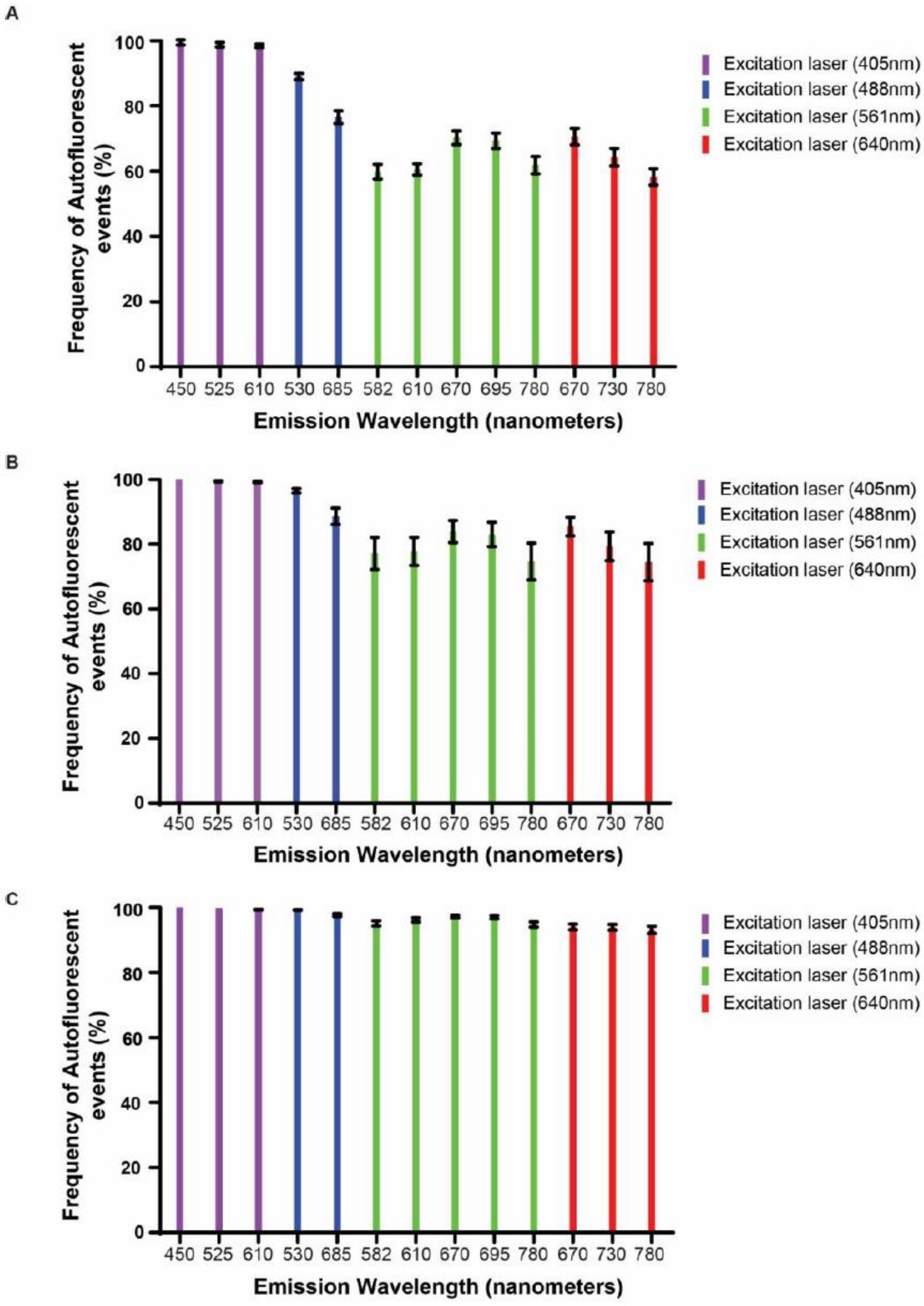
A
Frequency of Autofluorescent events (%)
0
20
40
60
80
100
450 525 610 530 685 582 610 670 695 780 670 730 780
Emission Wavelength (nanometers)
Excitation laser (405nm)
Excitation laser (488nm)
Excitation laser (561nm)
Excitation laser (640nm)
B
Frequency of Autofluorescent events (%)
0
20
40
60
80
100
450 525 610 530 685 582 610 670 695 780 670 730 780
Emission Wavelength (nanometers)
Excitation laser (405nm)
Excitation laser (488nm)
Excitation laser (561nm)
Excitation laser (640nm)
C
Frequency of Autofluorescent events (%)
0
20
40
60
80
100
450 525 610 530 685 582 610 670 695 780 670 730 780
Emission Wavelength (nanometers)
Excitation laser (405nm)
Excitation laser (488nm)
Excitation laser (561nm)
Excitation laser (640nm)

Figure 4.1 Enzyme digested DAT particles were autofluorescent across the visible spectrum. After treating unseeded DAT with (A) TrypLE Express^{TM}, (B) Liberase^{TM}, or (C) Collagenase for 1 hour at 37^{o}C, the digested scaffold was analyzed for autofluorescent particles by flow cytometry. Digested DAT produced autofluorescent events across the visible spectrum (450 - 780 nm). Autofluorescence was most pronounced when excited by the violet – blue laser (>95% of total events at 450 – 610 nm emission), reduced when using yellow - green or red excitation lasers (~60% – 70% of total events at 582 – 780 nm emission). However, the autofluorescent properties were most pronounced across all emission spectra when collagenase was used. Data represents mean ± SD (N=3).

Figure 4.2

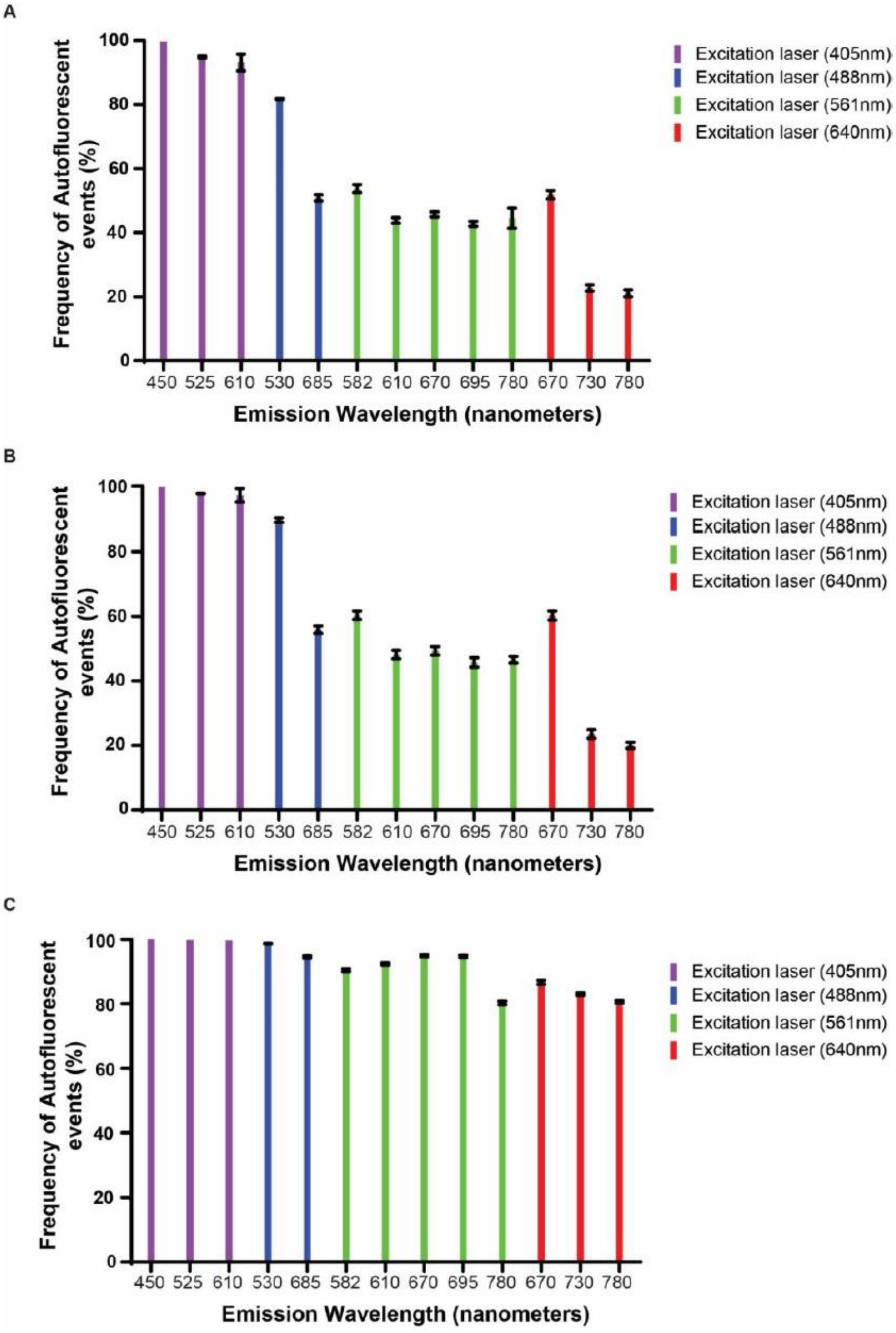
A
B
C
Frequency of Autofluorescent events (%)
0
20
40
60
80
100
450 525 610 530 685 582 610 670 695 780 670 730 780
Emission Wavelength (nanometers)
Excitation laser (405nm)
Excitation laser (488nm)
Excitation laser (561nm)
Excitation laser (640nm)

Figure 4.2 Enzyme digested DCT was autofluorescent across the visible spectrum. After treating unseeded DCT with (A) TrypLE Express^{TM}, (B) Liberase^{TM}, or (C) Worthington's type I collagenase for 1 hour at 37^{o}C, the digested scaffold was analyzed for autofluorescent particles by flow cytometry. Digested DCT produced autofluorescent events across the visible spectrum (450 - 780 nm). Autofluorescence was most pronounced across all channels when the DCT was digested using collagenase. In all cases, scaffold autofluorescence was the most pronounced when excited by smaller wavelength light sources (i.e. Violet-Blue) while autofluorescence from longer wavelength excitation sources was produced to a lesser degree. Data represents mean ± SD (N=3).

Figure 4.3

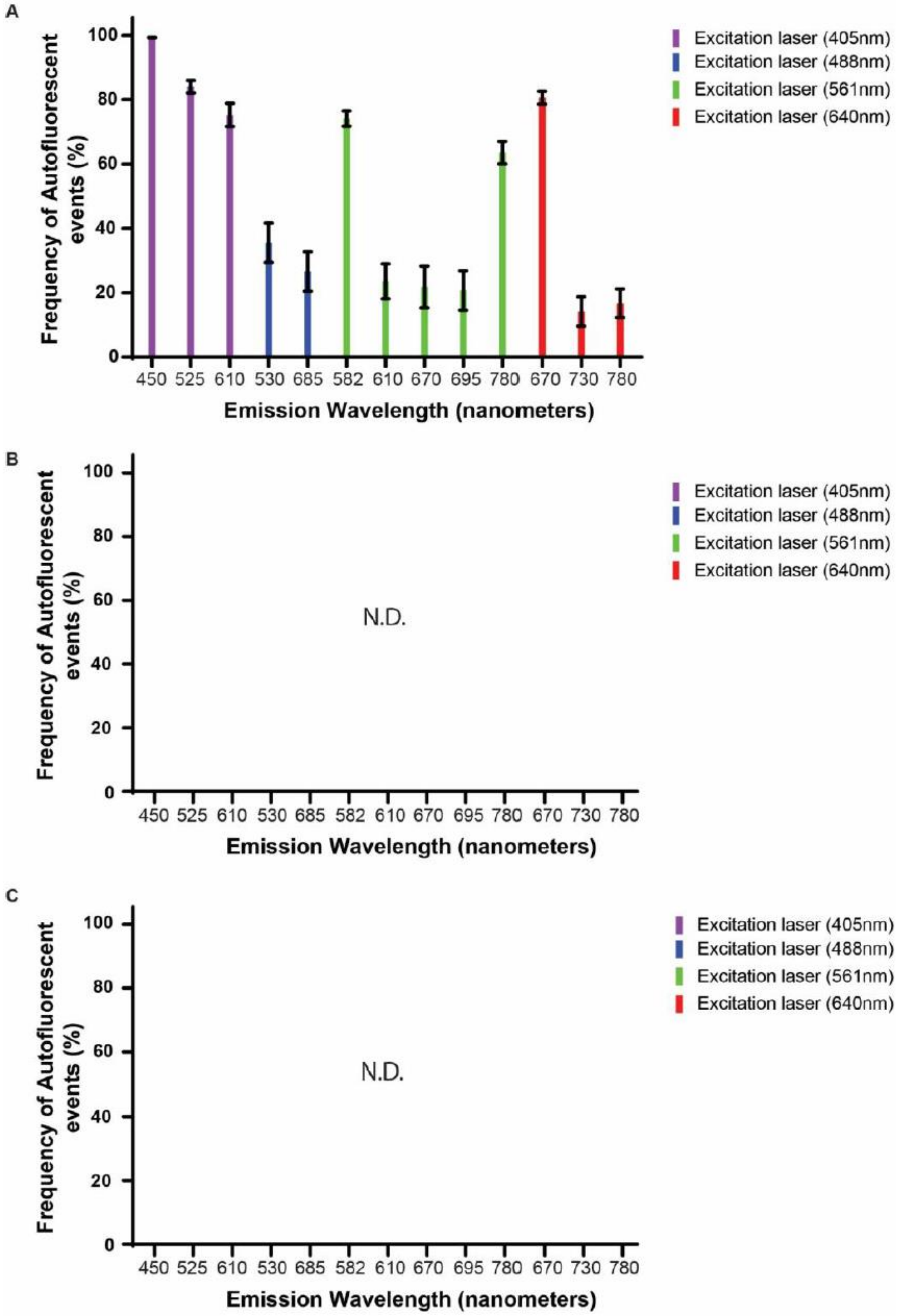
A
Frequency of Autofluorescent events (%)
0
20
40
60
80
100
450 525 610 530 685 582 610 670 695 780 670 730 780
Emission Wavelength (nanometers)
Excitation laser (405nm)
Excitation laser (488nm)
Excitation laser (561nm)
Excitation laser (640nm)
B
Frequency of Autofluorescent events (%)
0
20
40
60
80
100
N.D.
450 525 610 530 685 582 610 670 695 780 670 730 780
Emission Wavelength (nanometers)
Excitation laser (405nm)
Excitation laser (488nm)
Excitation laser (561nm)
Excitation laser (640nm)
C
Frequency of Autofluorescent events (%)
0
20
40
60
80
100
N.D.
450 525 610 530 685 582 610 670 695 780 670 730 780
Emission Wavelength (nanometers)
Excitation laser (405nm)
Excitation laser (488nm)
Excitation laser (561nm)
Excitation laser (640nm)

Figure 4.3 Enzyme digested pure bovine collagen was autofluorescent across the visible spectrum. After treating unseeded collagen with (A) TrypLE Express^{TM}, (B) Liberase^{TM}, or (C) Worthington's type I collagenase for 1 hour at 37^{o}C, the digested scaffold was analyzed for autofluorescent particles by flow cytometry. Digested collagen produced autofluorescent events across the visible spectrum (450 - 780 nm). When digested with trypsin, collagen autofluorescence was the most pronounced when excited by smaller wavelength light sources (i.e. Violet-Blue) while autofluorescence from longer wavelength excitation sources was produced to a lesser degree. Due to complete solubilization of the collagen scaffold, digest preparations with Liberase and collagenase were unable to be detected via flow cytometry. Data represents mean ± SD, (N=3).

4.3.2 Scaffold debris obscures cell populations visualized by flow cytometry.

Next, ECFC (**Figure 4.4**) or MSC (**Figure 4.5**) seeded within scaffolds for 24 hours were enzymatically extracted and analyzed by flow cytometry for relative cell size (forward scatter) and cell complexity (side scatter). Calcein AM was used to discern live cellular content from the scaffold debris. Because protease cocktails such as Liberase^{TM} TL or Worthington's Type I Collagenase primarily digest scaffold proteins, sample preparations from DAT (**Figure 4.4A, Figure 4.5A**) or DCT (**Figure 4.4B, Figure 4.5B**) were comprised of a heterogeneous mixture of cells and scaffold debris. Although filtering the sample preparation was required to ensure large debris particles did not clog the fluidics system on the flow cytometer, filtering in fact, did not eliminate debris events that obscured cells usually discerned by forward versus side scatter selection. In contrast, Liberase^{TM} or Collagenase treatment of more highly purified bovine COL scaffolds resulted in complete scaffold digestion, yielding primarily cellular events (**Figure 4.4C, Figure 4.5C**). Taken together, these data indicated that digestion of decellularized tissue-based scaffolds using collagenase-containing enzyme cocktails produced autofluorescent debris that could obscure cellular events.

Figure 4.4

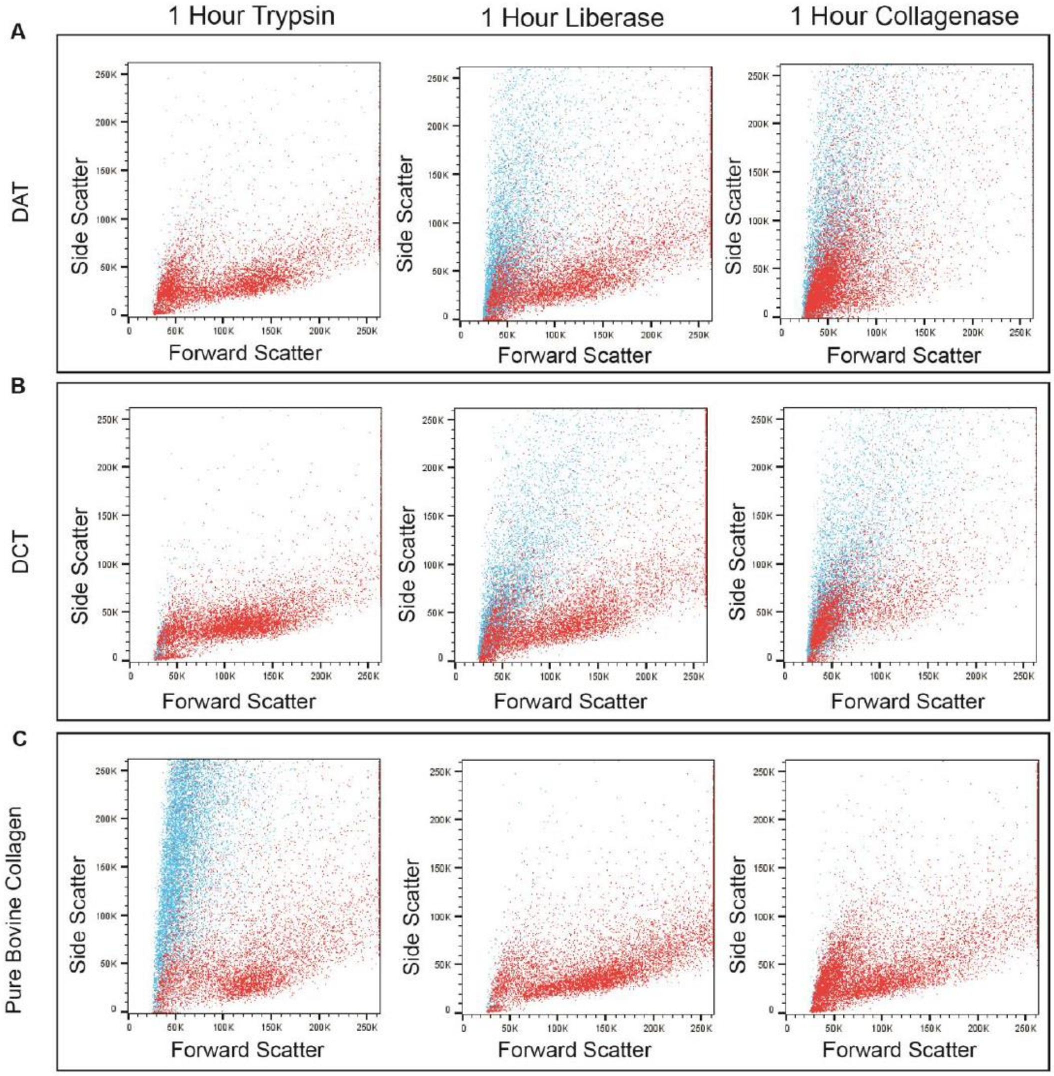

Figure 4.4 Debris particles from digested ECM obscured ECFC detected by flow cytometry. ECFC were seeded into DAT, DCT or bovine collagen matrices, cultured for 24h, and processed using digestive enzymes to release cells for subsequent analyses by flow cytometry. Cells (red dots) were visualized using Calcein AM and overlaid with the Calcein AM negative scaffold debris (blue dots) for each enzymatic treatment. Seeded (A) DAT and (B) DCT scaffolds treated with Liberase^{TM} or collagenase produced forward scatter (FSC) and side scatter (SSC) profiles where cellular events were obscured by scaffold particles. In contrast, DAT and DCT scaffolds treated with TrypLE Express^{TM} generated discernable cellular events with fewer contaminating scaffold particles. (C) Bovine collagen scaffolds showed almost complete digestion with few contaminating events after Liberase^{TM} or collagenase treatment. Flow cytometry plots are representative of 3 ECFC samples (N=3) seeded into each scaffold type and digested by each enzyme.

Figure 4.5

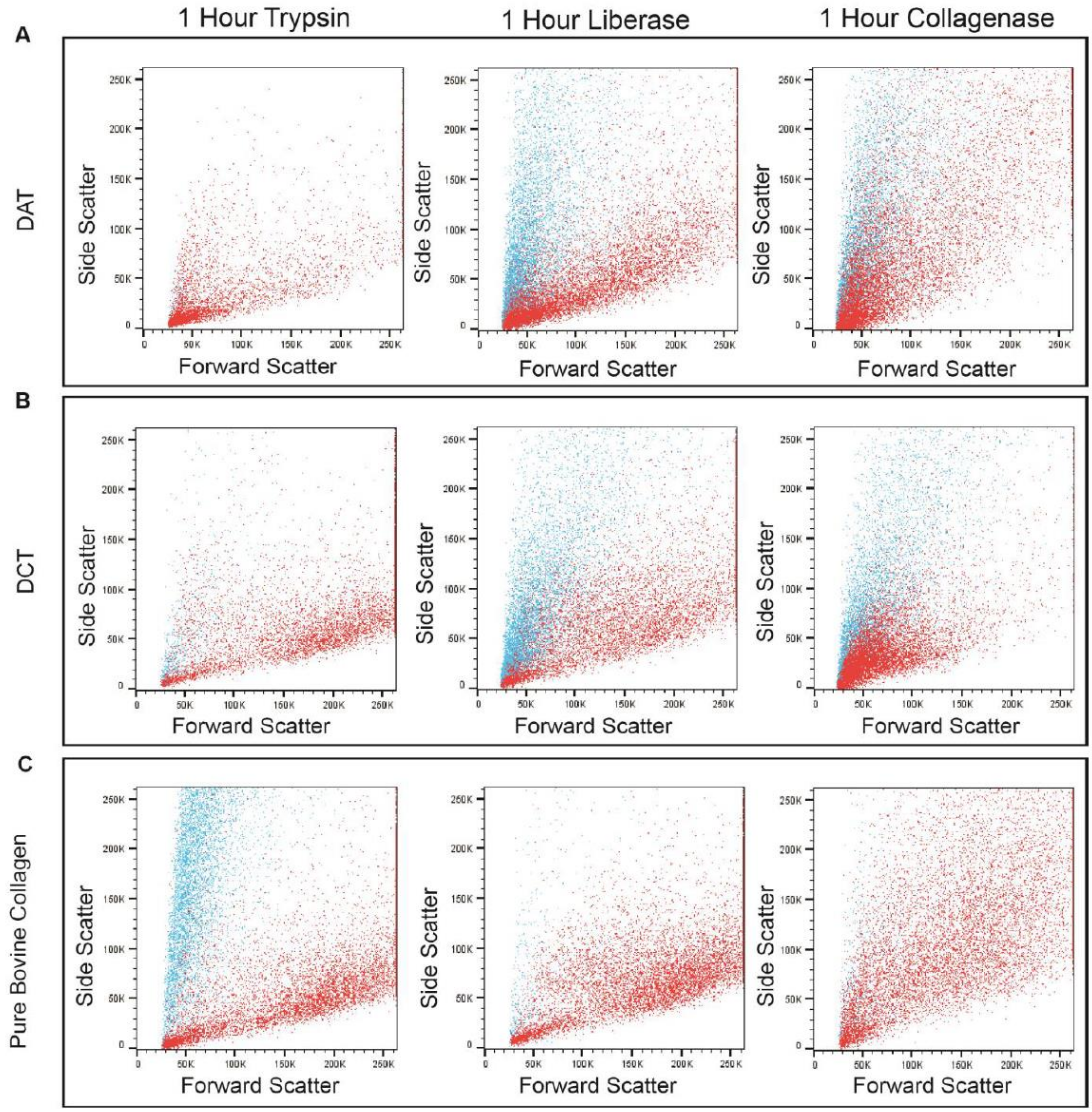

Figure 4.5 Debris particles from digested ECM obscured MSC detected by flow cytometry. MSC were seeded into DAT, DCT or bovine collagen matrices, cultured overnight, and processed using digestive enzymes to release cells for subsequent analyses by flow cytometry. Cells (red dots) were visualized using Calcein AM and overlayed with the Calcein AM negative scaffold debris (blue dots) for each enzymatic treatment. Seeded (A) DAT and (B) DCT scaffolds treated with Liberase^{TM} or collagenase produced forward scatter (FSC) and side scatter (SSC) profiles where cellular events were obscured by scaffold particles. In contrast, DAT and DCT scaffolds treated with trypsin generated discernable cellular events with fewer contaminating scaffold particles. (C) Bovine collagen scaffolds showed almost complete digestion with few contaminating events after Liberase^{TM} or collagenase treatment. Flow cytometry plots are representative of 3 MSC samples (N=3) seeded into each scaffold type and digested by each enzyme.

4.3.3 TrypLE express^{TM} digestion enabled cell preparation suitable for flow cytometry

To optimize the methodology to extract cells from bioscaffolds, ECFC or MSC were seeded into DAT, DCT and COL scaffolds for 24 hours. After extraction, cellular events were clearly identified by gating for Calcein AM^{+} events (**Figure 4.6A**). Although use of collagenase-containing proteases on DAT and DCT bioscaffolds produced sample preparations with abundant scaffold debris (<30% of total events detected were cells), TrypLE express^{TM} -digestion, generated sample preparations with >92% cellular events as measured by Calcein AM positive cells (**Figure 4.6B, C**). However, for the COL scaffolds, TrypLE express^{TM} digestion yielded substantial debris (<70% cell purity), while the collagenase-containing proteases completely digested the ECM resulting in cell purities of >95% (**Figure 4.6D**). The purity of the sample preparations did not differ significantly with treatment time or when comparing endothelial or mesenchymal cell types seeded in bioscaffolds. Therefore, digestion with TrypLE provided the purest sample preparation for the decellularized tissue-based materials, while cells within the more homogeneous COL matrices were best released by collagenase-containing enzyme cocktails.

Figure 4.6

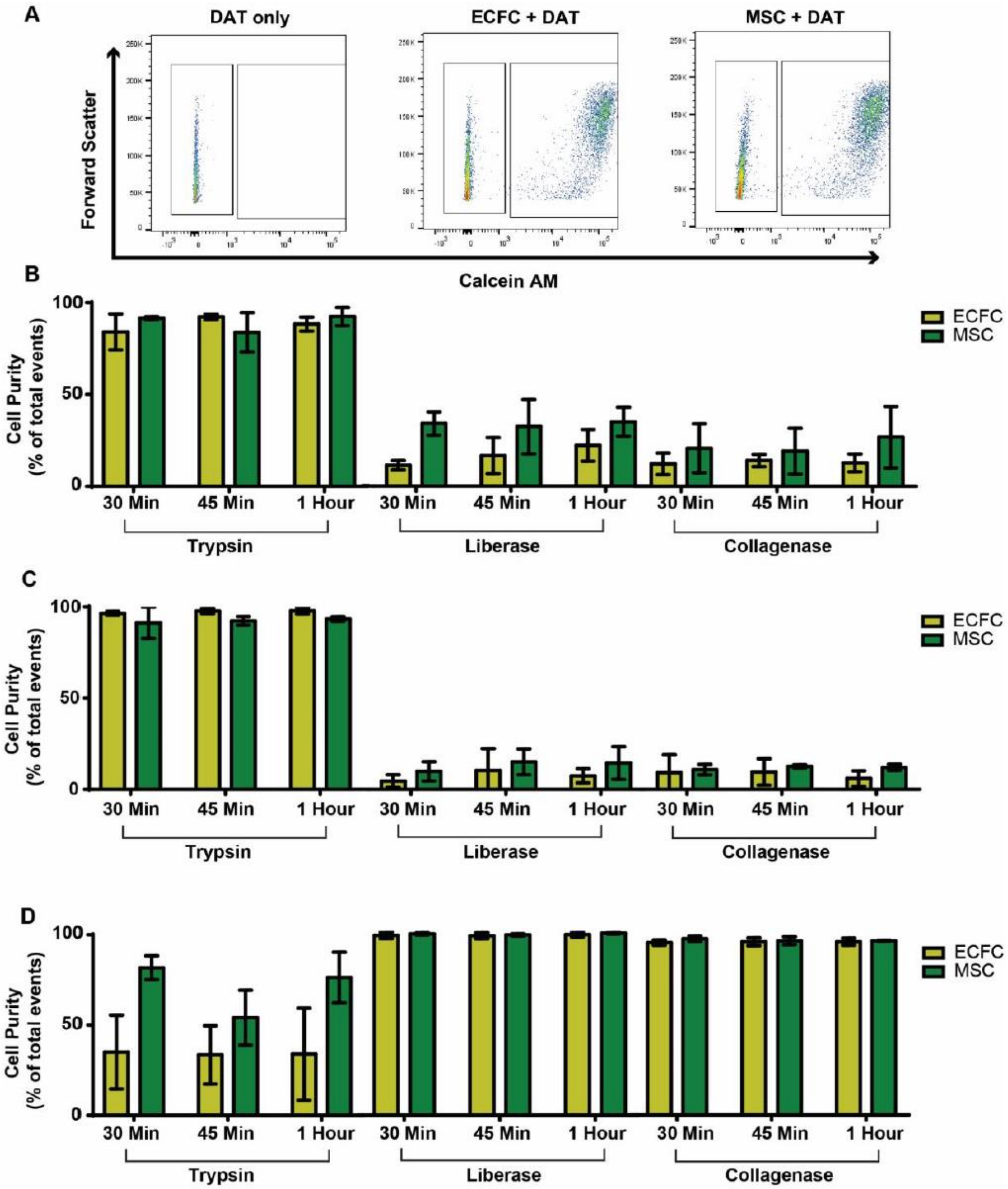
A
DAT only
ECFC + DAT
MSC + DAT
Forward Scatter
Calcein AM
250K
200K
150K
100K
50K
0
-10^3
0
10^3
10^4
10^5
B
C
D
Cell Purity
(% of total events)
100
50
0
30 Min
45 Min
1 Hour
Trypsin
Liberase
Collagenase
ECFC
MSC

Figure 4.6 TrypLE Express^{TM}-treated bioscaffolds produced cell preparations suitable for flow cytometry. To broadly determine the best methodology to extract cells from various bioscaffolds, we seeded ECFC or MSC into DAT, DCT, or bovine collagen preparations for 24h. In addition, (A) Representative flow cytometry dot plots demonstrate our gating strategy using Calcein AM to distinguish live cellular events from debris after treatment with Liberase^{TM}. We then tested 3 protease cocktails: TrypLE express^{TM}, Liberase^{TM}, and Worthington's type I collagenase^{TM} treatment for 30 minutes, 45 minutes, or 1 hour. Trypsin-treatment of (B) DAT and (C) DCT preparations achieved high cell purity (>92%) by flow cytometry. In contrast, (D) bovine collagen preparation achieved optimal purity (>95%) using Liberase or collagenase. Data represents mean ± SD for 3 ECFC and MSC samples (N=3).

4.3.4 Cell extraction efficiency was proportional to the length of enzymatic treatment.

To assess cell yield after seeding and culture, cells were extracted using the most favourable enzymatic conditions identified in the previous studies for each scaffold group and cell viability was enumerated by trypan blue exclusion. The highest MSC and ECFC yield was achieved from scaffolds treated for 1 hour at 37 ^{o}C (**Figure 4.7A, B**). Cell extraction efficiency was quantified by the cell yield from the scaffolds divided by the seeding efficiency. Briefly, the seeding efficiency is equal to the minuend between the initial plating number and the cell number that did not seed into the scaffolds. Notably, MSC extraction efficiency was ~46% in TrypLE express^{TM} -treated DAT and was further reduced in DCT bioscaffolds. In contrast, cell yield extracted from bovine collagen was nearly 100% of the initially seeded dose. This suggests that not all MSC were being completely liberated from the DAT or DCT scaffolds. Interestingly, ECFC did not efficiently detach from the DAT or DCT scaffolds (**Figure 4.7A**), with only ~15% cell extraction efficiency achieved at 1-hour TrypLE express^{TM} digestion. Because of the differences observed between the yields of each cell type, the potential for the enzyme efficiency to vary on a cell-type basis was assessed. The MSC and ECFC were mixed and seeded in specific ratios on both DAT and DCT scaffolds (**Figure 4.7C, D**) and the cell frequencies of extracted cells from both scaffolds matched the starting ratios, indicating that there was no cell-specific selectivity after TrypLE express^{TM} treatment.

Figure 4.7

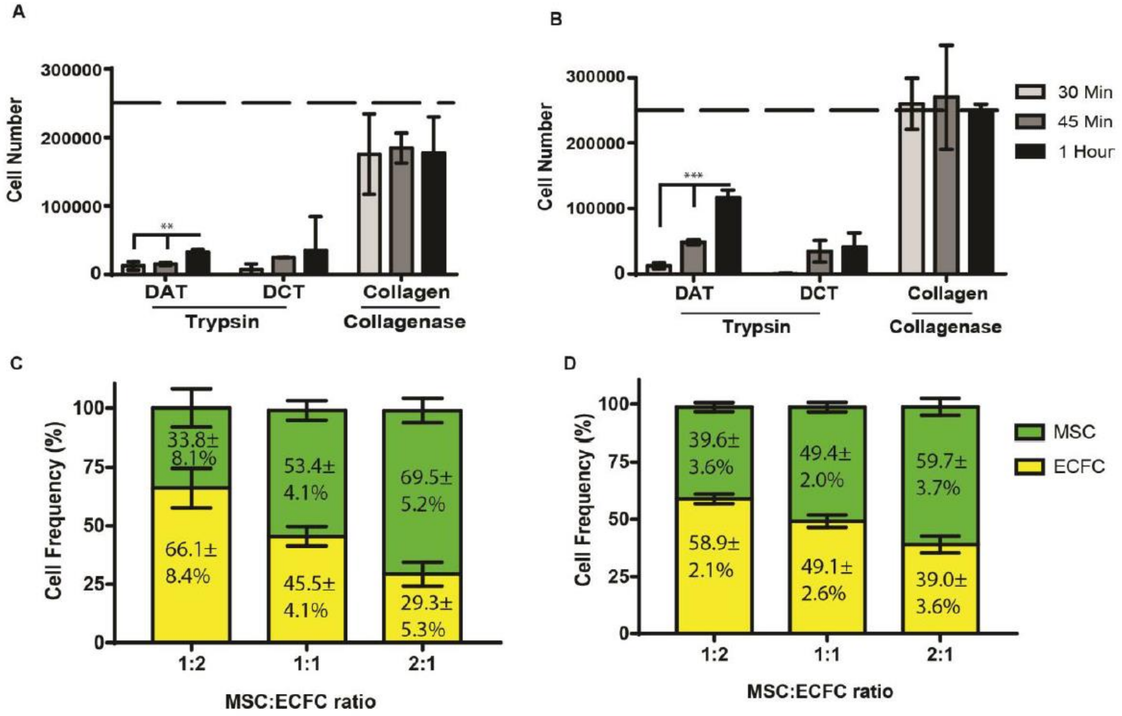

Figure 4.7 Cell extraction efficiency is proportional to protease treatment time. For cell extraction efficiency quantification, the enzymatic conditions that yielded the highest purity for each scaffold type was selected. For DAT and DCT, trypsin was used and for bovine collagen scaffolds, collagenase was used. For the extraction of (A) ECFC and (B) MSC from the DAT scaffolds, trypsin treatment of 1 hour produced the greatest cell yield. The dotted line represents the number of cells plated. To determine if MSC or ECFC were selectively liberated from the DAT or the DCT upon exposure to trypsin, we seeded specific ratios of ECFC and MSC and analyzed the ratio of cells coming off the scaffolds using flow cytometry. Both of the (C) DAT and (D) DCT scaffolds produced nearly identical ratios from what was initially seeded in the scaffolds. During these experiments, the pure bovine cartilage scaffolds were used as a positive control for cell yield because the scaffolds dissolved in solution. Data represents mean ± SD; (** $P<0.01$, *** $P<0.0001$, N=3).

4.3.5 Cell extraction using a density gradient improved cell purity, yield, and viability.

Because the filtration method shown in **Figure 4.7** produced suboptimal cell yield using trypLE express^{TM} treatment, another approach was used to try and improve cell yield. Given the impressive cell yield from the collagenase-treated condition in COL, digestion of the whole scaffold into small fragments may be the most efficient means to maximize the cell yield. To separate cells from debris, a density gradient was used in conjunction with Liberase^{TM} treatment. Liberase^{TM} was used as it contains a diverse set of proteases and caused substantial breakdown of the scaffold. The increased surface area of the homogenized scaffold material may maximize cell yield while minimizing protease exposure time. To remove the scaffold debris, the sample preparations were centrifuged on Hypaque-Ficoll and subsequently filtered after collecting cells from the mononuclear cell layer. MSC purity of >99% was achieved, and the MSC yield was increased to approximately 75% in DAT scaffolds and approximately 50% in DCT scaffolds (**Figure 4.8A, B**). Interestingly, the extraction efficiency of ECFC in either DAT or DCT did not improve using the ficoll-based isolation, suggesting ECFC extraction remained less complete compared to MSC. Because the COL scaffolds fully digested after protease treatment, this condition served as a positive control for determining cell yield.

Figure 4.8

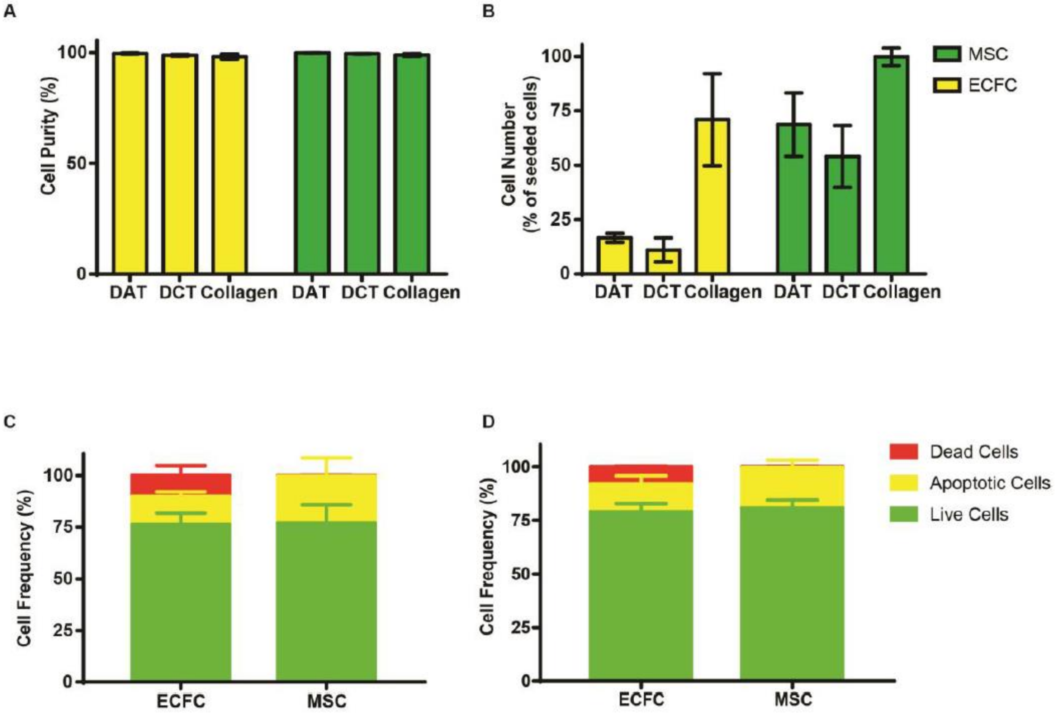

Figure 4.8 Cell extraction using Hypaque-Ficoll improved cell purity, yield, and viability. Both DAT and DCT were treated with Liberase^{TM} at 37^{o}C and agitated every 5 minutes for a total of 15 minutes until scaffolds dissociated. The (A) purity of the extracted ECFC and MSC was >99% and the (B) cell yield was >50% of cells seeded for MSC in either DAT or DCT. Interestingly, the cell yield for ECFC was <25% from either the DAT or DCT scaffolds. Assessing the viability of the MSC and ECFC in (C) DAT or (D) DCT resulted in a higher proportion of ECFC death. The frequency of apoptotic MSC was approximately 20% of cells in both the DAT and DCT. Data represents mean ± SD, (N=3).

4.3.6 Cell extraction did not impair detection of cell viability or cell surface phenotype.

Although >95% cell purity was achieved after TrypLE express^{TM} treatment, the potential for enzymatic treatment to alter cell viability or surface antigen expression was assessed. Our gating strategy to determine cellular content was through selection using DRAQ5^{+} events (**Figure 4.9A, B**). Subsequently, cell viability was assessed through Calcein AM and Annexin V staining (**Figure 4.9C, D**). After treating the DAT scaffolds with TrypLE express^{TM} for 1 h at 37^{o}C, the frequency of viable cells (Calcein+/DRAQ5+/Annexin V-) was high for both ECFC and MSC at 88 ± 2.9% and 85 ± 1.5% respectively (**Figure 4.9E**, **Figure 4.10**), with ~12% apoptotic cells identified (Calcein+/DRAQ5+/Annexin-V+). Importantly, when extracting ECFC and MSC from bovine COL scaffolds, the frequency of apoptotic cells was 63.9 ± 5.7% and 45.0 ± 10.6%, respectively indicating prolonged exposure to collagenase negatively affected cell viability (**Figure 4.9D, E**).

When isolating cells using the density gradient isolation methods with Liberase^{TM}, the viability of MSC was 77 ± 8.7% while the ECFC was 76.3 ± 5.5%. Isolated MSC contained a negligible frequency of dead cells (0.3%) while the ECFC had ~10% dead cell content from both DAT and DCT sample preparations (**Figure 4.8C, D**).

To assess if prolonged enzymatic treatment altered the detection of cell surface marker expression, MSC extracted from DAT scaffolds were stained using a multichromatic flow cytometry antibody panel consisting of 4 lineage-specific cell surface markers and for the viability marker Calcein AM. Each of the antibodies used in the multichromatic panel yielded nearly identical expression frequencies compared to previous work performed on tissue culture plastic[22] using well-accepted stromal cell markers (>95% CD73+, CD90+, CD105+; **Figure 4.11C, E**) and lack of expression of the pan-leukocyte marker (<5% CD45+; **Figure 4.11D, E**). Thus, detection of cell surface antigen expression was not impaired by prolonged enzymatic treatments used for extraction. Taken together these data indicate viable cells expressing known cell surface markers could be quantified after prolonged enzymatic cell extraction procedures.

Figure 4.9

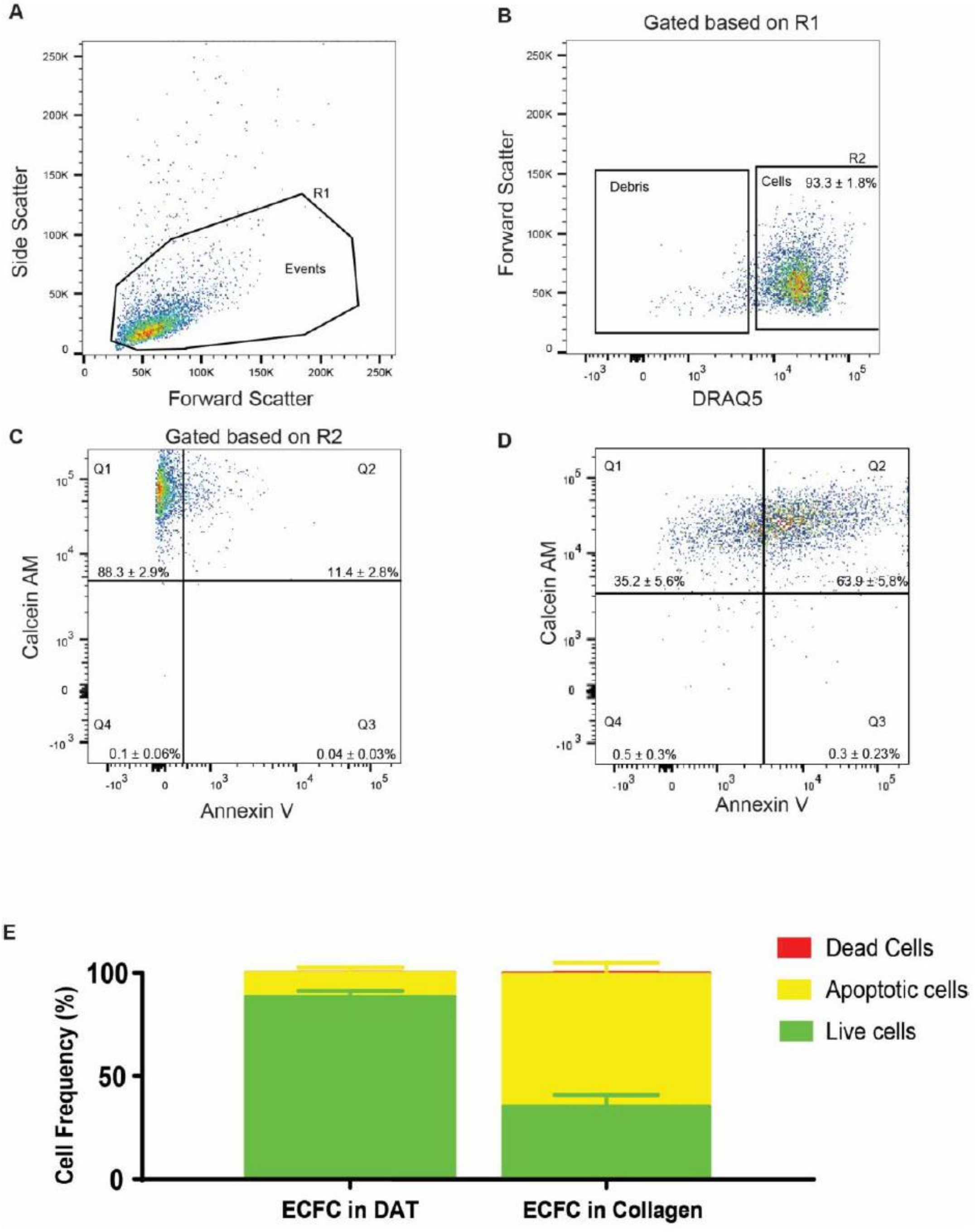
A
250K
200K
150K
100K
50K
0
Side Scatter
R1
Events
0
50K
100K
150K
200K
250K
Forward Scatter
B
Gated based on R1
Forward Scatter
Debris
R2
Cells 93.3 ± 1.8%
-10³
0
10³
10⁴
10⁵
DRAQ5
C
Gated based on R2
Calcein AM
Q1
Q2
88.3 ± 2.9%
11.4 ± 2.8%
Q4
Q3
0.1 ± 0.06%
0.04 ± 0.03%
Annexin V
D
Calcein AM
Q1
Q2
35.2 ± 5.6%
63.9 ± 5.8%
Q4
Q3
0.5 ± 0.3%
0.3 ± 0.23%
Annexin V
E
Cell Frequency (%)
100
50
0
ECFC in DAT
ECFC in Collagen
Dead Cells
Apoptotic cells
Live cells

Figure 4.9 Prolonged enzymatic extraction reduced ECFC survival in collagenase-treated bovine collagen bioscaffolds. ECFC extracted from DAT bioscaffolds were stained with Calcein AM, Annexin V, and DRAQ5. Our gating strategy selected cells based on (A) forward versus side scatter, with (B) DRAQ5 to discern cells from debris, and ECFC seeded in (C) DAT or (D) bovine collagen were analyzed for Calcein AM to label viable cells and Annexin V to label phosphatidyl serine in the external leaflet of the plasma membrane of apoptotic cells. (E) Despite exposure to trypsin for 1 hour, 88 ± 2.9% of ECFC were viable with 11 ± 2.8% of cells undergoing apoptosis. In contrast, prolonged exposure of the ECFC in collagenase resulted in 35.2 ± 5.6% ECFC viability, with 63.9 ± 5.7% of the cells undergoing apoptosis. Data represents mean ± SD for 4 ECFC samples (N=4).

Figure 4.10

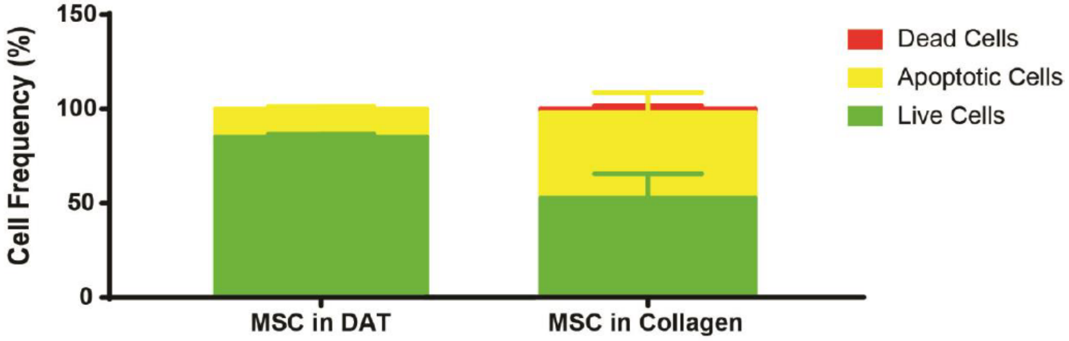

Figure 4.10 MSC viability was reduced in collagenase-treated bovine collagen bioscaffolds. To assess cell viability, we stained MSC extracted from decellularized adipose tissue scaffolds with Calcein AM, Annexin V, and DRAQ5. MSC seeded in decellularized adipose tissue or pure bovine collagen were subsequently analyzed for positive Calcein AM and Annexin V staining to determine sample viability. MSC extracted from DAT using TrypLE Express^{TM} for 1 hour 85 ± 1.5% were viable with 14.9 ± 1.5% of the cells undergoing apoptosis. However, prolonged exposure of the collagen-extracted MSC in collagenase resulted in 45 ± 10.6% of the cells becoming apoptotic. Data represents mean ± SD, (N=4).

Figure 4.11

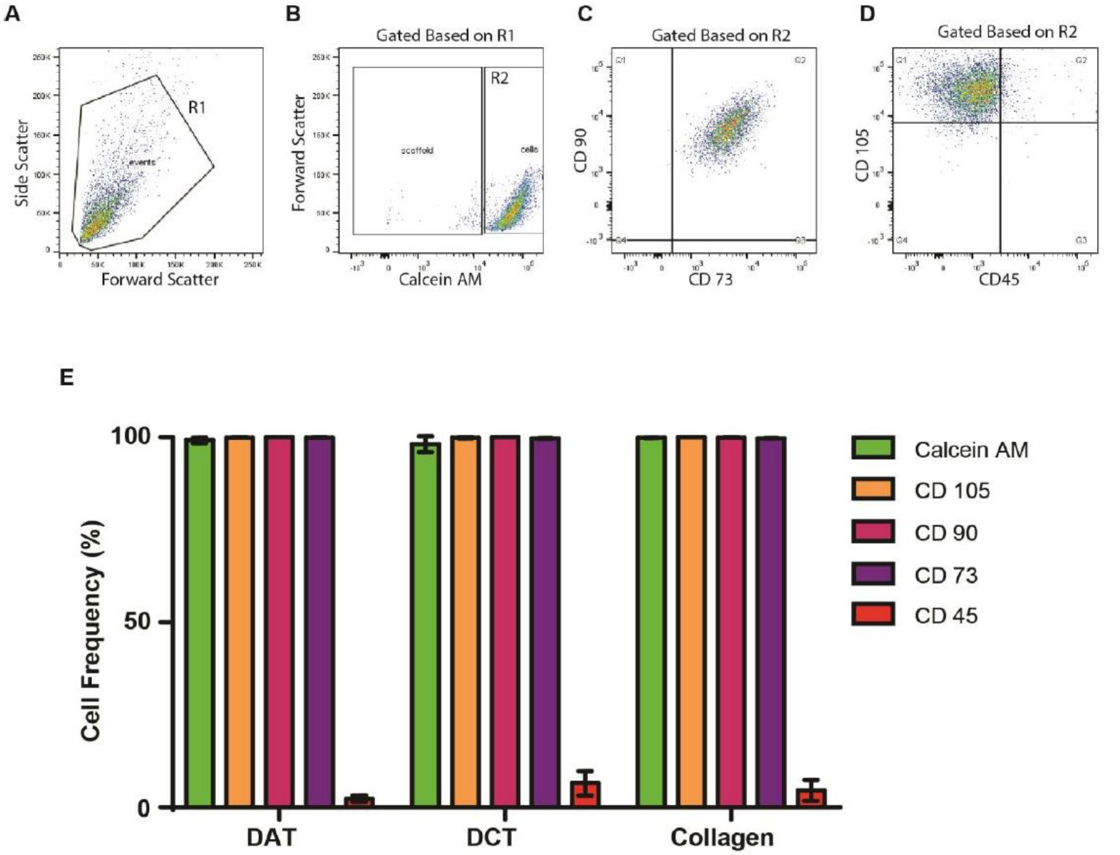

Figure 4.11 Prolonged enzymatic treatment did alter predicted cell surface antigen detection. For DAT and DCT bioscaffolds, seeded MSC were extracted using TrypLE express^{TM} and Liberase^{TM} was used for MSC seeded in bovine collagen. Cell surface phenotype analyses using a 5-color flow cytometry panel revealed that (A, B) viable (Calcein^{+}) MSC highly expressed (C, D) mesenchymal stromal markers (CD73, CD90, and CD105), but did not express the pan-leukocyte marker (CD45). Using this gating strategy each sample preparation was >98% viable. Similar to culture of MSC on tissue culture plastic, the frequency of stromal marker expression was >99% with hematopoietic marker expression (CD45) <6.5%. Data represents mean ± SD for 3 MSC samples (N=3).

4.4 Discussion

In this study, protocols were developed for the analysis of extracted cell populations seeded in decellularized adipose, cartilage, and collagen bioscaffolds using flow cytometry. The primary challenge was to acquire reliable data from adherent cells detached from 3-dimensional bioscaffolds while minimizing the generation of digested scaffold debris. When using enzymes with collagen-digestive functions, digestion of heterogeneous DAT and DCT scaffolds produced a plethora of autofluorescent particles with a forward versus side scatter profile that obscured analyses of the released cells. Importantly, analyses with contaminating autofluorescent debris could generate false positive events and aberrantly alter the detection of important biomarkers. Therefore, development of consistent methods to discern true cellular events from autofluorescent scaffold debris required careful optimization using scaffold-specific enzymatic digestion protocols and cell marking dyes to minimize false positive events detected by flow cytometry.

By altering 3 tested parameters: cell type, bioscaffold composition, and digestive enzyme exposure, we determined that adherent cell types (ECFC or MSC), seeded into bioscaffolds sourced from varying ECM sources (DAT or DCT), required prolonged digestion with TrypLE express^{TM} to generate a cell suspension suitable for flow cytometric analyses. If more aggressive protease treatments such as Liberase^{TM} is utilized, the duration of exposure should be reduced by dissociating the sample to maximize cell viability. The debris generated by Liberase^{TM} treatment required the use of density gradient centrifugation to purify the cell preparation and improve cell yield. To quantify the purity of sample preparations, Calcein-AM viability dye was an effective tool for discerning live cellular events from contaminating scaffold debris. Calcein AM exposure resulted in fluorescent accumulation in viable cells as the compound is metabolized by cytosolic esterase activity[23]. Fortunately, Calcein AM produced a signal notably brighter than the autofluorescence exhibited by contaminating scaffold particles. Ultimately, this allowed us to modify cell extraction methodologies and maximize the signal to noise ratio. Using these optimized protocols, sample purity of >95% was consistently achieved when extracting cells from DAT and DCT using the filtration method, potentially eliminating the requirement for Calcein-AM which occupies one of the most common detectors used for fluorochrome-conjugated antibody-mediated cell surface phenotype analyses by flow cytometry.

The scaffolds used in these studies were fabricated from suspensions of cryomilled decellularized tissue particles pre-molded for use. The ability to shape these natural, cell-supportive constructs greatly increases their versatility for use as a delivery vehicle for pro-regenerative cells in a clinical setting. However, milled constructs can also result in the generation of considerable debris after enzymatic digestion. Interestingly, differences between ECM composition were evident through distinct autofluorescent spectra observed between each tissue-derived scaffold type utilized in this study.

If density gradients are not being utilized during sample preparation, TrypLE express^{TM} was the most effective enzyme treatment for producing a discernable cell suspension from the complex decellularized scaffolds such as DAT and DCT. Although Trypsin is unable to degrade intact collagen triple helices[24], TrypLE express^{TM} can potentially degrade ECM-associated proteins. Both the DAT and DCT scaffolds treated with TrypLE express^{TM} did not generate scaffold fragments in solution, and large particle debris could be minimized by filtration prior to flow cytometry analyses. In agreement, previous studies have demonstrated that trypsin was unable to physically alter collagen-rich tissues[25]. In contrast, when collagenase or Liberase^{TM} were used, these enzyme mixtures primarily targeted abundant bioscaffold components and the macroscopic structure of the scaffolds readily broke down after collagen fragmentation, leaving behind debris that could obscure true cellular events assessed by flow cytometry. To minimize scaffold debris when using Liberase^{TM}, the use of a density gradient was required to effectively remove contaminating debris. The exception to this was the use of collagenase on the purified bovine COL scaffolds. This enzymatic treatment resulted in complete digestion and solubilization of the COL bioscaffold with minimal detectable autofluorescent scaffold debris. However, gentle digestion conditions with short duration are recommended when using commercially available enzyme cocktails as we observed cell viability was reduced after prolonged enzymatic treatment with collagenase.

Two cell types, MSC and ECFC were compared to determine if interactions between different cell types seeded within the various scaffolds would require different enzymatic treatments or exposure durations. Both adherent cell types required TrypLE express^{TM} incubation for an extended period (1h) to obtain sufficient cellular events for flow cytometric applications. When exposed to Liberase^{TM}, the ECFC and MSC required only 15 minutes incubation before density gradient centrifugation. Regardless of the scaffolds, enzymatic treatment or methodological approach used, ECFC consistently showed a reduced cell yield. Because different enzymatic treatments did not preferentially liberate either ECFC or MSC when co-cultured, the low ECFC yield was likely due to reduced cell survival after enzymatic treatment. Although detected cell viability was similar between the MSC and ECFC, these methods cannot account for cells that have completely broken down after cell death. Interestingly, the disconnect between the ECFC cell yields and the ratio between ECFC and MSC after seeding may be explained by the pro-survival effect MSC exerts on ECFC[26]. Collectively, the most efficient methodology to maximize cell numbers was the use of collagenase-containing protease cocktails used in conjunction with density gradient centrifugation. For example, Liberase^{TM} produced higher cell yields from decellularized scaffold materials because the scaffolds were broken down entirely. Subsequent use of a density gradient was required to separate all the cellular components from the scaffold debris in solution. Importantly, prolonged exposure of cells to a collagenase-containing enzymatic digestion negatively impacted cell viability.

4.5 References

1. Badylak, S.F., D. Taylor, and K. Uygun, *Whole-organ tissue engineering: decellularization and recellularization of three-dimensional matrix scaffolds.* Annual review of biomedical engineering, 2011. **13**: p. 27-53.

2. Chattopadhyay, S. and R.T. Raines, *Review collagen-based biomaterials for wound healing.* Biopolymers, 2014. **101**(8): p. 821-833.

3. Taqvi, S. and K. Roy, *Influence of scaffold physical properties and stromal cell coculture on hematopoietic differentiation of mouse embryonic stem cells.* Biomaterials, 2006. **27**(36): p. 6024-6031.

4. Su, N., et al., *Fibrous scaffolds potentiate the paracrine function of mesenchymal stem cells: A new dimension in cell-material interaction.* Biomaterials, 2017. **141**: p. 74-85.

5. O'Brien, F.J., et al., *The effect of pore size on cell adhesion in collagen-GAG scaffolds.* Biomaterials, 2005. **26**(4): p. 433-441.

6. Chen, H., et al., *Cell–scaffold interaction within engineered tissue.* Experimental cell research, 2014. **323**(2): p. 346-351.

7. Marcos-Campos, I., et al., *Bone scaffold architecture modulates the development of mineralized bone matrix by human embryonic stem cells.* Biomaterials, 2012. **33**(33): p. 8329-8342.

8. Ng, S.L., et al., *Lineage restricted progenitors for the repopulation of decellularized heart.* Biomaterials, 2011. **32**(30): p. 7571-7580.

9. Shapiro, H.M., *Practical flow cytometry*. 2005: John Wiley & Sons.

10. Roederer, M., *Spectral compensation for flow cytometry: visualization artifacts, limitations, and caveats.* Cytometry Part A, 2001. **45**(3): p. 194-205.

11. Wagnieres, G.A., W.M. Star, and B.C. Wilson, *In vivo fluorescence spectroscopy and imaging for oncological applications.* Photochemistry and photobiology, 1998. **68**(5): p. 603-632.

12. Manning, H.B., et al., *Detection of cartilage matrix degradation by autofluorescence lifetime.* Matrix Biol, 2013. **32**(1): p. 32-8.

13. Hed, J., *The extinction of fluorescence by crystal violet and its use to differentiate between attached and ingested microorganisms in phagocytosis.* FEMS Microbiology letters, 1977. **1**(6): p. 357-361.

14. Mosiman, V.L., et al., *Reducing cellular autofluorescence in flow cytometry: an in situ method.* Cytometry, 1997. **30**(3): p. 151-156.

15. Fishman, J.M., et al., *Immunomodulatory effect of a decellularized skeletal muscle scaffold in a discordant xenotransplantation model.* Proceedings of the National Academy of Sciences, 2013. **110**(35): p. 14360-14365.

16. Yu, C., et al., *Porous decellularized adipose tissue foams for soft tissue regeneration.* Biomaterials, 2013. **34**(13): p. 3290-3302.

17. Martin, P.M., et al., *Decellularized Adipose Tissue Scaffolds for Soft Tissue Regeneration and Adipose-Derived Stem/Stromal Cell Delivery.* Adipose-Derived Stem Cells: Methods and Protocols, 2018: p. 53-71.

18. Xu, H., et al., *Comparison of decellularization protocols for preparing a decellularized porcine annulus fibrosus scaffold.* PloS one, 2014. **9**(1): p. e86723.

19. Yu, C., et al., *Decellularized adipose tissue microcarriers as a dynamic culture platform for human adipose-derived stem/stromal cell expansion.* Biomaterials, 2017. **120**: p. 66-80.

20. Kornmuller, A., et al., *Fabrication of Extracellular Matrix-derived Foams and Microcarriers as Tissue-specific Cell Culture and Delivery Platforms.* Journal of visualized experiments: JoVE, 2017(122).

21. Ingram, D.A., et al., *Identification of a novel hierarchy of endothelial progenitor cells using human peripheral and umbilical cord blood.* Blood, 2004. **104**(9): p. 2752-60.

22. Sherman, S.E., et al., *High aldehyde dehydrogenase activity identifies a subset of human mesenchymal stromal cells with vascular regenerative potential.* Stem Cells, 2017. **35**(6): p. 1542-1553.

23. Bratosin, D., et al., *Novel fluorescence assay using calcein-AM for the determination of human erythrocyte viability and aging.* Cytometry Part A, 2005. **66**(1): p. 78-84.

24. Gratzer, P.F., R.D. Harrison, and T. Woods, *Matrix alteration and not residual sodium dodecyl sulfate cytotoxicity affects the cellular repopulation of a decellularized matrix.* Tissue engineering, 2006. **12**(10): p. 2975-2983.

25. Keech, M.K., *The effect of collagenase and trypsin on collagen. An electron microscopic study*. The Anatomical Record, 1954. **119**(2): p. 139-159.

26. Souidi, N., et al., *Stromal Cells Act as Guardians for Endothelial Progenitors by Reducing Their Immunogenicity After Co-Transplantation.* Stem Cells, 2017. **35**(5): p. 1233-1245.

Chapter 5

5 Transplantation of endothelial and mesenchymal progenitor cells in decellularized adipose tissue scaffolds for the recovery of acute ischemic injury.

5.1 Introduction

Peripheral artery disease (PAD) is characterized by atherosclerosis-induced ischemia in the extremities, and approximately 10 million individuals in North America are diagnosed with PAD[1, 2]. Although many PAD cases go unrecognized, critical limb ischemia (CLI), the most severe form of PAD, can develop. CLI is characterized by resting pain, non-healing ulcers, and increased risk of infection in the ischemic limb, leading to amputation in 25-30% of patients within one year of diagnosis. Within five years of diagnosis > 60% of patients will have died from cardiovascular complications[3]. The development of an effective means to treat PAD is critical to improve patient outcomes and reduce related health care costs associated with ischemic vascular diseases. Cellular therapies that promote the stimulation of angiogenesis, or the formation of new blood vessels from pre-existing vessels, is an attractive strategy to combat severe vascular diseases.

The architecture and function of the cardiovascular system is crucial in maintaining homeostasis of all organ systems. The basic vascular structure is comprised of multiple cell types including endothelial cells, smooth muscle cells, and pericytes. In order to maintain well-functioning vasculature, these cell types synergistically function with hematopoietic cells to balance blood vessel growth and regression. In the context of vascular disease, these interactions are disrupted[4]. Endothelial colony forming cells (ECFC) spontaneously form tubules *in vitro* and directly incorporate into newly forming blood vessels *in vivo*[5, 6]. Although generally accepted as a pro-vascular cell type, other studies lack demonstration of ECFC incorporation into blood vessels[7]. Importantly, several studies have implicated ECFC as the building blocks of blood vessels during angiogenic processes after injury to the vasculature[8]. However, during chronic cardiovascular disease ECFC numbers are depleted and ECFC dysfunction impairs angiogenic response to ischemia[9].

Perivascular cells, or pericytes, reside adjacent to the endothelial cell layer of blood vessels and act to promote vessel stability through paracrine and direct contact signaling mechanisms[10]. Although closely associated with endothelial cells, pericytes do not express common endothelial markers such as CD31, CD44, or von Willebrand factor (vWF). However, CD146 is expressed on all pericytes and has been used to isolate pericytes from almost every adult organ and from fetal human tissue, including the umbilical cord and placenta. CD146+ cells expanded *in vitro* also express multipotent-stromal cell (MSC) markers: CD73+, CD90+, and CD105+ without the expression of hematopoietic antigens (CD45)[11]. Importantly, expanded CD146+ pericytes associate with blood vessels after intramuscular (I.M.) transplantation into rats subjected to vascular injury[12]. Whether referred to as pericytes or MSC, CD146+ cells efficiently expand adherent to plastic and can differentiate into three distinct mesenchymal lineages: fat, bone, and cartilage *in vitro*. Furthermore, allogenic MSC have been safely transplanted in patients following myocardial infarction to aid in repair and revascularization of cardiac tissue[13]. MSC are a readily available cell source which can be isolated from various human tissue such as bone marrow (BM), adipose tissue and umbilical cord blood.

BM-derived MSC promote survival and proliferation of endothelial cells under hypoxic conditions *in vitro*[14]. After transplantation, BM-MSC may incorporate into vascular structures as pericytes[12, 15]. However, the therapeutic benefit of BM-MSC is contingent on the local microenvironment such as ECM composition, growth factors and conditions such as hypoxia. Regardless, BM-MSC are able to home to sites of vascular injury signaling-axis and secrete factors such as vascular endothelial growth factor (VEGF) and platelet derived growth factor (PDGF) to support angiogenesis[16]. Mice receiving combinatorial xenograft transplantation comprised of endothelial cells with BM-MSC have shown increased vascularization and increased vessel stability[15, 17]. Multiple factors make combinatorial transplantation of MSC and ECFC an attractive strategy. Both MSC and ECFC can be readily obtained from autologous or allogeneic sources, they can be efficiently expanded *ex vivo*, and combined to support robust angiogenesis when transplanted into pre-clinical models of ischemic disease[18].

Many clinical trials have experienced modest outcomes after cell transplantation which may be attributed to transient cell engraftment or poor integration within host tissues[19]. Therefore, transplantation strategies which promote cell engraftment may provide long term benefit in a clinical setting. Due to recent development of innovative biomaterial solutions, biological scaffolds have emerged as a promising means to augment recovery in patients while minimizing immunological responses in the patient. Biological scaffolds resemble the ECM component of a tissue encompassing structural proteins, cell-adhesion proteins, glycoproteins, and other extracellular signaling molecules found in native tissues[20]. These components of ECM are highly conserved across species and thus do not elicit detrimental immune responses in host tissues during xenotransplantation[21]. There are several commercially available biological scaffolds currently used in clinical trials demonstrating both safety and efficacy[22]. Clinically-relevant biological scaffolds can be derived from both synthetic and decellularized tissue sources[23], where each scaffold type provides both advantages and disadvantages. Principally, synthetic scaffolds can be mass-manufactured, physical properties can be tailored to meet the demands of specific applications, and synthetic scaffolds can be transplanted using minimally invasive techniques such as injection. However, synthetic scaffolds have been unable to entirely recapitulate the ECM of the tissues they are designed to mimic. The native ECM in many different tissue types differs not only by protein composition, but they also differ in their structural and spatial arrangement of the ECM proteins[24]. Another advantage to using biological scaffolds in a regenerative context is to improve the engraftment and survival of cells loaded into these matrices[25]. Lastly, previous studies have demonstrated that biological scaffolds can be designed to degrade within tissues after exerting their regenerative effect, thus addressing any concern that foreign scaffold materials will remain within the patient[26, 27].

Biomaterial design and production is continuously improving and currently permits the manipulation of several physical and chemical properties of decellularized bioscaffolds. For example, the additional processing of decellularized adipose tissues (DAT) to be tailored into any size, shape, or concentration for transplantation[28]. These novel processing steps enables the scaffold material to be manipulated like synthetic scaffolds while retaining the chemical and biological composition reflective of native adipose tissue. Human adipose tissue is relatively easy to obtain in the form of discarded tissue from human procedures, such as liposuction clinics. Thus, adipose-derived scaffolds could serve as a readily available tool to promote tissue regeneration at local sites of ischemia[29]. Because adipose tissue is effectively vascularized and immunologically inert, seeding scaffolds with vessel-forming cell types (MSC and ECFC) may prolong donor cell engraftment, and prolong the capacity for transplanted cells to stimulate revascularization of ischemic tissues[30]. The use of biological scaffolds derived from tissue sources provides a composition which closely represents the endogenous ratios of ECM and embedded proteins of biological tissues as compared to some of the synthetic options available[24]. In this study, we demonstrate that DAT foam scaffolds act as an effective carrier to improve the survival and retention of vessel-forming MSC and ECFC after transplantation into an immunodeficient mouse model with femoral artery/vein ligation-induced (FAL) hind limb ischemia.

5.2 Methods

5.2.1 MSC and ECFC isolation and culture.

MSC and ECFC were isolated from human bone marrow and human umbilical cord blood, respectively. Briefly, MNC from each tissue were obtained after centrifugation on hypaque-ficoll density gradient (GE Healthcare, Chicago, USA), and MNC were plated on tissue culture plastic at 270,000 cells/cm^2. Cells were incubated for 14 days in Amniomax media + supplement (Life Technologies, Carlsbad, USA) or in endothelial growth media (EGM-2; Lonza, Basel, Switzerland) to obtain MSC or ECFC colonies respectively. After colony outgrowth, cells were dissociated using trypsin, MSC and ECFC were re-plated at 4000 cells/cm^2 and subsequently passaged when cultures reached 80% confluency. Cell lines were cryopreserved at passage 3 prior to use in experiments.

5.2.2 DAT preparation and seeding.

Collection and preparation of human adipose tissues into DAT foam scaffolds was performed as previously described[27, 31]. Briefly, the adipose tissue was subjected to a detergent-free, 5-day processing protocol beginning with multiple freeze-thaw cycles followed by enzymatic digestion to detach the cells from the ECM. Next, the tissues were subjected to several polar solvent washes to remove lipid content from the ECM scaffold. After rinsing out the polar solvent, the tissues were exposed to another enzymatic digestion, rinsed, and exposed to another series of polar solvent washes and final rinses before the solubilization protocol. After the decellularization process, the scaffolds were then subjected to α-amylase for 72 hours. After rinsing the α-amylase, 0.2M acetic acid was used to solubilize the DAT. 500 µL of the solubilized DAT was loaded into a well of a 48-well plate where it was lyophilized and stored for further use[32]. To seed cells, the foams were re-hydrated and 250,000 MSC and/or ECFC were dispensed on the DAT foams and incubated for 24 hours at 37$^{o.}$C.

5.2.3 Determining cell proliferation and cell surface phenotype via flow cytometry.

MSC and/or ECFC were seeded on DAT foams or tissue culture plastic and incubated at 37^{o}C + 5% CO_2 for 12 hours before adding 1 µMolar of EdU to the cultures. To assess MSC or ECFC surface marker expression after seeding on the DAT foam scaffolds via flow cytometry, the samples were prepared to minimize scaffold debris. Briefly, seeded scaffolds were incubated in Liberase™ TL (Sigma-Aldrich, St. Louis, USA) at 37^{o}C for 15 minutes with intermittent vortexing every 5 minutes until the sample preparation dissociated in suspension. Next, the sample was layered on a Hypaque-ficoll density gradient where the cell fraction was centrifuged, collected, and filtered using a 50 µM filter (Sysmex, Kobe, Japan). To decipher between MSC and ECFC in coculture experiments, the cells were stained with antibodies against CD90 and CD31, respectively. In conjunction with CD90 and CD31, CD73 and CD105 were used to phenotype the MSC while TIE2 and CD105 (BD Biosciences) were used to phenotype ECFC. To detect proliferating ECFC, 1 µMolar of EdU (Thermo Fisher Scientific, Waltham, USA) was added to the EGM-2 for 72 hours before analysis of proliferation. For co-culture assays, MSC proliferation was not measured because the MSC required >20-fold higher concentrations of EdU in which impaired ECFC viability. To measure cell proliferation by EdU incorporation, cells were fixed in 10% formaldehyde (ThermoFisher) for 5 minutes before permeabilization with saponin buffer for 15 minutes. The Alexafluor 647 azide cocktail was prepared as per manufacturer’s instructions (ThermoFisher) and applied to the samples for ½ hour before analysis by flow cytometry.

5.2.4 Femoral artery ligation and transplantation.

Immunodeficient NOD/SCID mice at 8-12 weeks of age were used as xenotransplantation recipients to model hind limb ischemia induced by FAL surgery as previously reported[33]. Under anaesthesia an incision was made in the right thigh and the fat pad cauterized to reveal the femoral artery and vein. The femoral artery and vein were separated from the sciatic nerve and ligated on both the proximal and distal ends to allow for a 5mm section to be excised as previously described[34]. Seeded or unseeded DAT foam scaffolds with 250,000 MSC and/or ECFC were subcutaneously transplanted directly after excision of the femoral artery/vein. For intramuscular transplantation groups, 250,000 ECFC were injected into the quadriceps muscle at 3 locations around the site of injury at equal doses in 20 µL of PBS 24 hours after surgery.

5.2.5 Measurement of perfusion by laser doppler perfusion imaging.

Measurement of limb perfusion was assessed by laser Doppler perfusion imaging (LDPI, Moor Instruments, Devon, UK). Briefly, shaved NOD.SCID mice were placed on a heating pad at 37°C for 5 minutes prior to LDPI acquisition. LDPI was performed on anaesthetized mice at days 0, 7, 14, 21, 28, and 35 post-transplantation where flux images were obtained of the distal hindlimbs. To quantify the kinetics of blood flow recovery, the average flux units per foot were used to generate the perfusion ratios between the ischemic and non-ischemic limb.

5.2.6 Analysis of hind limb and scaffold tissue by immunofluorescence.

After euthanasia, tissue from the ischemic and non-ischemic quadriceps and gastrocnemius muscle was harvested and embedded in optimal cutting temperature medium (ThermoFisher) and frozen at -80°C. Each tissue block was cryosectioned at 12 µm thickness across 3.6 mm of tissue. Immunofluorescence was performed on tissue sections to assess human cell engraftment using the pan-HLA-A, B, C primary antibody (BD Biosciences) and visualized using a secondary antibody conjugated to Cy-5 (Vector Labs, Burlingame, USA). Cells were counter stained with DAPI prior to imaging on the

Leica-TSC SP8 confocal microscope (Leica, Wetzlar, Germany). Human cell quantification using HLA-A, B, C was also performed on tissue sections generated from the DAT scaffolds 14 days post-transplantation. To quantify the vessel density within tissue sections, an anti-mouse CD31 antibody (BD Bioscience) was used and visualized using a secondary antibody conjugated to Texas red (Vector). Tissue sections were counter-stained with DAPI (Sigma-Aldrich, St. Louis, USA) to visualize cell nuclei. Human cell engraftment and/or CD31+ blood vessel density was quantified in a blinded fashion from 12 photomicrographic fields at 20x magnification.

5.2.7 Immunohistochemical analysis of human cell engraftment and blood vessel recruitment within DAT foam scaffolds.

Immunohistochemistry was performed on DAT scaffold tissue sections due to a high degree of autofluorescence produced by the ECM. To quantify the vessel density within the scaffolds, an anti-mouse CD31 antibody (BD Bioscience) was used and visualized using an alkaline phosphatase-labeled secondary antibody stained with Vector blue (Vector). Tissue sections were counter-stained with methyl green (Vector Labs, Burlingame, USA) to visualize cell nuclei. Human cell engraftment was assessed using the NOD.SCID MPS type VII mouse lacking functional beta glucuronidase activity. To visualize human cells in this mouse model, tissue sections were stained with pararosaniline (Sigma). Human cell engraftment was quantified in a blinded fashion from 12 photomicrographic fields at 20x magnification. CD31 density within the scaffolds was quantified using ImageJ analysis of RGB-converted photomicrographs where signal intensity was measured by threshold gating.

5.2.8 Statistical analyses.

For the analysis of significance across assays, a one-way ANOVA with Tukey's multiple comparisons test was performed using Graphpad Prism software. A two-tailed T-test was performed to determine significance between the blood vessel density within the normal and ischemic thigh of the NOD.SCID mice. A two-way ANOVA with Tukey's post-hoc test was performed to determine significance between the HLA$^+$/MAC-1$^+$ cells compared to the HLA$^+$/MAC-1$^-$ cells from the DAT scaffold transplants.

5.3 Results

5.3.1 Seeding and culture in DAT scaffolds altered the surface marker expression of ECFC and MSC.

Because the DAT scaffold is a bio-active substrate, we wanted to assess whether the ECFC or MSC surface phenotype was altered after culture on DAT foam scaffolds compared to tissue culture plastic (TCP) controls. ECFC and MSC were co-seeded and cultured on DAT scaffolds or TCP for 72 hours before assessing ECFC and MSC surface phenotype using a multichromatic flow cytometry panel for: CD31, CD90, CD73, CD105, and TIE2. ECFC were distinguished from MSC using CD31 and CD90 expression, respectively (**Figure 5.1A)**. ECFC demonstrated consistently high expression of CD73 (99.9 ± 0.1%) and CD105 (98.5 ± 2.2%) under all conditions. However, 84.2 ± 7.1% of ECFC expressed TIE2$^+$ when co-cultured with MSC on TCP, and the frequency of TIE2+ ECFC increased to 99.1 ± 0.1% after co-culture on DAT foam scaffolds (**Figure 5.1B**). Alternatively, MSC demonstrated consistent expression of TIE2 (94.9 ± 0.9%) and CD73 (99.9 ± 0.1%) cells where the CD105+ cell frequency significantly decreased from 99.1 ± 0.2% to 88.2 ± 3.6% after co-culture in the DAT foam scaffolds (**Figure 5.1C**). Collectively, these results suggest that DAT scaffolds may modulate the phenotypes of ECFC and MSC during culture *in vitro.*

Figure 5.1

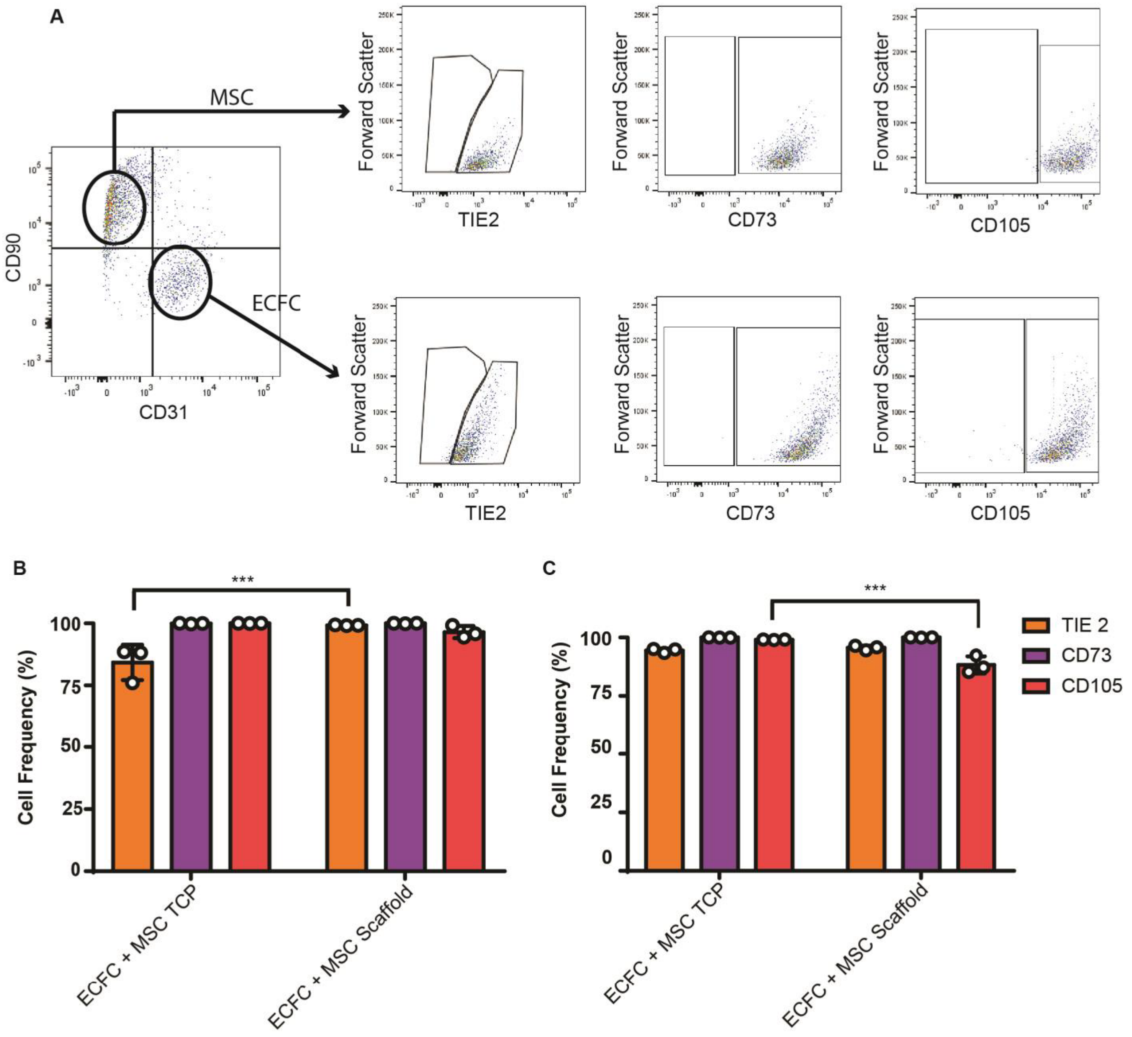

Figure 5.1 ECFC and MSC expression of TIE2 and CD105 was altered by culture in DAT foam scaffolds. The cell surface phenotype of ECFC and MSC cultured on tissue culture plastic or on DAT scaffolds for 72 hours was assessed using a multichromatic flow cytometry panel for: CD31, CD90, CD73, CD105, and TIE2. (A) Representative flow cytometry plots demonstrate the gating strategy to identify ECFC (CD31$^+$) and MSC (CD90$^+$) prior to analysis of other cell surface markers. (B) ECFC demonstrated consistent expression of CD73$^+$ (99.9 ± 0.1%) and CD105$^+$ (98.5 ± 2.2%) across all conditions. The frequency of TIE2$^+$ ECFC during co-culture with MSC on TCP was 84.2 ± 7.1% and was significantly increased to 99.1 ± 0.1% after co-culture on DAT foam scaffolds. (C) MSC demonstrated consistent expression of TIE2$^+$ (94.9 ± 0.9%) and CD73$^+$ (99.9 ± 0.1%) while the frequency of CD105 expression was decreased from 99.1 ± 0.2% after culture on TCP to 88.2 ± 3.6% after culture in the DAT foam scaffolds. Data represents the mean ± SD using cells from 3 UCB (ECFC) and 3 BM (MSC) samples (N=3; ***P<0.001 by one-way ANOVA using a Tukey’s post hoc test).

5.3.2 ECFC proliferation was diminished during culture with MSC or on DAT scaffolds.

To determine whether ECFC proliferation was affected by either the DAT foam scaffolds or direct co-culture with MSC, ECFC were grown in the nucleotide analogue EdU for 72 hours prior to analysis. To assess ECFC proliferation under direct co-culture conditions, cells were stained with a multichromatic panel containing CD31, CD90, and Alexafluor 647 azide to detect EdU incorporation during DNA replication (**Figure 5.2A**). Unfortunately, the concentrations of EdU required to measure MSC proliferation were toxic to the ECFC which prevented the quantification of MSC proliferation in co-culture conditions. After seeding into DAT scaffolds, ECFC division was decreased during the 72-hour culture (2.8 ± 2.0%) compared to ECFC expansion on tissue culture plastic (74 ± 14%). In co-culture with MSC, the rate of ECFC proliferation was minimal in the DAT foam scaffolds (10 ± 6.7%) and on TCP (6.3 ± 2.3%) (**Figure 5.2B**). Taken together these data indicate that ECFC proliferation was impaired when co-cultured with MSC and when cultured on DAT scaffolds.

Figure 5.2

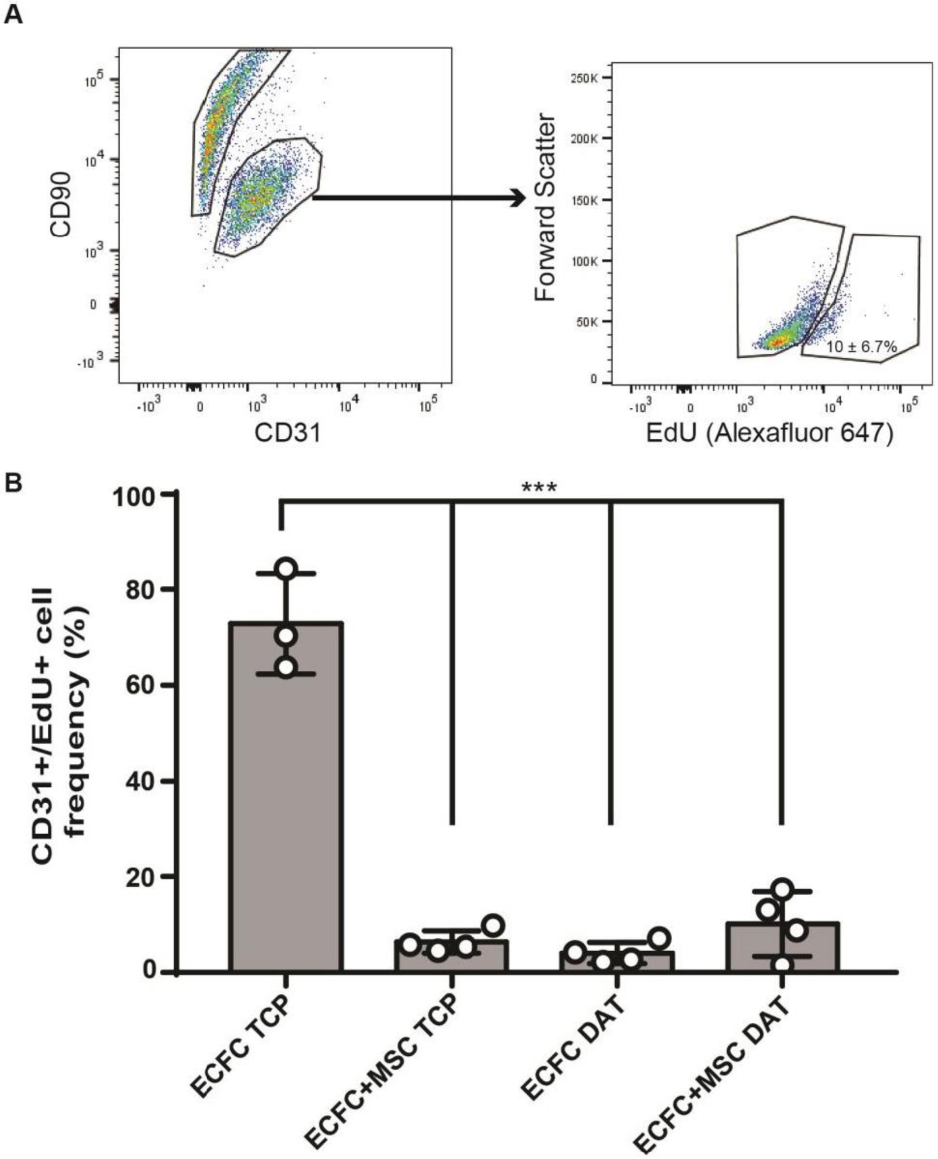

Figure 5.2 ECFC proliferation was decreased by culture on DAT scaffolds and by co-culture with MSC. ECFC were cultured on TCP or DAT scaffolds with or without MSC for 72 hours in media containing 1 µMolar EdU. (A) Representative flow cytometry plots demonstrate the gating strategy to identify ECFC ($CD31^+$) and MSC ($CD90^+$) prior to analysis of EdU-incorporation. During culture on tissue culture plastic, the 74 ± 14% of ECFC divided within 72 hours. During co-culture with MSC on TCP, only 6.3 ± 2.3% of ECFC divided within 72 hours. ECFC proliferation was also significantly decreased when cultured in DAT scaffolds alone (2.8 ± 2.0%) or with MSC (10 ± 6.7%). Data represents the mean ± SD using cells from 3 UCB (ECFC) and 3 BM (MSC) samples (N=3; ***P<0.001 by one-way ANOVA using a Tukey's post hoc test).

5.3.3 Intramuscular injection of ECFC and/or MSC did not improve perfusion in NOD.SCID mice with FAL.

To determine whether ECFC and/or MSC could enhance the recovery of perfusion in a FAL-induced ischemic limb, 250,000 ECFC, MSC or 125,000 ECFC with 125,000 MSC were transplanted via intramuscular injection. Blood flow was quantified by LDPI and the perfusion ratio between the ischemic and non-ischemic limbs was compared every 7 days for 35 days post-surgery. The recovery of the PBS-injected controls plateaued by day 14 (37.5 ± 17.3%), with a final perfusion ratio of 37.0 ± 14.9% by day 35. Similarly, intramuscular injected ECFC, MSC, and ECFC/MSC co-transplantation did not significantly improve perfusion over the 35-day time-course compared to PBS-injected controls (**Figure 5.3**). These results indicated that intramuscular injection of ECFC and/or MSC did not enhance the recovery of blood flow in the ischemic hind limb.

Figure 5.3

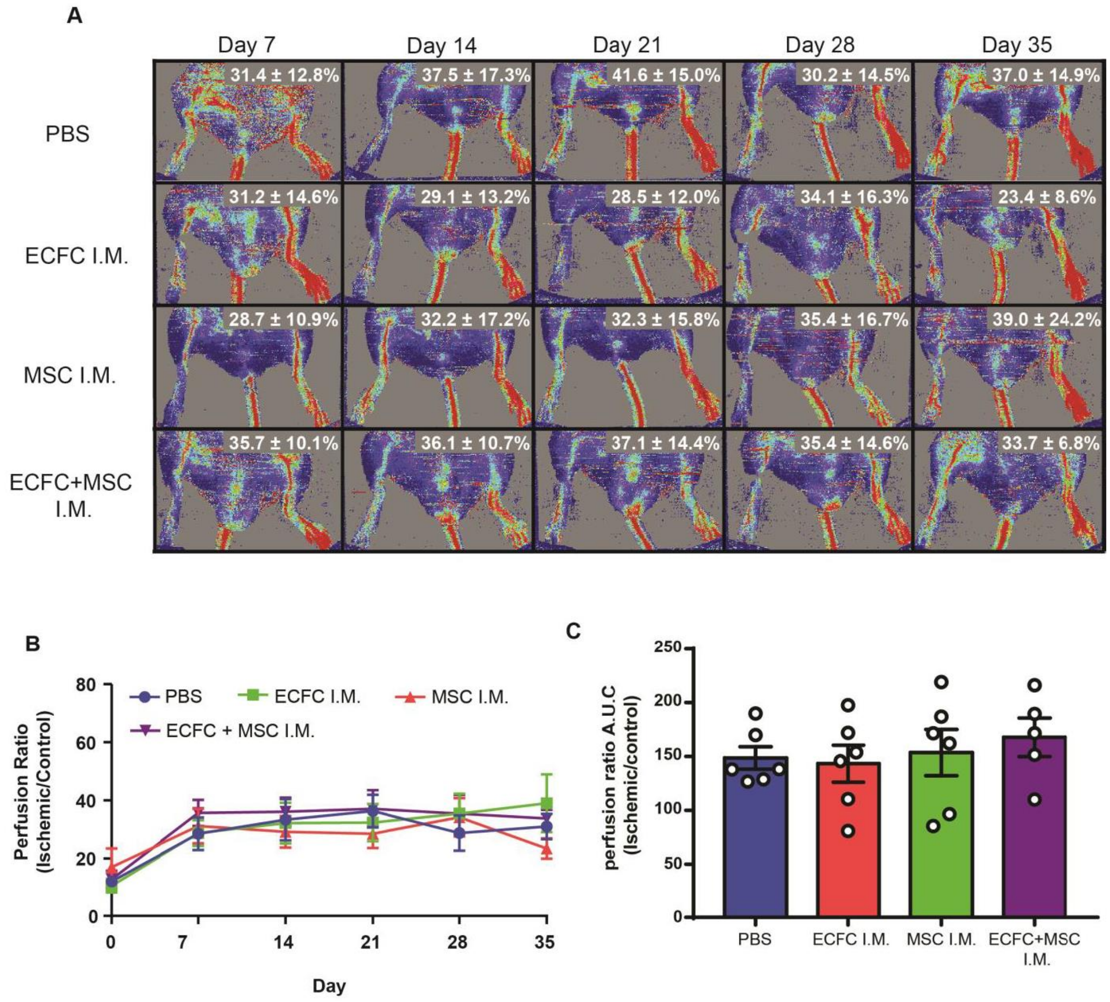

Figure 5.3 Intramuscular injection of ECFC and/or MSC did not improve limb perfusion in NOD.SCID mice after FAL. ECFC and/or MSC were injected into the ischemic thigh muscle of NOD.SCID mice following FAL-induced ischemia. (A) The recovery of limb perfusion was monitored every 7 days for 5 weeks by LDPI. (B) The recovery of perfusion in the ischemic limb of PBS-injected control mice plateaued at day 14 and reached a final perfusion ratio of 37.0 ± 14.9% at day 35. Intramuscular injection of ECFC, MSC, and ECFC/MSC did not significantly alter perfusion with perfusion ratios of 23.4 ± 8.6%, 39 ± 24.2%, and 33.7± 6.8% at day 35, respectively. (C) Similarly, area under the curve (AUC) analyses did not reveal any significant changes in blood perfusion compared to PBS-injected controls. Data represents the mean ± SEM using cells from 6 UCB (ECFC) and 6 BM (MSC) samples (N=6).

5.3.4 ECFC and/or MSC seeded DAT foam scaffolds did not improve perfusion in NOD.SCID mice with FAL.

Accordingly, we wanted to determine whether ECFC and/or MSC could enhance blood perfusion recovery *in vivo* after transplantation seeded on DAT foam scaffolds. Similar to the intramuscular transplantation, NOD.SCID mice with FAL-induced hind limb ischemia were transplanted with scaffold alone or seeded DAT foams with ECFC and/or MSC. After scaffold-only implantation, perfusion ratios plateaued by day 14 (42.0 ± 21.6%), reaching a final perfusion ratio of 36.6 ± 19.9% by day 35. DAT-seeded with ECFC, MSC, and ECFC/MSC did not significantly improve blood perfusion over the 35-day time-course with perfusion ratios at day 35 at 42.2 ± 17.4%, 48.5 ± 17.6%, and 37.3 ± 23.2%, respectively (**Figure 5.4**). Collectively, these results indicated that transplantation of ECFC and/or MSC seeded within DAT foam scaffolds did not improve the recovery of blood perfusion in the ischemic hind limb of NOD.SCID mice. Collectively, the cellular transplantation treatment groups for both I.M. injection and DAT scaffold transplantation did not enhance the recovery of blood perfusion as measured by an area under the curve analysis (**Figure 5.3C, 5.4C**).

Figure 5.4

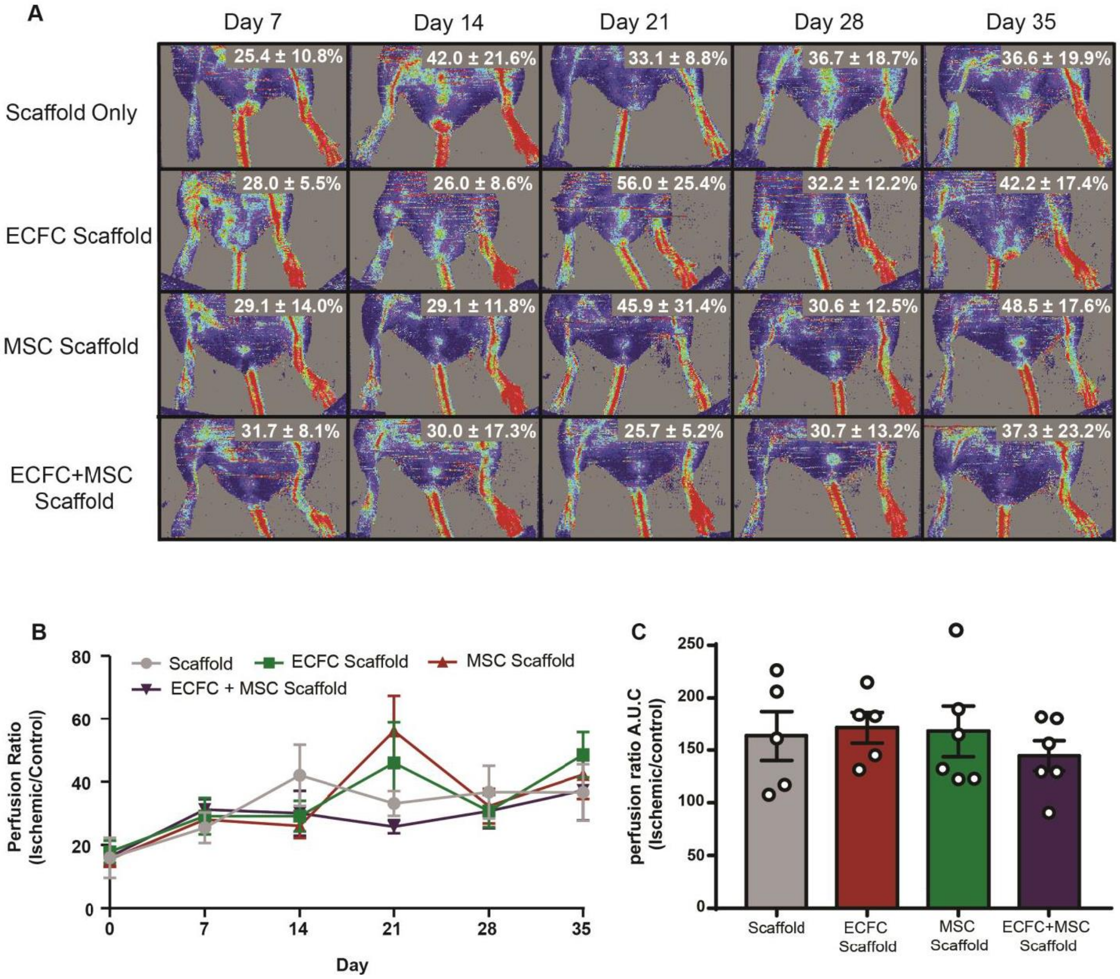

Figure 5.4 Implantation of ECFC and/or MSC seeded into DAT scaffolds did not improve limb perfusion in NOD.SCID mice with FAL. ECFC and/or MSC seeded DAT scaffolds were implanted subcutaneously into the ischemic limb of NOD.SCID mice following FAL-induced ischemia. (A) The recovery of limb perfusion was monitored every 7 days for 5 weeks by LDPI. (B) Control mice implanted with scaffold-only reached a final perfusion ratio of 36.6 ± 19.9% at day 35. Implantation of DAT scaffolds seeded with ECFC, MSC, and ECFC/MSC did not significantly improve perfusion with perfusion ratios of 42.2 ± 17.4%, 48.5 ± 17.6%, and 37.3 ± 23.2% at day 35, respectively. (C) Similarly, area under the curve (AUC) analyses did not reveal any significant changes in blood perfusion compared to scaffold-only controls Data represents the mean ± SEM using cells from 6 UCB (ECFC) and 6 BM (MSC) samples (N=6).

5.3.5 Transplantation of ECFC and/or MSC increase blood vessel density within the ischemic thigh muscle.

Because DAT scaffolds have been previously demonstrated to promote murine endothelial cell recruitment, we next wanted to determine if the ECFC and/or MSC could potentiate murine vessel formation in the ischemic hind limb at the site of implantation. After euthanasia, the ischemic and contralateral thigh muscles were collected, cryosectioned, and analyzed by immunofluorescence using HLA-A,B,C and CD31 to quantify human cell engraftment alongside mouse blood vessel density, respectively. Representative photomicrographs showing CD31+ vessel density in the ischemic limb for each treatment group are shown in **Figure 5.5A, 5.6A**. Interestingly, intramuscular injection of ECFC and MSC (256.8 ± 6.9 cells/mm^2) significantly augmented blood vessel density in the ischemic limb compared to PBS-injected (213.6 ± 24.9 cells/mm^2) controls. Alternatively, the ECFC (255.6 ± 43.4 cells/mm^2) and MSC (233.8 ± 24.2 cells/mm^2) injected mice demonstrated blood vessel densities similar to the PBS controls (**Figure 5.5B**). Interestingly, mice transplanted with the DAT scaffold alone (212.4 ± 11.5 cells/mm^2) had similar CD31$^+$ vessel density in the ischemic limb compared to the ECFC (244.3 ± 12.9 cells/mm^2), MSC (218.0 ± 27.7 cells/mm^2), and ECFC/MSC (239.8 ± 42.8 cells/mm^2) seeded scaffolds (**Figure 5.6B**). After comparing the blood vessel density within the ischemic versus non-ischemic limb, only the PBS-injected and DAT scaffold-alone transplanted controls showed significantly decreased vessel densities compared to the non-ischemic limb. Conversely, all the cellular transplantation conditions showed statistically equivalent blood vessel densities compared to the non-ischemic limb (**Table 5.1**). Collectively, intramuscular injection of ECFC/MSC significantly increased blood vessel density within the ischemic limb. Moreover, all cellular transplantation conditions, with and without the use of DAT scaffolds showed recovered blood vessel density similar to the non-ischemic limb.

Figure 5.5

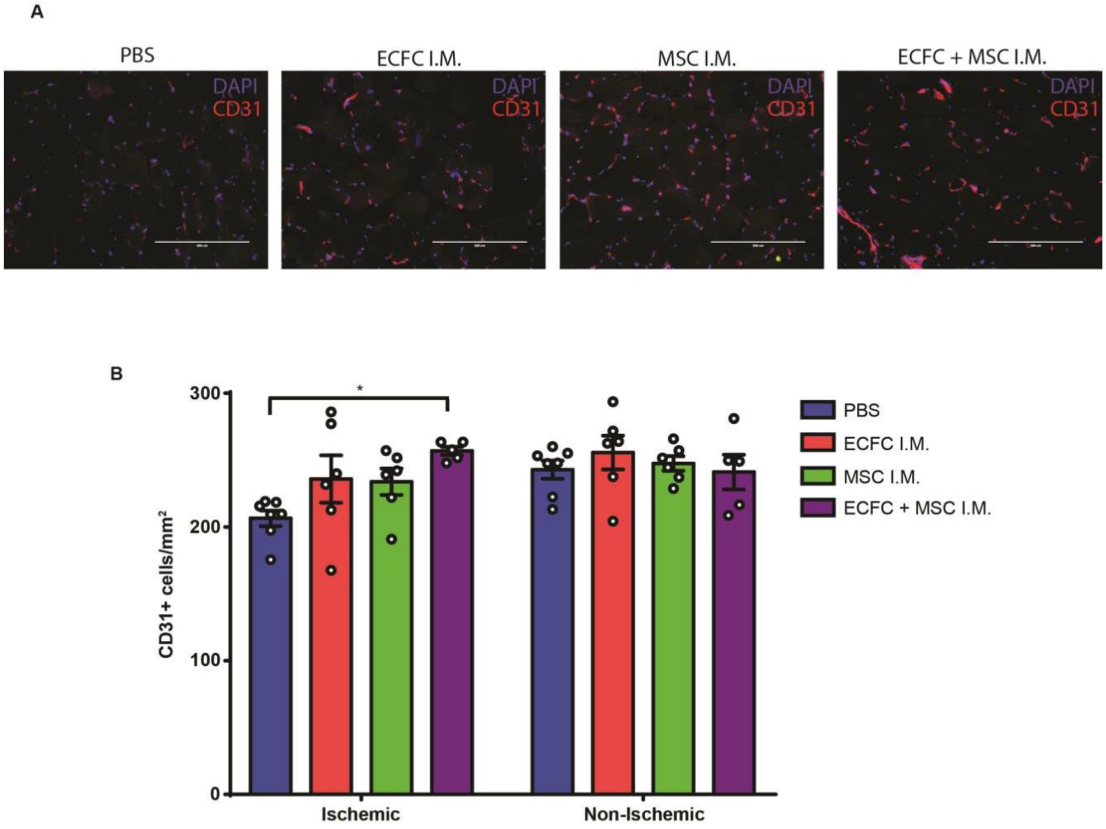

Figure 5.5 Intramuscular injection of ECFC with MSC increased blood vessel density in the ischemic limb of NOD.SCID mice after FAL. ECFC and/or MSC were injected into the ischemic thigh muscle of NOD.SCID mice following FAL-induced ischemia. (A) Blood vessel density was quantified using immunofluorescent photomicrographs of thigh muscle sections enumerating the number of $CD31^+$ cells co-localized with a nuclear signal (DAPI). Mice I.M.-injected with ECFC and MCS together (256.8 ± 6.9 cells/mm^2) showed significantly increased blood vessel density in the ischemic limb compared to mice I.M.-injected with PBS (213.6 ± 24.9 cells/mm^2). In contrast, blood vessel density in mice I.M.-injected with ECFC (255.6 ± 43.4 cells/mm^2), or MSC (233.8 ± 24.2 cells/mm^2) alone was not significantly different when compared to PBS controls. Data represents the mean ± SEM using cells from 6 UCB (ECFC) and 6 BM (MSC) samples (N=6, *$P<0.05$ by one-way ANOVA using Tukey's post hoc test).

Figure 5.6

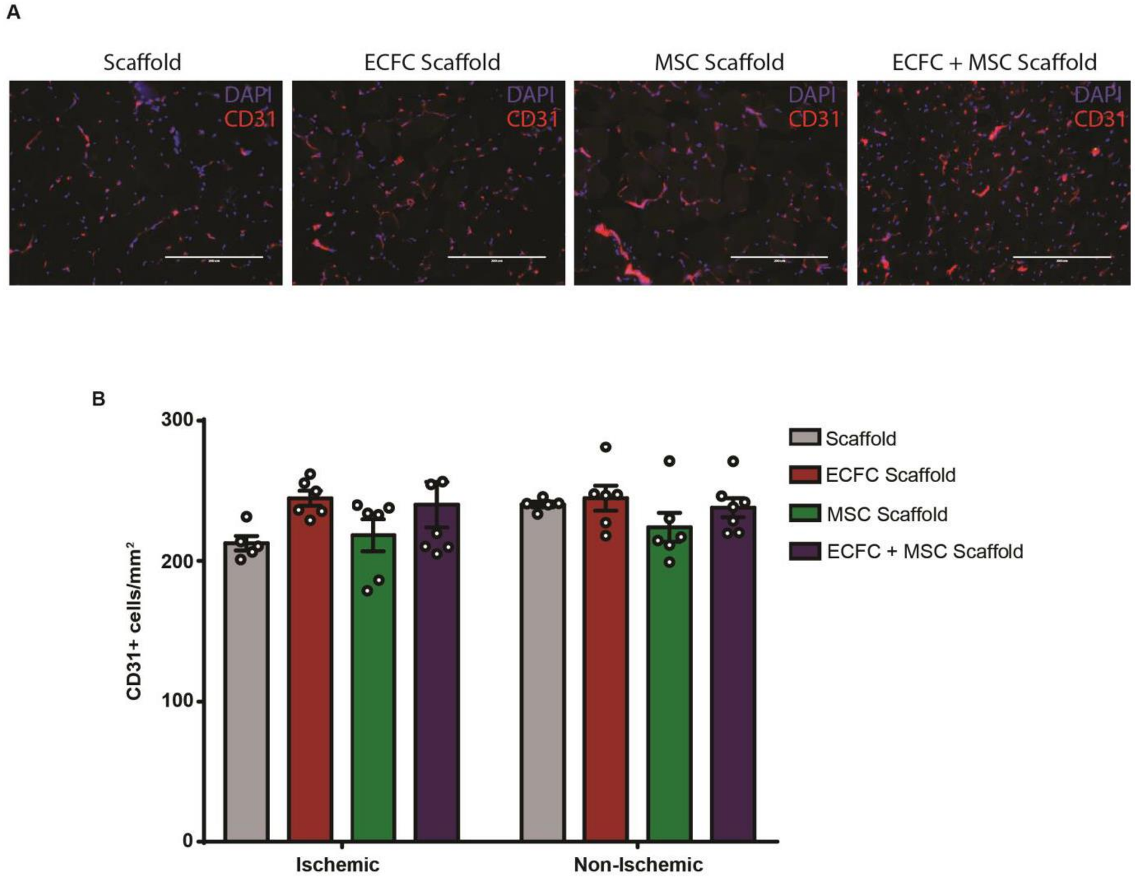

Figure 5.6 DAT scaffolds seeded with ECFC and/or MSC did not improve blood vessel density in the ischemic limb of NOD.SCID mice with FAL. ECFC and MSC seeded on DAT scaffolds were implanted into the ischemic limb of NOD.SCID mice following FAL-induced ischemia. Blood vessel density was quantified on immunofluorescent photomicrographs by enumerating the number of $CD31^+$ events co-localizing with a nuclear signal (DAPI). The ECFC (244.3 ± 12.9 cells/mm^2), MSC (218.0 ± 27.7 cells/mm^2), or both ECFC/MSC (239.8 ± 42.8 cells/mm^2) seeded in DAT scaffolds recovered blood vessel density comparable to the scaffold-treated (212.4 ± 11.5 cells/mm^2) mice. Data represents the mean ± SEM using cells from 6 UCB (ECFC) and 6 BM (MSC) samples (N=5-6, measured by one-way ANOVA using Tukey's post hoc test).

Table 5.1 T-test comparison of CD31$^+$ vessel density between the ischemic and normal thigh within treatment groups 35 days post FAL surgery.

Treatment	Ischemic limb	Normal Limb	P value
PBS	**213.65**	**249.10**	**0.0004**
Scaffold	**212.47**	**239.92**	**0.004**
ECFC I.M.	255.65	255.65	0.07
MSC I.M.	233.84	247.51	0.17
ECFC Scaffold	244.36	244.42	0.99
MSC Scaffold	218.10	223.73	0.68
ECFC + MSC Scaffold	239.81	237.70	0.86
ECFC + MSC I.M.	256.86	241.06	0.34

5.3.6 Human ECFC or MSC engraftment was improved within the DAT scaffolds.

To ensure sensitive detection of human cell engraftment without the use of human-specific cell surface marker detection, ECFC or MSC were transplanted into NOD.SCID MPS type VII mice that lack functional beta glucuronidase (GUSB) activity. Because the human ECFC and MSC transplanted ubiquitously expressed GUSB, human cells can be tracked at single cell sensitivity using this unique mouse model using pararosanalin (red) staining for GUSB enzymatic activity[33, 35]. Similarly, immunohistochemical staining of the DAT scaffolds from the NOD.SCID MPS type VII mice was performed to avoid tissue autofluorescence impeding human cell detection. At 14 days after I.M.-injection, single GUSB+ human cells were rarely detected within the ischemic thigh. The detection of GUSB+ cells occurred in only one of three transplanted mice throughout 0.35 mm of sectioned thigh muscle tissue (**Figure 5.7A, C**). Interestingly, human cell engraftment within the ischemic thigh was also observed within mice transplanted with ECFC or MSC-seeded DAT scaffolds (**Figure 5.7B, D**). In contrast, human GUSB+ cells were abundantly detected within DAT scaffolds at 14 days post-transplantation (**Figure 5.8A, B**). The amount of human cell engraftment within the DAT scaffolds averaged 6.12 ± 2.9 cells/mm^2 for ECFC and 5.7 ± 6.0 cells/mm^2 for MSC (**Figure 5.8C**). Prolonged human cell engraftment within the DAT scaffolds was detected 35 days post-transplantation (**Figure 5.9**). Furthermore, human cell engraftment was detected and quantified within the DAT scaffolds using flow cytometry after 14 days post-transplantation. Cells extracted from the DAT scaffolds were stained with CD31, CD90, and Calcein AM to stain the live human ECFC and MSC (**Figure 5.8D**). The frequency of ECFC seeded within DAT scaffolds was 0.46 ± 0.56% which was significantly improved when seeded in DAT scaffolds with MSC (3.44 ± 1.49%). MSC frequency was unaffected with or without the presence of ECFC (1.65 ± 0.50% versus 1.82 ± 1.40%, respectively) (**Figure 5.8E**). These data suggest that human ECFC and MSC survival and retention was increased within the implanted DAT scaffold compared to intramuscular injection. Moreover, the survival of ECFC within the DAT scaffolds was augmented in the presence of MSC. In addition, human cell extravasation from the DAT scaffold into surrounding muscle tissue was detectable but extremely rare.

Figure 5.7

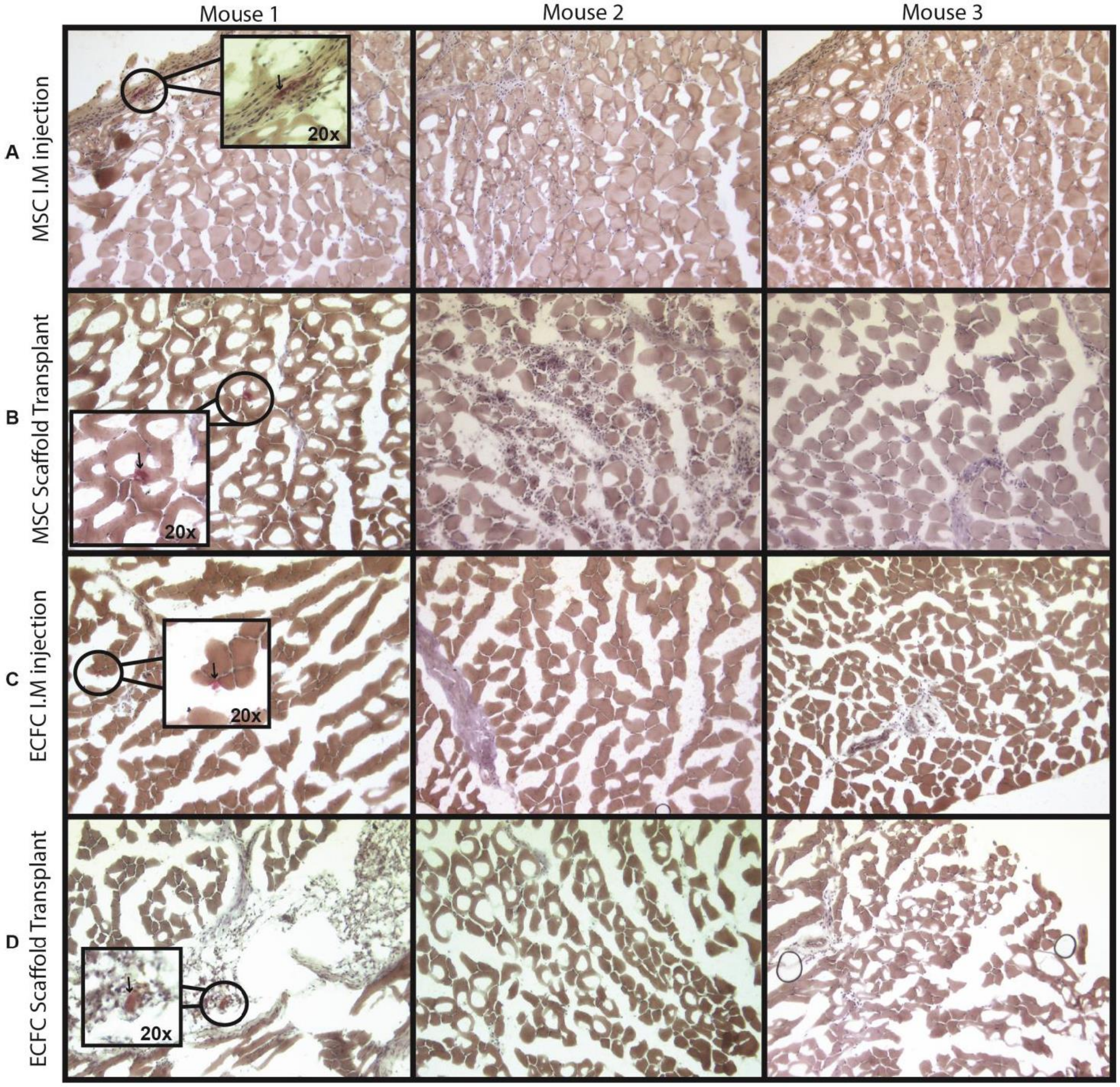
Mouse 1
Mouse 2
Mouse 3
A
MSC I.M injection
B
MSC Scaffold Transplant
C
ECFC I.M injection
D
ECFC Scaffold Transplant
20x
20x
20x
20x

Figure 5.7 Human cell engraftment was rare in the ischemic thigh after scaffold implantation or I.M injection. ECFC or MSC were transplanted intramuscularly or implanted subcutaneously within DAT scaffolds in MPS type VII NOD.SCID mice. At 14 days post-transplantation, human cells were detected using pararosaniline staining for beta glucuronidase activity. Within the ischemic thigh, only one of the three I.M or scaffold-transplanted mice contained detectable human cells (red) within 350um of sectioned tissue. When transplanted via I.M injection, the presence of human ECFC or MSC were exceedingly rare within the ischemic thigh. Although extremely rare, human cells were also detected in the ischemic thigh of mice transplanted with DAT scaffolds seeded with ECFC or MSC. Photomicrographs show human cells detected within 3 mice transplanted using cells from 3 UCB (ECFC) and 3 BM (MSC) samples per group (N=3).

Figure 5.8

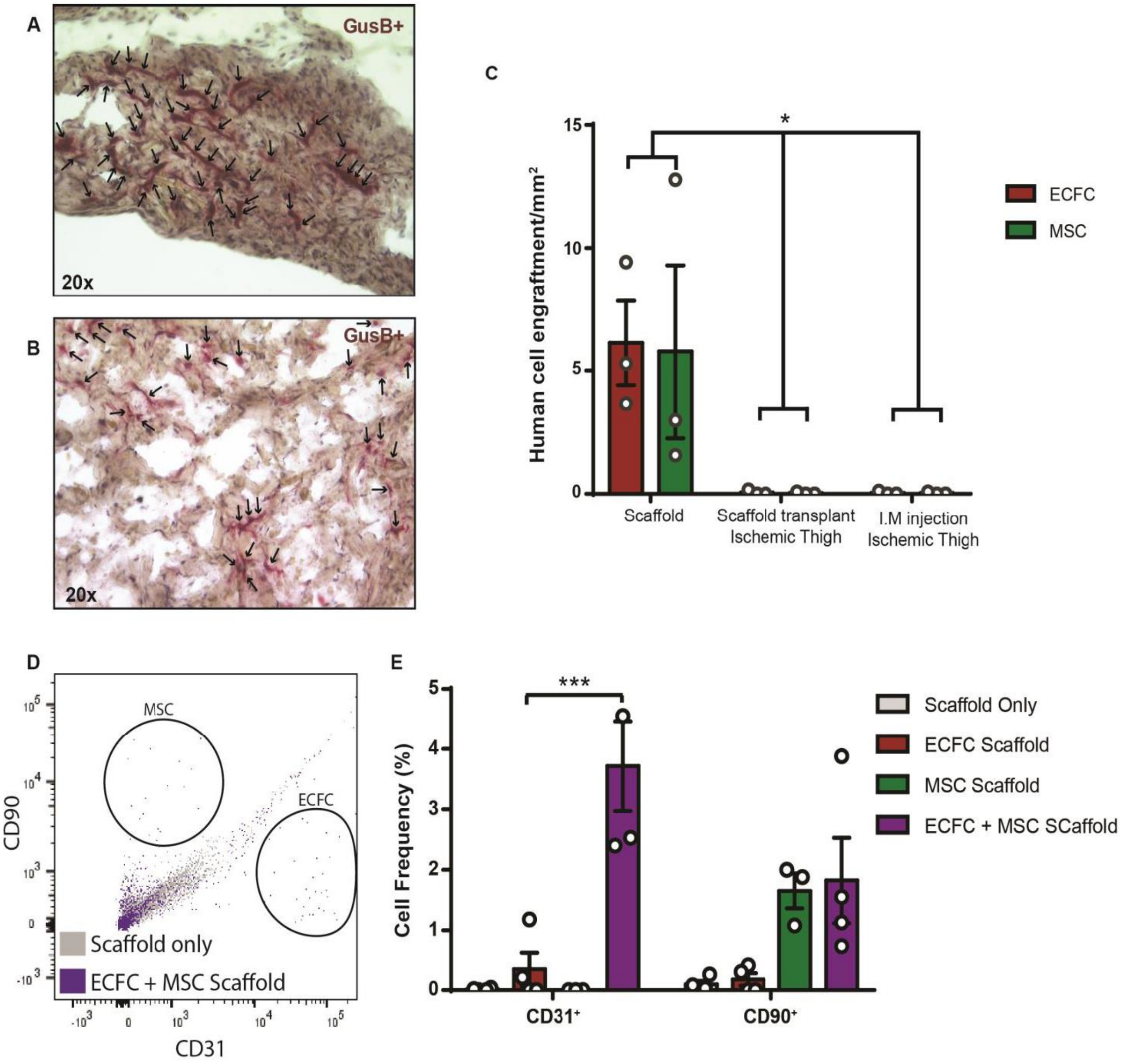
A
GusB+
20x
B
GusB+
20x
C
*
Human cell engraftment/mm²
15
10
5
0
Scaffold
Scaffold transplant Ischemic Thigh
I.M injection Ischemic Thigh
ECFC
MSC
D
MSC
ECFC
CD90
CD31
Scaffold only
ECFC + MSC Scaffold
E
***
Cell Frequency (%)
5
4
3
2
1
0
CD31⁺
CD90⁺
Scaffold Only
ECFC Scaffold
MSC Scaffold
ECFC + MSC SCaffold

Figure 5.8 Human cell engraftment was increased in DAT scaffolds at 14 days post-transplantation. ECFC or MSC were seeded in DAT scaffolds and implanted subcutaneously at the site of FAL surgery in MPS type VII NOD.SCID mice. After 14 days, the presence of human cells was detected using pararosaniline staining for functional beta glucuronidase activity. Human (A) ECFC or (B) MSC seeded into DAT scaffolds were abundantly detected at 14 days post-transplantation into MPS type VII NOD.SCID mice. (C) Within the ischemic thigh, only one of the three I.M or scaffold-transplanted mice contained a single human cell across three stained tissue sections. Human cells were detected at 6.1 ± 2.9 ECFC/mm^2 and 5.7 ± 6.0 MSC/mm^2 within the DAT scaffolds at 14 days post-transplantation. (D) Flow cytometry was performed on DAT scaffolds 14-days post-transplantation to assess the frequency of human ECFC (CD31+) and MSC (CD90+) persisting within the scaffolds. (E) The frequency of ECFC seeded within DAT scaffolds was 0.46 ± 0.56% which was significantly improved when seeded in DAT scaffolds with BM-MSC (3.44 ± 1.49%). MSC frequency was unaffected with or without the presence of ECFC (1.65 ± 0.50% versus 1.82 ± 1.40%, respectively). Data represents the mean ± SEM using cells from 3 UCB (ECFC) and 3 BM (MSC) samples (N=3; *P<0.05, ***P<0.01 by two-way ANOVA using a Tukey’s post hoc test).

Figure 5.9

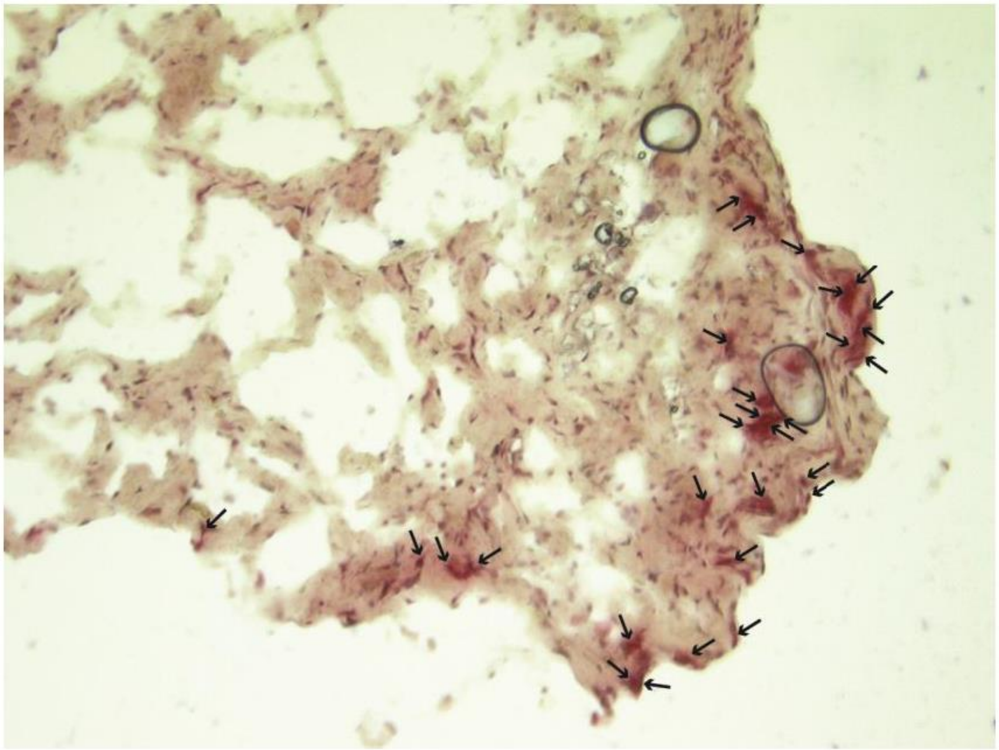

Figure 5.9 Human cell detection in the DAT scaffolds at 35 days post-transplantation in MPS type VII NOD.SCID mice. ECFC were seeded in DAT scaffolds and implanted subcutaneously at the site of FAL surgery for 35 days in MPS type VII NOD.SCID mice. Numerous human cells were detected within the scaffolds (Black arrows) at 35 days post-transplantation.

5.3.7 The murine cells recruited to the DAT scaffolds were primarily MAC-1+ and took up HLA from the DAT scaffolds.

After 14 days post-transplantation, unseeded DAT scaffolds or DAT scaffolds seeded with ECFC and MSC were stained for HLA and DAPI to observe human cell engraftment via confocal microscopy. A line-scan analysis was performed to quantify HLA$^+$ features in each image (**Figure 5.10A, B)**. In both the Scaffold-only and cell-seeded conditions, several HLA$^+$/DAPI$^+$ cells were observed throughout the scaffolds (**Figure 5.10A-iii, B-iii**). To validate these findings, flow cytometry was performed to broadly assess the types of cells recruited to the scaffold using MAC-1 and whether murine cells were presenting HLA. First, we compared the MAC-1$^+$ cell content between murine bone marrow and the cells extracted from unseeded DAT scaffolds (**Figure 5.11A**). The frequency of observed MAC-1$^+$ cells from unseeded DAT scaffolds totaled 80.9 ± 5.2%, similar to DAT seeded with ECFC (79.9 ± 3.0%) or MSC (69.3 ± 2.7%) alone. Interestingly, DAT scaffolds seeded with ECFC and MSC recruited significantly fewer MAC-1$^+$ murine cells (52.8 ± 13.5%) (**Figure 5.11B**). Upon further analysis, we compared the HLA+ cell frequency within the MAC-1- and MAC-1$^+$ cells from bone marrow and DAT scaffolds (**Figure 5.11C, D**). Within the MAC-1$^+$ cells, the frequency of HLA$^+$ cells totaled >80% while <3% of the MAC-1$^-$ cells were HLA$^+$ across all DAT transplant conditions (**Figure 5.11E**).

Figure 5.10

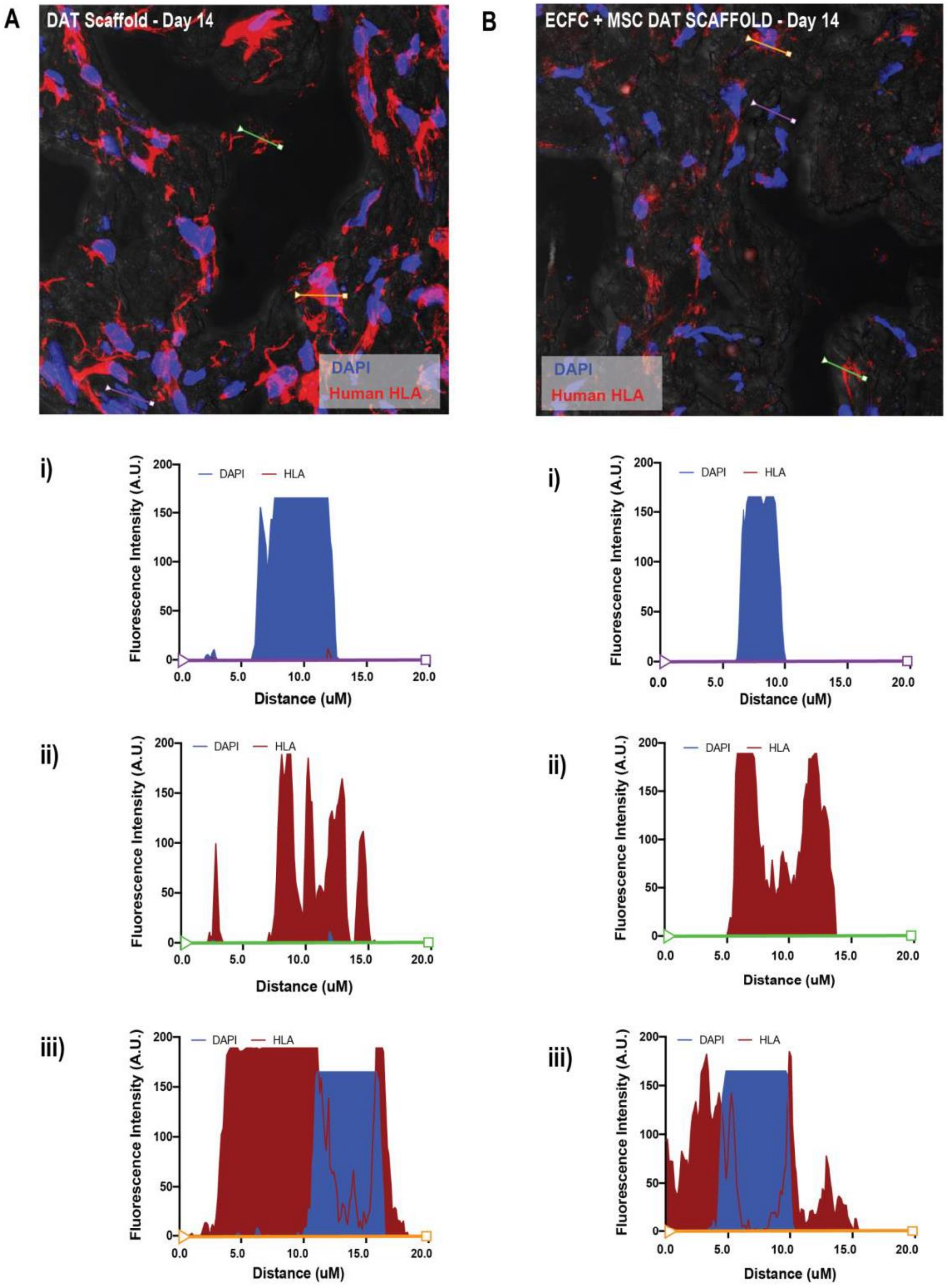
A
DAT Scaffold - Day 14
DAPI
Human HLA
B
ECFC + MSC DAT SCAFFOLD - Day 14
DAPI
Human HLA
i)
ii)
iii)
Fluorescence Intensity (A.U.)
0
50
100
150
200
DAPI
HLA
Distance (uM)
0.0
5.0
10.0
15.0
20.0

Figure 5.10 Human leukocyte antigen was detected in DAT scaffolds and invading murine cells 14 days post-transplantation. ECFC and MSC-seeded DAT scaffolds or unseeded DAT scaffolds were implanted subcutaneously at the site of FAL surgery in NOD.SCID mice. After 14 days, the DAT scaffolds were retrieved, cryosectioned and stained for the presence of HLA. Confocal images were taken at 63x magnification and a line-scan analysis was performed to quantify HLA+ features in each image. A representative photomicrograph indicates where the line scan analyses were performed for (A) unseeded DAT scaffolds and (B) ECFC + MSC-seeded DAT scaffolds. 3 Different regions for each photomicrograph was chosen to represent (A-i, B-i) DAPI-only events, (A-ii, B-ii) HLA-only events, and (A-iii, B-iii) HLA in close proximity to DAPI. In both the Scaffold-only and cell-seeded conditions, several HLA+/DAPI+ cells were observed throughout the scaffolds. Photomicrographs represent 3 different transplant conditions of unseeded DAT scaffolds and DAT scaffolds seeded with 3 UCB (ECFC) and 3 BM (MSC) samples (N=3).

Figure 5.11

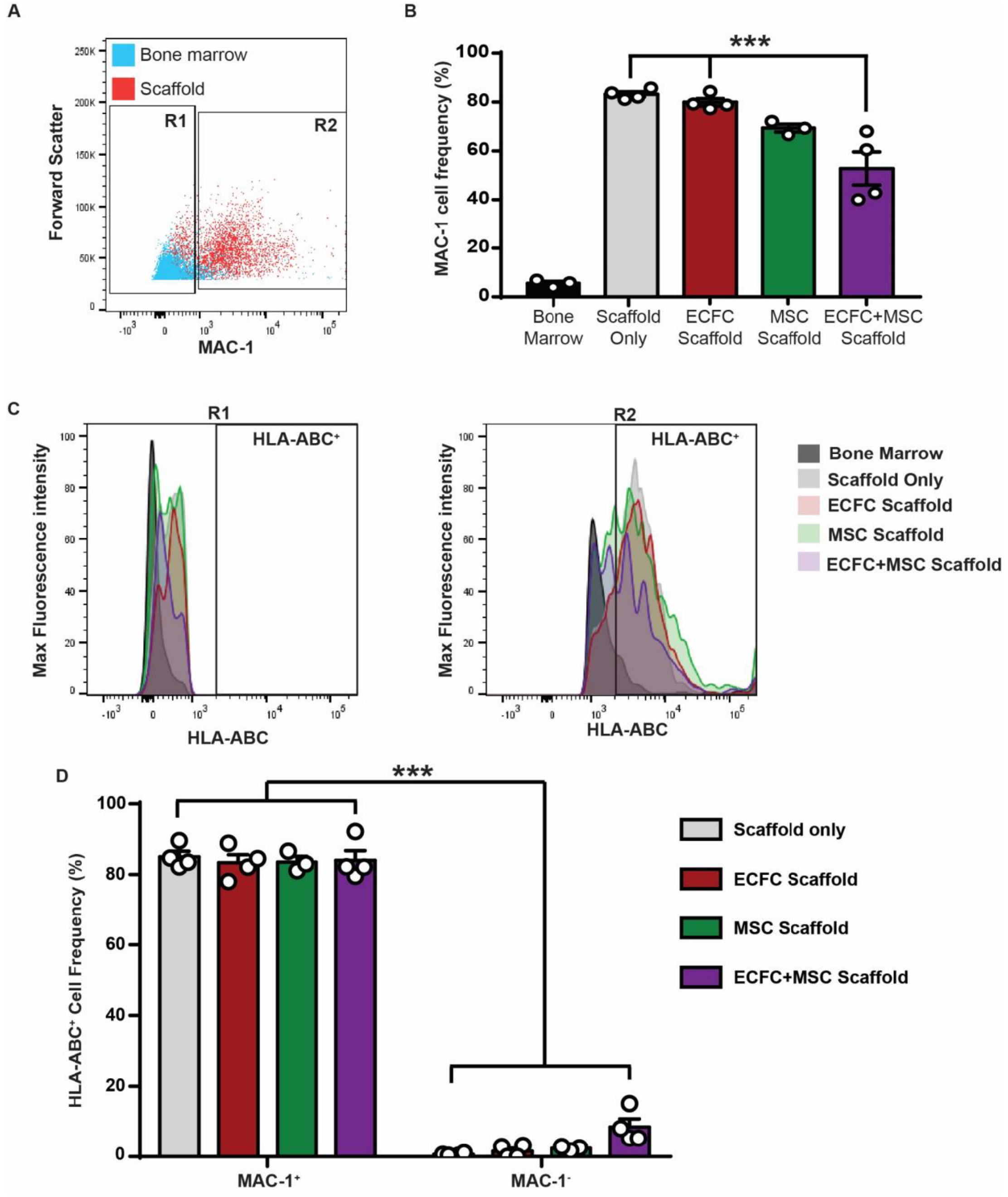
A
Bone marrow
Scaffold
Forward Scatter
R1
R2
MAC-1
B
***
MAC-1 cell frequency (%)
100
80
60
40
20
0
Bone Marrow
Scaffold Only
ECFC Scaffold
MSC Scaffold
ECFC+MSC Scaffold
C
R1
R2
HLA-ABC⁺
Max Fluorescence intensity
HLA-ABC
Bone Marrow
Scaffold Only
ECFC Scaffold
MSC Scaffold
ECFC+MSC Scaffold
D
***
HLA-ABC⁺ Cell Frequency (%)
Scaffold only
ECFC Scaffold
MSC Scaffold
ECFC+MSC Scaffold
MAC-1⁺
MAC-1⁻

Figure 5.11 Murine cells recruited to DAT scaffolds were primarily MAC-1$^+$ and presented the human-specific marker, HLA. Unseeded DAT scaffolds or DAT scaffolds seeded with ECFC and/or MSC were implanted subcutaneously for 14 days at the site of FAL surgery in NOD.SCID mice. After retrieval, the DAT scaffolds were stained for MAC-1 and HLA and quantified by flow cytometry. (A) A representative dot plot represents the MAC-1$^+$ murine cell content overlaid with the MAC-1$^+$ cell content of the DAT scaffold. (B) Quantification of the MAC-1+ cells in the DAT scaffold revealed a significant decrease in the frequency of recruited MAC-1+ cells to DAT scaffolds seeded with ECFC and MSC (52.8 ± 13.5%) compared to unseeded DAT (80.9 ± 5.2%) and DAT seeded with ECFC (79.9 ± 3.0%). After quantifying the HLA$^+$ cell content within the (C) MAC-1$^-$ and (D) MAC-1$^+$ cells, a notable amount of HLA$^+$ cells were observed (>80%) within MAC-1+ murine cells obtained from the DAT scaffolds (E). Data represents the mean ± SEM using cells from 3 UCB (ECFC) and 3 BM (MSC) samples (N=3; ***P<0.01 by one-way ANOVA in panel B and two-way ANOVA in panel E. Both statistical tests were performed using a Tukey's post hoc test).

5.3.8 DAT scaffolds contained CD31+ vessel-like structures.

At 35 days post-transplantation, DAT scaffolds were removed from the mice, sectioned and stained with a mouse anti- CD31 antibody to determine the vessel density within the scaffold. Contiguous vessel-like structures were observed within both human cell-seeded and DAT-only transplanted conditions (**Figure 5.12A**). When comparing the average CD31 signal intensity or CD31 signal area, no differences were observed between any of the cell-transplanted conditions and the un-seeded DAT scaffolds (**Figure 5.12B, C**). Together, these data suggested that the DAT foam scaffolds alone could support primitive vessel formation after implantation into an ischemic microenvironment.

Figure 5.12

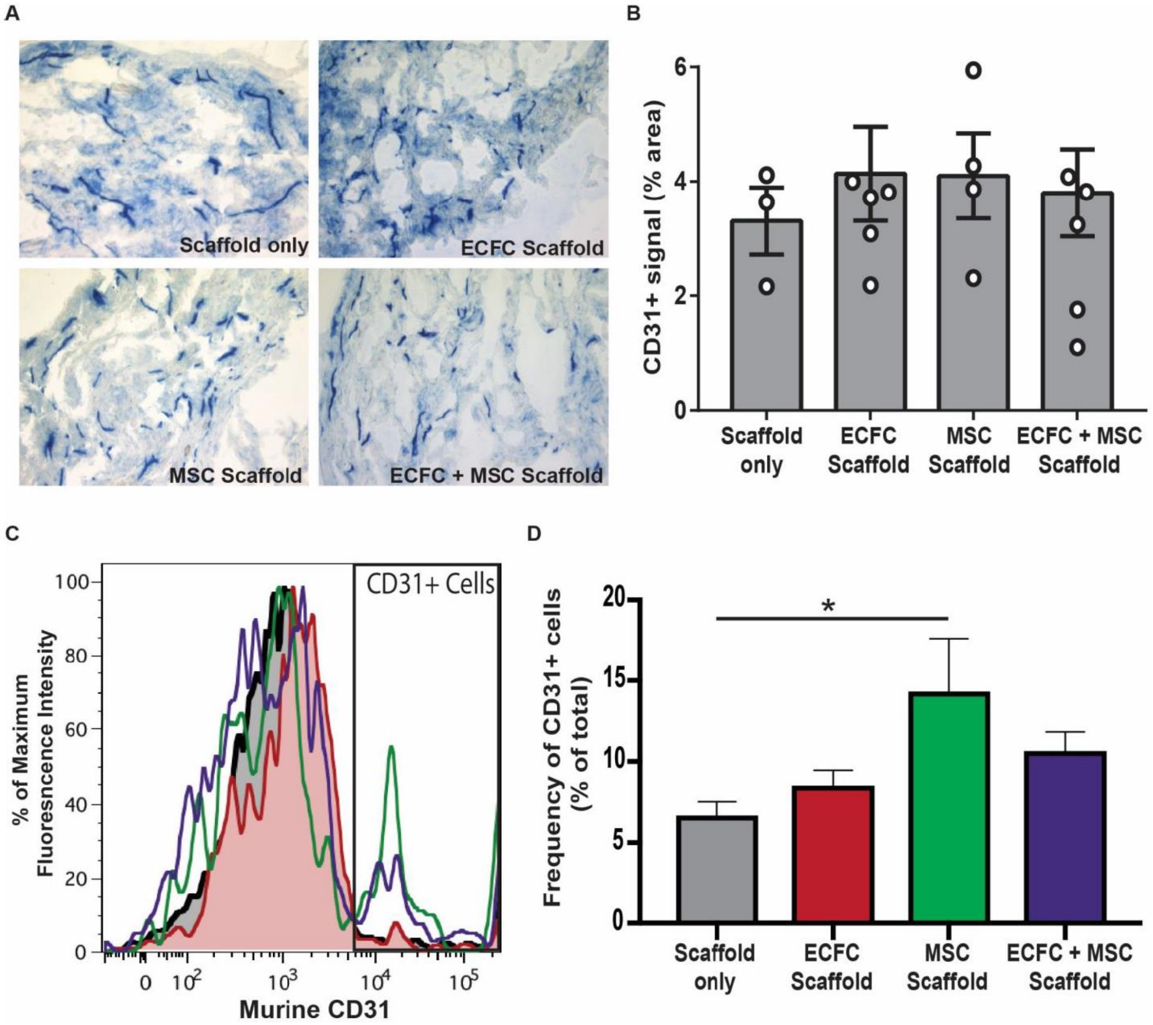

Figure 5.12 DAT scaffolds transplanted at the site of FAL surgery contained CD31+ vessel-like structures after 35 days post-transplantation. DAT scaffolds were transplanted with or without ECFC and/or MSC at the site of FAL surgery. Scaffolds were recovered 35 days post-transplantation and stained for CD31^{+} cells. (A) Representative photomicrographs of stained scaffolds revealed CD31^{+} vessel-like structures throughout the DAT scaffolds. Both the (B) CD31^{+} signal intensity and (C) CD31^{+} signal area was quantified using image-J threshold analyses on monochrome RGB scaffold photomicrographs. CD31^{+} signal intensity and signal area were not significantly different between cell-seeded and un-seeded DAT scaffolds. Data represents the mean ± SEM using cells from 6 UCB (ECFC) and 6 BM (MSC) samples (N=3-6).

5.4 Discussion

In the current study, we demonstrated the utility of DAT scaffolds as a novel modality for the transplantation of human ECFC and MSC into the ischemic limb of immunodeficient NOD.SCID mice after FAL surgery. We also documented a change in cell surface marker expression of ECFC and MSC when seeded in decellularized adipose scaffolds *in vitro*. Additionally, the proliferative potential of ECFC was attenuated upon co-culture with MSC and after seeding on DAT scaffolds. Unfortunately, we did not observe enhanced recovery of limb perfusion following the transplantation of ECFC and/or MSC intramuscularly or when seeded in DAT scaffolds implanted subcutaneously into FAL-induced ischemic hind limbs. Although no changes in limb perfusion was observed, co-transplantation of ECFC and MSC improved blood vessel density in the ischemic limb at the site of intramuscular injection, suggesting that these cells may exert a localized pro-angiogenic effect in the ischemic tissue. These findings did not indicate that the combination of ECFC and MSC could support the enhanced recovery of blood perfusion in the ischemic hind limb as suggested by Kang *et al.*[36]. The authors demonstrated that intramuscular injection of 2 million ECFC and MSC combined promoted the recovery of blood perfusion in the ischemic limb, a result that was not observed when the dose of cells transplanted was >2 million cells. Thus, the number of cells injected by Kang *et al.* were 8-fold higher than our cell dose and may indicate a minimal threshold of transplanted cells may be required to elicit a therapeutic effect. Although we transplanted substantially fewer cells (due to the low frequency of $CD34^+$ cells), we observed increased blood vessel density within the ischemic thigh muscle recovered to levels comparable to the non-ischemic limb. Another reason for our observed differences in the recovery of perfusion may be due to the differences in transplantation methodology. Here, we describe implantation of ECFC and/or MSC within DAT scaffolds or after direct intramuscular injection. In Kang et al.[36] cells were mixed within liquid Matrigel and injected into the muscle tissue permitting gelation at body temperature.

In intramuscular transplanted mice, we did not observe human cell engraftment in the ischemic thigh tissues after 35 days post-transplantation. The decline of human cell engraftment after intramuscular transplantation has also been observed previously for

ECFC[37] alone or co-transplanted with MSC[36]. We also observed an extremely low level of human cell engraftment within ischemic thigh muscles at 14 days post-transplantation using the sensitive NOD.SCID MPSVIII mouse model. Human cells within the ischemic muscle was exceedingly rare whether the cells were transplanted within DAT scaffolds or by intramuscular injection. Alternatively, we demonstrated robust survival of both ECFC and MSC within DAT scaffolds at 14 days post-transplantation into the ischemic hindlimb of NOD.SCID MPS VII mice. Furthermore, the NOD.SCID MPS VII mouse model enabled the detection of human cell survival within DAT scaffolds up to 35 days post-transplantation. As an alternative methodology, the detection of human cells within the DAT scaffold by using an HLA-A, B, C antibody was complicated by the presence of HLA throughout the scaffold. Interestingly, the murine cells recruited to the unseeded DAT scaffolds appeared to up-take HLA which appeared throughout the cytosol of the cells. To confirm this phenomenon, flow cytometry was used after extracting the murine cells from the DAT scaffolds 14 days post-transplantation. To address the question of the types of cells observed within the DAT scaffold, a MAC-1 antibody was used which has been noted to mark neutrophils, NK cells, monocytes, and macrophages[38]. Compared to mouse BM-MNC, we observed a dramatic enrichment of MAC-1 positive cells throughout the DAT scaffolds. We further dissected the MAC-$1^{+/-}$ populations to determine that HLA+ cells were enriched within the MAC-1^{+} cells obtained from the DAT scaffolds. Of note, the cell populations stained and analyzed by flow cytometry were live cells which suggests that HLA^{+} murine cells are presenting the HLA antigen on the cell surface for the antibody staining to occur. Fortunately, anti-CD31 and anti-CD90 antibodies were able to accurately quantify ECFC and MSC engraftment within the DAT scaffolds, respectively. In any given transplantation condition with human cells seeded within the DAT scaffolds, <4% of the total detected events were human cells while the remaining >96% were murine cells. Although the frequency of human cells was low, a significant improvement of ECFC engraftment was observed when co-transplanted with MSC. In summary, DAT scaffolds robustly recruit MAC-1^{+} cells which interact with the scaffold as measured by HLA presentation on these cells. Furthermore, the DAT scaffolds augmented human cell survival where ECFC survival was further improved upon seeding the cells in combination with MSC.

To determine if ECFC or MSC altered cell surface marker expression in response to contact culture within the DAT scaffolds, ECFC and MSC were cultured together for 72 hours on DAT scaffolds. MSC cultured in the DAT scaffolds showed a notable decrease in endoglin (CD105) expression after 72 hours compared to MSC cultured on tissue culture plastic *in vitro*. CD105 has been implicated to be involved in TGF-β signaling but also contains the integrin binding sequence, RGB[39]. Other studies suggest a connection between CD105 expression, TGF-β signaling and changes in integrin expression[40]. Our findings indicate that the interactions between DAT and MSC may provide cues that decrease CD105 expression by MSC. Interestingly, these results were not observed in ECFC that maintained CD105 expression. However, the frequency of TIE2$^+$ ECFC after culture in the DAT scaffolds was significantly increased. Further studies are warranted to determine if ECFC establish a vascular niche within DAT scaffolds, as previous studies have demonstrated TIE2 signaling pathways promote vessel stability and prevent vessel regression *in vivo*[41]. Similarly, *in vitro* culture of the highly proliferative ECFC on DAT scaffolds or ECFC with MSC on TCP both resulted in drastically diminished proliferation. Thus, MSC-ECFC, ECFC-DAT interactions may promote ECFC quiescence given the documented role of MSC to demonstrate pericyte properties [42-44].

Within the transplanted DAT scaffolds, we observed many invading murine cells as early as 14 days post-transplantation, detected by hematoxylin staining. This was anticipated as host cell invasion has been previously noted in other transplantation studies utilizing DAT scaffolds[45]. We also observed robust vascularization within unseeded DAT scaffolds, indicating that the bioactive properties of DAT scaffolds may have potent pro-vascular effects *in vivo*. Our observations corroborate previous studies that demonstrated endothelial cell recruitment to the transplanted DAT bioscaffolds[46]. Murine CD31+ cell recruitment was further improved in the DAT scaffolds seeded with MSC, measured by flow cytometry. The transplantation of DAT scaffolds did not recover blood vessel density in the ischemic thigh to levels measured within the non-ischemic limb. However, when the DAT scaffolds contained ECFC and/or MSC, blood vessel density within the ischemic thigh was comparable to the non-ischemic contralateral limb. These data suggest that DAT scaffolds alone can mediate a local angiogenic effect, whereas the ECFC and MSC were necessary to promote vascularization of the ischemic limb potentially through secreted paracrine factors[47, 48]. Although we did not observe blood perfusion recovery using this transplantation strategy, the blood vessel density within the ischemic thigh recovered to levels similar to the non-ischemic limb after transplantation with as little as 250,000 ECFC and/or MSC. The findings reported throughout this study suggest that the localized pro-vascular effects of the ECFC and MSC may have alternative clinical benefits. For example, the DAT foam scaffolds have been demonstrated to promote vascularization in wound healing setting[45] alongside ECFC seeded on bioscaffold constructs[49, 50]. Given our observations that the DAT scaffolds promote human cell survival, co-transplantation of ECFC and MSC to synergistically promote vascularization[51, 52] may improve wound healing through paracrine angiogenic effects.

5.5 References

1. Lovell, M., et al., *Peripheral arterial disease: Lack of awareness in Canada.* Canadian Journal of Cardiology, 2009. **25**(1): p. 39-45.

2. Hirsch, A.T., et al., *<Peripheral arterial disease detection, awareness and treatment in primary care.pdf>*. JAMA, 2001. **286**(11): p. 8.

3. Davies, J.E., *Criticial Limb Ischemia: Epidemiology.* MDCVJ, 2012. **3**(4): p. 1.

4. Carmeliet, P., *Mechanisms of angiogenesis and arteriogenesis.* Nature Medicine, 2000. **6**(3): p. 7.

5. Yoder, M.C., et al., *Redefining endothelial progenitor cells via clonal analysis and hematopoietic stem/progenitor cell principals.* Blood, 2007. **109**(5): p. 10.

6. Dubois, C., et al., *Differential effects of progenitor cell populations on left ventricular remodeling and myocardial neovascularization after myocardial infarction.* 2010. **55**(20): p. 2232-2243.

7. Jung, H.S., et al., *The potential of endothelial colony-forming cells to improve early graft loss after intraportal islet transplantation.* 2014. **23**(3): p. 273-283.

8. Critser, P.J. and M.C. Yoder, *Endothelial colony-forming cell role in neoangiogenesis and tissue repair.* Curr Opin Organ Transplant, 2010. **15**(1): p. 68-72.

9. Sata, M., *Role of circulating vascular progenitors in angiogenesis, vascular healing, and pulmonary hypertension.* Arteriosclerosis, thrombosis, and vascular biology, 2006. **26**(5): p. 1008-1014.

10. Fisher, M., *Pericyte signaling in the neurovascular unit.* Stroke, 2009. **40**(3 suppl 1): p. S13-S15.

11. Crisan, M., et al., *A perivascular origin for mesenchymal stem cells in multiple human organs.* Cell Stem Cell, 2008. **3**(3): p. 301-13.

12. Al-Khaldi, A., et al., *Therapeutic angiogeneis using autologous bone marrow stromal cells: improved blood flow in a Chronic Limb Ischemia model.* Ann Thorac Surg, 2003. **75**: p. 6.

13. Hare, J.M., et al., *A randomized, double-blind, placebo-controlled, dose-escalation study of intravenous adult human mesenchymal stem cells (prochymal) after acute myocardial infarction.* Journal of the American College of Cardiology, 2009. **54**(24): p. 2277-2286.

14. Hung, S.C., et al., *Angiogenic effects of human multipotent stromal cell conditioned medium activate the PI3K-Akt pathway in hypoxic endothelial cells to inhibit apoptosis, increase survival, and stimulate angiogenesis.* Stem Cells, 2007. **25**(9): p. 2363-70.

15. Melero-Martin, J.M., et al., *Engineering robust and functional vascular networks in vivo with human adult and cord blood-derived progenitor cells.* Circ Res, 2008. **103**(2): p. 194-202.

16. Ball, S.G., C.A. Shuttleworth, and C.M. Kielty, *Mesenchymal stem cells and neovascularization: role of platelet-derived growth factor receptors.* J Cell Mol Med, 2007. **11**(5): p. 1012-30.

17. Au, P., et al., *Bone marrow derived mesenchymal stem cells facilitate engineering of long lasting functional vasculature.* Blood, 2008. **111**(9): p. 9.

18. Caplan, A.I. and D. Correa, *The MSC: an injury drugstore.* Cell stem cell, 2011. **9**(1): p. 11-15.

19. Qadura, M., et al., *Concise review: cell therapy for critical limb ischemia: an integrated review of preclinical and clinical studies.* Stem Cells, 2018. **36**(2): p. 161-171.

20. Naba, A., et al., *The extracellular matrix: Tools and insights for the "omics" era.* Matrix Biol, 2016. **49**: p. 10-24.

21. Badylak, S.F., *Xenogeneic extracellular matrix as a scaffold for tissue reconstruction.* Transpl Immunol, 2004. **12**(3-4): p. 367-77.

22. Badylak, S.F., D.O. Freytes, and T.W. Gilbert, *Extracellular matrix as a biological scaffold material: Structure and function.* Acta Biomater, 2009. **5**(1): p. 1-13.

23. Vacanti, J.P. and R. Langer, *Tissue engineering: the design and fabrication of living replacement devices for surgical reconstruction and transplantation.* The Lancet, 1999. **354**: p. S32-S34.

24. Lutolf, M.P. and J.A. Hubbell, *Synthetic biomaterials as instructive extracellular microenvironments for morphogenesis in tissue engineering.* Nat Biotechnol, 2005. **23**(1): p. 47-55.

25. Casadei, A., et al., *Adipose tissue regeneration: a state of the art.* J Biomed Biotechnol, 2012. **2012**: p. 462543.

26. Fuchs, J.R., B.A. Nasseri, and J.P. Vacanti, *Tissue engineering: a 21st century solution to surgical reconstruction.* Ann Thorac Surg, 2001. **72**: p. 15.

27. Turner, A.E.B., et al., *The performance of decellularized adipose tissue microcarriers as an inductive substrate for human adipose-derived stem cells.* Biomaterials, 2012. **33**(18): p. 4490-4499.

28. Martin, P.M., et al., *Decellularized Adipose Tissue Scaffolds for Soft Tissue Regeneration and Adipose-Derived Stem/Stromal Cell Delivery.* Adipose-Derived Stem Cells: Methods and Protocols, 2018: p. 53-71.

29. Bura, A., et al., *Phase I trial: the use of autologous cultured adipose-derived stroma/stem cells to treat patients with non-revascularizable critical limb ischemia.* Cytotherapy, 2014. **16**(2): p. 245-257.

30. Sarnowska, A., et al., *Encapsulation of mesenchymal stem cells by bioscaffolds protects cell survival and attenuates neuroinflammatory reaction in injured brain tissue after transplantation.* Cell Transplant, 2013. **22 Suppl 1**: p. S67-82.

31. Flynn, L.E., *The use of decellularized adipose tissue to provide an inductive microenvironment for the adipogenic differentiation of human adipose-derived stem cells.* Biomaterials, 2010. **31**(17): p. 4715-24.

32. Yu, C., et al., *Porous decellularized adipose tissue foams for soft tissue regeneration.* Biomaterials, 2013. **34**(13): p. 3290-302.

33. Putman, D.M., et al., *Umbilical Cord Blood-Derived Aldehyde Dehydrogenase-Expressing Progenitor Cells Promote Recovery from Acute Ischemic Injury.* Stem Cells, 2012. **30**(10): p. 2248-2260.

34. Capoccia, B.J., et al., *Revascularization of ischemic limbs after transplantation of human bone marrow cells with high aldehyde dehydrogenase activity.* Blood, 2009. **113**(21): p. 5340-51.

35. Sly, W.S., et al., *Beta glucuronidase deficiency: report of clinical, radiologic, and biochemical features of a new mucopolysaccharidosis.* The Journal of pediatrics, 1973. **82**(2): p. 249-257.

36. Kang, K.-T., et al., *Endothelial colony forming cells and mesenchymal progenitor cells form blood vessels and increase blood flow in ischemic muscle.* Scientific reports, 2017. **7**(1): p. 770.

37. Flex, A., et al., *Human cord blood endothelial progenitors promote post-ischemic angiogenesis in immunocompetent mouse model.* Thrombosis research, 2016. **141**: p. 106-111.

38. Wada, H., et al., *Adult T-cell progenitors retain myeloid potential.* 2008. **452**(7188): p. 768.

39. Duff, S.E., et al., *CD105 is important for angiogenesis: evidence and potential applications.* The FASEB Journal, 2003. **17**(9): p. 984-992.

40. Boroujerdi, A., et al., *Chronic Cerebral Hypoxia Promotes Arteriogenic Remodeling Events that can be Identified by Reduced Endoglin (CD105) Expression and a Switch in β 1 Integrins.* Journal of Cerebral Blood Flow & Metabolism, 2012. **32**(9): p. 1820-1830.

41. Eklund, L. and P. Saharinen, *Angiopoietin signaling in the vasculature.* Experimental cell research, 2013. **319**(9): p. 1271-1280.

42. Wong, S.-P., et al., *Pericytes, mesenchymal stem cells and their contributions to tissue repair.* Pharmacology & therapeutics, 2015. **151**: p. 107-120.

43. Shafiee, A., et al., *Mesenchymal stem/stromal cells enhance engraftment, vasculogenic and pro-angiogenic activities of endothelial colony forming cells in immunocompetent hosts.* Scientific reports, 2017. **7**(1): p. 13558.

44. Betsholtz, C., P. Lindblom, and H. Gerhardt, *Role of pericytes in vascular morphogenesis*, in *Mechanisms of Angiogenesis*. 2005, Springer. p. 115-125.

45. Martin, P.M., et al., *Matrix composition in 3-D collagenous bioscaffolds modulates the survival and angiogenic phenotype of human chronic wound dermal fibroblasts.* Acta biomaterialia, 2018.

46. Han, T.T.Y., et al., *Adipose-derived stromal cells mediate in vivo adipogenesis, angiogenesis and inflammation in decellularized adipose tissue bioscaffolds.* Biomaterials, 2015. **72**: p. 125-137.

47. Liu, Y., et al., *Vasculogenic and Osteogenesis-Enhancing Potential of Human Umbilical Cord Blood Endothelial Colony-Forming Cells.* Stem cells, 2012. **30**(9): p. 1911-1924.

48. Doorn, J., et al., *Therapeutic applications of mesenchymal stromal cells: paracrine effects and potential improvements.* Tissue Engineering Part B: Reviews, 2011. **18**(2): p. 101-115.

49. Kim, K.L., et al., *Enhanced dermal wound neovascularization by targeted delivery of endothelial progenitor cells using an RGD-g-PLLA scaffold.* Biomaterials, 2009. **30**(22): p. 3742-3748.

50. Hendrickx, B., et al., *Integration of blood outgrowth endothelial cells in dermal fibroblast sheets promotes full thickness wound healing.* Stem Cells, 2010. **28**(7): p. 1165-1177.

51. Souidi, N., et al., *Stromal Cells Act as Guardians for Endothelial Progenitors by Reducing Their Immunogenicity After Co-Transplantation.* Stem Cells, 2017. **35**(5): p. 1233-1245.

52. Lin, R.-Z., et al., *Human endothelial colony-forming cells serve as trophic mediators for mesenchymal stem cell engraftment via paracrine signaling.* Proceedings of the National Academy of Sciences, 2014. **111**(28): p. 10137-10142.

Chapter 6

6 Summary and Discussion

6.1 Summary of findings.

The overall objective of my thesis was to improve the revascularization potential of culture expanded ECFC and MSC by assessing variables that improve engraftment and/or pro-vascular function following transplantation into an ischemic microenvironment. First, I employed a conventional strategy to determine if FACS-purification could select more potent pro-angiogenic progenitor cell subsets from clinically-applicable human MSC and ECFC populations after expansion. In Chapter 2, I discovered that MSC selected for high ALDH-activity, a conserved progenitor cell function, demonstrated enhanced pro-angiogenic secretory functions and represented a further purified, more homogeneous MSC subset amenable for vascular regenerative applications. In contrast, high ALDH-activity did not select for ECFC with enhanced colony or tubule forming capacity *in vitro.* Therefore, in Chapter 3, I used selection by the best-known EPC marker, the sialomucin CD34, to FACS-purify $CD34^{+/-}$ ECFC subsets with both phenotypic and functional differences after expansion *in vitro.* In Chapters 4 and 5, I utilized decellularized adipose-derived bioscaffolds as a novel cell delivery modality to improve the survival and engraftment of ECFC and MSC *in vivo*. Importantly, this research has demonstrated that DAT scaffolds enhance the survival of pro-angiogenic ECFC and MSC compared to intramuscular injection of either cell population. Ultimately, I predict the information generated in this thesis will contribute to the development of improved regenerative medicine strategies to combat ischemic diseases.

Clinical use of both EPC and MSC in clinical applications has been delayed due to the rarity of the cells and the lack of a selective cell surface marker that identifies therapeutic cells. Previously, our lab has demonstrated effective methods to purify progenitor cells from heterogeneous cell populations by selecting for cells with high ALDH-activity[1]. ALDH-activity provides cytoprotective function to protect progenitor cell pools of multiple lineages from damage or deletion after exposure to oxidative stressors[2, 3]. Thus, I sought to purify a pro-vascular progenitor cell subset from both ECFC and MSC cultures using high ALDH-activity. Notably, MSC selected for high ALDH-activity demonstrated enhanced pro-vascular capabilities *in vitro* and *in vivo*. Specifically, conditioned media generated from the ALDH^{hi} MSC promoted endothelial cell survival and proliferation *in vitro* and increased endothelial cell recruitment to areas of ischemia *in vivo*. On the other hand, high ALDH-activity did not enrich for ECFC with colony forming capacity *in vitro*. Similar to ALDH-activity, FACS purification using CD34 has isolated putative progenitor cell populations from the hematopoietic and endothelial lineages. Therefore, I investigated whether CD34^{+} ECFC demonstrated enhanced primitive (colony formation) or mature (tube formation) endothelial cell functions compared to CD34^{-} ECFC *in vitro*. Surprisingly, CD34^{+} ECFC showed reduced colony and tube forming function *in vitro,* thus suggestive of the existence of a potential endothelial hierarchy. Conversely, the capacity of CD34^{+} ECFC to form vessel-like structures in Matrigel plugs was equivalent to CD34^{-} ECFC 7-days after implantation in Matrigel into immunodeficient mice. Thus, the identity of a definitive marker (ALDH or CD34) to purify the elusive endothelial precursor cell after ECFC expansion *in vitro* remained elusive. Collectively, these studies demonstrated the feasibility of using progenitor cell functions (i.e. ALDH-activity) to FACS purify expanded MSC subsets with enhanced pro-vascular functions, whereas FACS was unable to segregate ECFC subsets with enhanced pro-angiogenic function *in vivo*. After combining ECFC and MSC as a transplantation strategy in a murine model of hindlimb ischemia, my results suggested that alternative strategies were needed to improve the engraftment of ECFC or MSC transplanted into an ischemic microenvironment. Ultimately, cell selection using high ALDH-activity, or the lack CD34-expression may help refine cell-based revascularization therapies currently under intense pre-clinical and clinical investigation for severe ischemic diseases[4-6].

6.1.1 Chapter 2 – ALDH^{hi} MSC demonstrate enhanced vascular regenerative potential.

In chapter 2, I investigated whether high ALDH-activity could be used as a marker to segregate a pro-vascular MSC subset from cultured BM-MSC. We have previously demonstrated the prospective purification of ALDH^{hi} cells from BM-MNC enriched for

MSC with CFU-F capacity[7]. However, as MSC are expanded *in vitro*, cell progeny have been shown to differentiate and lose their regenerative capacity[8]. Therefore, we hypothesized that MSC selection based on ALDH-activity after *ex vivo* expansion may reduce heterogeneity by segregating an MSC subset with enhanced vascular regenerative functions both *in vitro* and *in vivo*.

Initially, I demonstrated that both ALDH^{lo} versus ALDH^{hi} MSC expressed equivalent expression of 'classical' MSC surface markers and showed mesodermal multipotency generating bone, cartilage and adipose tissues *in vitro*. However, conditioned media generated by ALDH^{hi} MSC demonstrated a potent pro-survival and proliferative stimulation of human microvascular endothelial cells (HMVEC) under serum-free conditions. In addition, ALDH^{hi} MSC conditioned media exposure augmented HMVEC tube-forming capacity in growth factor-reduced matrices. After subcutaneous implantation within DIVAA implants into the flank of immunodeficient mice, DIVAA implants supplemented with ALDH^{hi} MSC (or conditioned media generated by ALDH^{hi} MSC) significantly promoted murine vascular cell recruitment and vessel infiltration compared to ALDH^{lo} MSC. Although both subsets demonstrated strikingly similar mRNA expression patterns by microarray, quantitative proteomic analyses performed on subset-specific conditioned media revealed ALDH^{hi} MSC robustly secreted several proteins associated with pro-angiogenic, chemo-attractant, and matrix-modifying functions. Collectively, MSC selected for high ALDH-activity demonstrated enhanced pro-angiogenic secretory function and represent a novel MSC subset, isolated after culture, that is amenable to vascular regenerative applications.

Utilization of high ALDH-activity to select for MSC with enhanced pro-regenerative functions holds promise for future clinical applications. The fluorescent ALDH substrate is non-toxic and has been used in clinical cell therapies in the past [9, 10]. Furthermore, selecting for cells with high ALDH-activity provides a means to isolate pro-regenerative cell populations that lack definitive cell surface markers for selection. Furthermore, selecting cells based on ALDH function also reduced heterogeneity commonly observed during the expansion primary cells. The heterogeneity of bulk-expanded MSC has been suggested to contribute to the lack of therapeutic efficacy of MSC *in vivo*[11, 12]. Therefore, selecting for ALDH^{hi} MSC to reduce cellular heterogeneity may contribute to the development of more efficacious vascular cell therapies.

6.1.2 Chapter 3 – CD34^{+} ECFC have attenuated vascular functions *in vitro*.

Because ECFC also lack markers to robustly identify primitive progenitor cell content, high ALDH-activity was also tested to identify an endothelial progenitor cell population with enhanced pro-vascular function. ECFC are highly proliferative endothelial cells isolated from human umbilical cord blood, peripheral blood, and bone marrow MNC[13]. ECFC primarily express endothelial cell surface markers, effectively form tubules *in vitro*, and can integrate into vasculature after transplantation *in vivo*[14]. Similar to MSC, we envision ECFC cultures as a heterogenous populations that will gradually lose progenitor cell functions with continuous passaging[8, 13]. Therefore, I hypothesized that FACS-purification of cultured ECFC based on ALDH-activity and/or primitive progenitor cell surface markers (CD34) would segregate a primitive progenitor cell subset with enhanced regenerative functions *in vitro* and *in vivo*.

In this study, I purified ECFC using FACS based on ALDH-activity and EPC markers (CD34, CXCR4) previously associated with the capacity to integrate into neovessels *in vivo*. After purification based on high versus low ALDH-activity, single ALDH^{lo} and ALDH^{hi} cells established colonies at a frequency equal to unpurified ECFC. In contrast, ECFC lacking CD34 or CXCR4 expression generated significantly more colonies compared to CD34^{+} or CXCR4^{+} ECFC. When seeded in growth factor-reduced Geltrex™ media, purified CD34^{+} ECFC also demonstrated a reduced tubule forming capacity compared to CD34^{-} ECFC. Comparing the cell surface proteome of CD34^{-} versus CD34^{+} ECFC revealed increased expression of several pro-angiogenic endothelial cell pathways on CD34^{+} ECFC including VEGFR2 and Jagged. Despite these functional differences between CD34^{+} versus CD34^{-} ECFC tested *in vitro*, both ECFC subsets equally orchestrated the formation of vessel-like structures within Matrigel plugs implanted subcutaneously into immunodeficient NOD.SCID mice. Moreover, detection of human cells was comparable between CD34^{+} and CD34^{-} ECFC, suggesting both ECFC subsets survived for 7 days following transplantation. Collectively, we demonstrated that CD34^{+}

versus CD34$^-$ ECFC subsets exhibited unexpected differences in clonogenicity and tubule formation *in vitro*; however, both ECFC subsets could assemble into vessel-like structures *in vivo*. Thus, the purification of ECFC subsets with enhanced vessel forming functions *in vivo* was not easily predicted by surrogate progenitor cell phenotypes. Thus, functional assays *in vitro* and *in vivo*, are encouraged to better predict pro-vascular potency for expanded ECFC populations.

6.1.3 Chapter 4 – Purification of human cells seeded within decellularized bioscaffolds for analysis by multiparametric flow cytometry.

In preparation of using flow cytometry to analyze cell populations implanted within DAT scaffolds in Chapter 5, the development of methods to generate cell preparations for flow cytometry that contained minimal scaffold debris were required. In this chapter, I demonstrated that enzymatic release of seeded cells from decellularized scaffolds produced debris with high levels of autofluorescence across the visible spectrum (450-780nm) that could obscure the assessment of cellular phenotype and function. In order to limit the enumeration of false positive events caused by scaffold debris, I developed a methodology to maximize cell retrieval and minimize cell debris, without impacting cell survival or phenotype, as these are two of the most insightful parameters to be measured during preclinical testing *in vitro* and *in vivo*.

Initially, I compared enzymatic digestion with trypLE express^{TM}, Liberase^{TM}, and collagenase to identify the protease formulation that generated pure cell preparations while minimizing the background generated by the autofluorescent scaffold debris. To demonstrate the broad utility of these methods, cell viability, and immunophenotype were assessed using human ECFC and MSC seeded on ECM-derived foams fabricated from human DAT, porcine DCT, or commercially-available bovine tendon collagen. The liberation of cells using TrypLE expess^{TM} incubation produced consistent sample preparations with high cell viability and minimized debris; however, the recovery remained lower relative to initial seeding density (<50%). In contrast, scaffold targeted digestion with collagenase-containing protease cocktails (>1 hr) negatively impacted cell viability and generated large amounts of debris that could interfere with sample analysis.

In order to maximize cell viability, scaffolds seeded with cells were digested with a collagenase-containing protease cocktails for less time. Next, cells could be effectively segregated from scaffold debris using Hypaque Ficoll density gradient centrifugation (>99% purity). In addition to increasing sample purity, the developed methodology supported both ECFC and MSC viability; in return, improving the total recoverable cell yield. Collectively, the development of these methods enabled the accurate detection and quantification of multiple cellular parameters during the co-culture of MSC and ECFC DAT scaffolds, described in Chapter 5.

6.1.4 Chapter 5 – ECFC and MSC demonstrate pro-vascular properties *in vivo*.

The aim in chapter 5 was to determine if the utilization of decellularized adipose tissue scaffolds could augment the pro-vascular function of ECFC and MSC following subcutaneous implantation of scaffold and cells into a murine model of FAL-induced hind limb ischemia. Previous pre-clinical studies have demonstrated the clinical potential for ECFC and MSC utilized as individual therapeutic cell populations[15-17]. Despite promising results, clinical trials testing therapeutic potential of ECFC or MSC have only observed modest benefits to date[18, 19]. One possibility for decreased cellular efficacy following transplantation may include how ECFC and MSC are isolated, cultured, and processed prior to transplantation. For example, endothelial cells expanded *in vitro* do not retain the same phenotype prior to isolation *in vivo* which may negatively impact cell function[20, 21]. This phenomenon may occur as a result of standard culture conditions being devoid of 3-D architecture, ECM-related signaling molecules, and/or the activation of mechano-sensing pathways during culture on stiff substrates (i.e. tissue culture plastic)[22-24]. For these reasons, I investigated the potential benefit of biological active decellularized scaffolds derived from a readily available tissue type (i.e. adipose tissue)[25]. I hypothesized that DAT scaffolds would augment ECFC and MSC survival and enhance vascular regenerative functions following transplantation into a murine model of hindlimb ischemia.

Initially culturing ECFC and MSC within DAT-foam scaffolds led to significant changes in the frequency of ECFC expressing TIE2 and MSC expressing CD105. I also observed a marked decrease in ECFC proliferation when cultured on the DAT scaffold, measured by EdU incorporation into dividing ECFC. Similarly, ECFC cultured with MSC also showed little ECFC proliferation with or without DAT scaffolds. Next, I investigated the pro-vascular potential of transplanted human ECFC and MSC, injected intramuscularly or within seeded DAT scaffolds, into our well-established NOD.SCID model of unilateral hindlimb ischemia. Subsequently, the recovery of blood perfusion was measured using LDPI on the distal hind limbs. Whether intramuscularly injected or seeded in DAT scaffolds, transplanted ECFC and/or MSC did not improve recovery of blood perfusion in the ischemic hind limb compared to PBS-injected controls. Next, I performed a histological analysis of the thigh muscles to screen for human cells and to enumerate the blood vessel density in both the ischemic and non-ischemic limbs. Human cell engraftment within the ischemic thigh tissue was not observed in any cell-treated mice 35 days post transplantation. Although exceedingly rare, both ECFC and MSC could be detected within the ischemic thigh 14 days post-transplantation after delivery within DAT scaffolds or by intramuscular injection. Conversely, human ECFC and MSC were abundantly detected within the DAT scaffolds 14 days post-transplantation and engraftment was easily observed up to 35 days post-transplantation. Although human cell engraftment was not observed 35 days after direct cell injection into murine muscle tissue, all mice receiving ECFC and/or MSC recovered blood vessel density to levels comparable to the non-ischemic contralateral limb. Only the mice intramuscularly injected with both ECFC and MSC significantly improved blood vessel density compared to the PBS-injected ischemic thigh. Mice receiving ECFC and/or MSC seeded within DAT scaffolds also recovered blood vessel density within the ischemic thigh comparable to the non-ischemic limb. Moreover, the scaffolds promoted murine cell recruitment into the DAT and showed the formation of vessel-like structures throughout the scaffold. Taken together, this data indicated that the ECFC and MSC are pro-vascular cell types which may only exert their effects in the local tissue environment immediately surrounding the site of transplantation. Although recovery of hind limb perfusion was not observed, increased vessel density in the ischemic thigh suggested that combinatorial transplantations of ECFC and MSC may provide local, vessel-forming benefit.

To summarize the data generated, **Figure 6.1** provides a theoretical model for the pro-vascular processes of ECFC and MSC transplanted into an ischemic setting. Here, I postulated that hypoxic signals in local muscle tissue recruits both ECFC and MSC to promote the formation of new vasculature. This is supported by my observation of human cell engraftment within the ischemic thigh of scaffold-implanted mice, indicating the migration of human cells from the scaffold towards the ischemic muscle. Concurrently, the bioscaffold itself promoted mouse endothelial cell recruitment likely due to bioactive substrates within DAT scaffolds. These findings were supported by my observation that unseeded DAT scaffolds displayed similar recruitment of $CD31^+$ murine cells within the scaffold compared to the ECFC and/or MSC seeded DAT scaffolds. Unfortunately, engraftment was extremely rare by day 14 within the ischemic thigh of the mouse and human cells were not detected by day 35 post-transplantation. These observations suggest that the human cells are targeted by murine innate immune cells, such as NK cells or residual macrophages. Human cells were subsequently diluted by murine cells which enables the increase in blood vessel density while diminishing human cell engraftment[6]. Lastly, DAT scaffolds stimulated the recruitment of murine endothelial cells, leading to vascularization of the transplanted bioscaffolds. Nonetheless, I also postulate that DAT scaffolds may provide additional survival cues within the ECM that promotes human cell survival during transplantation into harsh microenvironments.

Figure 6.1

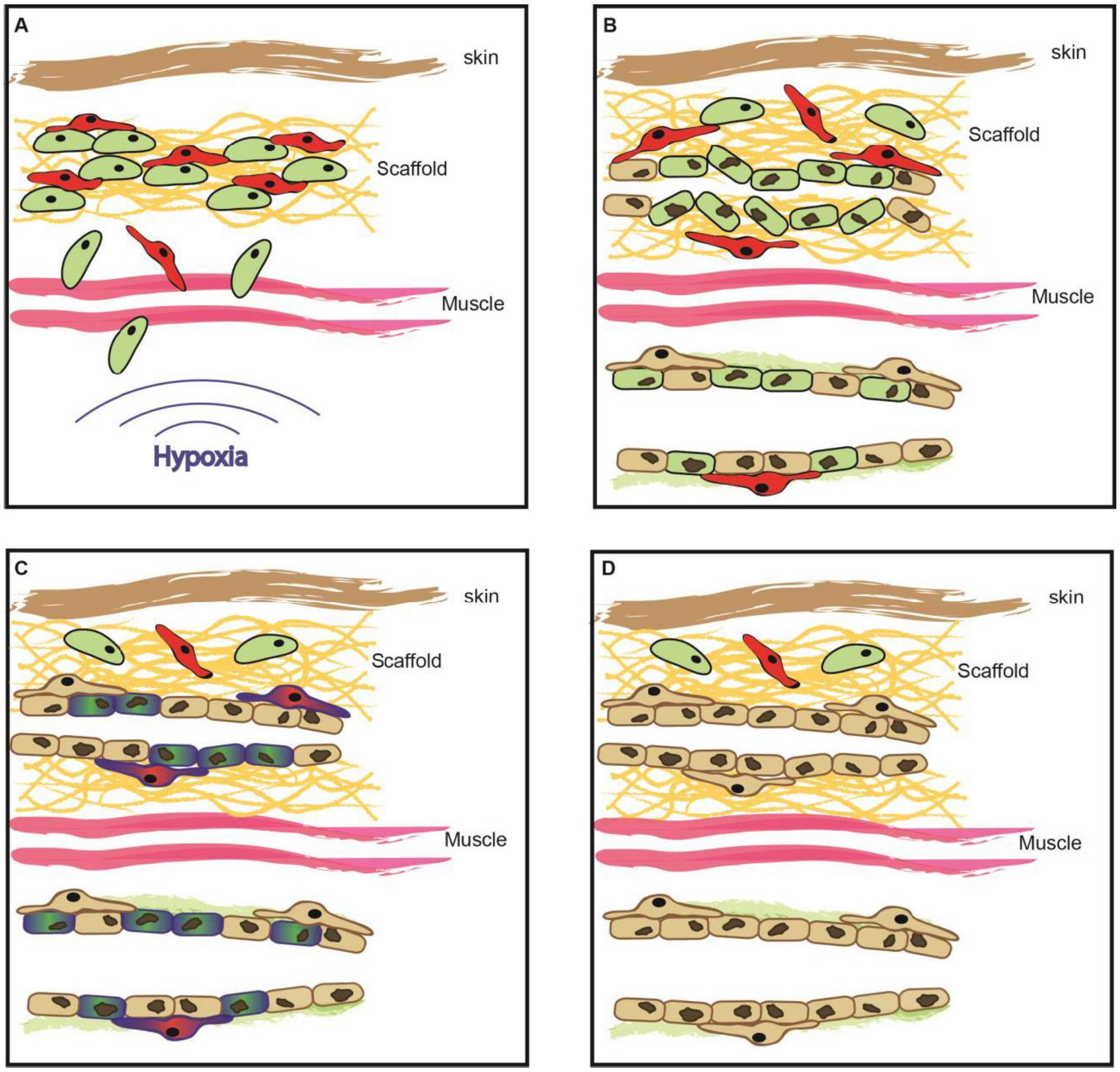
A
skin
Scaffold
Muscle
Hypoxia
B
skin
Scaffold
Muscle
C
skin
Scaffold
Muscle
D
skin
Scaffold
Muscle

Figure 6.1 A working model of DAT-seeded ECFC and MSC contribution to revascularization after transplantation in an ischemic hindlimb. (A) After transplantation, human ECFC (green cells) and MSC (red cells) migrate from the DAT scaffold (yellow/orange lines). (B) Human ECFC and MSC also recruit mouse endothelial cells (brown cells) and mediate the formation of new vasculature. Concurrently, DAT scaffolds also recruit mouse endothelial cells and other cell types into the DAT scaffold. (C) Human cells integrated into newly formed vessels may be selected against by residual innate immune cells of the mouse (Blue cells). (D) Mouse cells replace any human cells integrated into vascular structures while some human cells persist within the revascularized DAT scaffolds.

6.2 Clinical significance

MSC harbor multifaceted regenerative functions that have been utilized in numerous clinical trials, ranging from heart repair following cardiac infarction to treating life-threatening autoimmune diseases[26-28]. MSC are a highly secretory cell type that release multiple stimuli with pro-regenerative functions, and also possess the capacity to suppress the immune system[29]. In this thesis, I demonstrate that ALDH^{hi} MSC possess a pro-vascular secretory phenotype that enhanced the survival and function of endothelial cells *in vitro*. Considering MSC have been safely transplanted in the clinic for over a decade and demonstrate pro-regenerative functions in pre-clinical models of vascular disease[30, 31], MSC hold promise in the development of pro-vascular therapies. Unfortunately, the first trials using autologous MSC transplantation for treating CLI have only provided modest benefits[18, 19]. A likely reason for this may be the induction of MSC dysfunction due to chronic exposure to damaging stimuli associated with atherosclerosis and type 2 diabetes, which is documented to restrict circulating progenitor cell function in patients with CLI[32]. Transplanting a pro-vascular cell type such as healthy allogeneic ALDH^{hi} MSC may provide pro-regenerative stimuli to a non-responsive tissue environment shaped by chronic illness.

Initial clinical and pre-clinical studies indicated a lack of vascular response within elderly and/or diabetic patients treated with pro-angiogenic therapies. The diminished cellular response in these settings provided rationale for Asahara to investigate the existence of EPC to replace the exhausted tissue[32, 33]. After the discovery of circulating cells with post-natal vasculogenic potential, ECFC were subsequently isolated and expanded *ex vivo* and provided promise for the treatment of vascular dysfunction in the adult[13]. With expandable human ECFC available for pre-clinical testing, utilizing the pro-vascular signaling properties of MSC in conjunction with ECFC to promote vascularization in a mouse model of hind limb ischemia became the focus of my study. Interestingly, the intramuscular injection ECFC and/or MSC did not improve perfusion in the FAL-induced ischemic hindlimb mouse model. Based on a similar study, the pro-vascular effects of the ECFC and MSC could have been improved with the transplantation of more cells[6]. Although a significant improvement of limb perfusion was not observed, blood vessel density in the ischemic hindlimb was significantly increased compared to PBS-injected controls. These findings suggest that the ECFC and/or MSC demonstrate cooperative pro-vascular effects at the site of transplantation but had limited impact on downstream ischemia areas. Because this mouse model is subjected to a severe and immediate ischemic event, there likely exists sites of varying ischemia all throughout the afflicted limb. Thus, it is likely that the ECFC and/or MSC are responding to these localized ischemic microenvironments at the point of transplantation and fail to influence the distal ischemic sites. Previous studies have indicated that injection of 2-million ECFC and MSC (8-fold more than our studies) within Matrigel demonstrated recovery of perfusion in the distal hindlimb[6]. Thus, the number of cells injected in this context may be critical as more cells may migrate to benefit distal regions of the limb where perfusion was being measured. Our studies add that using decellularized bioscaffolds that provide supportive architecture and/or bioactive stimuli can increase the survival and engraftment of the human cells following transplantation. After implantation of the DAT with ECFC and/or MSC, the blood vessel density in the ischemic thigh was observed to be equivalent to the non-ischemic limb, again suggesting revascularization was stimulated by the local paracrine effects of the delivered ECFC and MSC.

Considering DAT scaffolds can improve the engraftment of ECFC and MSC with pro-angiogenic functions localized to the site of transplantation, cell-supplemented DAT scaffold implantation may have therapeutic potential in a wound healing setting. Wound healing in the human body requires the temporal organization of multiple cell types, including the initial invasion of immune cells that function to clear cellular debris and minimize the risk of infection. Next, cells surrounding the wound edge will proliferate into the wound and generate a provisional ECM network to facilitate endothelial cell invasion and angiogenesis[34]. At this early stage in the healing process, supplementation of ECFC and MSC within DAT may augment a localized re-vascularization process and augment wound healing. Similarly, bioactive stimuli embedded within transplanted DAT scaffolds may further augment tissue regeneration[35]. Likewise, purification of cells with enhanced pro-regenerative functions such as the ALDH^{hi} MSC subset may further enhance the wound healing process. Collectively, this proposed strategy warrants pre-clinical testing to investigate the role of ECFC and MSC in a wound healing setting.

6.3 Limitations of *in vitro* culture.

It is well established that endothelial cells will undergo phenotypic changes when removed from their native microenvironment subjected to culture expansion[20, 21]. Similarly, MSC also lose progenitor cell functions while undergoing drastic phenotypic and molecular changes *in vitro*[36, 37]. Although these are inherent limitations of *in vitro* culture, valuable *in vitro* assays have been developed to elucidate fundamental biological processes and cell-cell interactions of both ECFC and MSC[17]. The data presented in chapter 3 demonstrated functional differences between the $CD34^+$ versus $CD34^-$ ECFC *in vitro*. Although, functional differences were observed *in vitro*, $CD34^+$ and $CD34^-$ ECFC exhibited comparable endothelial functions when transplanted *in vivo*. In my opinion, the disconnect between established *in vitro* and *in vivo* assays used in these studies exist for several reasons. First, I observed dynamic CD34 expression on ECFC *in vitro* that was contingent on cell density. Given the functional differences between the CD34+ and $CD34^-$ ECFC, the dynamic nature of CD34 expression suggests that the cellular functions of $CD34^+$ ECFC may also be dynamic. Secondly, the microenvironment that an endothelial cell experiences *in vivo* is vastly different to the surrogate microenvironment *in vitro*. For example, *in vitro* conditions fail to recapitulate the 3-dimentional cell-ECM and cell-cell interactions in tissues[38, 39]. For these reasons, I speculate that our observations that $CD34^+$ ECFC resemble an endothelial cell phenotype with ‘decreased function’ may be due to the cell density in culture. Specifically, as the endothelial cells proliferate and become confluent in culture, the number of cell-cell contacts may promote the expression of mature endothelial cell markers. Moreover, our results suggest that culture conditions and/or cell density may regulate states of activation or quiescence in ECFC. Although identifying a progenitor cell subset within ECFC remained elusive, the plasticity and high proliferative potential of ECFC *in vitro* may be a good metric for vasculogenic potential *in vivo*.

Despite the inherent challenges of maintaining progenitor cell phenotype and function *in vitro*, expansion serves as an efficient means to generate large-scale quantities of therapeutic cell populations for regenerative therapies. In chapter 5, I demonstrated that the culture of ECFC on DAT scaffolds or in co-culture with MSC attenuated ECFC proliferation. This suggests that ECFC assume *in vivo*-like phenotype as endothelial cell turnover *in vivo* is limited[40]. If this hypothesis is true, using culture expansion to generate high cell numbers and subsequently ‘conditioning’ the cells in co-culture and/or on decellularized scaffolds may be efficacious to enhance the cellular response *in vivo*. Although *in vitro* assays can provide valuable insight to cellular processes within or between cell populations, but care must be taken to ensure *in vitro* findings are validated *in vivo*.

6.4 Future directions

The results obtained following ECFC/MSC co-transplantation within DAT suggested promising pro-vascular responses that could be optimized by the purification of pro-angiogenic ALDH^{hi} MSC prior to implantation into the NOD.SCID mouse model of FAL-induced ischemia. Furthermore, increasing the number of transplanted ECFC and/or MSC may improve the recovery of hind limb blood perfusion, as supported by previous studies[6]. As postulated earlier, transplantation of ECFC and/or MSC seeded on DAT scaffolds into a cutaneous wound healing model to study the local revascularization properties of these therapeutic strategies is warranted.

We did not identify human cells incorporating into murine vasculature within the ischemic hind limb of NOD.SCID mice. This may be due to a transient survival of human cells while revascularization of the microenvironment was stimulated, suggested by the rare occurrence of human cells within mouse ischemic muscle at 14 days post-transplantation. This is followed by the recruitment of murine endothelial cells in response to signals contained within the DAT or generated by engrafted human cells, as suggested by the increase in blood vessel density in the ischemic thigh after intramuscular injection of ECFC and MSC together. Because the thickness of the mouse thigh is close to 1 cm, the limit of bioluminescent detection within tissue (< 1cm) would allow for effective cell tracking methodologies to track the human cells post-transplantation[41, 42]. Cell tracking experiments would provide insight to determine if the human cells are migrating from the site of transplantation or being selected against within the tissue microenvironment. Furthermore, transplanting human cells within an interleukin 2 receptor gamma null NOD.SCID mouse would address whether residual innate immune cells in NOD.SCID mice are potentially selecting against the human ECFC or MSC[43]. Last, we noted a plethora of mouse cells recruiting to the DAT scaffolds, indicated by hematoxylin-stained nuclei throughout the scaffolds 14 days post-transplantation. Many of these cells were not CD31 positive and were not detected by pararosaniline staining. Thus, in order to fully describe the murine response to the DAT scaffold, we must identify the phenotype of these CD31$^-$ mouse cells recruited to the scaffolds.

Ischemia induced in the hindlimb of mice is acute and may not accurately reflect the ischemic microenvironment created by chronic atherosclerosis in CLI patients. Atherosclerosis-induced CLI in humans has many contributing factors to the disease state such as: dyslipidemia, smoking, lack of exercise, etc.[44] that are difficult to recapitulate in pre-clinical models. Notably, lifestyle choices may also contribute to the manifestation of co-morbidities such as type II diabetes. Accumulating research has demonstrated that the microenvironment of chronic disease will lead to stem/progenitor cell exhaustion, ultimately attenuating the regenerative functions of stem cell pools in systemic tissues[45, 46]. Although it is possible to promote an atherosclerotic environment in mice with a high-fat diet, the physiology of the mouse makes it resistant to developing life-threatening plaques as observed in human patients[47]. To better recapitulate stem cell exhaustion, comorbidities of CLI (i.e. diabetes) could be mimicked by the induction of hyperglycemia following streptozotocin (STZ)-induced beta cell ablation[48]. Hyperglycemic mice, conditioned with a high-fat diet, would be subjected to FAL-induced hind limb ischemia to mimic human CLI patients with common comorbidities. Ultimately, a more fine-tuned murine model of CLI may help to improve the translation of efficacy from pre-clinical research to clinical applications aimed at treating severe ischemic disease.

During *in vitro* studies comparing the colony and tube forming function of CD34$^+$ versus CD34- ECFC, I observed functional responses which contradicted other studies in the literature[49, 50]. In these published studies, ECFC were derived from various tissue sources (peripheral blood, placenta) which may contribute to functional differences observed. For this reason, a thorough head-to-head comparison between endothelial cell populations derived from different tissue sources is warranted. For example, proteomic, transcriptomic, and functional comparisons of peripheral blood ECFC, human microvascular endothelial cells (HMVEC), human umbilical vein endothelial cells (HUVEC), and human aortic endothelial cells (hAEC) would provide valuable insight into functional differences observed between endothelial cell populations *in vitro* and *in vivo*[51]. Collectively, in-depth molecular and functional comparisons between endothelial cell populations may elucidate functional and phenotypic characteristics which may confirm the existence of a putative endothelial cell hierarchy *in vitro*.

Finally, our lab has previously demonstrated the pro-vascular potential of the ALDH^{hi}-purified hematopoietic progenitor cells (HPC) from umbilical cord blood MNC[52]. Given the documented contribution of hematopoietic cells to promote vessel formation[53], transplantation of the ALDH^{hi} HPC may provide secretory cues that direct and augment the pro-vascular activity of the ECFC or MSC. During this transplantation strategy, the ECFC and MSC could be seeded on DAT scaffolds and transplanted at the surgical site after FAL surgery. HPC would be injected intravenously to utilize systemic circulation and to home to sites of ischemia[52]. I propose the functions of infused HPC would be to provide instructional cues to promote vessel formation by ECFC and stabilization by MSC during the revascularization of ischemic tissues.

6.5 References

1. Hess, D.A., et al., *Functional characterization of highly purified human hematopoietic repopulating cells isolated according to aldehyde dehydrogenase activity.* Blood, 2004. **104**(6): p. 1648-55.

2. Jones, R.J., et al., *Assessment of aldehyde dehydrogenase in viable cells.* Blood, 1995. **85**(10): p. 2742-2746.

3. Moreb, J.S., *Aldehyde dehydrogenase as a marker for stem cells.* Current stem cell research & therapy, 2008. **3**(4): p. 237-246.

4. Shafiee, A., et al., *Mesenchymal stem/stromal cells enhance engraftment, vasculogenic and pro-angiogenic activities of endothelial colony forming cells in immunocompetent hosts.* Scientific reports, 2017. **7**(1): p. 13558.

5. Souidi, N., et al., *Stromal Cells Act as Guardians for Endothelial Progenitors by Reducing Their Immunogenicity After Co-Transplantation.* Stem Cells, 2017. **35**(5): p. 1233-1245.

6. Kang, K.-T., et al., *Endothelial colony forming cells and mesenchymal progenitor cells form blood vessels and increase blood flow in ischemic muscle.* Scientific reports, 2017. **7**(1): p. 770.

7. Capoccia, B.J., et al., *Revascularization of ischemic limbs after transplantation of human bone marrow cells with high aldehyde dehydrogenase activity.* Blood, 2009. **113**(21): p. 5340-51.

8. Bell, G.I., et al., *Transplanted human bone marrow progenitor subtypes stimulate endogenous islet regeneration and revascularization.* Stem Cells Dev, 2012. **21**(1): p. 97-109.

9. Perin, E.C., et al., *Rationale and design for PACE: patients with intermittent claudication injected with ALDH bright cells.* Am Heart J, 2014. **168**(5): p. 667-73.

10. Perin, E.C., et al., *Randomized, double-blind pilot study of transendocardial injection of autologous aldehyde dehydrogenase–bright stem cells in patients with ischemic heart failure.* American heart journal, 2012. **163**(3): p. 415-421. e1.

11. Phinney, D.G., *Biochemical heterogeneity of mesenchymal stem cell populations: clues to their therapeutic efficacy.* Cell cycle, 2007. **6**(23): p. 2884-2889.

12. Tripathy, N.K., et al., *Cardiomyogenic Heterogeneity of Clonal Subpopulations of Human Bone Marrow Mesenchymal Stem Cells.* Journal of stem cells & regenerative medicine, 2018. **14**(1): p. 27.

13. Ingram, D.A., et al., *Identification of a novel hierarchy of endothelial progenitor cells using human peripheral and umbilical cord blood.* Blood, 2004. **104**(9): p. 2752-60.

14. Lin, R.-Z. and J.M. Melero-Martin, *Fibroblast growth factor-2 facilitates rapid anastomosis formation between bioengineered human vascular networks and living vasculature.* Methods, 2012. **56**(3): p. 440-451.

15. Melero-Martin, J.M., et al., *Engineering robust and functional vascular networks in vivo with human adult and cord blood-derived progenitor cells.* Circ Res, 2008. **103**(2): p. 194-202.

16. Au, P., et al., *Bone marrow derived mesenchymal stem cells facilitate engineering of long lasting functional vasculature.* Blood, 2008. **111**(9): p. 9.

17. Paschalaki, K.E. and A.M. Randi, *Recent advances in Endothelial Colony Forming Cells toward their use in clinical translation.* Frontiers in medicine, 2018. **5**: p. 295.

18. Tateishi-Yuyama, E., et al., *Therapeutic angiogenesis for patients with limb ischaemia by autologous transplantation of bone-marrow cells: a pilot study and a randomised controlled trial.* The Lancet, 2002. **360**(9331): p. 427-435.

19. Matoba, S., et al., *Long-term clinical outcome after intramuscular implantation of bone marrow mononuclear cells (Therapeutic Angiogenesis by Cell Transplantation [TACT] trial) in patients with chronic limb ischemia.* Am Heart J, 2008. **156**(5): p. 1010-8.

20. Milici, A., M. Furie, and W. Carley, *The formation of fenestrations and channels by capillary endothelium in vitro.* Proceedings of the National Academy of Sciences, 1985. **82**(18): p. 6181-6185.

21. Rubin, L., et al., *A cell culture model of the blood-brain barrier.* The Journal of cell biology, 1991. **115**(6): p. 1725-1735.

22. Yeung, T., et al., *Effects of substrate stiffness on cell morphology, cytoskeletal structure, and adhesion.* Cell motility and the cytoskeleton, 2005. **60**(1): p. 24-34.

23. Discher, D.E., P. Janmey, and Y.-l. Wang, *Tissue cells feel and respond to the stiffness of their substrate.* Science, 2005. **310**(5751): p. 1139-1143.

24. Discher, D.E., D.J. Mooney, and P.W. Zandstra, *Growth factors, matrices, and forces combine and control stem cells.* Science, 2009. **324**(5935): p. 1673-1677.

25. Martin, P.M., et al., *Decellularized Adipose Tissue Scaffolds for Soft Tissue Regeneration and Adipose-Derived Stem/Stromal Cell Delivery.* Adipose-Derived Stem Cells: Methods and Protocols, 2018: p. 53-71.

26. Le Blanc, K., et al., *Mesenchymal stem cells for treatment of steroid-resistant, severe, acute graft-versus-host disease: a phase II study.* Lancet, 2008. **371**(9624): p. 1579-86.

27. Duijvestein, M., et al., *Autologous bone marrow-derived mesenchymal stromal cell treatment for refractory luminal Crohn's disease: results of a phase I study.* Gut, 2010. **59**(12): p. 1662-9.

28. Hare, J.M., et al., *A randomized, double-blind, placebo-controlled, dose-escalation study of intravenous adult human mesenchymal stem cells (prochymal) after acute myocardial infarction.* Journal of the American College of Cardiology, 2009. **54**(24): p. 2277-2286.

29. Nauta, A.J. and W.E. Fibbe, *Immunomodulatory properties of mesenchymal stromal cells.* Blood, 2007. **110**(10): p. 3499-506.

30. Giordano, A., U. Galderisi, and I.R. Marino, *From the laboratory bench to the patient's bedside: an update on clinical trials with mesenchymal stem cells.* Journal of cellular physiology, 2007. **211**(1): p. 27-35.

31. Bernardo, M.E. and W.E. Fibbe, *Safety and efficacy of mesenchymal stromal cell therapy in autoimmune disorders.* Annals of the New York Academy of Sciences, 2012. **1266**(1): p. 107-117.

32. Isner, J.M. and T. Asahara, *Angiogenesis and vasculogenesis as therapeutic strategies for postnatal neovascularization.* The Journal of clinical investigation, 1999. **103**(9): p. 1231-1236.

33. Asahara, T., *Isolation of Putative Progenitor Endothelial Cells for Angiogenesis.* Science, 1997. **275**(5302): p. 964-966.

34. Falanga, V., *Wound healing and its impairment in the diabetic foot.* The Lancet, 2005. **366**(9498): p. 1736-1743.

35. Martin, P.M., et al., *Matrix composition in 3-D collagenous bioscaffolds modulates the survival and angiogenic phenotype of human chronic wound dermal fibroblasts.* Acta biomaterialia, 2018.

36. Baxter, M.A., et al., *Study of telomere length reveals rapid aging of human marrow stromal cells following in vitro expansion.* Stem cells, 2004. **22**(5): p. 675-682.

37. Rombouts, W. and R. Ploemacher, *Primary murine MSC show highly efficient homing to the bone marrow but lose homing ability following culture.* Leukemia, 2003. **17**(1): p. 160.

38. Abbott, A., *Cell culture: biology's new dimension*. 2003, Nature Publishing Group.

39. Ben-Ze'ev, A., et al., *Cell-cell and cell-matrix interactions differentially regulate the expression of hepatic and cytoskeletal genes in primary cultures of rat hepatocytes.* Proceedings of the National Academy of Sciences, 1988. **85**(7): p. 2161-2165.

40. Cines, D.B., et al., *Endothelial cells in physiology and in the pathophysiology of vascular disorders.* Blood, 1998. **91**(10): p. 3527-3561.

41. Kim, J.E., S. Kalimuthu, and B.-C. Ahn, *In vivo cell tracking with bioluminescence imaging*. Nuclear Medicine and Molecular Imaging, 2015. **49**(1): p. 3-10.

42. Troy, T., et al., *Quantitative comparison of the sensitivity of detection of fluorescent and bioluminescent reporters in animal models.* Molecular imaging, 2004. **3**(1): p. 15353500200403196.

43. Ishikawa, F., et al., *Development of functional human blood and immune systems in NOD/SCID/IL2 receptor γ chainnull mice.* Blood, 2005. **106**(5): p. 1565-1573.

44. Association, A.D., *8. Cardiovascular disease and risk management.* Diabetes care, 2016. **39**(Supplement 1): p. S60-S71.

45. Tongers, J.r., J.G. Roncalli, and D.W. Losordo, *Therapeutic angiogenesis for critical limb ischemia: microvascular therapies coming of age*. 2008, Am Heart Assoc.

46. Rauscher, F.M., et al., *Aging, progenitor cell exhaustion, and atherosclerosis.* Circulation, 2003. **108**(4): p. 457-463.

47. Breslow, J.L., *Mouse models of atherosclerosis.* Science, 1996. **272**(5262): p. 685-688.

48. Schnedl, W.J., et al., *STZ transport and cytotoxicity: specific enhancement in GLUT2-expressing cells.* Diabetes, 1994. **43**(11): p. 1326-1333.

49. Patel, J., et al., *Self-Renewal and High Proliferative Colony Forming Capacity of Late-Outgrowth Endothelial Progenitors Is Regulated by Cyclin-Dependent Kinase Inhibitors Driven by Notch Signaling.* Stem Cells, 2016. **34**(4): p. 902-12.

50. Ferreras, C., et al., *Segregation of late outgrowth endothelial cells into functional endothelial CD34- and progenitor-like CD34+ cell populations.* Angiogenesis, 2015. **18**(1): p. 47-68.

51. Jeong, H.E., et al. *The angiogenic sprouting of endothelial cells in three-dimensional collagen gel matrix*. in *17th International Conference on Miniaturized Systems for Chemistry and Life Sciences, MicroTAS 2013*. 2013. Chemical and Biological Microsystems Society.

52. Putman, D.M., et al., *Umbilical Cord Blood-Derived Aldehyde Dehydrogenase-Expressing Progenitor Cells Promote Recovery from Acute Ischemic Injury.* Stem Cells, 2012. **30**(10): p. 2248-2260.

53. Rafii, S., et al., *Contribution of pro-angiogenic hematopoietic cells to vascularization of tumor and ischemic tissue.* Angiogenesis: From Basic Science to Clinical Applications, 2006. **3**: p. 163.

Appendices.

Appendix 1 Permission to reproduce Sherman et al. in Springer eBook.

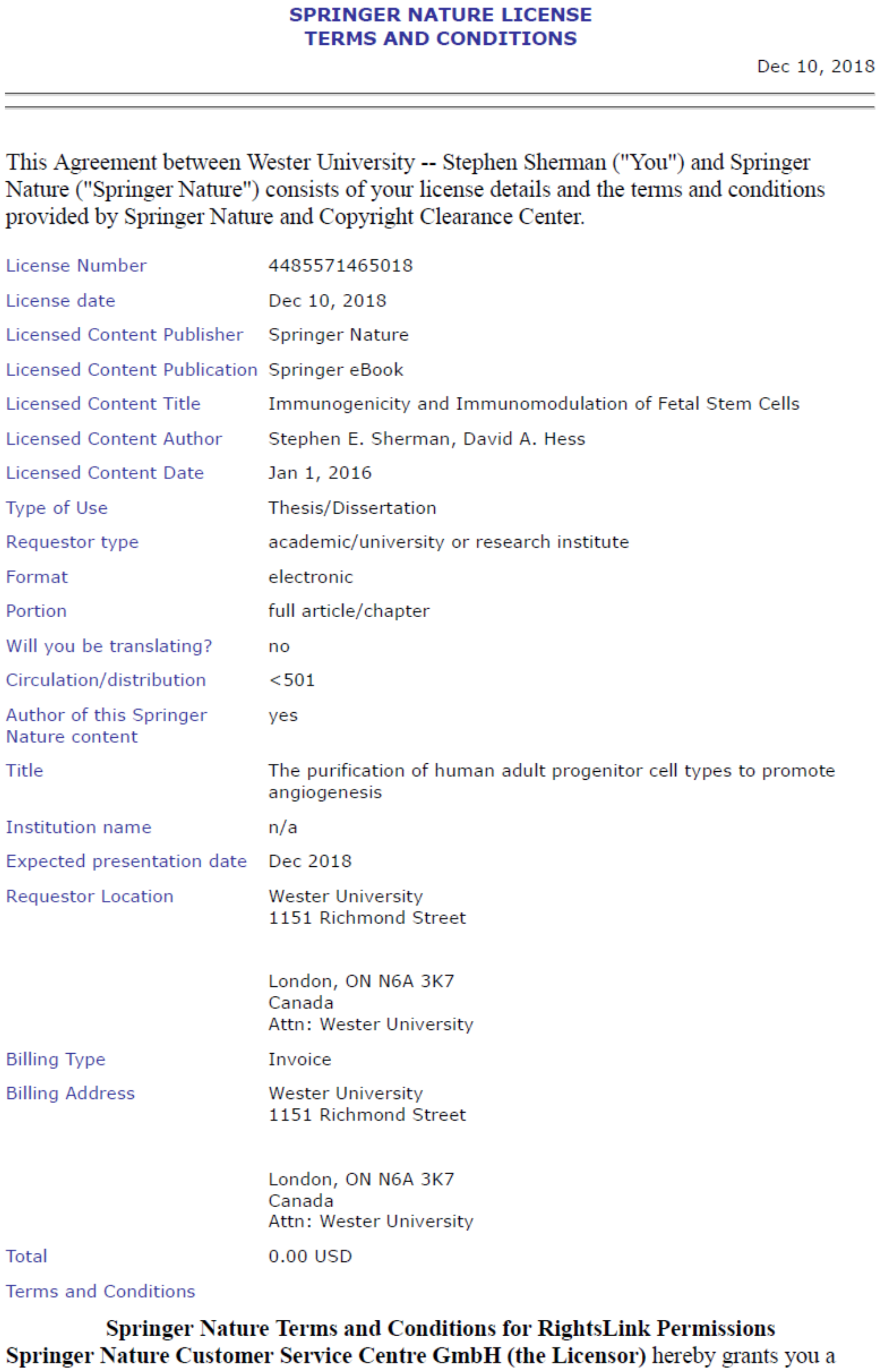

SPRINGER NATURE LICENSE
TERMS AND CONDITIONS

Dec 10, 2018

This Agreement between Wester University -- Stephen Sherman ("You") and Springer Nature ("Springer Nature") consists of your license details and the terms and conditions provided by Springer Nature and Copyright Clearance Center.

License Number	4485571465018
License date	Dec 10, 2018
Licensed Content Publisher	Springer Nature
Licensed Content Publication	Springer eBook
Licensed Content Title	Immunogenicity and Immunomodulation of Fetal Stem Cells
Licensed Content Author	Stephen E. Sherman, David A. Hess
Licensed Content Date	Jan 1, 2016
Type of Use	Thesis/Dissertation
Requestor type	academic/university or research institute
Format	electronic
Portion	full article/chapter
Will you be translating?	no
Circulation/distribution	<501
Author of this Springer Nature content	yes
Title	The purification of human adult progenitor cell types to promote angiogenesis
Institution name	n/a
Expected presentation date	Dec 2018
Requestor Location	Wester University 1151 Richmond Street London, ON N6A 3K7 Canada Attn: Wester University
Billing Type	Invoice
Billing Address	Wester University 1151 Richmond Street London, ON N6A 3K7 Canada Attn: Wester University
Total	0.00 USD
Terms and Conditions	

Springer Nature Terms and Conditions for RightsLink Permissions
Springer Nature Customer Service Centre GmbH (the Licensor) hereby grants you a

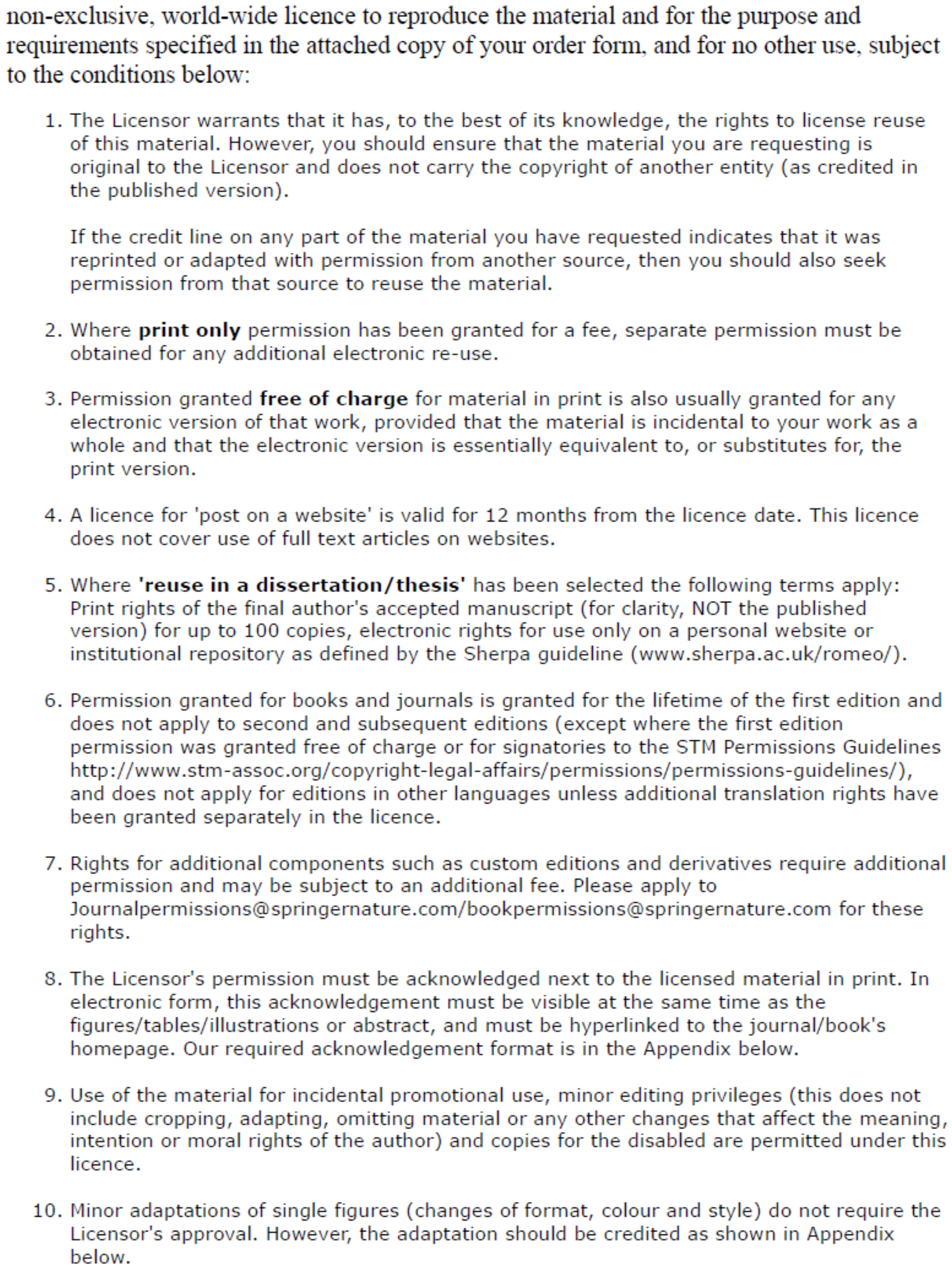

non-exclusive, world-wide licence to reproduce the material and for the purpose and requirements specified in the attached copy of your order form, and for no other use, subject to the conditions below:

1. The Licensor warrants that it has, to the best of its knowledge, the rights to license reuse of this material. However, you should ensure that the material you are requesting is original to the Licensor and does not carry the copyright of another entity (as credited in the published version).

   If the credit line on any part of the material you have requested indicates that it was reprinted or adapted with permission from another source, then you should also seek permission from that source to reuse the material.

2. Where **print only** permission has been granted for a fee, separate permission must be obtained for any additional electronic re-use.
3. Permission granted **free of charge** for material in print is also usually granted for any electronic version of that work, provided that the material is incidental to your work as a whole and that the electronic version is essentially equivalent to, or substitutes for, the print version.
4. A licence for 'post on a website' is valid for 12 months from the licence date. This licence does not cover use of full text articles on websites.
5. Where **'reuse in a dissertation/thesis'** has been selected the following terms apply: Print rights of the final author's accepted manuscript (for clarity, NOT the published version) for up to 100 copies, electronic rights for use only on a personal website or institutional repository as defined by the Sherpa guideline (www.sherpa.ac.uk/romeo/).
6. Permission granted for books and journals is granted for the lifetime of the first edition and does not apply to second and subsequent editions (except where the first edition permission was granted free of charge or for signatories to the STM Permissions Guidelines http://www.stm-assoc.org/copyright-legal-affairs/permissions/permissions-guidelines/), and does not apply for editions in other languages unless additional translation rights have been granted separately in the licence.
7. Rights for additional components such as custom editions and derivatives require additional permission and may be subject to an additional fee. Please apply to Journalpermissions@springernature.com/bookpermissions@springernature.com for these rights.
8. The Licensor's permission must be acknowledged next to the licensed material in print. In electronic form, this acknowledgement must be visible at the same time as the figures/tables/illustrations or abstract, and must be hyperlinked to the journal/book's homepage. Our required acknowledgement format is in the Appendix below.
9. Use of the material for incidental promotional use, minor editing privileges (this does not include cropping, adapting, omitting material or any other changes that affect the meaning, intention or moral rights of the author) and copies for the disabled are permitted under this licence.
10. Minor adaptations of single figures (changes of format, colour and style) do not require the Licensor's approval. However, the adaptation should be credited as shown in Appendix below.

Appendix 2 Permission to reproduce Sherman et al. in Stem cells.

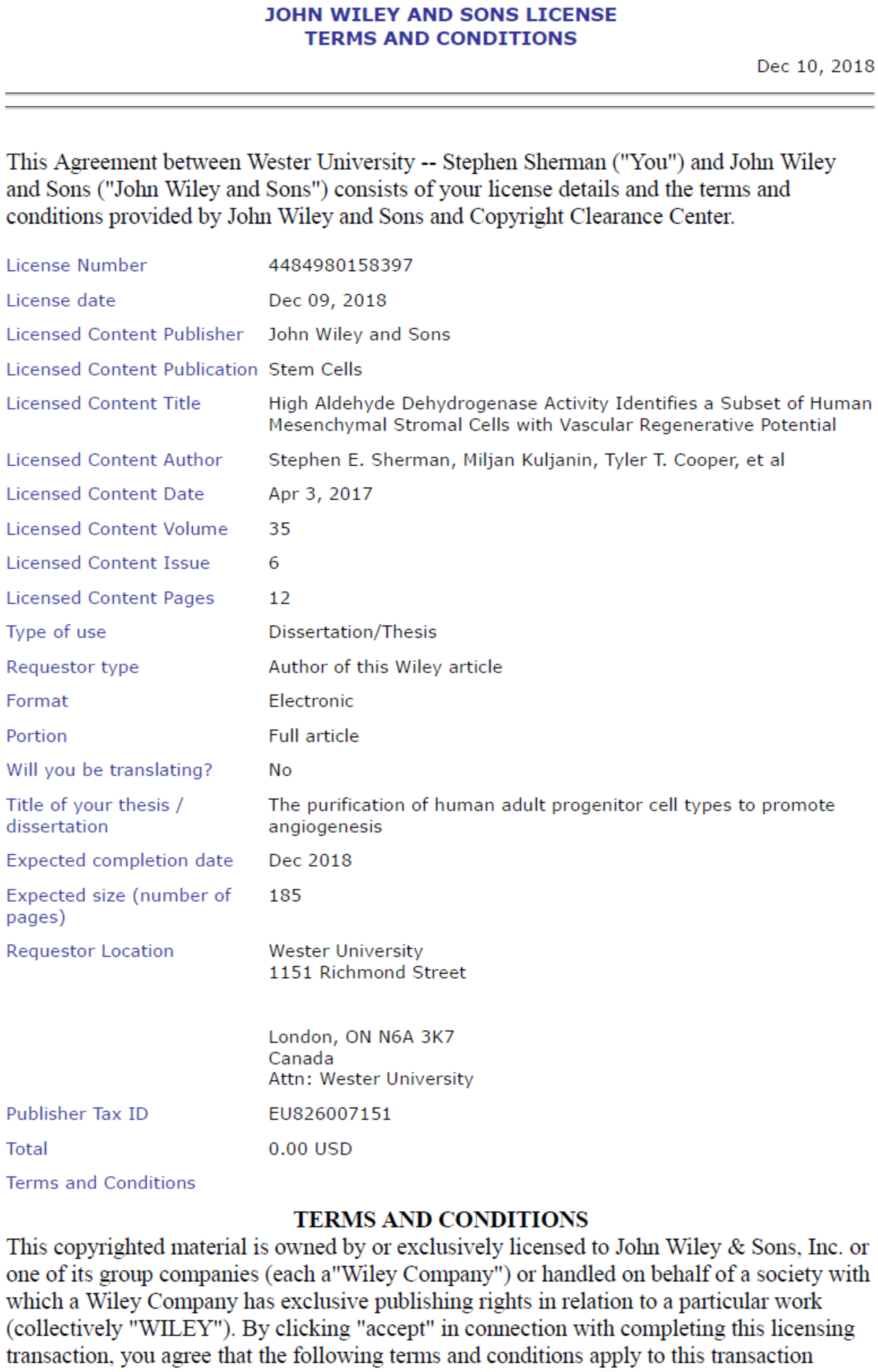

JOHN WILEY AND SONS LICENSE
TERMS AND CONDITIONS

Dec 10, 2018

This Agreement between Wester University -- Stephen Sherman ("You") and John Wiley and Sons ("John Wiley and Sons") consists of your license details and the terms and conditions provided by John Wiley and Sons and Copyright Clearance Center.

License Number	4484980158397
License date	Dec 09, 2018
Licensed Content Publisher	John Wiley and Sons
Licensed Content Publication	Stem Cells
Licensed Content Title	High Aldehyde Dehydrogenase Activity Identifies a Subset of Human Mesenchymal Stromal Cells with Vascular Regenerative Potential
Licensed Content Author	Stephen E. Sherman, Miljan Kuljanin, Tyler T. Cooper, et al
Licensed Content Date	Apr 3, 2017
Licensed Content Volume	35
Licensed Content Issue	6
Licensed Content Pages	12
Type of use	Dissertation/Thesis
Requestor type	Author of this Wiley article
Format	Electronic
Portion	Full article
Will you be translating?	No
Title of your thesis / dissertation	The purification of human adult progenitor cell types to promote angiogenesis
Expected completion date	Dec 2018
Expected size (number of pages)	185
Requestor Location	Wester University 1151 Richmond Street London, ON N6A 3K7 Canada Attn: Wester University
Publisher Tax ID	EU826007151
Total	0.00 USD
Terms and Conditions	

TERMS AND CONDITIONS

This copyrighted material is owned by or exclusively licensed to John Wiley & Sons, Inc. or one of its group companies (each a"Wiley Company") or handled on behalf of a society with which a Wiley Company has exclusive publishing rights in relation to a particular work (collectively "WILEY"). By clicking "accept" in connection with completing this licensing transaction, you agree that the following terms and conditions apply to this transaction (along with the billing and payment terms and conditions established by the Copyright Clearance Center Inc., ("CCC's Billing and Payment terms and conditions"), at the time that you opened your RightsLink account (these are available at any time at http://myaccount.copyright.com).

Terms and Conditions

- The materials you have requested permission to reproduce or reuse (the "Wiley Materials") are protected by copyright.

- You are hereby granted a personal, non-exclusive, non-sub licensable (on a stand-alone basis), non-transferable, worldwide, limited license to reproduce the Wiley Materials for the purpose specified in the licensing process. This license, **and any CONTENT (PDF or image file) purchased as part of your order,** is for a one-time use only and limited to any maximum distribution number specified in the license. The first instance of republication or reuse granted by this license must be completed within two years of the date of the grant of this license (although copies prepared before the end date may be distributed thereafter). The Wiley Materials shall not be used in any other manner or for any other purpose, beyond what is granted in the license. Permission is granted subject to an appropriate acknowledgement given to the author, title of the material/book/journal and the publisher. You shall also duplicate the copyright notice that appears in the Wiley publication in your use of the Wiley Material. Permission is also granted on the understanding that nowhere in the text is a previously published source acknowledged for all or part of this Wiley Material. Any third party content is expressly excluded from this permission.

- With respect to the Wiley Materials, all rights are reserved. Except as expressly granted by the terms of the license, no part of the Wiley Materials may be copied, modified, adapted (except for minor reformatting required by the new Publication), translated, reproduced, transferred or distributed, in any form or by any means, and no derivative works may be made based on the Wiley Materials without the prior permission of the respective copyright owner.**For STM Signatory Publishers clearing permission under the terms of the STM Permissions Guidelines only, the terms of the license are extended to include subsequent editions and for editions in other languages, provided such editions are for the work as a whole in situ and does not involve the separate exploitation of the permitted figures or extracts,** You may not alter, remove or suppress in any manner any copyright, trademark or other notices displayed by the Wiley Materials. You may not license, rent, sell, loan, lease, pledge, offer as security, transfer or assign the Wiley Materials on a stand-alone basis, or any of the rights granted to you hereunder to any other person.

- The Wiley Materials and all of the intellectual property rights therein shall at all times remain the exclusive property of John Wiley & Sons Inc, the Wiley Companies, or their respective licensors, and your interest therein is only that of having possession of and the right to reproduce the Wiley Materials pursuant to Section 2 herein during the continuance of this Agreement. You agree that you own no right, title or interest in or to the Wiley Materials or any of the intellectual property rights therein. You shall have no rights hereunder other than the license as provided for above in Section 2. No right, license or interest to any trademark, trade name, service mark or other branding ("Marks") of WILEY or its licensors is granted hereunder, and you agree that you shall not assert any such right, license or interest with respect thereto

- NEITHER WILEY NOR ITS LICENSORS MAKES ANY WARRANTY OR REPRESENTATION OF ANY KIND TO YOU OR ANY THIRD PARTY, EXPRESS, IMPLIED OR STATUTORY, WITH RESPECT TO THE MATERIALS OR THE ACCURACY OF ANY INFORMATION CONTAINED IN THE MATERIALS, INCLUDING, WITHOUT LIMITATION, ANY IMPLIED WARRANTY OF MERCHANTABILITY, ACCURACY, SATISFACTORY QUALITY, FITNESS FOR A PARTICULAR PURPOSE, USABILITY, INTEGRATION OR NON-INFRINGEMENT AND ALL SUCH WARRANTIES ARE HEREBY EXCLUDED BY WILEY AND ITS LICENSORS AND WAIVED BY YOU.

- WILEY shall have the right to terminate this Agreement immediately upon breach of this Agreement by you.

- You shall indemnify, defend and hold harmless WILEY, its Licensors and their respective directors, officers, agents and employees, from and against any actual or threatened claims, demands, causes of action or proceedings arising from any breach of this Agreement by you.

- IN NO EVENT SHALL WILEY OR ITS LICENSORS BE LIABLE TO YOU OR ANY OTHER PARTY OR ANY OTHER PERSON OR ENTITY FOR ANY SPECIAL, CONSEQUENTIAL, INCIDENTAL, INDIRECT, EXEMPLARY OR PUNITIVE DAMAGES, HOWEVER CAUSED, ARISING OUT OF OR IN CONNECTION WITH THE DOWNLOADING, PROVISIONING, VIEWING OR USE OF THE MATERIALS REGARDLESS OF THE FORM OF ACTION, WHETHER FOR BREACH OF CONTRACT, BREACH OF WARRANTY, TORT, NEGLIGENCE, INFRINGEMENT OR OTHERWISE (INCLUDING, WITHOUT LIMITATION, DAMAGES BASED ON LOSS OF PROFITS, DATA, FILES, USE, BUSINESS OPPORTUNITY OR CLAIMS OF THIRD PARTIES), AND WHETHER OR NOT THE PARTY HAS BEEN ADVISED OF THE POSSIBILITY OF SUCH DAMAGES. THIS LIMITATION SHALL APPLY NOTWITHSTANDING ANY FAILURE OF ESSENTIAL PURPOSE OF ANY LIMITED REMEDY PROVIDED HEREIN.

- Should any provision of this Agreement be held by a court of competent jurisdiction to be illegal, invalid, or unenforceable, that provision shall be deemed amended to achieve as nearly as possible the same economic effect as the original provision, and the legality, validity and enforceability of the remaining provisions of this Agreement shall not be affected or impaired thereby.

- The failure of either party to enforce any term or condition of this Agreement shall not constitute a waiver of either party's right to enforce each and every term and condition of this Agreement. No breach under this agreement shall be deemed waived or excused by either party unless such waiver or consent is in writing signed by the party granting such waiver or consent. The waiver by or consent of a party to a breach of any provision of this Agreement shall not operate or be construed as a waiver of or consent to any other or subsequent breach by such other party.

- This Agreement may not be assigned (including by operation of law or otherwise) by you without WILEY's prior written consent.

- Any fee required for this permission shall be non-refundable after thirty (30) days from receipt by the CCC.

- These terms and conditions together with CCC's Billing and Payment terms and conditions (which are incorporated herein) form the entire agreement between you and WILEY concerning this licensing transaction and (in the absence of fraud) supersedes all prior agreements and representations of the parties, oral or written. This Agreement may not be amended except in writing signed by both parties. This Agreement shall be binding upon and inure to the benefit of the parties' successors, legal representatives, and authorized assigns.

- In the event of any conflict between your obligations established by these terms and conditions and those established by CCC's Billing and Payment terms and conditions, these terms and conditions shall prevail.

- WILEY expressly reserves all rights not specifically granted in the combination of (i) the license details provided by you and accepted in the course of this licensing transaction, (ii) these terms and conditions and (iii) CCC's Billing and Payment terms and conditions.

- This Agreement will be void if the Type of Use, Format, Circulation, or Requestor Type was misrepresented during the licensing process.

- This Agreement shall be governed by and construed in accordance with the laws of the State of New York, USA, without regards to such state's conflict of law rules. Any legal action, suit or proceeding arising out of or relating to these Terms and Conditions or the breach thereof shall be instituted in a court of competent jurisdiction in New York County in the State of New York in the United States of America and each party hereby consents and submits to the personal jurisdiction of such court, waives any objection to venue in such court and consents to service of process by registered or certified mail, return receipt requested, at the last known address of such party.

Appendix 3 Animal use protocol ethics approval

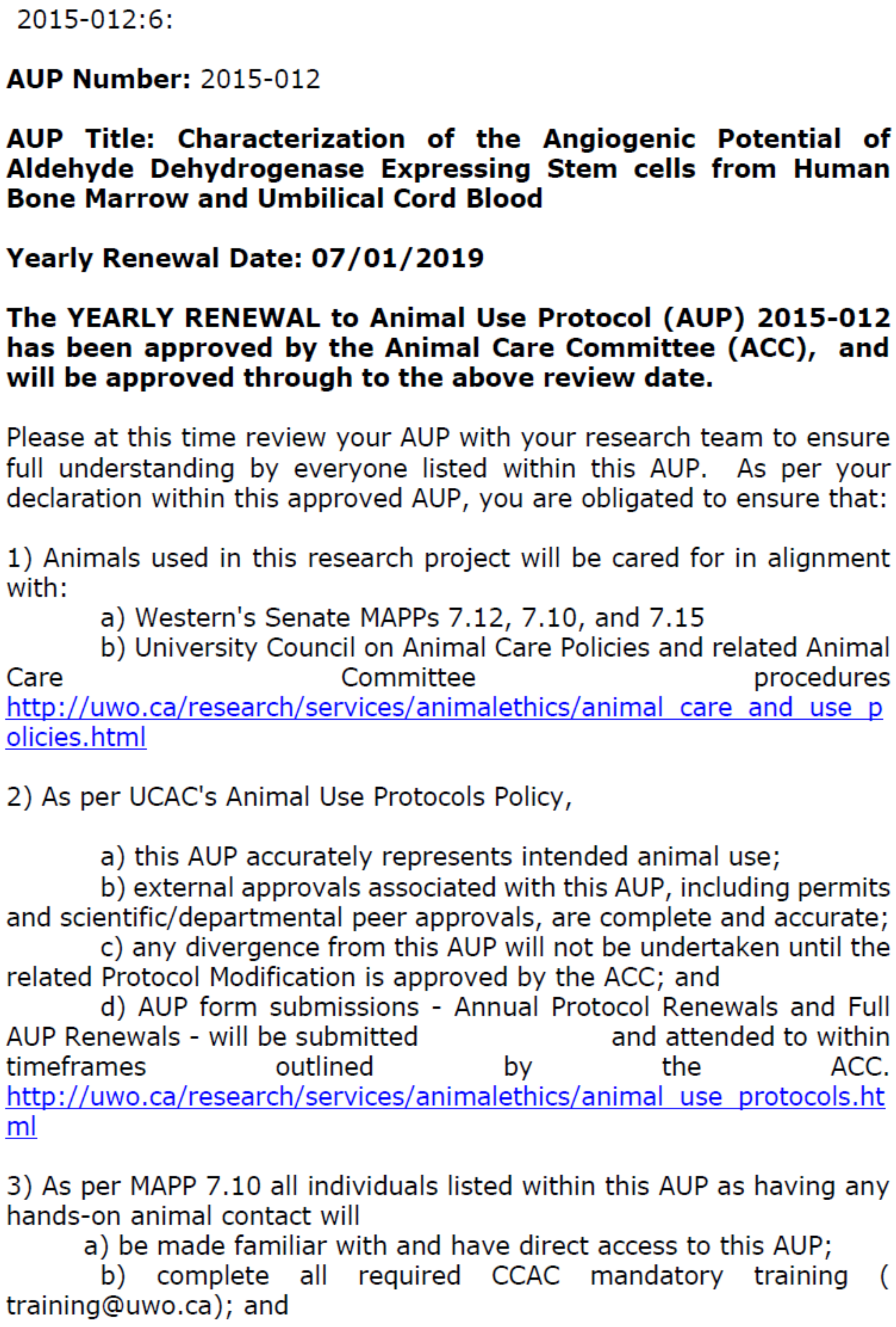

2015-012:6:

AUP Number: 2015-012

AUP Title: Characterization of the Angiogenic Potential of Aldehyde Dehydrogenase Expressing Stem cells from Human Bone Marrow and Umbilical Cord Blood

Yearly Renewal Date: 07/01/2019

The YEARLY RENEWAL to Animal Use Protocol (AUP) 2015-012 has been approved by the Animal Care Committee (ACC), and will be approved through to the above review date.

Please at this time review your AUP with your research team to ensure full understanding by everyone listed within this AUP. As per your declaration within this approved AUP, you are obligated to ensure that:

1) Animals used in this research project will be cared for in alignment with:
    a) Western's Senate MAPPs 7.12, 7.10, and 7.15
    b) University Council on Animal Care Policies and related Animal Care Committee procedures http://uwo.ca/research/services/animalethics/animal_care_and_use_policies.html

2) As per UCAC's Animal Use Protocols Policy,

    a) this AUP accurately represents intended animal use;
    b) external approvals associated with this AUP, including permits and scientific/departmental peer approvals, are complete and accurate;
    c) any divergence from this AUP will not be undertaken until the related Protocol Modification is approved by the ACC; and
    d) AUP form submissions - Annual Protocol Renewals and Full AUP Renewals - will be submitted and attended to within timeframes outlined by the ACC. http://uwo.ca/research/services/animalethics/animal_use_protocols.html

3) As per MAPP 7.10 all individuals listed within this AUP as having any hands-on animal contact will
    a) be made familiar with and have direct access to this AUP;
    b) complete all required CCAC mandatory training (training@uwo.ca); and

c) be overseen by me to ensure appropriate care and use of animals.

4) As per MAPP 7.15,

a) Practice will align with approved AUP elements;

b) Unrestricted access to all animal areas will be given to ACVS Veterinarians and ACC Leaders;

c) UCAC policies and related ACC procedures will be followed, including but not limited to:

i) Research Animal Procurement
ii) Animal Care and Use Records
iii) Sick Animal Response
iv) Continuing Care Visits

5) As per institutional OH&S policies, all individuals listed within this AUP who will be using or potentially exposed to hazardous materials will have completed in advance the appropriate institutional OH&S training, facility-level training, and reviewed related (M)SDS Sheets, http://www.uwo.ca/hr/learning/required/index.html

Submitted by: Copeman, Laura on behalf of the Animal Care Committee
University Council on Animal Care

The University of Western Ontario
Animal Care Committee / University Council on Animal Care
London, Ontario Canada N6A 5C1
519-661-2111 x 88792 Fax 519-661-2028
auspc@uwo.ca�
http://www.uwo.ca/research/services/animalethics/index.html

Appendix 4 Human research ethics approval

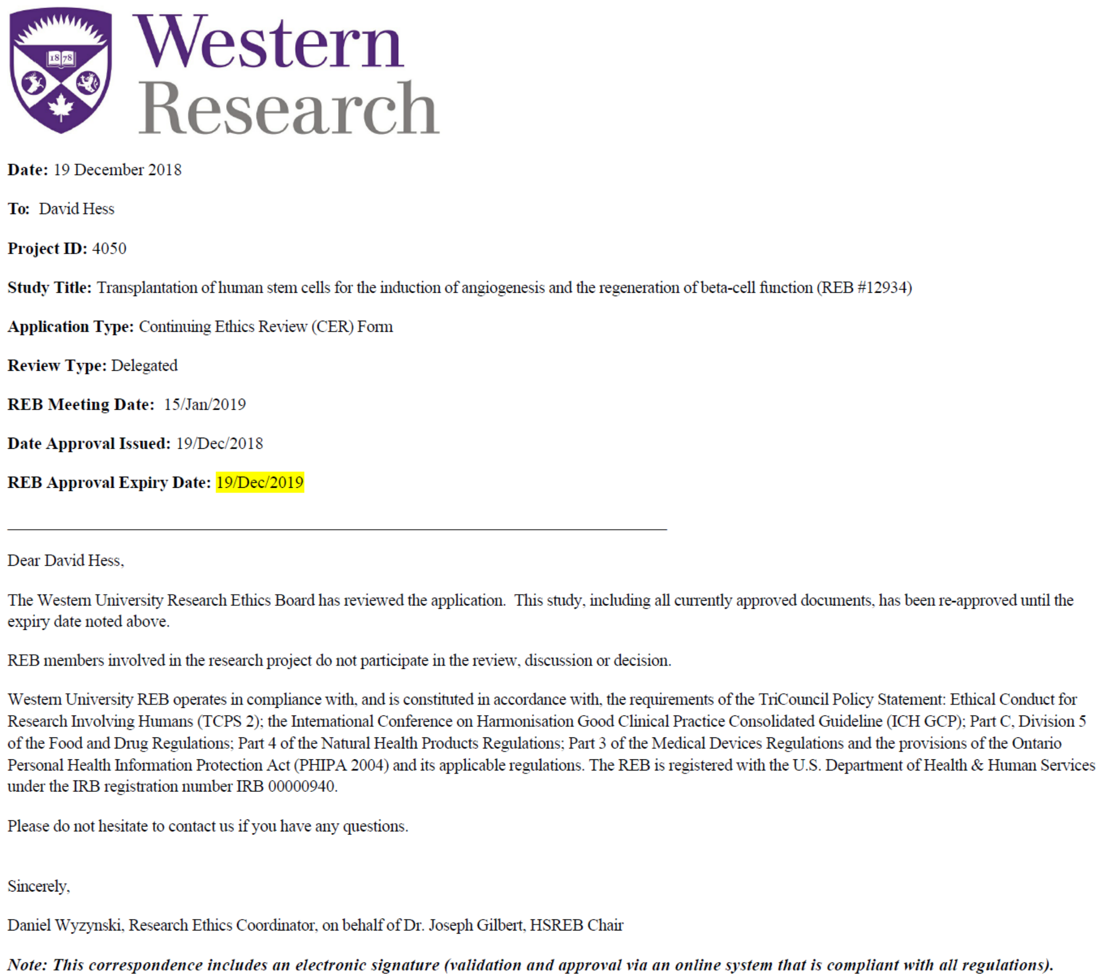

Western
Research

Date: 19 December 2018

To: David Hess

Project ID: 4050

Study Title: Transplantation of human stem cells for the induction of angiogenesis and the regeneration of beta-cell function (REB #12934)

Application Type: Continuing Ethics Review (CER) Form

Review Type: Delegated

REB Meeting Date: 15/Jan/2019

Date Approval Issued: 19/Dec/2018

REB Approval Expiry Date: 19/Dec/2019

Dear David Hess,

The Western University Research Ethics Board has reviewed the application. This study, including all currently approved documents, has been re-approved until the expiry date noted above.

REB members involved in the research project do not participate in the review, discussion or decision.

Western University REB operates in compliance with, and is constituted in accordance with, the requirements of the TriCouncil Policy Statement: Ethical Conduct for Research Involving Humans (TCPS 2); the International Conference on Harmonisation Good Clinical Practice Consolidated Guideline (ICH GCP); Part C, Division 5 of the Food and Drug Regulations; Part 4 of the Natural Health Products Regulations; Part 3 of the Medical Devices Regulations and the provisions of the Ontario Personal Health Information Protection Act (PHIPA 2004) and its applicable regulations. The REB is registered with the U.S. Department of Health & Human Services under the IRB registration number IRB 00000940.

Please do not hesitate to contact us if you have any questions.

Sincerely,

Daniel Wyzynski, Research Ethics Coordinator, on behalf of Dr. Joseph Gilbert, HSREB Chair

Note: This correspondence includes an electronic signature (validation and approval via an online system that is compliant with all regulations).

Curriculum Vitae

Name:	**Stephen Sherman**
Post-secondary Education and Degrees:	University of Western Ontario London, Ontario, Canada 2009-2013 B.Sc.
Honours and Awards:	Province of Ontario Graduate Scholarship 2016-2017, 2017-2018
	Children's Hospital Foundation Graduate Scholarship 2015-2016
	Platform Presentation Award, London Health Research Day 2016
	2nd Place Poster Award, Annual Physiology and Pharmacology Research Day 2014
	University of Western Ontario Dean's Honor List, 2009-2013
Related Work Experience	Teaching Assistant University of Western Ontario 2015-2019

Publications:

- Dhillon J, Young SA, **Sherman SE**, Bell GI, Amsden BG, Hess DA, Flynn LE. Investigation of Peptide-Modified Methacrylated Glycol Chitosan Hydrogels as a Pro-Angiogenic Cell Delivery Platform for Human Adipose-derived Stem/Stromal Cells. JBMR: Part A. Nov. 2018.
- **Sherman SE**, Bell GI, Teoh H, Al-Omran M, Connelly KA, Bhatt DL, Hess DA, Verma S. Canagliflozin improves the recovery of blood flow in an experimental model of severe limb ischemia. JACC: BTS. Jan 2018.
- Cooper TT, **Sherman SE**, Kuljanin M, Bell GI, Lajoie GA, Hess DA. Inhibition of aldehyde dehydrogenase-activity expands multipotent myeloid progenitor cells with vascular regenerative function. Stem cells. Jan 2018.
- Young SA, **Sherman SE**, Cooper TT, Brown C, Anjum F, Hess DA, Flynn LE, Amsden BG. Mechanically resilient injectable scaffolds for intramuscular stem cell delivery and cytokine release. Biomaterials. Jan 2018.

- Kuljanin M, Bell GI, **Sherman SE**, Lajoie GA, Hess DA. Proteomic characterisation reveals active Wnt-signalling by human multipotent stromal cells as a key regulator of beta cell survival and proliferation. Diabetologia. Oct 2017.
- Putman DM, Cooper TT, **Sherman SE**, Seneviratne AK, Hewitt M, Bell GI, Hess DA. Expansion of Umbilical Cord Blood Aldehyde Dehydrogenase Expressing Cells Generates Myeloid Progenitor Cells that Stimulate Limb Revascularization. Stem cells translational medicine. July 2017.
- **Sherman SE**, Kuljanin M, Cooper TT, Putman DM, Lajoie GA, Hess DA. High Aldehyde Dehydrogenase Activity Identifies a Subset of Human Mesenchymal Stromal Cells with Vascular Regenerative Potential. Stem cells. Mar 2017.
- Lavoie JR, Creskey MM, Muradia G, Bell GI, **Sherman SE**, Gao J, Steward DJ, Cyr TD, Hess DA, Rosu-Myles M. Brief Report: Elastin Microfibril interface 1 and integrin-linked protein kinase are novel markers of islet regenerative function in human multipotent mesenchymal stromal cells. Stem cells. Aug 2016.
- Seneviratne AK, Bell GI, **Sherman SE**, Cooper TT, Putman DM, Hess DA. Expanded hematopoietic progenitor cells reselected for high aldehyde dehydrogenase activity demonstrate islet regenerative functions. Stem cells. Dec 2015.
- **Sherman SE**, Hess DA**.** Immunogenicity and immunomodulation of fetal stem cells. In Fetal Stem Cells in Regenerative Medicine 2016 (pp. 57-79). *Springer, New York, NY.*